BENEFICIATION OF FINE COAL USING THE AIR-SPARGED HYDROCYCLONE

A thesis submitted to the
UNIVERSITY OF CAPE TOWN
in fulfillment of the requirements
for the degree of
MASTER OF SCIENCE IN ENGINEERING

by
ASHLEY WAYNE BREED B.Sc. (Chem. Eng.) (Cape Town)

Department of Chemical Engineering
University of Cape Town
Rondebosch, 7700
South Africa

October 1992

SYNOPSIS

The Air-Sparged Hydrocyclone (ASH) is a high capacity flotation device which is alleged to be more efficient for the flotation of fine particles than conventional flotation equipment. The principal aims of this thesis were to investigate the use of an ASH in the flotation of South African coal *ultrafines* (-150 micron), and to determine the effect of various design and operating parameters on the performance of the process, in terms of the product yields and grades obtainable.

The testwork was carried out on a typical Witbank coal, from the Kleinkopje Colliery, with an ash content of 23.7 %. The coal was characterised by means of size, ash-by-size and float-and-sink analyses. Batch flotation experiments were carried out to provide a benchmark against which the ASH could be compared. Preliminary ASH work was carried out to determine the required collector and frother dosages and the optimal slurry feed rate.

A fractional factorial design, at two levels, was carried out to investigate the effects of the underflow configuration (the use of an orifice and a baffle instead of the conventional pedestal/annular opening), the ratio of the overflow to underflow openings (A^*), the ASH length to diameter ratio (L_c/d_c), the ratio of the air to slurry feed rates (Q^*), the ratio of the vortex-finder length to the cyclone diameter (L_{vf}/d_c) and the size of the slurry inlet (A_{inlet}). The effect of pulp density was investigated separately.

The results of the testwork showed that the ASH beneficiated the coal successfully at capacities of up to 300 times those possible in conventional (batch) flotation, and in the region of 1500 times those achieved using the same coal in a column cell. The overall results, in terms of concentrate ash contents at particular yields, showed that the ASH results were comparable with those of the batch cell, but not as good as those of the column cell.

The nature of the material being floated resulted in collector dosages in the region of 36 kg/ton being used in the factorial design to achieve concentrate yields in the region of 50 %. However, use of the optimal ASH configuration reduced this required collector dosage to about 25 kg/ton, without loss in performance.

A typical (good) ASH result achieved was a yield of 47.7 % at a concentrate ash content of 8.8 %.

Size analyses indicated that the ASH product is recovered by both flotation and classification with the result that, for the small diameter ASH and Kleinkopje coal sample used, the ASH could not be considered to be a *more efficient device for the flotation of fine particles*, but rather a *less efficient device for the recovery of coarse particles*. However, the ASH performance in the *ultrafine* size fractions (-150 micron) was comparable with that of the batch cell.

The underflow configuration, A^* and L_c/d_c all had a significant effect on the performance of the ASH. Q^* had a minor effect, L_{vf}/d_c may have had an effect and A_{inlet} had no effect on the performance of the ASH. In addition, increasing the pulp density from 1.6 to 9.4 % (mass/volume) had no effect on the performance of the ASH.

It is recommended that future research include the investigation of pre-conditioning for the flotation of poorly floatable (inertinite rich) South African coals, the use of an ASH on more floatable coals, the determination of the limit to which the pulp density can be increased (without loss in flotation performance) and the determination of scale-up criteria for the ASH.

ACKNOWLEDGEMENTS

The author would like to extend his thanks to the following people who assisted with the work presented in this thesis:

Prof. J-P. Franzidis for his assistance and guidance throughout the testwork and write-up phase of this study.

My friend and colleague Sean von Holt for his constructive advice throughout the testwork, and assistance with the statistical analysis.

Helen Divey and Lorna Wall for their assistance in the ash and float-and-sink analyses.

The Foundation for Research and Development (FRD) for funding the research.

Colleagues and staff in the Department of Chemical Engineering at the University of Cape Town for their interest and assistance whenever needed.

My parents and family, without whom this would not have been possible.

Meriel, who was always there when needed.

For my late father, LOUIS BREED, and his belief in education

CONTENTS

CHAPTER THREE

LIST OF TABLES

LIST OF FIGURES

NOMENCLATURE

A_{inlet}	ASH slurry inlet area; mm^2
A_{of}, $A_{overflow}$	ASH overflow area; mm^2
A_{uf}, $A_{underflow}$	ASH underflow area; mm^2
A^*	A_{of}/A_{uf} ratio; dimensionless
C_{vb}	volumetric fraction of the bubble phase, dimensionless
dof	degrees of freedom
d_b^{cr}	critical air bubble diameter, mm
d_c	ASH diameter; mm
d_o	ASH underflow orifice diameter; mm
d_p	particle diameter; μm
d_p, $d_{pedestal}$	ASH pedestal diameter; mm
d_{vf}, $d_{vortex-finder}$	ASH vortex-finder diameter; mm
g	acceleration due to gravity, 9.8 m/s^2
IEP	iso-electric point
L_c	ASH length; mm
lk	contrast
L_{vf}	ASH vortex-finder length; mm
MSe	mean square of the error
MSlk	mean square of the contrast
n	number of samples
PZC	point of zero charge
Q_{air}	air flow rate; slpm
Q_{slurry}	slurry flow rate; l/min
Q^*	Q_{air}/Q_{slurry} ratio; dimensionless
se	standard error

CHAPTER ONE

INTRODUCTION

1.1 Background

1.1.1 Coal fines and ultrafines in South Africa

Of the 224 Mt of run-of-mine (ROM) production of South African collieries in 1988, approximately 20 % (DMEA Report, 1989) reported to discards, representing about 10 % of the energy content of the ROM production (Grobbelaar, 1988).

The high proportion of discard material can be attributed to the increased mechanisation of coal mining in South Africa, the market demands for size-specific coal products and the friability of the coal seams. The increased use and capacity of mechanised mining methods has led to the employment of heavier charges and less selective mining of the coal seams. This, together with opencast mining methods, has resulted in an increase in the proportion of dirt and fines delivered to the washing plants. The above, coupled with the demand for size specific thermal (13 to 14 % ash) and low-ash (7.0 to 7.5 % ash) coal (LAC), has resulted in 30 to 40 % of the ROM coal fed to washing plants reporting to the discard stream.

The discard material varies greatly in terms of both size and quality. However, the liberation which accompanies the reduction in particle size results in the fines fraction of the discards containing a relatively large proportion of liberated high grade material.

In the South African coal industry -0.5 mm material is considered to be fines, and constitutes 8 to 12 % of the ROM coal. However, inefficiencies in the classification circuits result in the actual top size being in the region of 1 mm. Until the mid 1980's, these fines were generally discarded or (in the case of two-product mines) added to the middlings for use as steam coal. An exception was in the plants producing metallurgical coal, where the fines have for a long time been regarded as a source of high grade product and therefore beneficiated by froth flotation.

The most recent discard and duff coal inventory in South Africa was carried out in 1985 (DMEA Report, 1987). It showed that South African coal mines were discarding 3.7 million tons of bituminous slurry each year. The ash content of this coal ranged from 6 to 58 %, and the calorific value from 15.0 to 26.8 MJ/kg. The sulphur content varied from 0.66 to 2.20 %. There was great potential for producing some saleable product from this material through appropriate beneficiation.

The introduction of spirals has been the most significant development in the beneficiation of coal fines during the last decade. Spiral plants have been introduced into at least 17 collieries since 1984, and currently treat more than 5 Mtpa of +0.1 mm material (Franzidis, 1992). Spirals are low capacity, low cost devices which, on account of their poor separation efficiency are generally used to produce a single product which is added to the steam coal product. In spite of the installation of spiral plants at numerous mines, the -0.1 mm ultrafines are still discarded.

There are both economic and environmental advantages to recovering a saleable product from the discard material (both coarse and fine) that is currently stockpiled or dumped. Among the economic advantages are increased mining costs, the higher coal price and reclamation and stockpiling/dumping costs of 1.32 to 8.75 Rands/ton (DMEA Report, 1987). The environmental advantages of reducing the size and energy

content of stockpile/discard dumps are the following:

i) they are a source of acid ground water;
ii) they reduce the value of the land adjacent to the discard dumps; and
iii) it would reduce the possibility of spontaneous combustion and the associated atmospheric pollution.

In addition, it is expected that so called "green" issues will become increasingly important political factors in the future, both within South Africa and in terms of pressure from trading partners.

Consideration of the above suggests that it might be economically and environmentally advantageous to subject the ultrafines discards to further processing, as they contain a larger proportion of liberated, high grade product than the coarser discard material. No additional mining cost would be incurred, the disposal cost would be reduced, and the potential for environmental pollution would be curtailed. The generation of more saleable product from the same ROM feed would increase the profitability of the mine and extend the life of the reserves.

Methods for fines beneficiation can be broadly classified into those which exploit differences in the bulk properties of the valuable and gangue materials (through the use of water and dense medium cyclones, jigs, shaking tables and spirals) and those which use differences in the surface properties (e.g. froth flotation, oil agglomeration and selective flocculation). Below a particle size of 0.1 mm the efficiency of separation processes based on bulk properties drops off rapidly despite the associated increase in liberation. This led Horsfall and Franzidis (1988) to propose that the fines fraction be subdivided into fines (-750+150 micron) and ultrafines (-150 micron) fractions. In addition they proposed that differences in bulk properties (viz. gravity) be used to beneficiate the fines fraction while differences in surface properties be used to beneficiate the ultrafines.

Of the three surface-based technologies mentioned above, froth flotation is the most commercially viable (Aplan, 1987). Despite this, and the widespread use of flotation, both locally and internationally, in the beneficiation of mineral ores, flotation of coal fines, both locally and internationally, is limited. This can be attributed to:

i) the high capital and running costs of conventional cells versus the low unit value of coal;
ii) the inability of these cells to make clean separations at finer sizes; and
iii) high dewatering costs.

In addition, South African coals (Gondwanaland deposits) are generally more difficult to float than Northern Hemisphere coals (Laurasian coals) as a result of their petrographic composition and mineral content/associations. In spite of this numerous workers have shown that South African coal *ultrafines* can be beneficiated by both conventional and column flotation. However, the problems listed above and the low capacity of column cells (especially in the flotation of low rank coals) has resulted in the limited use of froth flotation in South African coal washing plants.

Oil agglomeration and selective flocculation have not been used commercially on South African coals. Since early 1990 a local company has achieved promising results carrying out oil agglomeration plant trials using a mobile pilot plant; this work is still in progress. No testwork results using selective flocculation have been published.

Until the 1980's flotation of coal fines was limited to metallurgical coal fines. At present 6 South African collieries use conventional flotation to beneficiate the ultrafines, only one of which is a non-coking mine (Franzidis, 1992). The most important coalfield in South Africa, viz. Witbank, has no flotation plants. The factors discussed above indicate the need and desirability to find a low cost, high capacity method/device for the flotation of these untreated *ultrafines*.

1.1.2 The air-sparged hydrocyclone

The Air-Sparged Hydrocyclone (ASH) is a high capacity flotation device invented by Professor J.D. Miller of the University of Utah in the early 1980's. It consists of two concentric right vertical tubes, the inner of which is porous; a conventional cyclone header and vortex-finder; and a froth pedestal at its base. A diagrammatic representation of the ASH is given in Figure 1.1 below.

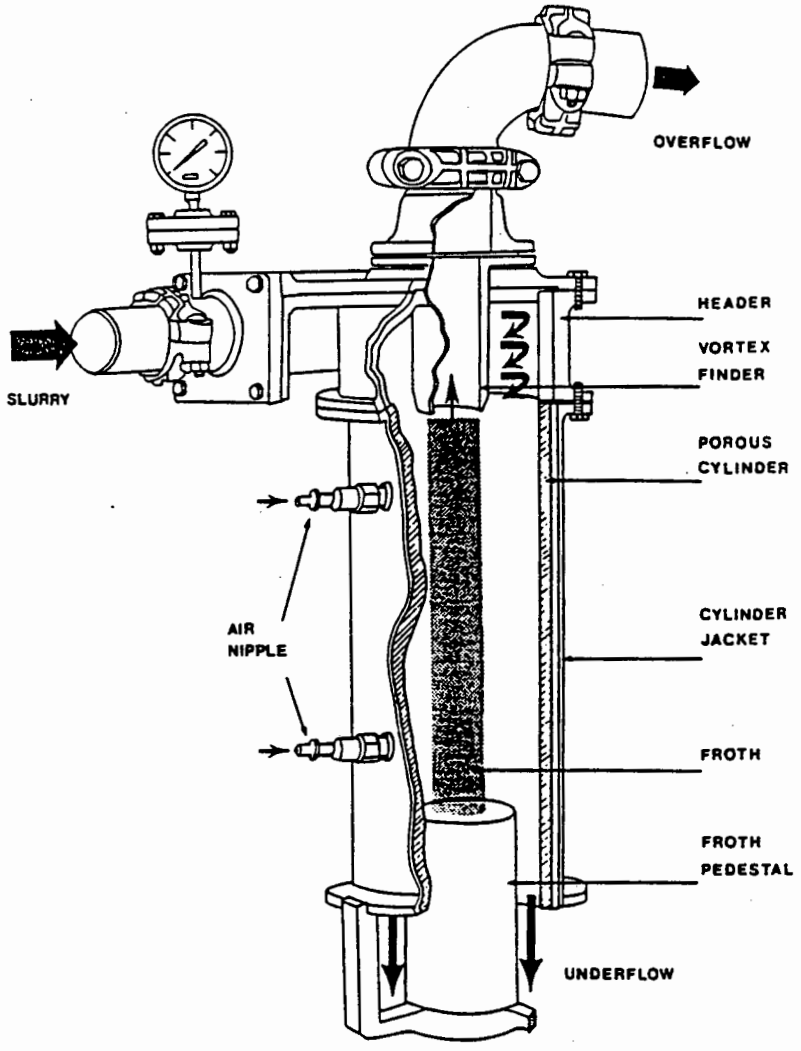

Figure 1.1: Diagrammatic representation of the ASH (after Ye et al, 1988)

Slurry is fed via the header into the porous cylinder. As the slurry moves axially down the ASH, hydrophobic particles collide with (and become attached to) air bubbles produced by sparging air through the

porous cylinder. The particle/bubble aggregates move to the cyclone axis, and form a froth phase supported at the base by the pedestal. The froth phase moves axially up the ASH to be discharged via the vortex-finder (overflow). The slurry phase is discharged via the annular opening between the pedestal and the porous cylinder wall (underflow).

The small air bubbles (formed as a result of the micron size pores of the porous cylinder and the high shear forces at the cyclone wall), the increased particle inertia (caused by the centrifugal forces) and the directed particle-bubble motion together result in the *increased collision efficiency of small particles*. This in turn extends the lower limit of fine particle flotation and increases the flotation rate of these particles. In addition, the high volumetric rates result in a short residence time, i.e. a *large volumetric capacity*. Other advantages of the ASH are reported to be:

i) their flotation performance is comparable with that obtained in batch cells;
ii) coal concentrate dewatering may not be necessary; and
iii) an ASH circuit may be much cheaper than a conventional circuit in capital and operating costs.

It is the potential of the ASH for achieving particle separations better than, or comparable to, those obtained in conventional cells, at far greater capacities than those achievable in other flotation machines, that make it worth investigating for the beneficiation of South African coal *ultrafines*.

To date testwork using the ASH in South Africa has only been carried out by Burger (1986) and Nieuwoudt et al (1990), both of whom used pyrite. Burger commissioned and modified an ASH, and carried out a preliminary investigation. Nieuwoudt et al further modified the ASH and investigated the effects of the design and operating parameters on the performance of the ASH. To the author's knowledge, no one has previously investigated the use of an ASH for the beneficiation of South African coal *ultrafines*.

1.2 Aims and Scope of the Investigation

The aims of this research were to investigate the use of an ASH in the flotation of South African coal *ultrafines*, and to determine the effect of various design and operating parameters on the performance of the process, in terms of product yields and grades obtainable.

The ASH used by Nieuwoudt et al (1990) was modified for use in this investigation. The ASH rig was located at the University of Stellenbosch. The coal selected for the investigation was a "typical" Witbank coal on which conventional and column flotation work had already been performed at the University of Cape Town. The sample was collected in such a way as to ensure that it was uniform in both composition and nature. Care was also taken to ensure that the sample splitting procedure followed resulted in representative subsamples for the ASH investigation.

The coal was characterised by size, ash-by-size and float-and-sink analyses. Batch flotation experiments were carried out for comparison with the results obtained in the ASH. Preliminary work was done to become familiar with the operation of the ASH, and to obtain an idea of the range of operating parameters to use in the detailed ASH work. The detailed ASH investigation was carried out using the method of factorial design, so as to identify the most important parameters and interactions between them. Follow-up work was done to investigate the effect of specific parameters on the ASH operation.

1.3 Thesis Outline

Chapter Two begins with a description of the structure of coal and how it is formed. This is followed by a description of South African coal. Finally the factors affecting the flotation of coal are discussed.

Chapter Three is a literature review pertinent to the ASH. It begins with a description of the unit and how it operates. Advantages and disadvantages are then described. This is followed by a review of the

design and operating parameters which have been found to determine the performance of the ASH. Finally the work of previous researchers on the flotation of coal in the ASH is described and discussed.

Chapter Four is a description of the experimental equipment used in this investigation and of the methods followed in the ASH testwork and coal characterisation work. The analytical techniques followed are also described.

The results of the preliminary investigation are reported in Chapter Five. These consisted of the sample preparation, coal characterisation (size, ash-by-size, float-and-sink and release flotation analysis, and batch flotation) and two-phase and preliminary three-phase ASH results.

Chapter Six begins with a description and analysis of the results obtained in the fractional factorial design investigation. This is followed by the results of further work carried out to investigate the effect of pulp density, air rate and collector dosage. The Chapter concludes with a general discussion of the effects of the various parameters on the performance of the ASH, and with an evaluation of the feasibility of using the ASH to float South African coals.

Conclusions drawn from the results and recommendations for further work are given in Chapter Seven.

CHAPTER TWO

THE NATURE OF COAL AND FACTORS AFFECTING COAL FLOTATION

The diversity of the original plant material from which a coal was formed, and the conditions under which it formed, have a significant impact on the physical and chemical behaviour of that coal. The emphasis of this Chapter is directed towards describing and discussing those factors which affect the flotation of coal. The Chapter begins by describing how coal was formed, and goes on to discuss its composition on both the microscopic and macroscopic scale. This is followed by a discussion of South African coals, their characteristics, the extent of the reserves, and the current status of fine coal beneficiation. Finally a review of the factors affecting the flotation of coal is presented.

2.1 The Origin of Coal

Coal was formed during the Carboniferous, Permian and early Cretaceous periods. Decaying plant matter was deposited in swamps, with most of the vegetation growing on site, although some was carried into the swamps by rivers. This period of plant death and decay, to form peat, is known as the biochemical stage of coal formation (Horsfall, 1980, p203). This stage was rapid, and had a variety of end products, depending on the original vegetation and the conditions in the swamp. The thick beds of peat were covered by layers of sandstone and shale. The above process was then repeated.

For coal formation it was necessary for the peat to be covered by water, and the layers of silt, clay and sand resulted in an increase in the pressure and temperature of the peat. After the burial of the peat the bacterial activity ceased, and the rate of transformation of the material slowed. This metamorphic stage of the coalification process resulted in a reduction of the oxygen and water contents of the material, with a corresponding increase in carbon content.

With time, and under the influence of climatic and tectonic changes, the material underwent physical and chemical changes, which resulted in the formation of coal.

The behaviour of different coals are a result of the composition, deposition, biochemical degradation and metamorphosis of the original organic constituents. These factors determine the *type*, *rank* and *grade* of the coal.

i) The coal *type* (petrography) is the characteristic organic composition of the coal. It is determined by the proportions and chemical composition of the organic constituents of the original material and the biochemical degradation which the material has undergone. The end products are the macerals described in Section 2.2.1.1.

ii) The coal *rank* is a measure of the maturity of the coal, and it ranges from peat (unconsolidated product of decomposition found in bogs and marshes), through lignite or brown coal, to sub-bituminous coal, to bituminous coal, to semi-anthracite or lean coal, to anthracite, of which the most mature form is known as meta-anthracite. A marked reduction in the amount of volatiles becomes apparent in the higher rank stages of bituminous coal.

iii) The coal *grade* is the proportion of inorganic mineral sediments in the coal. These minerals can be syngenetic (inherent) or epigenetic (extraneous) as described in Section 2.2.1.2 below.

2.2 The Composition of Coal

Coal is a physically heterogeneous and chemically complex solid. It consists chiefly of carbonaceous material (C, H, O and lesser amounts of N and S), moisture and inorganic minerals. The composition of coal may be described or characterised at various levels, as is discussed in the sections below.

2.2.1 The microscopic structure of coal

At the microscopic level coal can be seen to consist of discrete particles of carbonaceous and mineral matter. These particles range in size from 1 to 50 micron (Falcon, 1986). The composition of the carbonaceous and mineral matter is discussed below.

2.2.1.1 carbonaceous material

The carbonaceous material in coal is nonhomogeneous, and consists of different *macerals*, which are analogous to minerals. The macerals are the result of the primary accumulation and early coalification of the different parts of the original plant material. The three major maceral groups are discussed below.

i) *Vitrinite* was formed from cell wall material and the cell fillings of the woody tissue of plants (trunks, branches, twigs, roots and leaf tissue). For preservation as vitrinite such material in the peat swamp needed to fall into, or be covered by, water or sediment to prevent severe biochemical oxidation from taking place (i.e. the decomposition was anaerobic). Vitrinite contains less volatile matter than exinite, but more than inertinite. It has a SG of 1.27 - 1.80 (Falcon, 1986) and an intermediate H:C ratio.

ii) *Inertinite* results from plant material that has been strongly altered and degraded by oxidation during the peat stage. The parent material is the same as that of vitrinite, but it has undergone aerobic or subaerobic decomposition during the oxidation process. Inertinite contains the least amount of volatile matter and has the lowest H:C ratio of the major macerals, and has a SG of 1.35 - 1.70 (Falcon, 1986).

iii) *Exinite* consists of the chemically-resistant vegetable matter like spores, cuticles, cell walls, resins, waxes, fats and oils. It is the maceral containing the most volatile material, has the highest H:C ratio, and a SG of 1.18 - 1.25 (Falcon, 1986).

These maceral groups have different optical, physical and chemical properties, which enables them to be readily identified by means of a petrographic analysis (under the microscope). A summary of the major characteristics of the maceral groups is presented in Table 2.1 below.

As may be seen from Table 2.1, the chemical and physical properties of the macerals change with changing rank. As the rank of a coal increases the differences in the properties of the different macerals become less marked. Coal rank is measured by the reflectance of vitrinite. Vitrinite is used as the reference maceral as it is the most homogeneous, and its reflectance varies linearly with changing rank.

2.2.1.2 minerals

The mineral matter present in coal can be divided into two broad categories, intrinsic and extrinsic or introduced mineral matter. Intrinsic mineral matter is material that was present in the original living organism. These minerals are ultimately trapped in the form of sub-microscopic grains and organo-metallic complexes. Extrinsic mineral matter can be divided into two categories:

Table 2.1: A summary of the major constituents of the three maceral groups in hard coal (after Falcon, 1978:12)

Maceral Group	Plant Origin	Reflectance			Chemical Properties		Technological Characteristics						
		Description	Rank	% Reflected Light	Characteristic Element	Typical Products on Heating		Combustion			Pyrolysis		Hydrogenation and Liquifaction
								Ignition	Burn Out	Smoke	Coke	Liquors	
VITRINITE	woody trunks, branches, stems, bark, leaf tissue, shoots and detrital organic matter gelified/vitrinitized in acquatic reducing conditions.	Dark to medium grey	Low rank to Medium rank Bituminous	0.5-1.1	Intermediate hydrogen content	Light hydrocarbons	Intermediate volatiles decreasing rank	###	###	**	**	***	##	###
				1.1-1.6				##	##	*	****	(*)	#	##
		Pale grey	High rank Bituminous	1.6-2.0	-	-		#	#	(*)	(*)		(#)	(#)
		White	Anthracite	2.0-10.0	-	-		#	#	-	-	-		
EXINITE	cuticles, spores, resin, algae accumulating in sub-aquatic conditions.	Black-brown	Low rank	0.0-0.5	Hydrogen rich	Early methane gas	Volatile-rich decreasing with rank	####	####	****	*	****	####	##
		Dark grey	Bituminous	-0.5-0.9				###	###	***	*	**	###	###
				-0.9-1.1		Oil		#	#	**	*	*	#	#
		Pale grey	Medium rank Bituminous	-1.1-1.6		Condensates wet gases decreasing		(#)	(#)	(*)	(*)	(*)	-	
		Pale grey (-vitrinite) to white shadows	High rank Bituminous to Anthracite	-1.6-10.0	-	-	-	-	-	-	-	-	-	
INERTINITE	As for vitrinite, but fusinitised in aerobic oxidising conditions.	Medium grey	Low rank Bituminous	0.7-1.6	Hydrogen poor	-	Low volatiles in all ranks	#	#	*	-	-	-	-
		Pale grey to white and yellow-white	Medium rank Bituminous to Anthracite	-1.6-1.6				#	#	(*)	-	-	-	-
				-1.6-10.0	-	-		(#)	(#)	-	-	-	-	

KEY	
#	: Capacity or rate
####	: Fast
#	: Slow
	: Zero
*	: Proportion
****	: High
*	: Low
-	: Absent

i) *Syngenetic* or primary mineral matter consists of matter that accumulated at the time of peat accumulation, as a result of wind and water, or *in situ* precipitation. As these minerals are intimately intergrown with the coal, they are difficult to liberate from the coal.

ii) *Epigenetic* or secondary mineral matter is matter that was carried by water into fractures, cavities and pores within the coal seam long after the initial accumulation of the peat. Coals containing these minerals are easily liberated.

Turning to the minerals which are known to be associated with coal, the minerals most commonly found are clay, quartz, carbonates, iron sulphides, apatite, barite, gypsum and sphalerite, all of which have a SG greater than 1.8 (Falcon, 1986).

i) *Clay* is the mineral found most commonly in coal. It occurs as minute grains (1 to 2 micron in diameter), as small lenses, as microscopically visible bands, as fillings in cell cavities, as a replacement to cell structures to form clay petrifications and as veins (Falcon, 1986). Clay has a SG of 2.3 - 2.6 (Falcon, 1978).

ii) *Quartz* generally occurs in small quantities, as isolated grains, 5 to 20 micron in diameter (Falcon, 1986). Where a seam has been invaded by silica, quartz veins, petrifications and cell fillings occur. Quartz has a SG of 2.65.

iii) *Carbonates* usually occur as nodules of siderite, or as veins and cell fillings of calcite (SG of 2.7), dolomite (SG of 2.9) and ankerite (SG of 3.5 - 3.8).

iv) *Iron sulphides* such as pyrite, melnikovite pyrite and marcasite have a SG of 5 and are only ever present in small quantities. Where pyrite is abundant, it is usually present in the form of petrifications and nodules.

v) *Apatite*, *barite*, *gypsum* and *sphalerite* rarely occur in coal, but may be significant in a particular region.

Coal always contains a certain amount of water (inherent moisture). This water is present in the pores, and it cannot be removed by draining, centrifuging or by evaporation at normal temperatures. This water is only removed by heating the coal to above the boiling point of water.

2.2.2 The macroscopic structure of coal

Lumps of coal show bands of different texture and brightness, running parallel to the bedding plane of the coal. These bands are known as vitrain, durain, clarain and fusain and are described below.

2.2.2.1 vitrain

Vitrain is black and shiny. It normally occurs in thin layers up to half an inch thick. In higher rank coals it can be soft and brittle. Vitrain is mainly responsible for the coking properties of a coal.

2.2.2.2 durain

Black durain is black in colour, but it is not shiny. It is composed of altered residues of leaves and seeds. Grey durain is grey in colour and consists of an intimate mixture of vitrain and material similar to fusain. The lustre of the grey durain increases as the vitrain content increases.

2.2.2.3 clarain

Clarain consists of very thin alternating bands of vitrain and black durain, which results in a satiny appearance.

2.2.2.4 fusain

Fusain does not usually form continuous bands in coal. It usually occurs as discrete flat pieces. It looks like charcoal, and if the pores are not filled with mineral matter it is very soft. Fusain represents the most altered material in the coal seam.

2.2.3 The characterisation of coal

Coal has traditionally been characterised by means of proximate and ultimate analyses. Proximate analyses determine the relative amounts of light organic compounds (volatiles) as opposed to the amount of non-volatiles (fixed carbon). Proximate analyses also determine the moisture content of the coal and the amount of inorganic ash after combustion. In ultimate analyses the total amounts of the principal elements occurring in coal, viz. C, H, N, O and S are determined.

As the above analyses give no indication of the technological and beneficiation properties of the coal it is necessary to carry out a petrographic analysis (including an analysis of the type, form and proportion of the mineral matter present) to infer the above properties. Float-and-sink tests are also carried out to determine the liberation characteristics of the coal, i.e. the yield of product coal that is theoretically achievable at a certain grade (ash content).

In addition to the above, tests are also carried out to evaluate the suitability of a coal for specific purposes. Some of these user specific properties are: the ash fusion temperature (AFT) test, the Hardgrove grindability index (HGI), the swelling index (SI), etc..

2.3 Coal in South Africa

2.3.1 Characteristics of South African coals

2.3.1.1 petrography

As a result of the differences in the vegetation and climatic conditions between the Northern and Southern Hemispheres at the time of coal deposition and formation, the coals formed in South Africa differ from those of Europe and America. In addition South African coals tend to be chemically rather than physically changed. This is the result of their shallow burial depth, and hence a lack of pressure effects, and because of temperature effects caused by widespread igneous intrusions.

Northern Hemisphere, or Laurasian, coals are rich in vitrinite, which is highly reactive, while those of the Southern Hemisphere, also known as Gondwana coals, contain mainly inertinite, which except for semi-fusinite and macrinite, is largely unreactive. Exinite is present in small quantities. Table 2.2 below summarises the relative proportions of the various macerals in South African, German and U.S.A coals.

Table 2.2: Average maceral proportions (% by volume) of the three principal coal regions of the world (after Falcon 1977)

		Location		
Macerals	Reactivity	Carboniferous Coals (Germany)	Permian (South Africa)	Tertiary Permian (U.S.A)
Vitrinite	reactive	70	40	82
Exinite	reactive	15	0	8
Inertinite	non to partially reactive	15	60	10
Syngenetic minerals	non-reactive	3	14	2

2.3.1.2 mineral associations

As South African coalfields were freshwater deposits, they contain mainly syngenetic minerals whereas those of the Northern Hemisphere contain mainly epigenetic minerals (see Table 2.2). The result is that the Northern Hemisphere coals as mined consist largely of clean coal and mineral matter as discrete particles. The particles will have very different densities on account of the difference in density between the coal macerals and the mineral matter in coal (Section 2.2.1). Particles of intermediate density, or middlings, consist of pieces of coal with gangue attached to them. On crushing, these "false middlings" break into separate coal and gangue particles, which can then be separated.

In Southern Hemisphere coals, the "false middlings" represent a small portion of the intermediate density material; the result is that crushing results in little liberation unless carried out to below 1 micron. South African coals contain a high proportion of "true middlings".

In South African coals, clays constitute about 70 % of the mineral impurities, and are below 1 micron in size (Falcon, 1978). The major minerals present are kaolinite, illite and chlorite. These clay minerals are present throughout the coal matrix, and are associated with all the maceral groups. This results in them being very difficult to liberate.

Quartz constitutes about 20 % (Sanders and Brookes, 1986) of the mineral impurities in South African coals, and is present as coarse wind or water deposited material (syngenetic), or as fine material deposited with the clay during coal formation (epigenetic).

South African coals are low in syngenetic carbonates (siderite, ankerite, dolomite and calcite) as a result of the high redox potential present during the time of coal formation.

Sulphide minerals are important as a result of the detrimental effect of sulphur on coke or boiler coal. However, South African coals are low in both syngenetic (pyrite) and epigenetic sulphides.

2.3.1.3 rank

The rank of South African coals increases from west to east. The coal of the Orange Free State and Karoo basin is of low rank. The Transvaal coals are higher in rank, and the coal in certain parts of Natal are very high rank coals.

2.3.2 South African coal reserves

South Africa possesses 2 % of the world coal reserves, about 166 000 Mt of *in situ* mineable coal (Alberts, 1987). However, about 75 % of this coal has an ash content of greater than 21.5 %, and the bulk of it is not economically washable (Falcon, 1977).

70 % of South Africa's coal occurs in the Transvaal, and the balance is found in the Orange Free State and Natal (Falcon, 1977). The coal found in the Orange Free State is low rank, high ash bituminous coal, used mainly in power stations. The Transvaal coals are medium rank bituminous coals with minor variations. Significant reserves of coking and blend coking coals occur in the Northern Transvaal. Natal coals are varied in type and rank, and include the only high rank coals and anthracites in the main Karoo basin.

The traditional mining region comprises the fields in the Eastern Transvaal (the Witbank-Middelburg region), the Northern Orange Free State and Northern Natal. The newer mining region consists of the Waterberg and Soutpansberg fields in the Northern Transvaal and the Springbok Flats in the Central Transvaal. The location of the major South African coalfields is shown in Figure 2.1 below. The location and estimated size of the reserves of the various types of coal is indicated in Table 2.3 below.

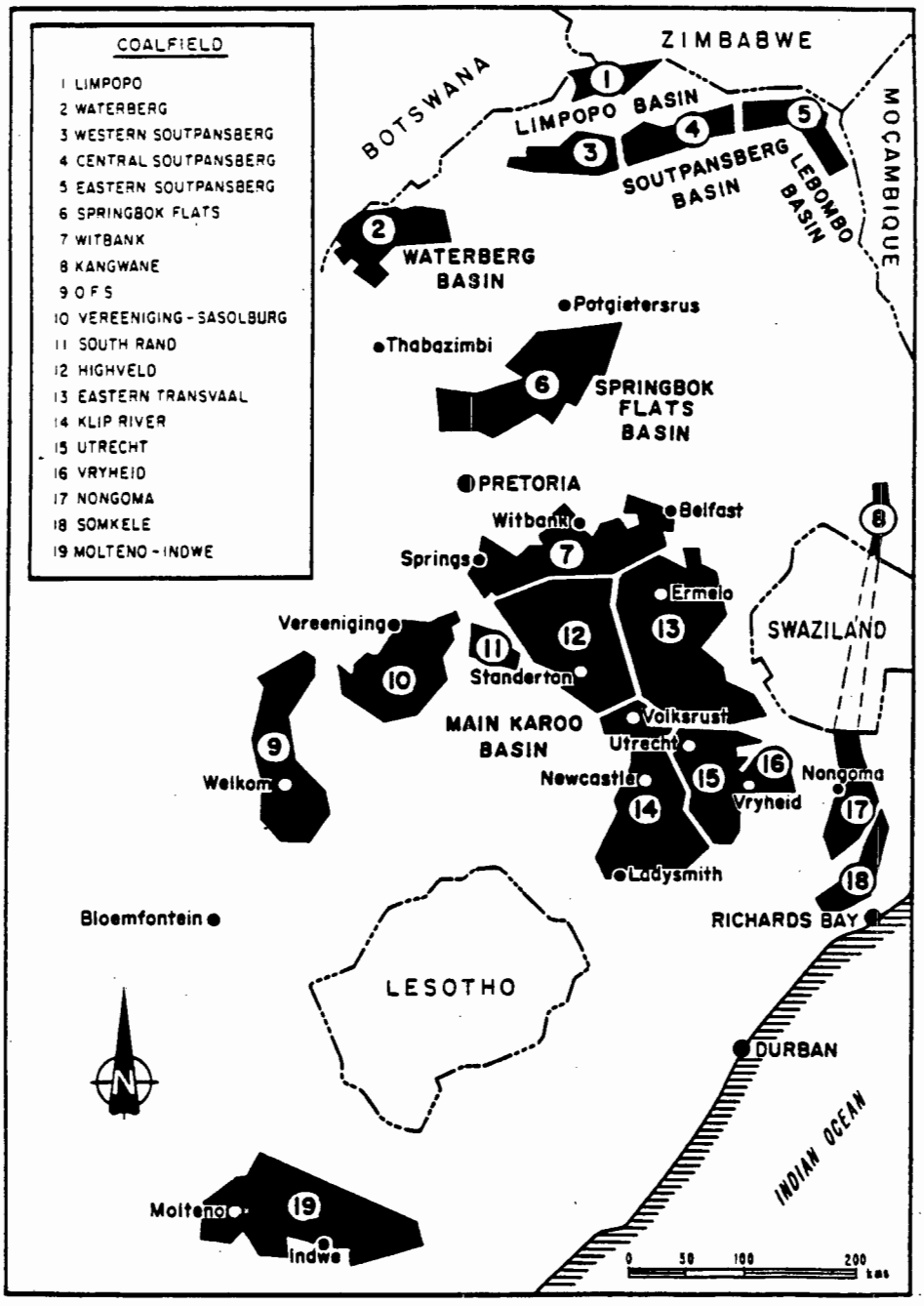

Figure 2.1: Location of the coalfields of South Africa (after Chamber of Mines, 1981)

Table 2.3: Location and amounts of South African coal reserves (in megatons) (Alberts, 1987:378; modified using data from Alberts [1987:385,386])

	Bituminous Coal		Metallurgical bituminous coal			Anthracite Coal					
						Anthracite			Lean Coal		
Coalfield	in situ mineable	Recoverable	Saleable * (high grade)	In situ mineable containing met. coal	Recoverable benefic.	in situ mineable	Recoverable	Recoverable benefic.	in situ mineable	Recoverable	Recoverable benefic.
Witbank	16241.17	12460.96	6455.28	1839.53	400.88	-	-	-	-	-	-
Highveld	16909.43	10979.03	1513.12	567.21	230.57	-	-	-	-	-	-
Southrand	3072.11	730.11	-	-	-	-	-	-	-	-	-
Springbok Flats $	3250.01	1700.01	1700.01	1050.01	150.01	-	-	-	-	-	-
Waterberg Upper @	56461.01	12760.01	3000.01	Substantial	Substantial	-	-	-	-	-	-
Lower	20276.01	15224.01	1883.01	-	-	-	-	-	-	-	-
Limpopo	256.01	202.01	107.01	256.01	107.01	-	-	-	-	-	-
Soutpansberg +	1450.01	-	267.01	1450.01	1267.01	-	-	-	-	-	-
Western Areas	-	-	-	-	-	-	-	-	-	-	-
Utrecht	749.54		316.43	202.01	102.01						
Klip River #	705.38	100.01	314.12	462.01	158.01	1082.27	711.65	475.65	395.36	266.02	141.62
Vryheid	86.57		55.58	86.01	39.01						
Eastern Transvaal	7052.83	4538.11	2450.66	29.81	16.14						
KwaZulu	-	-	-	-	-	256.75	172.83	98.68	-	-	-
Kangwane	-	-	-	-	-	467.01	227.51	147.11	-	-	-
Sasolburg-Vereniging	4757.11	2233.32	-	-	-	-	-	-	-	-	-
Orange Free State	-	-	-	-	-	-	-	-	-	-	-
Remainder	8876.01	4919.61	-	-	-	-	-	-	-	-	-
Old Springfield	-	-	-	-	-	-	-	-	-	-	-
Total	140143.2	65847.19	18062.24	5942.61	2470.65	1806.03	1111.99	721.44	395.36	266.02	141.62

* Included in recoverable

$ For the Springbok Flats, in situ beneficiated mineable product (a 50% factor) was calculated , 60% mining yield (extractability) assumed, and a total of 250 Mt mining loss (ie. geological loss) allowed for.

@ The amount of recoverable bituminous coal was estimated as being the average of the amounts given in assesments A and B by Alberts (1987:385)

\+ Excluding the Republic of Venda

\# The amount of recoverable bituminous coal is a total value for Utrecht, Vryheid and Klip River

The amounts given for the anthracite coal are total values for Utrecht, Vryheid, Klip River and the Eastern Transvaal

The Waterberg coal field is the major contributor to the total coal reserves of South Africa. It is 88 km in length (from east to west) and 40 km wide, and forms part of a larger coal field which extends into Botswana. The coal body consists of different zones, but the rank generally decreases from east to west. It contains 76 000 Mt of the 140 000 Mt of *in situ* mineable bituminous coal in South Africa (Alberts, 1987) and substantial amounts of metallurgical bituminous coal which can be recovered by beneficiation. However the ash content of the coal is high, averaging about 45 % (Botha, 1980). In addition the ash is relatively finely intergrown.

The Witbank coal field has been the centre of the coal mining industry since 1890 and still produces more than any other coal field. It has reserves of recoverable (by beneficiation) metallurgical bituminous and bituminous coal.

The best quality coking coals are found in Natal, formed locally by the thermal effect of dolerite intrusions on good quality bituminous coal. Part of this coalfield, to the south-east of Vryheid, is the only region in South Africa where anthracite and lean coal occur.

2.4 The Beneficiation of Fine Coal by Flotation

Beneficiation can be defined as the processing carried out on ROM coal to prepare it for the market. This processing can be divided into 5 levels, ranging from simply crushing the ROM coal to a particular topsize for use in power generation and oil from coal plants (Level 1) to re-crushing the coarse product with another stage of fines beneficiation (Level 5).

Coarse (+6.0 mm) and small (-15+0.5 mm) coal is generally beneficiated using gravity separation units. The coarse coal is treated in either dense medium baths or jigs, with the general trend in South Africa being towards baths. The small coal is generally treated in centrifugal units, e.g. cyclones and Dynawhirlpool washers.

In South Africa the -0.5 mm coal is considered to be fines. However, inefficiencies in the classification circuits can result in the topsize being in the region of 1 mm. Horsfall and Franzidis (1988) suggested that the fines be subdivided into fine coal (-0.5+0.1 mm) and ultrafine coal (-0.1 mm) fractions. Treating the fine and ultrafine coal separately has been found to achieve better results in both size fractions (Amcoal, 1987). It was further suggested (Horsfall and Franzidis, 1988) that the fine coal be beneficiated by gravity techniques (spirals, water and dense medium cyclones, jigs, separating tables and upward current washers) and the ultrafine coal be beneficiated using surface properties (froth flotation, oil agglomeration and selective flocculation).

As was mentioned in Section 1.1.1 above, spirals have been introduced into many coal washing plants in South Africa during the last decade, to treat the -0.5+0.1 mm fines. However much of the -0.1 mm ultrafines are still discarded. The traditional and most widely used method of beneficiating this size fraction is flotation.

In the flotation of coal the primary objective is the rejection of ash-forming minerals. A major problem is the heterogeneous nature of both the carbonaceous and inorganic material. The carbonaceous material is naturally hydrophobic and this hydrophobicity can be extended by the addition of oily collectors (e.g. fuel oil, kerosene, etc.). However the mineral surface reacts in a more complex manner, which depends on numerous factors, including the pH, cation concentration, etc.. The bubble size in coal flotation is controlled (and reduced) by the addition of frothers, usually alcohols (e.g. methylisobutylcarbinol (MIBC), tri-ethoxybutane (TEB), pine oil, etc.). These and other factors affecting coal flotation are discussed in detail in Section 2.5 below.

Coal flotation circuits are generally very simple - often consisting of only a rougher stage, or sometimes a rougher followed by a cleaner stage. In spite of the widespread use of flotation in mineral processing, the use of coal flotation is limited throughout the world. This has been attributed to the cost of the process versus the low value of coal (per ton) and the inability of flotation to produce high grades at very small particle sizes.

Coal flotation in South Africa is even more limited than internationally. This can be attributed to the problems described above and the fact that South African coals are more difficult to float than Northern Hemisphere coals, as a result of the different petrographic composition and mineral content and association (Section 2.3.1). In spite of the above, numerous workers have shown that the flotation of South African coals is possible in both column and conventional flotation cells. At present 6 collieries, one of which is a non-coking coal producer, have flotation plants. However, there are no flotation plants in the most commercially important coalfield, viz. the Witbank field.

2.5 Factors Affecting the Flotation of Coal

The flotation response of coal is related to its physical (size, shape, porosity, moisture content, electrical properties, maceral and mineral matter content), chemical (ash content, chemical structure, functional groups, oxidising ability) and surface (hydrophobicity, surface functional groups, zeta potential, point of zero charge [PZC] in solution) properties. These properties are inter-related and cannot be dealt with independently.

Sun (1968) and Aplan (1988) proposed the existence of different sites of varying hydrophobicity on the surface of coal particles. The different sites proposed by Aplan (1988) were:

i) strongly hydrophobic;
ii) weakly hydrophobic; and
iii) hydrophilic.

The number and ratio of these different sites on the surface of a coal particle depend on its rank, petrography, degree of oxidation, mineral content and size, as well as on the reagent addition and conditioning; hence, these factors determine the floatability of that particle. These factors, and their effect on coal floatability, are discussed in the sections which follow.

2.5.1 Coal rank

High rank coal which is low in volatiles is easier to float in terms of yield and reagent consumption than low rank coal which is high in volatiles. This trend reverses for anthracite which is more difficult to float than high volatile bituminous coal (Ye et al, 1989; Engel and Smitham, 1988; Ye and Miller, 1988; Horsfall, 1980, p203). The results obtained by Ye and Miller (1988), who carried out reagentless flotation of different rank coals in a Hallimond tube micro-flotation cell, are given in Figure 2.2 below.

The increasing floatability with increasing rank is apparent, as is the very sharp reversal in going from low volatile bituminous coal to anthracite. The rank of a coal influences its floatability in several ways as described below.

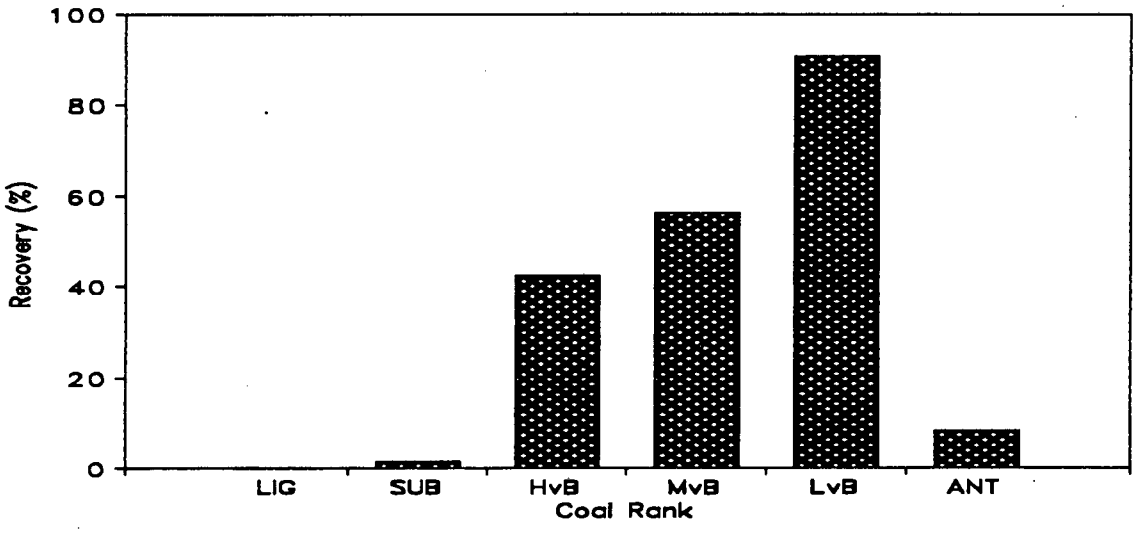

Figure 2.2: Maximum reagentless Hallimond-tube flotation recovery at pH 6.0 for coals of different rank (particle size 100x200 mesh) (after Ye and Miller, 1988)

2.5.1.1 hydrophobicity

As the coal rank increases, the aromatic lamellae grow in size and proportion, and their alignment becomes more perfect. As the aromaticity increases, the number of substituted functional groups decreases resulting in a decrease in the number of hydrophilic

sites. This results in an increase in the coal hydrophobicity (Tsai, 1982, p98).

The equilibrium hydrophobicity is measured by determining the contact angle of the coal. A high contact angle results from high hydrophobicity. Therefore, as the rank increases, so does the contact angle, except for the reversal which occurs with anthracite (Aplan, 1988; Ye end Miller, 1988). The above is clear from further results obtained by Ye and Miller (1988), plotted in Figure 2.3 below.

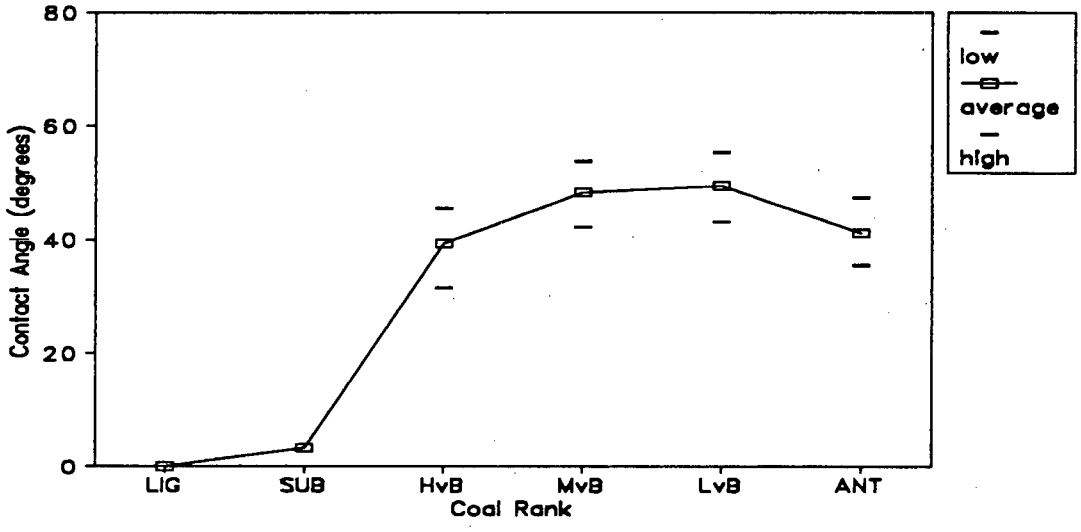

Figure 2.3: Measured contact angles at pH 6.0 for coals of different rank (particle size 100x200 mesh) (after Ye and Miller, 1988)

The contact angle has traditionally been used as an indication of the floatability of coal, but numerous researchers have found that contact angle measurements cannot describe the behaviour of coal particles whose flotation behaviour is pH dependent (Ye et al, 1989). For this reason Ye et al (1989) used induction time measurements to describe coal floatability, with the induction time consisting of the actual induction time (film rupture time) and the time taken for the liquid film to be displaced to such an extent that the aggregate was sufficiently strongly attached to resist

detachment caused by the movement of the aggregate (film displacement time#). The induction time defined in this manner would be expected to decrease with increasing coal floatability.

Ye et al (1989) showed that the induction time described above displayed a trend similar to that followed by the contact angle. In addition the induction times measured were able to describe the pH dependent behaviour of coal particles. The results obtained by Ye et al (1989) are plotted in Figure 2.4 below.

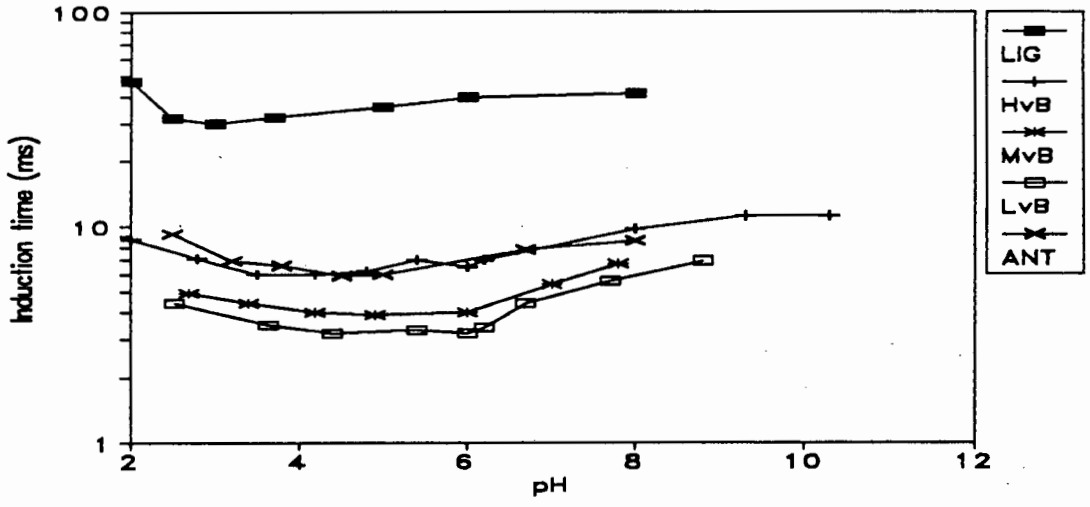

Figure 2.4: Measured induction times for coals of different rank (particle size 100x200 mesh) as a function of pH (after Ye et al, 1989)

From Figure 2.4 it is apparent that the induction times for the different rank coals pass through a minimum between a pH of 4 and 6. However the order of floatability by rank remains the same.

2.5.1.2 porosity

Coal porosity varies with rank. Low rank coals have an "open" structure and are highly porous: the pore sizes are in the macropore size range of 300 - 30 000 Å (Gan et al, 1972). Coking coals have a "liquid" structure, with a very low porosity. High rank coals have

It is this film displacement time which results in an increase in the measured induction time with an increase in the particle size.

an "anthracite" structure and are also highly porous. However, the pores are in the micropore range of 4 - 12 Å (Gan et al, 1972).

The macropores of low rank coals become filled with water (Tsai, 1982, p14; Aplan, 1988), and this results in an increase in the hydrophilic nature of the coal (Falcon, 1978). Voges (1991) postulated that the collector can be absorbed into the coal particle, thereby leaving the outside surface uncoated. This could explain the increase in the flotation recovery of certain low rank coals, obtained with a reduction in the conditioning time.

2.5.1.3 functional groups

The oxygen content of coal increases with decreasing rank. This oxygen is usually present in the form of carboxylic (COOH) or phenolic (OH) groups (Aplan, 1988; Campbell and Sun, 1970). These groups form polar covalent or ionic bonds in solution and their negative charge in water results in hydrophilic sites (Wen and Sun, 1977). This contributes to the low floatability of low rank coals.

2.5.1.4 pH, point-of-zero charge (PZC) and isoelectric point (IEP)

Numerous workers have used the PZC and IEP interchangeably. The IEP, defined by Park (1970) is, "The pH at which zero surface charge can be detected by electrokinetic means" and the PZC is, "The pH at which equal adsorption of H^+ and OH^- occur". However, "In the absence of any ionic or polar species and of any other sources of charge the PZC and the IEP are equal." (Wen and Sun, 1977). The PZC must be measured by direct measurement of adsorption densities.

Wen and Sun (1977) found that the hydroxyl and hydronium ions are potential determining for all coals examined except lignite. Ye et al (1989), Wen and Sun (1977) and numerous other workers found that coal flotation results were best at a pH where the zeta potential was zero (i.e. at the isoelectric point; IEP). Ye et al (1989) and Wen and Sun (1977) found that as the coal rank decreases the IEP moves to a lower pH. The results obtained by Ye et al (1989) are plotted in Figure 2.5 below.

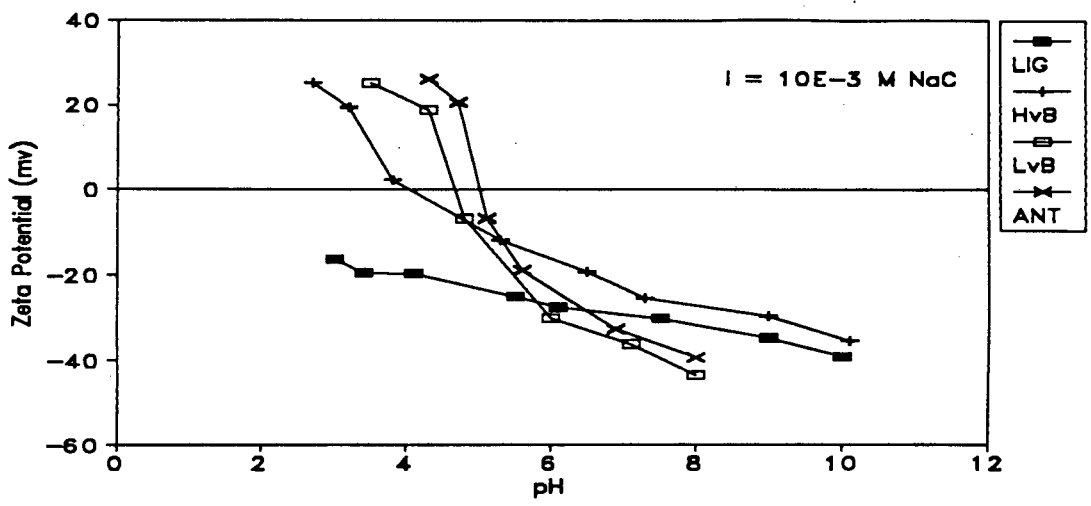

Figure 2.5: Measured zeta potentials for coals of different rank, as a function of pH (after Ye et al, 1989)

Comparison of Figures 2.4 and 2.5 indicates that the minimum induction time for a given coal occurs at the pH value corresponding to a zeta potential of zero for the coal (IEP). Therefore a superior flotation response should result if the flotation was carried out at the IEP of naturally hydrophobic material.

However Onlin and Aplan (1988) found that adding No. 2 fuel oil to various ranks of coal did not significantly alter the PZC although the flotation response was affected. Onlin and Aplan (1988) also found that nitrogenous cationic collectors raised the PZC of medium and high ranking coals, but did not affect the PZC of lower rank coals. It was concluded that, as the charge on the dispersed oil drops (collectors) is negative (MacKenzie, 1969; Mishra, 1987; Ng, 1982) an electrokinetic barrier to collector adsorption exists, especially for lower rank coals. This was substantiated by Collins and Jameson (1976, 1977), who found that the bubble and particle charges have a significant effect on the flotation response of small particles. They also found that the best results were obtained when the particles and bubbles were uncharged.

2.5.2 Petrographic analysis

Burdon (1962) found that the maceral content of flotation concentrates changes with time. This is because the flotation rates of the various macerals are different. In his work Burdon (1962) found that the flotation rate of vitrinite was greater than that of semi-fusinite. In addition to the above, Campbell and Sun (1970) found that the different anthracite lithotypes have different PZC's and could therefore be expected to exhibit different flotation rates.

2.5.3 Oxidation level

Numerous workers have shown that even very floatable coals are difficult to float when oxidised. Wen and Sun (1981) showed that adding a few percent of oxidised coal reduced overall floatability of a coal.

The oxidation of coal increases the number of oxygen groups on the coal particle's surface. These carboxyl and hydroxyl groups result in an increase in the number of hydrophilic sites on the coal surface. In addition, oxidation of the coal results in an increase in the amount of water soluble humic acids which serve to reduce the floatability of the coal (see Section 2.5.4 below).

The net effect of the above is a reduction in the equilibrium contact angle (Wen and Sun, 1977) and in the PZC moving to a lower pH, i.e. becoming more negative. In this way oxidation of the coal has the same effect as lowering the coal rank (Aplan, 1988). The results obtained by Wen and Sun (1977) are shown in Figure 2.6 below; the effect of oxidation can be clearly seen by comparison of Figures 2.5 and 2.6.

Gray et al (1976) found that the ease with which the coal macerals are oxidised decreases with increasing rank, and in the order vitrinite (most easily oxidised), exinite, inertinite (least easily oxidised).

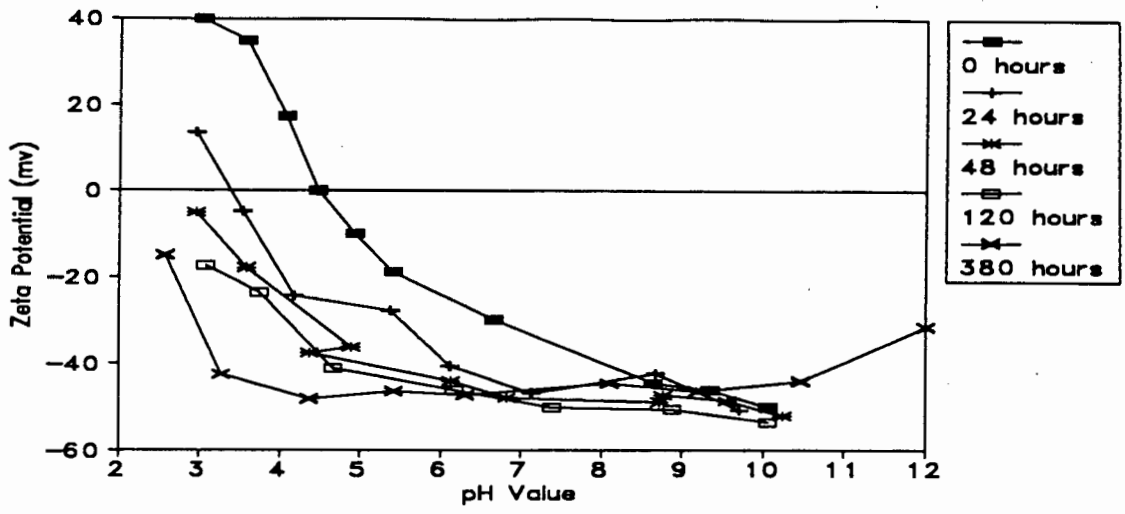

Figure 2.6: Effect of oxidation time on electrokinetic behaviour of HVA-bituminous vitrain at 125° C (Wen and Sun, 1977)

Wen and Sun (1977) found that cationic amines reduce the negative nature of the PZC of oxidised coals and can be used to increase the flotation recovery of oxidised coals. The above was substantiated by Nimerick and Scott (1980) who found that oxidised coals can be floated using cationic compounds (especially amines) as collectors or activators.

2.5.4 Mineral content

In conventional flotation the amount of fine mineral matter, especially clays, found in the froth product is directly proportional to water recovery in the concentrate (Trahar, 1981; Aplan, 1988). This phenomenon, known as entrainment, reduces the quality or grade of the product. This led to the development of flotation columns, which use froth washing to ensure a downward mass flow of water, which eliminates the entrainment of gangue in the concentrate (Breed and Inglis, 1989, p56).

The leaching of the mineral matter in coal, especially low rank coals, results in large quantities of humic acids in solution. Numerous workers, including Laskowski et al (1986) and Lai et al (1989), have found that humic acids in solution depress the flotation of coal. Lai et al (1989) found that, even at a concentration as low as 10 ppm,

humic acids led to a reduction in the coal floatability. Lai et al (1989) also found that the maximum adsorption of humic acids occurs at the pH where PZC=0 which resulted in the flotation recovery of coal being a minimum when carried out in the presence of humic acids.

In addition the hydrophilic nature of the mineral matter results in hydrophilic sites on the surface of the coal particles. This further depresses the floatability of coal with a high syngenetic mineral matter content.

2.5.5 Particle size

Numerous workers have found that, for any flotation system, the flotation rates of fine and coarse particles are low in comparison with those of intermediate sizes (Miller et al, 1985; Jameson et al, 1977; Mehrotra and Kapur, 1974; Trahar and Warren, 1976).

The reduced flotation rate of coarse particles can be attributed to the hydrodynamics of the flotation system and the particle hydrophobicity. Increasing the turbulence within a flotation system reduces the upper particle size limit to flotation as a result of the breakup of large particle/bubble aggregates. The upper particle size limit to flotation at a certain level of turbulence is also affected by the hydrophobicity (induced and natural) of the particles being floated, i.e. for large particles to float they must be very hydrophobic.

The low flotation rate of fines can be attributed to both the hydrodynamics within the flotation system and surface effects. The hydrodynamics result in a reduced collision efficiency of fine particles as a result of:

i) insufficient inertia to deviate from the fluid streamlines around the air bubbles, i.e. hydrodynamics of the system; and
ii) electrical repulsive forces between similarly charged particles and air bubbles.

In addition to the above Guy (1937) found that as the coal particle size decreases, the percent surface moisture increases. This results

in an increase in the proportion of hydrophilic surface sites, thereby reducing the hydrophobic nature of the coal, and making it less floatable.

The above led Bennet, Chapman and Dell (1958) to propose that each size fraction has its own flotation rate. This has since been substantiated by numerous workers including Reay and Ratcliff (1973) and Collins and Jameson (1976, 1977). In addition Ye and Miller (1988) and Ye et al (1989) found that as the particle size increases so does the induction time, irrespective of the coal rank, resulting in a reduction in the flotation rate. The results obtained by Ye et al (1989) are shown in Figure 2.7 below. It is of interest that the order of floatability by rank is not changed.

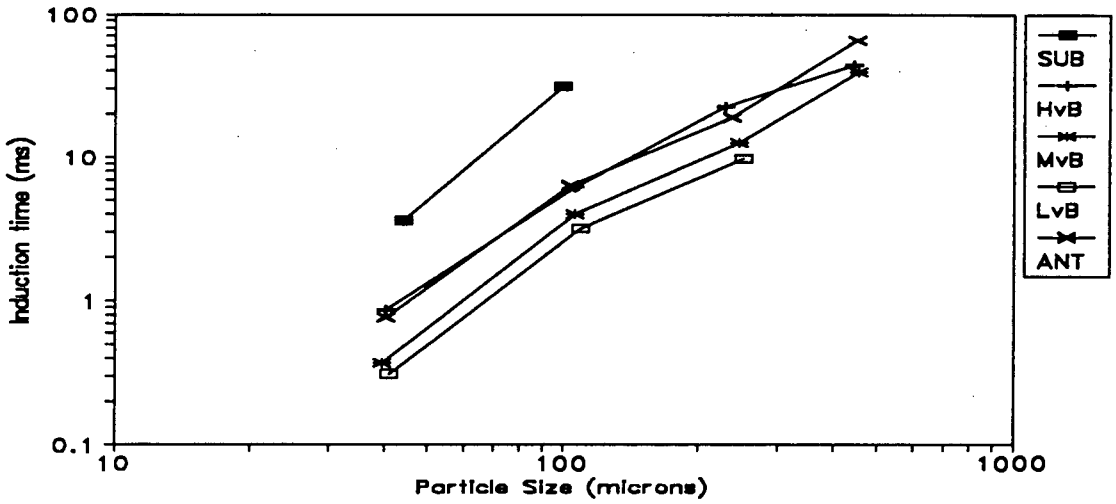

Figure 2.7: Effect of particle size on induction time of various rank coals (after Ye et al, 1989)

In addition to the reduced *rate* of flotation of fine particles, the presence of fines results in a reduction of the concentrate grade obtained. Engel and Smitham (1988) found that fine hydrophobic particles, especially high rank coals, stabilise the concentrate froth by preventing drainage of the liquid film. This results in an increase in entrainment and reduced concentrate grades.

Burdon (1962) also found that as the particle size decreased, so did the difference in the flotation rates for different macerals. In South

African coals most of the syngenetic clays are associated with the inertinite (Falcon, 1986) macerals. Therefore, a decreasing trend in the average particle size of a coal will be associated with a decreasing trend in the flotation selectivity.

The reduced hydrophobicity of fine particles described above, the fact that collector oils adsorb faster onto finer particles (Anderson, 1988, p207) and the increased surface area of fines per unit mass result in fine particles requiring more reagent than particles of an intermediate size. Increasing the collector dosage increases the recovery of fine particles, but the added availability of collector in the system results in the recovery of other "middlings" particles. This results in a further reduction in the concentrate grade.

The problems described above are compounded by the presence of clay slimes (d_p<20 micron). The colloidal nature of these slimes cause them to coat the coal particles. This reduces the hydrophobicity (contact angle) of the coal particles (Szczypa et al, 1973; Engel and Smitham, 1988) and results in a reduction in the flotation rate of the coal and an increase in the concentrate ash content.

2.5.6 Reagent addition

As coal is a low value product on a R/ton basis compared with other minerals, and because flotation is an expensive process, reagent costs in industrial coal flotation have thus far been minimised by the use of cheap reagents. To date there has been no economic incentive to develop selective collectors, depressants, activators or pH modifiers for coal flotation. In addition the ease with which overseas coals can be floated has resulted in little research into reagents for coal flotation, although Horsfall (1976) highlighted the need for selective collectors for South African coals more than a decade ago.

2.5.6.1 collectors

Collectors adsorb preferentially onto the valuable mineral, thereby imparting or increasing its hydrophobicity. Adsorption can be either chemical or physical. Chemisorption is a more selective

process. In coal flotation the collector physisorbs onto the hydrophobic sites on the coal particles while the gangue particles remain hydrophilic. This process has limited selectivity as coal particles contain both hydrophobic and hydrophilic sites. This results in the hydrophobicity of the coal being extended and not induced by the collector.

To date the collectors used in coal flotation have been the oily by-products of the chemical and petrochemical industries, such as paraffin, kerosene and diesel oil. The collector addition rate depends on the flotation conditions employed and the rank of the coal being floated, and can range from 0.5 kg/ton to over 50 kg/ton Aplan (1988). Anderson (1988, p207) found that aromatic collectors adsorbed onto an unwashed coal faster than aliphatic collectors, but that the aliphatics were more selective towards the carbonaceous material. Aromatic collectors also have a frothing ability, especially when high dosages are used.

2.5.6.2 frothers

Frothers facilitate the production of a stable froth which has the function of carrying the solids until the froth is removed from the flotation cell. Klaasen and Mokrousov (1963) found that the froth is also capable of enriching the solids, by selectively holding the valuable mineral while the tailings drain with the water from the interstitial lamellae. The frother does this by spreading at the air/water interface to form oil/water and oil/air interfaces (Anderson, 1988, p254). This reduces the cumulative interfacial tension, stabilising the air bubble. The addition of frother also produces bubbles with a uniform (reduced) bubble size.

Frothers are generally heteropolar compounds. Alcohol frothers have been found to be the most efficient for coal flotation.

2.5.7 Conditioning

In coal flotation plants the reagents are generally added to the coal slurry (either in the first cell or a conditioning vessel) and are

broken up into droplets at the impeller. The oil droplets are then dispersed throughout the pulp by bulk turbulence. The above method of conditioning is adequate in most instances. However, Burkin and Bramley (1961) found that the method of reagent (especially the collector) addition and the conditioning step can be the determining factors in the flotation of coal, especially low rank coals, and Misra and Anazia (1987) found that the method of collector dispersion affected the flotation of fine coal.

The poorer flotation of low rank coals mentioned above can be attributed to:

i) the repulsive forces arising from the electrical double-layer, between the negatively charged oil droplets and coal particles;

ii) the particle and bubble charges being of similar sign and magnitude (Collins and Jameson, 1977); and

ii) the flotation rate of -20 micron particles being proportional to the magnitude of the charges on the bubbles and particles (Collins and Jameson, 1977).

The above forces can be overcome by increasing the reagent dosage or the degree of agitation in the conditioning vessel and/or flotation cell (Burkin and Bramley, 1961). Von Holt (1992) carried out coal flotation experiments in a column and laboratory batch flotation cell at different collector dosages using different methods of collector dispersion and addition. Von Holt (1992, p123) found that the increased reagent dosage required in the flotation of low rank coals in the column cell (in comparison to that required in the batch cell) could be attributed to the limited degree of agitation in the column cell conditioning vessel. The power input per unit volume in the batch cell was in the region of 60 W/l while that in the column cell conditioning vessel was in the region of 3 W/l.

In addition the collector dispersion can be enhanced by mixing the oily collector and the frother prior to conditioning. Other methods of improving collector dispersion include predispersion in water using

water jets, aerosol sprays or venturi mixers. Misra and Anazia (1987) designed and tested a high intensity collector dispersion unit. In this unit the collector and air are fed to a mixing chamber and atomised oil droplets are formed. The collector aerosol, consisting of oil encapsulated air bubbles, is then fed to the flotation cell. Misra and Anazia found that this conditioning method enhanced dispersion, selectivity and flotation rate.

2.6 Chapter Summary

South African coals, like other Gondwanaland coals, were formed during the Permian period. As a result of the differences in the vegetation and climatic conditions in the Northern and Southern Hemispheres during the period of coal formation, the coals from the two regions differ both physically and chemically.

Northern Hemisphere coals are rich in vitrinite and exinite, while South African coals consist chiefly of inertinite. Northern Hemisphere coals are generally of a higher rank than South African coals. In addition South African coals contain chiefly syngenetic minerals (especially clays) whereas Northern Hemisphere coals contain chiefly epigenetic minerals. The high inertinite and syngenetic mineral contents of South African coals result in a large proportion of "true middlings" which cause difficulties in the production of a high grade product.

Until recently South African coal fines, except metallurgical coal fines, have been discarded or added (unbeneficiated) to the middlings product (in the case of two-product mines). However, modern trends are towards beneficiating the fine (-0.5+0.1 mm) coal by gravity methods and the ultrafine (-0.1 mm) coal by surface dependent processes. Of the surface dependent processes flotation seems to be the most economically feasible.

The flotation of coal is affected by a number of physical and chemical factors. These factors determine the relative proportion, and strength, of the hydrophobic and hydrophilic sites on the surface of the coal, which in turn determines the coal floatability. The factors referred to above

include the rank, petrographic composition, surface oxidation level, mineral content and particle size of the coal, as well as reagent addition and the type and degree of agitation in the conditioning step.

Coal floatability increases with increasing rank, except for anthracite which is more difficult to float than high volatile bituminous coal. As the rank of a coal increases so does the hydrophobicity, as measured by the contact angle and induction time (except for the reversal with anthracite). This can be attributed to the reduction in the number of hydrophilic sites caused by the reduction in the porosity (in the macropore range) and a reduction in the number of surface oxygen groups, with increasing coal rank.

In general South African coals are more difficult to float than Northern Hemisphere coals. This is a result of their low vitrinite and exinite contents (these are the most floatable macerals). In addition, the high syngenetic clay mineral content of South African coals results in an increase in the number of hydrophilic surface sites, soluble humic acids and slimes, all of which reduce the flotation rate and/or concentrate grade.

CHAPTER THREE

THE AIR-SPARGED HYDROCYCLONE - A NOVEL FLOTATION DEVICE

The air-sparged hydrocyclone (ASH) differs from other flotation devices in both appearance and mode of operation. This results in the hydrodynamics within the ASH being completely different to those in other flotation devices. This in turn results in the ASH having numerous advantages over other methods of flotation, and its performance being governed by different parameters.

The aim of this Chapter is to describe the ASH, and its operation, and to discuss the possible advantages it may have in the processing of "ultrafine" coal. A further objective is to review the design and operating parameters of the ASH, and their effect on the performance of the ASH, with a view to developing the experimental programme to be described in the Chapters which follow.

The Chapter begins with a description of the physical appearance of the ASH and how it operates. This is followed by a more detailed description of the fluid-flow within the ASH and the alleged advantages and disadvantages which result from the hydrodynamics. The effect of the design and operating parameters on the performance of the ASH, as found by previous researchers, are then described and discussed. Finally a review of the work done, and results achieved by previous researchers, using the ASH for the flotation of coal is given.

3.1 Physical Description of the Air-Sparged Hydrocyclone

The air-sparged hydrocyclone (ASH) was designed during the early 1980's by Professor J.D. Miller at the University of Utah. It is a novel flotation device combining elements of flotation and cyclone separation. The optimal configuration was found to be a vertically orientated cyclone with a tangential feed at the top (Miller and Van Camp, 1982). This configuration provides forced vortex flow within the cyclone thereby ensuring that the tangential velocity component is not a maximum near the cyclone axis. This favours the formation of a quiescent froth phase at the centre of the cyclone (Miller and Van Camp, 1982).

The ASH consists of two concentric right vertical cylinders#. The inner cylinder is a porous tube made of either high density polyethylene, stainless steel (Miller and Van Camp, 1981), ceramic (Burger, 1986; Cloete, 1987; van Deventer et al, 1988; Nieuwoudt et al, 1990), or sintered bronze (Nieuwoudt et al, 1990). The mean pore size diameter ranges from 1 to 120 micron (Baker et al, 1987). The outer cylinder serves as a non-porous jacket to ensure equal distribution of the air through the porous cylinder. The outer jacket is generally made of metal or PVC.

To date most ASH work has been carried out using cyclones with an internal diameter in the region of 5 cm. However, work has been done with diameters up to 15 cm. ASH lengths between 15.24 and 67.5 cm, corresponding to length to diameter ratios (L_c/d_c) from 2.71 to 11.4, have been investigated. A review of the available literature led Baker et al (1987) to conclude that an L_c/d_c ratio of 10 was optimal.

Slurry is fed tangentially via a conventional cyclone header at the top of the porous cylinder. The froth overflow is withdrawn by a central vortex-finder. Like the outer jacket the cyclone header and vortex-finder are generally made of metal or PVC. The base of the froth phase is supported and stabilised by a circular froth pedestal located on the cyclone axis.

A diagrammatic representation of the ASH is given in Figure 1.1 in Chapter 1

This pedestal has been constructed of a number of materials such as brass, stainless steel, polyethylene, PVC, etc. The slurry underflow is withdrawn through an annular opening between the froth pedestal and the porous cylinder wall. The pedestal diameters generally used have resulted in the width of the annular opening being between 6 and 15 % of the porous cylinder radius. The vortex-finder diameters have been chosen in such a way that the ratio of the overflow (A_{of}) to underflow (A_{uf}) area, A^*, has ranged between 0.5 and 5.

Burger (1986, p28) found that controlling the underflow rate by means of the width of the annular opening between the froth pedestal and the porous cylinder resulted in blockages by extraneous large particles, such as wood chips. This led to a larger annular opening being used, and the underflow rate being controlled by means of an orifice plate held in position below the annular opening by the spigot (Van Deventer et al, 1988).

A further development by Nieuwoudt et al (1990) was a spigot in which the underflow rate was controlled by means of a horizontal baffle placed above a flow limiting orifice; no pedestal was employed. This underflow configuration was made of PVC. To date very little work has been carried out using the orifice/baffle underflow configuration, hence the review which follows refers to work carried out using the pedestal/annular opening underflow configuration unless otherwise stated. Diagrammatic representations of the underflow configurations with and without a pedestal are shown in Figures 4.4 and 4.5 in Chapter 4.

3.2 Operation of the Air-Sparged Hydrocyclone

The slurry is fed tangentially via the cyclone header into the porous cylinder of the ASH. It develops a swirl flow in the radial direction, against the wall of the cylinder, as it travels axially down the cyclone. Everything within the cyclone is in swirl-flow, but the term "swirl-layer" is used to describe the slurry layer against the wall of the porous cylinder. The thickness of this slurry layer is known as the swirl-layer thickness. For a 5 cm diameter cyclone the slurry rates tested have

ranged between 15 and 130 lpm, at pulp densities ranging from 10 to 45 % solids.

Air, at feed rates of 50 to 500 slpm for a 5 cm ASH, is sparged through the walls of the porous cylinder. The high centrifugal forces at the wall cause the air to be sheared into innumerable small bubbles by the swirl-layer. The hydrophobic particles in the slurry collide with and become attached to these freshly formed air bubbles. After bubble/particle attachment, the tangential velocity of the aggregate is significantly reduced and it is transported radially into the froth phase as indicated in Figure 3.1 below.

The froth phase forms on the axis of the cyclone and is stabilised and constrained by the froth pedestal. The mechanism of froth "support" in the orifice/baffle configuration has yet to be defined. However, the results obtained by Nieuwoudt et al (1990) suggest that the transport of the froth to the overflow is also facilitated in an ASH with a orifice/baffle configuration. It may be that the baffle and the centrally located orifice cause sufficient "blocking" at the base of the ASH to support the froth on the cyclone axis. This froth phase moves axially upwards, countercurrent to the slurry phase. At the vortex-finder the froth is withdrawn as an overflow product. The hydrophilic particles remain in the swirl-layer and are discharged through the annular opening at the base of the cyclone.

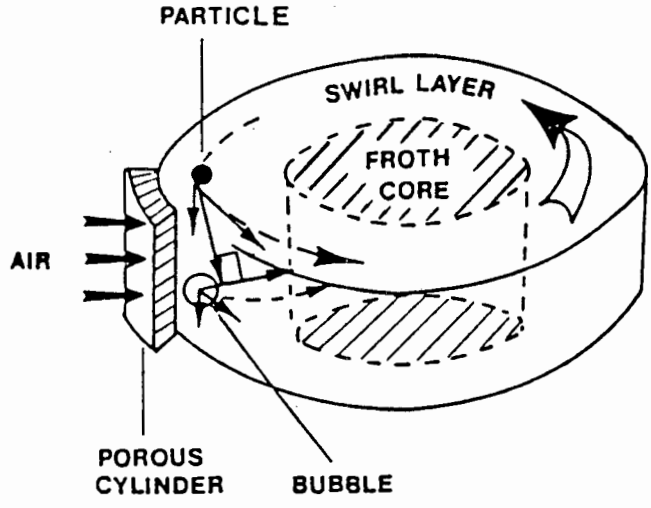

Figure 3.1: Schematic drawing of the particle and bubble motion in the ASH (after Ye et al, 1988).

The turbulence, the directed particle/bubble motion caused by the orthogonal (perpendicular) flow of the slurry and gas phases, and the small bubble sizes result in intimate contact between the air and the solid particles. Centrifugal forces increase the inertia of the particles, thereby increasing the collision efficiency of the fine particles. In addition the forces generated result in a pronounced separation between the slurry and froth phases.

While the ASH is in operation, the region closest to the walls consists chiefly of water and the region nearest the centre consists chiefly of air. The solid particles in the feed distribute across the cyclone diameter according to their density, size, shape and interaction with air. Large hydrophilic particles are forced to the cyclone walls while smaller hydrophilic particles are distributed throughout the water. The distribution of the hydrophobic particles depends on the mass of the particle/bubble aggregates.

A schematic drawing showing the simplified flotation pattern in the ASH is given in Figure 3.2 below.

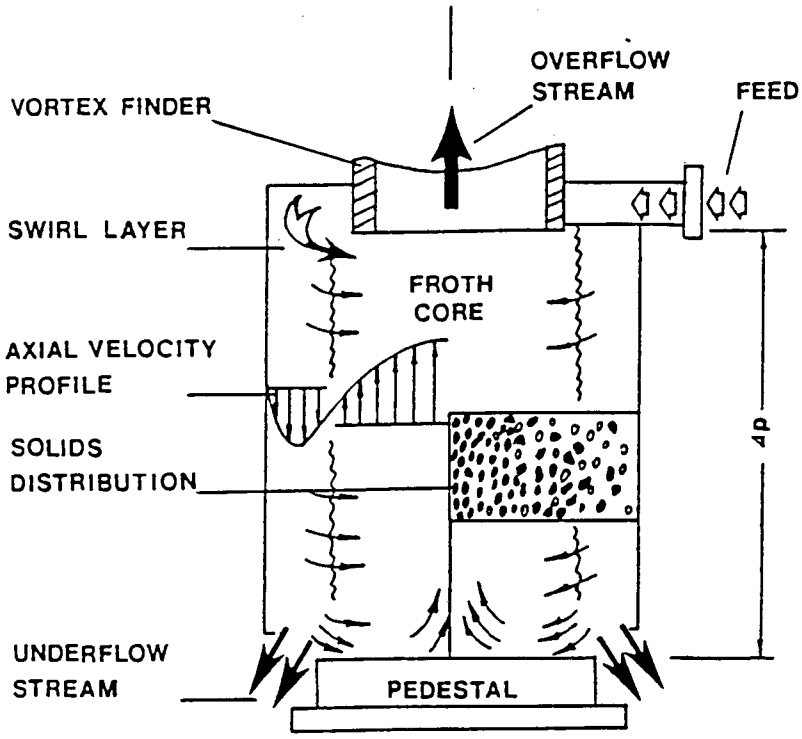

Figure 3.2: Schematic drawing showing the simplified flotation pattern in the ASH (after Ye et al, 1988).

3.3 Fluid-Flow in the Air-Sparged Hydrocyclone

Observations using a specially designed Plexiglass ASH (Van Camp, 1981), and confirmed by X-Ray computed tomography (CT) (Ye and Miller, 1988), have identified 3 distinct fluid regions within the ASH, viz. a swirl-layer, a froth phase and a transition region. These regions are described and discussed below.

3.3.1 The swirl-layer

The "swirl-layer" is defined as that part of the slurry that has a net axial velocity towards the annular opening at the base of the cyclone. The swirl-layer thickness in a (water only) right vertical non-porous cylinder is between 7.6 and 8.8 % of the cylinder (Miller and Kinneberg, 1984). In a right vertical porous cylinder (an ASH without a pedestal and in the absence of air) the swirl-layer thickness (water only) is about 8 to 12 % of the cyclone radius (Miller et al, 1985). This difference is caused by the roughness of the porous cylinder.

These values closely match the thickness of 10 % calculated by Taylor (1948) using inviscid theory for swirl-flow nozzles, and the thickness of 6 % calculated from continuity equations and a momentum balance (Miller et al, 1985). Taylor's equations differ from the experimental result because his equations do not consider the decay in the axial and tangential velocities down the length of the cyclone. Inaccuracies in Miller's method result from the equation for the kinematic viscosity being for pipe flow; hence it is only applicable at the entrance to the cyclone.

The average thickness of the swirl-layer (water only) increases slightly with an increase in the feed rate and cyclone length (Baker et al, 1987). This is because the absolute thickness of the swirl-layer increases in the direction of axial flow as a result of the decay in the tangential velocity, i.e. decay in the centrifugal forces.

The tangential and axial velocities of the slurry both decrease rapidly just below the inlet, and then increase again. Thereafter the

tangential velocity decays significantly with axial distance whereas the axial velocity only decays slightly. However, at any height in the cyclone the ratio of the tangential to axial velocities across the swirl-layer is constant and is independent of the slurry flow rate (Miller and Kinneberg, 1984). This is in agreement with inviscid theory and with the observed and measured results of Miller et al (1985).

As the radial velocity at the wall is zero and the swirl-layer thickness is small, the radial velocity across the swirl-layer is assumed to be zero (Miller et al, 1985).

If the annular underflow opening in an air-sparged hydrocyclone (in the absence of frother) is decreased in size from being greater than the swirl-layer thickness to being smaller than the swirl-layer thickness, the flow in the cyclone undergoes an abrupt transition from swirl to choked-flow. In this way decreasing the size of the annular opening increases the slurry hold-up volume. To date hold-up volume measurements have not been carried out using the orifice/baffle configuration. However, it would be expected that decreasing the orifice diameter would have the same effect as decreasing the width of the annular opening, but without exhibiting the same abrupt transition from swirl to choked flow. The latter would be the result of the ASH with a orifice/baffle configuration always operating under conditions of choked flow.

Hold-up volume measurements on an ASH have shown that the swirl-layer thickness in the two phase system is greater than that in the one phase system. The swirl-layer thickness in an ASH increases to between 11 and 14 % with an increase in the air rate, depending on the operating conditions (Baker et al, 1987). The thickness also increases slightly with an increase in frother addition. This increase in thickness can be attributed to the stabilisation of the fine air bubbles (increase in frother), or to the disturbance of the swirl flow by the air bubbles (increase in air rate). In addition, the transition from swirl to choked flow is not as abrupt when frother is added.

Hold-up volume measurements have also shown that in swirl-flow about 40 to 50 % of the ASH is occupied by water, and in choked-flow about 70 to 80 % of the ASH is occupied by water (Baker et al, 1987). The mean residence time of the water in the ASH also follows this trend. The mean residence time of the water in swirl-flow is about 0.5 seconds and in choked flow it is about 1.2 seconds (Baker et al, 1987).

In a three phase system the swirl-layer thickness is also affected by the pulp density of the slurry. This can be attributed to the increase in the viscosity of the slurry phase with an increase in its solids content (Miller et al, 1985).

3.3.2 The froth phase

The air sparged through the porous cylinder is sheared by the swirl-layer into innumerable small bubbles which form an annular froth phase on the axis of the porous cylinder. The centre of the porous cylinder is occupied by an air core (Miller and Van Camp, 1982; Gopalakrishnan et al, 1990). The high unit capacity of the ASH results in the froth phase being discharged from the ASH at a high velocity. This results in the froth characteristics in ASH flotation being more complex than in conventional flotation.

As the air bubbles penetrate the swirl-layer and enter the air core they have both axial and tangential velocity components. However, their motion can be simplified and considered to be orthogonal to the particle motion (Ye et al, 1988). In order to obtain an estimate of the bubble size Miller and Kinneberg (1984) assumed that, at high slurry velocities, detachment of the bubble from the capillary occurs when the centre of the bubble has been displaced a distance equal to the length of an arc with a chord whose length equals the sum of the radii of the bubble and the capillary. If the effect of surface tension is neglected, then when the bubbles are significantly larger than the capillary, the bubble size is independent of the capillary size and only dependent on the air and slurry rates.

The relations described above have not been tested for capillary sizes below 100 micron because of difficulties in measuring such small bubbles (Miller and Ye, 1989).

In an ASH the sizes of the bubbles are also affected by the following factors which cause the air rates through the pores to vary from pore to pore (Miller and Ye, 1989):

i) the distance of the pore from the roof of the cyclone; and
ii) the non-uniformity of pore sizes (a porous cylinder has a pore size distribution).

By using an ASH with Plexiglass windows it has been found that bubble coalescence does not occur and that the movement of individual bubbles follows Stoke's law (Miller et al, 1985). From these findings it can be assumed that the bubble sizes are similar to the pore sizes and that the bubble size distribution follows the pore size distribution (Miller and Ye, 1989).

For a multipore system the following assumptions can also be made (Miller et al, 1985):

i) the air flow rate through all the pores is the same;
ii) the resistance of the porous wall is so high that the bubbles are formed at a constant air rate;
iii) the air flow used is high enough for all pores to operate; and
iv) the number of bubbles formed is equal to the number of pores.

However, it may be that there is a limiting pore size or air rate below which the size of the bubble does not decrease any further. This lower bubble size limit may be determined by the boundary layer thickness and/or by the size of the turbulent eddies in the system (Miller et al, 1985).

The residence time of air bubbles in the ASH are generally no more than a few seconds. The residence time of an individual bubble depends on the axial level at which it is formed (Miller et al, 1985). However, the residence time of a bubble swarm is longer by a factor of

$(1-C_{vb})^{-4.6}$, where C_{vb} is the volumetric fraction of the bubble phase (Miller et al, 1985). For this reason the capacity of the ASH is limited by the bubble residence time.

Miller et al (1985) found that the air split to the overflow is independent of the water feed rate. This was for water feed rates of between 50 and 100 lpm, frother concentrations of between 20 and 80 ppm, and an ASH with a diameter of 5 cm. Approximately 85 % of the air fed to the system left the cyclone via the cyclone overflow. However, the dependence of the air split on the air rate has not yet been completely established. At NTP the overflow product contains between 50 and 80 % air by volume (Miller et al, 1985).

The addition of frother controls the diameter of the froth phase. When the froth core is small the axis of the froth core has a small amount of circular drift, which results in the transport of slurry to the overflow stream (Ye et al, 1988).

A pressure gradient exists between the froth pedestal and the vortex-finder outlet. This pressure gradient is the driving force for the axial transport of the froth phase (Ye et al, 1988). The ASH is usually operated under choked conditions, with the annular opening less than the swirl-layer thickness, to ensure that the required pressure gradient is obtained.

3.3.3 The transition region

A transition region exists between the swirl-layer and the froth annulus. The net axial velocity of the transition region is either zero or a low value in the same direction as the froth phase. A zero axial velocity exists when the froth core is large and hence the transition region is small. A low axial velocity towards the cyclone roof exists when the froth core is small and the transition region is large. In this case the ASH operates as if part of it were filled with water or slurry (Ye et al, 1988), as observed from hold-up volume measurements (Baker et al, 1987). For effective flotation the latter condition should be avoided.

3.4 Alleged Advantages of the Air-Sparged Hydrocyclone

The unique configuration of, and hydrodynamics within, an ASH are alleged to have a number of advantages. These advantages arise from the high slurry velocity, the formation of small air bubbles and the directed (perpendicular) particle/bubble motion. The alleged advantages are the extension of the lower limit of fine particle flotation, the production of very small bubbles, the increased flotation rate, the increased capacity/unit volume, the possibility of concentrate dewatering being unnecessary and the possibility of an ASH circuit being cheaper than a conventional circuit. These alleged advantages are discussed below.

3.4.1 Fine particles

Numerous workers, including Dobby and Finch (1987), Mehrotra and Kapur (1974), Flint and Howarth (1971), Trahar (1981) and Gaudin et al (1931) have shown that the flotation recovery of fine and coarse particles is less than that of intermediate sizes in conventional sub-aeration flotation cells. However, in any flotation system, the upper and lower particle size limits are determined by the collision efficiency of particles with air bubbles and can be considered to be a function of the bubble/fluid/particle system (Flint and Howarth, 1971). In general the optimum particle size is in the region of 30 micron, and the lower limit to fine particle flotation is about 10 micron.

In conventional flotation cells, the random motion of the particles and air bubbles results in a low probability of collision. In addition the -20 micron particles have insufficient inertia to deviate from the fluid streamlines around the air bubble in order to contact with the air bubble (Miller et al, 1985; Trahar and Warren, 1976; Evans, 1954). This results in the reduced flotation rate of these particles.

In addition to the low collision efficiency of these fine particles, their long contact time caused by the low particle velocity over the bubble surface (Dobby and Finch, 1987) and their shorter induction time (Ye and Miller, 1988), compared with that of larger particles, result in poor selectivity in the ultrafine sizes.

The ASH was designed to accomplish the fast flotation of fine particles by subjecting them to a centrifugal field which imparts sufficient inertia to them for collision to occur. The increased inertia of these fine particles, and the high density of freshly formed small bubbles moving orthogonally to the particles, increases the collision efficiency of the bubbles and particles (Miller et al, 1985; Nonaka and Uchio, 1984).

Furthermore, the turbulent conditions caused by the air passing through the swirl-layer result in intimate contact between the gaseous and solid phases. The conditions of high collision efficiency and intimate contact result in the increased recovery and grade of fine particles. In this way flotation in a centrifugal field extends the fine particle flotation limit to particles as small as 1 micron (Miller et al, 1986).

In the flotation of gold from Colorado river sand, in which the highest grade was in the -400 mesh fraction, Miller et al (1986) found that the ASH was more efficient than a conventional cell for the flotation of the finer particles. The ASH recovered 81 % of the gold while the conventional cell recovered only 56 % of the gold. Miller and Van Camp (1982) (coal) and Misra et al (1983) (oil shale) also achieved better separations, in the finer size fractions, in the ASH than in the batch cell. However, Van Deventer et al (1988) achieved similar pyrite recoveries in the -20 micron fraction using an ASH and a conventional cell, and Cloete et al (1990) found the batch cell to be more efficient than the ASH when floating fine pyrite.

3.4.2 Bubble size

In conventional flotation the air bubbles are approximately 1 mm in diameter. Miller and Kinneberg (1984) derived an expression which predicts that the diameter of the bubbles formed in an ASH are approximately equal to the diameter of the pores in the porous cylinder, when the cyclone radius is very much larger than the pore and bubble radii. However, experimental difficulties in accurately measuring the size of small bubbles have prevented experimental verification below 600 micron.

Small air bubbles are alleged to be more effective in the flotation of very finely ground particles (Miller, 1984; Jameson et al, 1977; Trahar and Warren, 1976; Nonaka and Uchio, 1984; Reay and Ratcliff, 1973). However, Szatkowski and Freyberger (1985) found that a critical bubble size, d_b^{cr}, exists, below which the bubble buoyancy is counteracted by the mass of solids attached to it, resulting in the bubble being unable to report to the froth. This confirms results obtained by Flint and Howarth (1971) and Dobby and Finch (1987), who found that an optimum bubble size existed for a particular flotation system. This led to Szatkowski and Freyberger (1985) postulating that smaller bubbles may improve certain aspects, but not necessarily the overall rate, of flotation. Furthermore, Dobby and Finch (1987) found that small bubbles increase the flotation rate of fine particles, but do not improve the selectivity of their flotation.

In addition the air flow rate and dispersion in conventional cells may limit flotation rates (Miller and Kinneberg, 1984). This fact is also indicated by the results of Flint and Howarth (1971), who found that the collision efficiency of particles and bubbles increased as the number of bubbles increased.

3.4.3 Flotation rate

In most flotation models, the flotation rate is considered to be a function of the particle and air bubble sizes, and their relative motion (Flint and Howarth, 1971; Jameson et al, 1977; Dobby and Finch, 1987, Szatkowski and Freyberger, 1985). Further analysis shows that the flotation rate constant is proportional to the magnitude of the force field that exists in the flotation machine (Van Camp and Miller, 1982; Nonaka and Uchio, 1984). Therefore, the flotation rate in an ASH, where the force fields may be as high as 100 g, will be much higher than those in conventional flotation cells, where the force fields are seldom higher than 5 g (Miller et al, 1986).

3.4.4 Residence time

Conventional flotation cells have a solids residence time of at least 2 minutes per cell. In contrast, the residence time in the ASH is between 0.5 and 1 second (Baker et al, 1987).

This results in the ASH having a capacity of 3 500 tonnes/day.m^3 of cell volume (Miller et al, 1988), which is up to 100 times greater (Stoessner, 1989) than the capacity of 35 to 70 tonnes/day.m^3 (Miller and Ye, 1989) of conventional froth flotation cells. The large capacity of the ASH means that little floor space is required; this favours its use where land is either expensive, or where the retrofitting of a plant is being carried out.

3.4.5 Concentrate dewatering

The slurry product from the flotation of coal in an ASH looks, burns and can be pumped like heavy oil. If the coal is to be used for the generation of thermal energy the drying stage can be eliminated. This also prevents coal dust pollution.

3.4.6 Economic considerations

As in the conventional hydrocyclone, the inlet slurry rate of the ASH, and hence the capacity, is related to the square root of the pressure drop. In both cases the recovery of water to the overflow has the same linear relationship to the feed water rate (Miller and Kinneberg, 1984). However, the dependence of the capacity of the ASH on the particle size distribution and density of the feed have not yet been established.

At present there are no scale-up relations for the ASH. However, the following have resulted in the ASH being assumed to act as a conventional cyclone:

i) the equations relating the capacity and pressure drop are similar;
ii) the classification curves are similar; and

iii) the influence of the flow rate on the cut-size is similar (Miller and Kinneberg, 1984).

If the cut-size is used as the scale-up criterion, then the volumetric flow rate is proportional to the cyclone diameter. Therefore, if the cyclone cut size is to remain constant, the pressure drop across the cyclone must be increased as the diameter is increased. This would result in the size of the cyclone being limited by pressure constraints.

Miller and Kinneberg (1984) compared the installed cost and energy consumption of an ASH circuit and a conventional flotation circuit for the flotation of low grade copper porphyry ore. The calculations excluded the cost of buildings and other indirect costs. A complete economic analysis was not carried out as at present there is no data involving maintenance costs of the porous cylinders. The calculations were carried out using 3 different sets of ASH operating conditions, obtained from experimental data using an ASH with a diameter of 5 cm. The results obtained showed that the ASH circuit gave the following savings:

i) capital cost savings of 18-35 %; and
ii) power savings of 3-30 %.

3.4.7 Summary of advantages

The advantages offered by the ASH can be summarised as follows:

i) it extends the lower limit of fine particle flotation, down to a diameter of 1 micron without loss of selectivity;
ii) the increased number and small size of the air bubbles increases the bubble/particle collision efficiency;
iii) the flotation rate is greater than in conventional cells;
iv) it has a large volumetric capacity which results in less floor space being required;
v) in certain cases dewatering of the concentrate may not be necessary; and

vi) an ASH circuit may be much cheaper than a conventional flotation circuit in capital and operating costs.

3.5 Disadvantages of the ASH

The turbulence inside the ASH results in the alleged advantages of the ASH being accompanied by certain disadvantages. These alleged disadvantages are discussed below.

3.5.1 Coarse particles

The recovery of coarse particles in the ASH is reduced in comparison with conventional flotation cells (Miller and Kinneberg, 1984). This is a result of the classification effect of the ASH and because the larger particle/bubble aggregates are often broken up by the turbulence inside the ASH.

In the flotation of a coarse Witwatersrand pyrite ore, viz. -300 micron, Cloete et al (1987) found that the recovery of +100 micron particles was lower in the ASH than in a conventional cell.

3.5.2 Reagent consumption

The need for a stable froth phase and very hydrophobic particles in the ASH often requires frother and collector dosages which are greater than those required in conventional flotation.

In the flotation of pyrite ore, Cloete et al (1987) found that to achieve similar recoveries the ASH required three times as much collector as a conventional cell.

3.6 ASH Design Parameters

In this section the effect of the design parameters on the performance of the ASH (as found by previous researchers) are reviewed and discussed.

3.6.1 Cyclone length/diameter ratio (L_c/d_c)

Increasing the ASH length at a constant cyclone diameter increases both the coarse and fine particle recoveries. This is because the swirl-layer velocity decreases down the length of the cyclone resulting in a region of reduced turbulence (Miller et al, 1985) as well as a longer residence time (Miller and Van Camp, 1982). Miller et al (1985) found that the size of larger eddies in the region of reduced turbulence at the base of the cyclone increases with increasing cyclone length. These eddies are able to carry larger particles to the cyclone axis, increasing the overall yield.

The above is confirmed in the results of Kinneberg and Miller (1983) who found that increasing the L_c/d_c from 10 to 15 increased the recovery of copper porphyry ore in the +400 mesh fraction, but did not affect the recovery of the -400 mesh fraction. Miller and Van Camp (1982) found that increasing the L_c/d_c from 2.7 to 4.8 resulted in an increase in yield and grade when floating a coal sample. Stoessner et al (1990) found that increasing the L_c/d_c ratio above 10 had a negligible effect on the yield, but decreased the grade. Nieuwoudt et al (1990) found that increasing the L_c/d_c ratio from 5.2, through 6.58, to 10.87 resulted in a significant improvement in the performance of the ASH for a pyritic ore, but that the recovery trend was less marked for a finer ore, although similar grades were obtained.

An increase in the cyclone diameter at a constant cyclone length results in a decrease in the centrifugal forces. This results in an increase in the upper size limit to flotation. Nieuwoudt et al (1990) postulated that the flotation effect in smaller diameter cyclones was inhibited, with the result that they acted primarily as splitters.

3.6.2 Underflow configuration

Most researchers investigating flotation in the ASH have not examined different types of underflow configurations, but have only used the pedestal and annular opening. Exceptions to the above are Van Deventer et al (1988) and Nieuwoudt et al (1990). Van Deventer et al found that blockage of the annular opening by woodchips was a problem in the flotation of a pyrite ore. The problem was solved by using a smaller diameter pedestal and controlling the underflow rate by means of an orifice mounted below the annular opening. Van Deventer et al found that this underflow configuration produced similar results, in terms of recoveries and grades, to those obtained using a pedestal and an annular opening.

Nieuwoudt et al (1990) used a spigot in which the underflow rate was controlled by means of a horizontal baffle placed 30 mm above a flow limiting orifice. The baffle was found to be necessary to decelerate the swirl-layer and thus enable the slurry to migrate to the axis of the cyclone and exit the base of the ASH. Nieuwoudt et al (1990) found that this configuration yielded better results than those obtained using the configuration used by Van Deventer et al (1988).

3.6.3 $A_{overflow}/A_{underflow}$ ratio (A*)

When the underflow rate is limited by the width of the annular opening, the width of the opening is critical to the operation of the ASH (Miller and Van Camp, 1982; Miller and Kinneberg, 1984; Miller et al, 1985; Miller et al, 1986; Baker et al, 1987; Miller et al, 1988; Ye et al, 1988). If the width of the annular opening is greater than the swirl-layer thickness then the froth phase will be discharged to the underflow and no concentrate will be obtained. Decreasing the width of the annular opening increases the water split to the overflow. This leads to an increase in the concentrate coal recovery but reduces the concentrate grade as a result of the entrainment of hydrophilic gangue as found by Gopalakrishnan et al (1990) and Miller and Ye (1989).

In contrast to the above workers, Stoessner et al (1990) found that increasing the underflow opening resulted in a negligible effect on the

recovery although it resulted in a strong improvement in coal concentrate grade. Miller and Kinneberg (1984), Miller et al (1985), Miller et al (1986) and Burger (1986) have reported the optimum annular opening to be in the region of 10 % of the cylinder radius. As the swirl-layer thickness in an ASH is in the region of 11 to 14 % this means that the ASH operates optimally under semi-choked conditions, with about 50% of the cyclone filled with slurry (Baker et al, 1987).

Ye et al (1988) proposed that the concentrate grade and solids concentration by mass are greatest at the centre of the froth core. Therefore the concentrate recovery and grade could be altered by changing the diameter of the vortex-finder and thereby varying the size of the froth core that is withdrawn. The above is confirmed by results obtained by Miller et al (1988) who found that decreasing the vortex-finder diameter resulted in an increase in the coal grade and a reduction in the coal recovery. Nieuwoudt et al (1990) found the above to be true at higher pyrite slurry rates. However, beyond a certain vortex-finder diameter and at low slurry feed rates, increasing the vortex-finder diameter resulted in a decrease in both the grade and recovery. Nieuwoudt et al (1990) attributed the above to the drop in the axial pressure gradient in the ASH having a more pronounced effect than the increase in the vortex-finder diameter. Stoessner et al (1990) also found that increasing the vortex-finder diameter resulted in a decrease in both the ash content and the recovery of coal. Unfortunately the above results were reported as a general trend; no slurry rates or vortex-finder diameters were reported.

In the region in which the ASH is generally operated (in coal flotation), its flotation performance is independent of the absolute values of the areas of the overflow and underflow openings, but dependent on the ratio (A^*) of these values (Miller et al, 1988; Gopalakrishnan et al, 1990). This is because both the overflow and underflow openings affect the axial pressure drop over the froth phase. The above is especially true for the water split, and hence the concentrate grade (Miller and Ye, 1989). This is supported by results obtained by Gopalakrishnan et al (1990) who found that at a constant A^* the water split, and hence the concentrate grade, was independent of the ratio of the air to slurry flow rates (Q^*).

Gopalakrishnan et al (1990) found that increasing A^* from 0.1 to 10, using a coal with a feed ash of 16 % and at a Q^*=4.7, resulted in the recovery increasing from 7 to 75 %, with a corresponding reduction in the grade from an ash content of 5 to 8 %. In addition, Gopalakrishnan et al (1990) found that increasing A^* above 1.0 yielded no appreciable increase in the recovery, but resulted in a reduction in the grade. The above led Baker (1991) to suggest that the optimum A^* was in the region of 1.

3.6.4 Vortex-finder length (L_{vf})

Burger (1986) found that the vortex-finder length did not have a significant effect on the flotation of pyrite in the ASH. In contrast Nieuwoudt et al (1990) found that increasing the vortex-finder length resulted in an increase in the recovery and a reduction in the grade (pyrite), until a certain vortex-finder length was reached, after which both the grade and recovery decreased.

The results obtained by Miller and Van Camp (1982) suggest that increasing the vortex-finder length should result in a reduction in the grade as a result of the grade being greatest at the top of the ASH. However, the recovery at short vortex-finder lengths is low as a result of the destabilisation of the froth phase by turbulence at the ASH inlet (Nieuwoudt et al, 1990). It therefore seems as though an optimum vortex-finder length exists, at an L_{vf}/d_c in the region of 1.0 (Nieuwoudt et al, 1990). Once the optimum vortex-finder length has been exceeded, the concentrate recovery decreases as a result of a reduction in the effective froth core length.

3.6.5 Inlet area

Few workers have investigated the effect of the inlet area on the performance of the ASH. However, Nieuwoudt et al (1990) found that the inlet area had little effect on the recovery of sulphur from a pyrite ore. They also found that the point of maximum sulphur grade shifted to higher feed rates with an increase in the slurry inlet area. The

latter can be attributed to the increase in the inlet area being counteracted by the increase in the slurry feed rate, to produce a similar inlet slurry rate per unit area, and hence similar centrifugal forces.

3.6.6 Cylinder porosity

Stoessner et al (1990) found that the pore size distribution of the porous inner cylinder of the ASH had no effect on the performance of the ASH in the flotation of coal. However, in the flotation of pyrite Nieuwoudt et al (1990) found that a smaller pore size distribution resulted in an increased recovery at a reduced grade. Nieuwoudt et al (1990) attributed the increased recovery to the production of smaller air bubbles, and the reduced grade to the associated increase in the water recovery.

3.7 ASH Operating Parameters

In this section the effect of the operating parameters on the performance of the ASH (as found by previous researchers) are reviewed and discussed.

3.7.1 Air rate/slurry rate (Q*)

Increasing the slurry feed rate, i.e. reducing Q^*, causes an increase in the centrifugal forces within the ASH. This results in a reduction in the concentrate recovery of coarse particles, caused by the breakup of large particle-bubble aggregates. This reduction in the coarse particle recovery can be partly counteracted by increasing the collector addition rate (Ye et al, 1988). However, increasing the slurry feed rate results in an increase in the recovery and grade of fine hydrophobic particles. The increased inertia imparted to the particles results in an increased hydrophobic particle collision efficiency, and an increased cleaning action on the misplaced hydrophilic particles.

Therefore, the optimum operating pressure (slurry feed rate) is one which balances the rupture of particle/bubble aggregates with the cleaning action on misplaced hydrophilic particles (Miller et al, 1985).

Initial work using the ASH was done using a Q^* in the region of 0.9. This ratio is similar to the Q^* used in column flotation. However, recent work has shown that the Q^* in the ASH can be as high as 10.0. Increasing the air rate, i.e. Q^*, has the following effect:

i) it increases the probability of collision and attachment;

ii) it increases the diameter of the froth core and stabilises the swirl motion of the slurry so that the flow is uniform throughout the cylinder - this reduces the slurry hold-up volume and the transition layer thickness to a minimum (Miller et al, 1988); and

iii) it increases the axial pressure gradient which ensures froth transport without the restriction of the slurry caused by a smaller annular opening (Ye et al, 1988).

Miller and Van Camp (1982) and Miller et al (1988) found that increasing Q^* increased the recovery without reducing the grade of the concentrate. Cloete et al (1988) found the above to be especially true when operating in the region of higher feed rates. In addition, Ye et al (1988) found that when the flotation performance is less dependent on A^*, the annular opening can be chosen to be the same width as the swirl-layer thickness and the vortex-finder diameter is chosen according to the required A^* ratio. The required recovery can then be obtained by increasing the air rate. The above can be attributed to the fact that about 85% of the air reports to the overflow, for most air rates (Miller et al, 1985; Miller and Kinneberg, 1984); the value decreases slightly with increasing slurry rate.

In contrast to the above, Stoessner et al (1990) and Gopalakrishnan et al (1990) found that increasing Q^* at a constant A^* increased both the recovery and the product ash content. Gopalakrishnan et al attributed the reduction in the grade to the increased water split to the overflow.

This increased water split results when the air rate is increased beyond a certain limit at a correspondingly low slurry pressure. A high air rate is also not effective if the froth is unstable or poorly mineralised (Ye et al, 1988). The former is clearly demonstrated by results obtained by Cloete et al (1987) who carried out experimental work in a 5 cm diameter by 50 cm long ASH which was operated in the absence of both solids and frother to determine the effect of the air rate and water pressure (feed rate) on the water split to the overflow. The results obtained are reproduced in Figure 3.3 below.

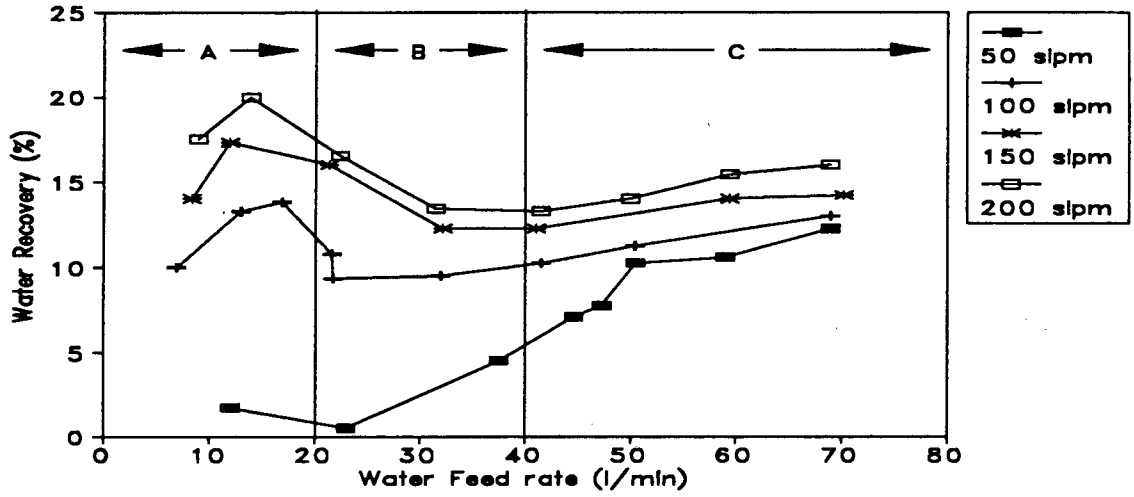

Figure 3.3: Recovery of water (at air rates of 50 to 200 slpm) to the overflow as a function of water flow rate (after Cloete et al, 1987)

From Figure 3.3 it can be seen that there are 3 distinct regions in which the ASH may be operated. Regions A and B are determined by the comparative strengths of the centrifugal forces (which depend on the water pressure) and the radial forces (which depend on the air rate), i.e. Q^*. Region C is determined by the physical limitations of the ASH, i.e. A^*. These 3 regions can be explained in the following way:

3.7.1.1 region A

In this region the radial forces dominate. Therefore, as the water rate is so low, increasing the water rate simply results in more water being available for transport to the overflow. This continues

until a maximum is reached, at which point the forces balance one another. A further increase in the water rate results in the centrifugal forces beginning to dominate and hence the water recovery decreases.

3.7.1.2 region B

In this region the centrifugal forces dominate. As the water rate is increased so the water recovery to the overflow decreases, until a minimum is reached. At this point the forces once again balance one another. From Figure 3.3 it can be seen that as the air rate is increased, so the point of minimum water recovery moves to a higher water rate. A further increase in the water rate results in the increased swirl-layer thickness limiting the flow of the water through the annular opening of the ASH.

3.7.1.3 region C

In this region increasing the water feed rate increases the water split to the overflow because of outlet restrictions.

The addition of frother to the system stabilises the froth and hence shifts the point of minimum water recovery to higher slurry flow rates, but does not affect air transport to the overflow.

The air flux through the porous cylinder has been investigated in different ways by various workers. Nieuwoudt et al (1990) and Van Deventer et al (1988) found that using inert sections at the base of the ASH increased both the pyrite grade and recovery when using a pedestal and annular opening. However, when using a baffle and a flow limiting orifice, poorer results were obtained when certain L_c/d_c ratios were chosen. In addition, Van Deventer et al (1988) found that the L_{vf} affected the ASH performance. In the work described above the volumetric air rate to the ASH was kept constant when the inert sections were used, hence increasing the air flux through the upper portion of the ASH. Stoessner et al (1990) found that having a region of increased air flux at the top of the ASH resulted in an increase in the clean coal recovery, but a reduction in the grade.

The above results can be attributed to both the tangential and axial velocities of the slurry passing through a local minimum below the slurry inlet as found by Miller et al (1985). Therefore increasing the air flux in this region results in an increase in the recovery and a corresponding reduction in the grade. It would also be expected that the vortex-finder length would affect the results obtained. Using inert sections at the base of the ASH would also effectively stabilise the swirl-layer in this region, facilitating its withdrawal via the annular opening, or inhibiting its withdrawal via a flow limiting orifice.

3.7.2 Pulp density

Kinneberg and Miller (1983) found that increasing the pulp density of the (copper porphyry ore) feed increased the viscosity of the slurry. This caused an increase in the swirl-layer thickness which, together with the reduced level of turbulence resulting from the increased solids content, resulted in an increase in the recovery of coarse particles. In addition, the reduced level of turbulence resulted in an increase in the water split to the overflow, which increased the fine particle recovery and hence reduced the grade of the concentrate. The latter has been confirmed by numerous workers including Stoessner et al (1990) (coal), Van Deventer et al (1988) (pyrite) and Nieuwoudt et al (1990) (pyrite); although Nieuwoudt et al (1990) found that the reduction in the grade was less apparent at increased slurry feed rates as a result of the increased centrifugal forces.

However, the effect of increasing the pulp density on the product recovery has been found to differ depending on the mineral being floated. Kinneberg and Miller (1983) found that increasing the pulp density did not affect the air split and hence the copper recovery remained unchanged. Van Deventer et al (1988) (pyrite), Cloete et al (1987) (pyrite) and Miller and Kinneberg (1984) (copper porphyry) found that increasing the pulp density of the feed slurry resulted in an increase in the recovery and Stoessner et al (1990) (coal) found that it reduced the recovery.

3.7.3 Feed characteristics

3.7.3.1 particle size

The inertia imparted to the fine particles by the centrifugal field enables them to deviate from the fluid streamlines and collide with the air bubbles. This results in the increased recovery of hydrophobic fines in the overflow. The classification effect also results in fine hydrophilic particles being transported to the overflow as a result of water transport to the overflow.

Coarse particles are easily recovered in the underflow as a result of the classification effect of the ASH and as a result of the particle/bubble aggregates being broken up by the turbulence. The upper size limit to flotation is in the region of 100 micron for a 5 cm diameter by 50 cm long ASH, but it is affected by the hydrophobicity and the liberation of the mineral being floated (Miller et al, 1988).

In the flotation of copper porphyry ore Kinneberg and Miller (1983) obtained a 100 % recovery for particles between 150 and 400 mesh, and a recovery of more than 80 % for the -100 micron fraction. They also found that the recovery of +100 micron particles decreased rapidly with increasing particle size, while that of the -400 mesh fraction decreased slowly with decreasing particle size.

3.7.3.2 hydrophobicity

In the ASH hydrophobic particles float against a centrifugal field. For this reason the stability of the particle/bubble aggregate is critical. The mineral particles to be floated need to be strongly hydrophobic and this often requires increased collector addition rates.

However, as the diameter of the cyclone increases this effect is expected to become less severe (Ye et al, 1988). An increase in particle hydrophobicity also increases the upper particle size limit.

3.7.4 Reagent addition

3.7.4.1 frother

Surface tension has very little effect on the size of the air bubbles formed in the ASH (Miller and Ye, 1989). However, the addition of frother is essential for effective flotation in the ASH. This is because flotation in the ASH requires that bubble coalescence does not occur and that the bubble/particle aggregates are very stable. If the froth phase is too weak it becomes entrained in the underflow, and if it is too stable it cannot be discharged via the overflow. The above conditions are controlled to a large extent by the addition of frother. The frother requirement in ASH flotation is often higher than in conventional flotation.

The addition of frother increases the thickness of the swirl-layer as a result of the stabilisation of the bubble phase. This increase in the swirl-layer thickness can be counteracted by increasing the slurry pressure which increases the centrifugal forces acting on the swirl-layer. Increasing the frother dosage also increases the size of the froth core and decreases the thickness of the transition layer. This increases the concentrate recovery as the transport of hydrophobic particles to the overflow is improved, but the grade may be reduced as a result of the entrainment of gangue into the stabilised froth (Cloete et al, 1987). There is a limit above which the further addition of frother has no effect (Baker et al, 1987).

3.7.4.2 collector

In the ASH the particle/mineral aggregate needs to be strongly hydrophobic for flotation to occur. This often requires a higher collector addition rate than in conventional flotation (Miller and Ye, 1989). However, in larger diameter cyclones the collector dosage is expected to be similar to that of conventional flotation.

In the flotation of a coarse Witwatersrand pyrite ore it was found that increasing the collector addition rate increased the recovery of pyrite in the concentrate without changing the grade, until a

limiting recovery was reached (Van Deventer et al, 1988). This limit depended on the slurry pressure. When the collector addition rate was further increased the concentrate grade decreased.

3.8 Previous Work using the ASH for Coal Flotation

Previous work using coal has shown that the overall results obtainable in the ASH are comparable, with respect to both grades and yields, to those obtainable in conventional batch flotation cells (Stoessner et al, 1988; Miller and Van Camp, 1982; Miller and Kinneberg, 1984). In certain instances the results obtained have approached the limit imposed by the washability of the coal (Miller et al, 1988). These results have been achieved at capacities which are up to 300 times greater than those of conventional flotation cells.

It has also been shown that although the extent of ash rejection varies from coal to coal, as a result of the variation of hydrophobicity with rank, extent of liberation and surface alteration (Miller et al, 1988), the best ash rejection occurs in the finer sizes in comparison to the upgrading which occurs in conventional cells (Miller and Kinneberg, 1984). However, contamination of the coal in the ultrafine sizes occurs as a result of the hydraulic transport of fine hydrophilic particles into the froth phase caused by the classification effect of the cyclone (Miller and Kinneberg, 1984). In addition the recovery of coarse particles is reduced in comparison with conventional cells (Miller and Kinneberg, 1984).

Miller and Van Camp (1982) used an ASH (d_c=150 mm, L_c=737 mm) to beneficiate a -590 micron coal sample from the feed stream to a water-only cyclone at the Cerro Marmon Coal Group at Boswell, PA. The coal was very fine, containing 50 to 70 % -38 micron material. The ash content varied between 22 and 25 %, with most of the ash being in the -38 micron fraction. The ASH was operated at a feed rate of 4 l/s, and a pulp density of 3 % solids. The reagent dosage used was 20 ppm of Dowfroth

1012. The air flow rate was kept at 6.6 l/s. The yield obtained was 75 %, at an ash content of 16.0 %. In a 2 minute batch flotation experiment in an Agitair bench cell, using 250 g/ton of Dowfroth 1012 a yield of 67 %, at an ash content of 15.5 %, was obtained.

Miller et al (1988) used a 5 cm diameter x 50 cm long ASH in the flotation of a medium-volatile bituminous coal from Pennsylvania. The feed material was 100 % -100 mesh and more than 60 % -400 mesh. The -400 mesh size fraction had an ash content of 22.6 % and the overall ash content was 17.8 %. Using kerosene as the collector (500 g/ton) and a feed rate of 0.5 tph, the ASH gave better results than those obtained in batch flotation experiments, with the results approaching the limits imposed by the washability characteristics of the feed (see Figure 3.4 below). In addition the ASH reduced the ash content of the -400 mesh fraction to 9.4 %.

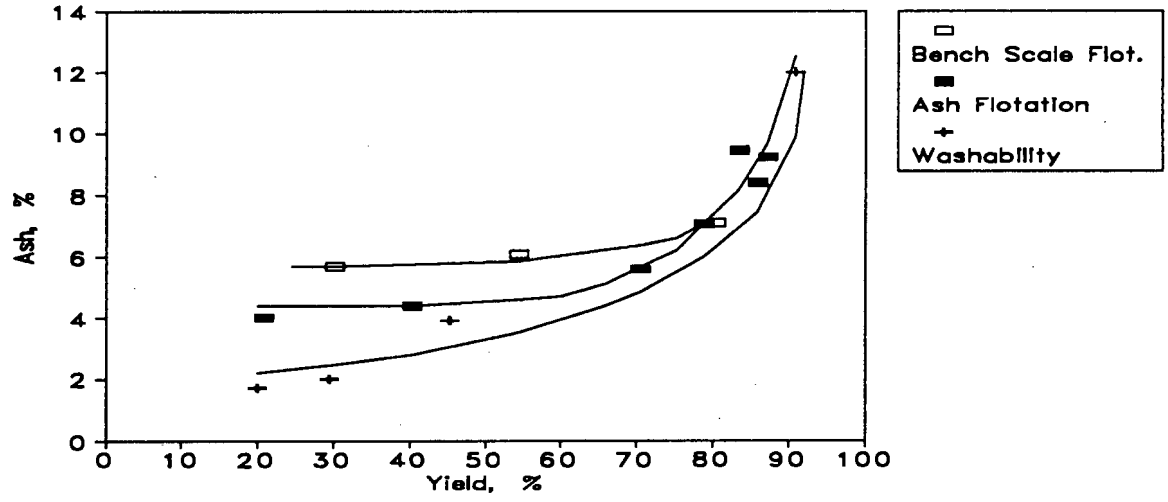

Figure 3.4: Flotation behaviour of medium-volatile bituminous coal compared to washability characteristics (after Miller and Ye, 1989)

In pilot plant studies at the EPRI Coal Quality Development Centre at Homer City, Stoessner et al (1988) used ASH's of various dimensions to beneficiate a 96 to 98 % -150 micron fines stream, with a feed ash that varied between 15 and 21 %. At a fuel oil (collector) addition rate of 2000 g/ton, and a MIBC (frother) addition rate of 1000 g/ton, yields of up

to 66.2 % were achieved, at grades in the region of 6.2 %. In comparison, conventional froth flotation resulted in a yield of 69.4 % at a grade of 5.0 %. At yields of greater than 70 % the ASH results were found to match the washability curve.

Previous work carried out using the ASH for the flotation of coal fines has shown that the most important features governing the flotation of coal in the ASH are:

i) Particle hydrophobicity
The particle hydrophobicity determines the upper particle size limit which can be recovered in the overflow product.

ii) Froth stability
The froth stability is determined by the particle hydrophobicity and the level of collector and frother addition.

iii) Solids recovery
In most cases about 80 % or more of the feed solids must be transported to the froth phase and recovered in the overflow product.

iv) Gangue size
The hydrophilic gangue is generally located in the finer sizes.

The operating conditions which have been found to give the best results are:

i) a low feed solids concentration, about 5 % by mass (Miller and Ye, 1989; Miller et al, 1988)
ii) modest air and slurry flow rates (Miller and Ye, 1989; Stoessner et al, 1990), i.e. $Q^* \approx 5$ (Baker, 1991)
iii) the minimum transfer of water to the overflow (Miller and Ye, 1989); this can be controlled by using the correct A^* ratio; i.e. $A^* \approx 1$ (Baker, 1991)
v) an L_c/d_c ratio of 10 for small diameter cyclones (Baker et al, 1987; Baker, 1991)

3.9 Chapter Summary

The Air-Sparged Hydrocyclone (ASH) consists of two concentric right vertical tubes, the inner of which is porous; a conventional cyclone header and vortex-finder; and a froth pedestal or orifice and baffle at its base. Slurry is fed into the porous cylinder and develops a swirl-layer (with a thickness in the region of 11 to 14 % of the cylinder radius). As the slurry moves down the ASH hydrophobic particles collide with (and become attached to) the micron sized air bubbles produced by sparging air through the porous cylinder. The particle/bubble aggregates move to the cyclone axis to form a froth phase. The underflow configuration restricts the slurry underflow and hence facilitates the discharge of froth via the overflow.

The small air bubbles, the increased particle inertia and the orthogonal particle/bubble motion is alleged to extend the fine particle flotation limit and to increase the flotation rate of these particles. The high slurry and air rates result in a short residence time which gives the ASH a specific volumetric capacity which is up to 100 times greater than that of conventional flotation cells. Other advantages of the ASH which have been reported are that the ASH performance is comparable to that of batch cells; that coal concentrate dewatering may not be necessary and that an ASH circuit may be cheaper than a conventional circuit.

Unfortunately the above advantages are accompanied by a reduction in the coarse particle recovery (in comparison with batch cells) and an increased reagent dosage (especially collector).

To date the effect of numerous design (L_c/d_c ratio, underflow configuration, A_{of}/A_{uf} ratio (A*), vortex-finder length (L_{vf}), inlet area (A_{inlet}) and cylinder porosity) and operating (air/slurry rate ratio (Q*), pulp density, feed particle characteristics and reagent addition) parameters on the performance of the ASH have been investigated.

At low L_c/d_c ratios, increasing the L_c/d_c ratio results in an increase in both the fine and the coarse particle recovery. However, at a certain cyclone length the fine particle recovery reaches a maximum. Further increases in L_c/d_c result in reduced grades. For coal the optimal L_c/d_c is alleged to be in the region of 10.

The underflow configuration has been found to have little effect (or none) on the performance of the ASH (using pyrite). However, the orifice/baffle configuration prevented blockages from being a problem.

A^* is the most important ASH parameter. Increasing A^* increases the recovery, but reduces the concentrate grades; A^* ratios in the region of 1.0 are alleged to be best for coal.

L_{vf}, A_{inlet} and the cylinder porosity have little effect on the performance of the ASH.

Decreasing Q^* causes an increase in the centrifugal forces in the ASH. This reduces the coarse particle recovery, but increases the grade and recovery of fine particles. However, above a certain Q^*, further increases result in an increase in the recovery and a reduction in the grade.

The effect of pulp density on the performance of the ASH seems to depend on the material being floated. This may be as a result of the absolute mass (or number) of particles reporting to the overflow.

The size and hydrophobicity of the particles being floated determines the collector dosage required to achieve a certain yield. Increasing the collector dosage increases the coarse particle recovery. In general the ASH requires collector dosages in the region of three times those required in batch cells. The frother dosage required is also greater than that required in batch cells.

Previous work using the ASH for the flotation of coal has shown that the ASH is capable of achieving separations comparable with those achieved in batch and conventional cells at greatly increased throughputs.

CHAPTER FOUR

EXPERIMENTAL DETAILS

As stated in Section 1.2 the aims of this research were to investigate the use of an ASH in the flotation of a South African coal, and to determine the effect of various design and operating parameters on the performance of the process, in terms of product yields and grades obtainable.

This Chapter sets out details of the equipment and experimental methods used in the investigation. The Chapter begins with a description of the coal chosen for the investigation. This is followed by a description of the ASH equipment and the experimental method used in the two-phase and three-phase ASH testwork. A brief description of the batch flotation apparatus and method follows. Finally the methods of carrying out the size, ash, and float-and-sink analyses are described.

4.1 Choice of Coal Sample

The coal chosen for use in this investigation was obtained from the Kleinkopje Colliery in Witbank. A Witbank coal was chosen because this coalfield is the most important (commercially) at present. In addition, coal from this colliery has been well characterised in both laboratory (batch and column cells) and plant (column cell) tests in a thesis recently submitted to the University of Cape Town (Von Holt, 1992). In fact, the sample used in this investigation is the same as that used by Von Holt (1992) in his laboratory work.

A description of the method of sample collection and preparation, together with a statistical analysis of the results obtained, is described in

Appendix A. The characterisation of the coal, by size analysis, proximate analysis, float-and-sink analysis and release and batch flotation experiments is described and discussed in Chapter Five, together with the results of the preliminary ASH work.

4.2 Air-Sparged Hydrocyclone Testwork

4.2.1 Experimental equipment

The air-sparged hydrocyclone rig used in this investigation was located at the University of Stellenbosch. The rig consisted of an agitated conditioning tank, a feed system (comprising a centrifugal pump, bypass stream, valve and magnetic flowmeter), a compressed air supply and the air-sparged hydrocyclone (ASH) itself. A photograph of the ASH rig appears in Figure 4.1 below; the rig is represented diagrammatically in Figure 4.2 below. In addition to the above equipment, a modified Leeds batch flotation cell was used to disperse the collector and frother prior to adding them to the coal slurry in the conditioning tank.

4.2.1.1 ASH units

Two different air-sparged hydrocyclone configurations, *ASH I* and *ASH II*, were used during the test program. These different configurations are described below.

i) *ASH I* consisted of a porous ceramic cylinder, 205 mm in length, with an internal diameter of 50 mm and an external diameter of 70 mm. The mean pore size of the cylinder was 1 micron. To prevent the erosion of the cylinder at the inlet and outlet, cylindrical non-porous sections of high density polyethylene, 30 mm long, were used at the top and base of the porous cylinder; as recommended by Burger (1986, p31). This resulted in an overall cyclone height of 265 mm.

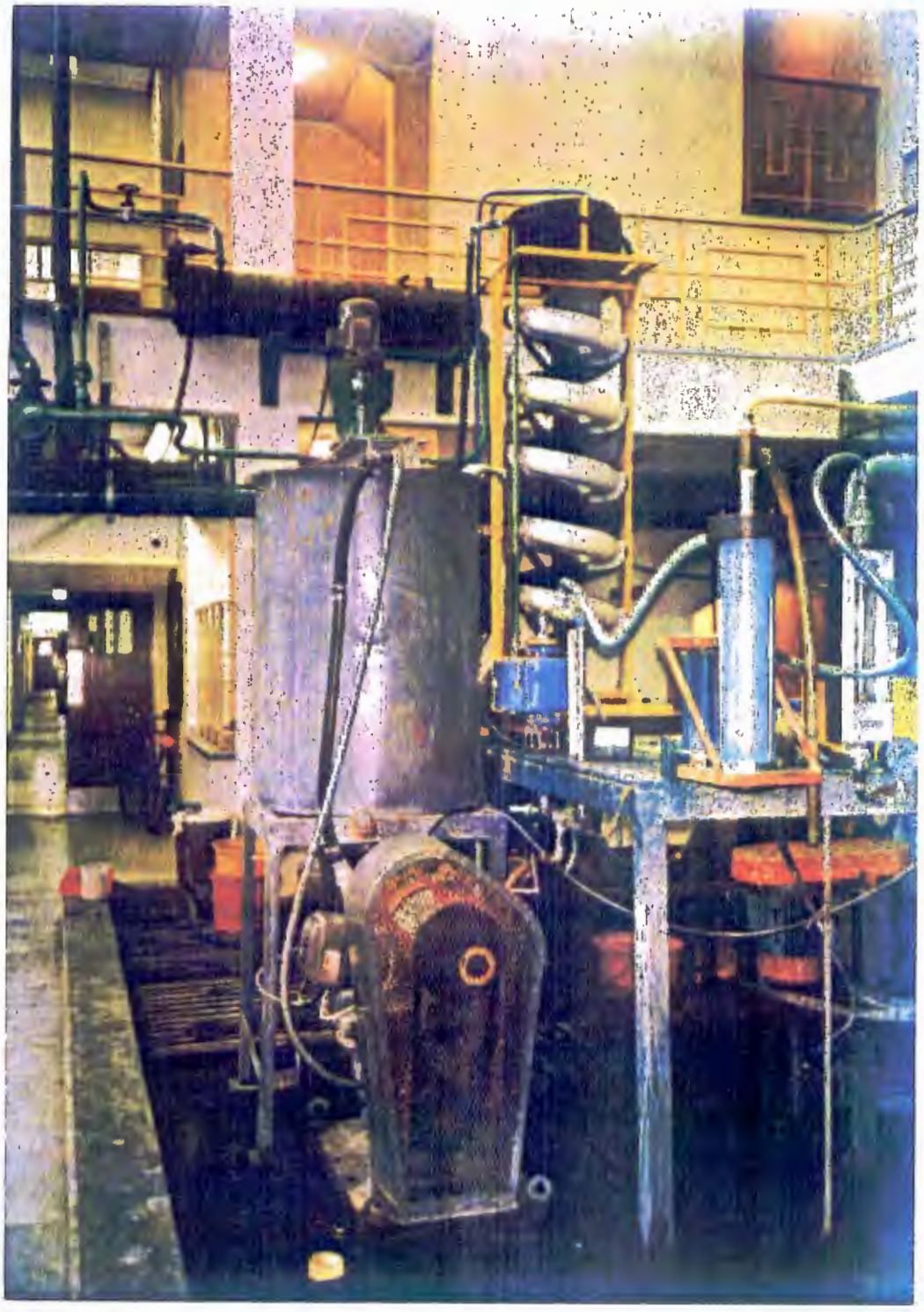

Figure 4.1: Photograph of the ASH rig

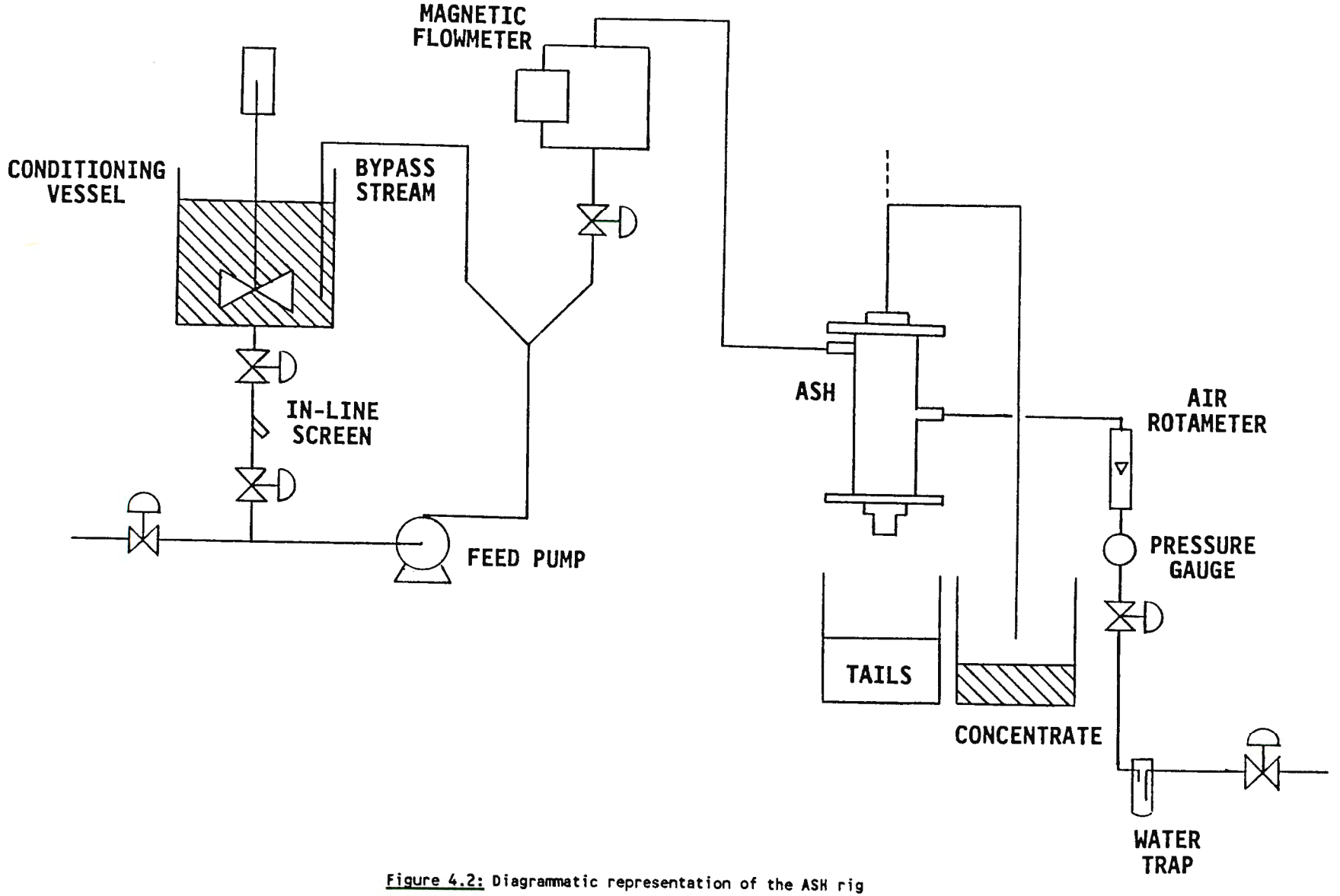

Figure 4.2: Diagrammatic representation of the ASH rig

The inlet area was 15x9 mm and the vortex-finder length was 37 mm. Vortex-finder diameters could be chosen to be either 10, 16, 21.5 or 27.5 mm, and pedestal diameters as either 44.1, 46 or 48.2 mm. The above pedestal diameters resulted in annular openings of 11.8, 8.0 and 3.6 % of the cylinder radius respectively. A diagrammatic representation of *ASH I* is given in Figure 4.3 below.

ii) *ASH II* consisted of sintered bronze porous cylinders 46 mm in diameter and varying length (300 and 500 mm). This enabled the testing of the influence of the L_c/d_c ratio on the flotation response. In addition, it was possible to choose various slurry inlet areas (15x9 mm and 15x12 mm) and different vortex-finder diameters (16 and 21.5 mm). The vortex-finder lengths were adjustable. The porous cylinders had an average pore size of 2 micron.

It was also possible to vary the underflow configuration of *ASH II*. Either an annular outlet opening (using a pedestal) or an orifice with a baffle positioned above it (as used by Nieuwoudt et al, 1990) could be used. The pedestal underflow configuration was constructed in such a way as to also allow the use of a large annular opening (i.e. a smaller pedestal) with a flow restricting orifice below (as used by Burger, 1986), in the event of blockages being a problem.

Diagrammatic representations of indicating the differences between the pedestal and orifice underflow configurations of *ASH II* are given in Figures 4.4 and 4.5 below.

4.2.1.2 ancillary equipment

The slurry was conditioned in a 470 l, rubber-lined, conditioning tank which was 70 cm in diameter and 1.5 m in height. The impeller used was a 3-blade pitched-blade propellor with a diameter of 40 cm. The impeller was located 40 cm from the base of the tank and was rotated at 300 rpm by a 0.37 kW motor.

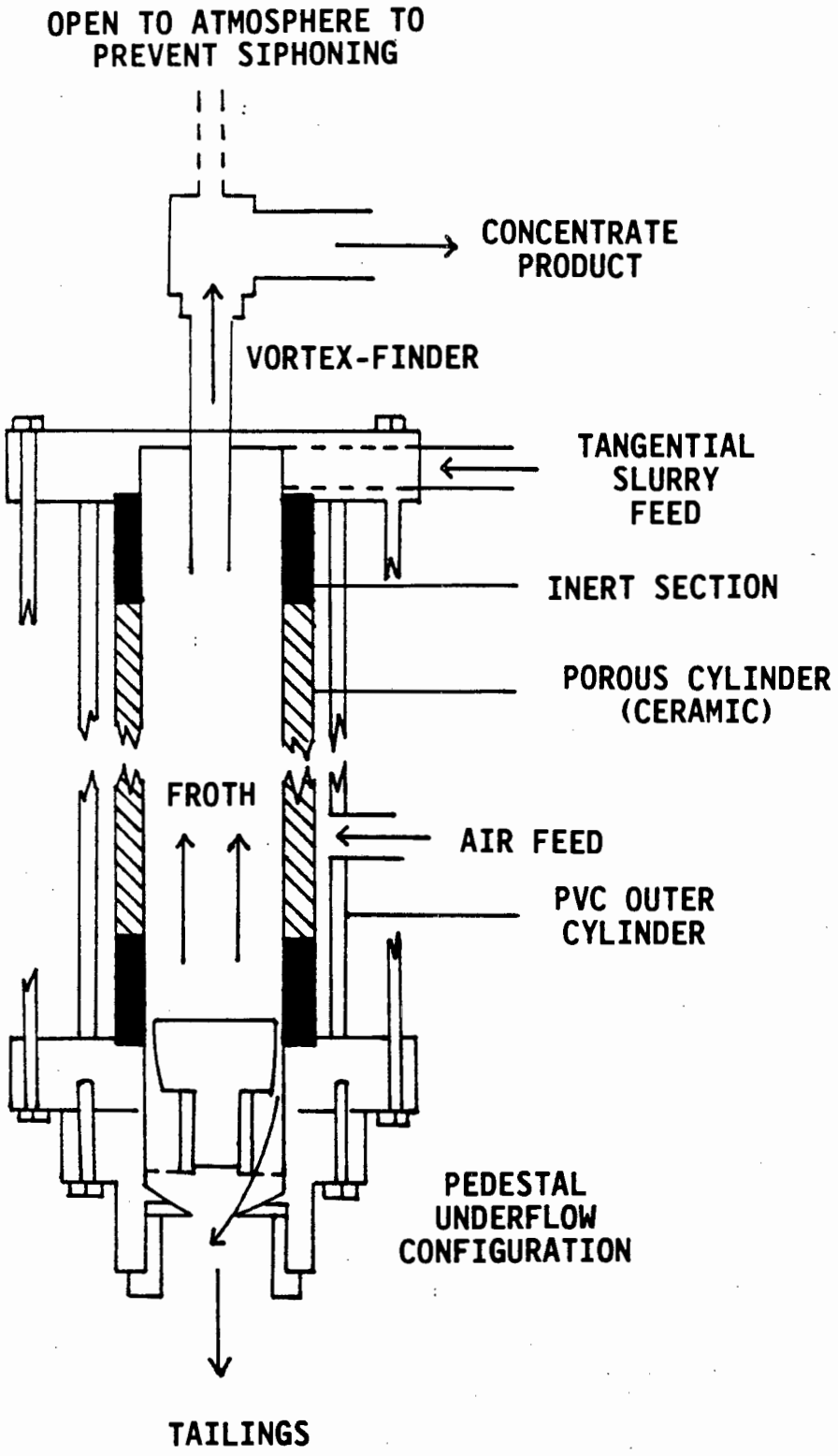

Figure 4.3: Diagrammatic representation of ASH I

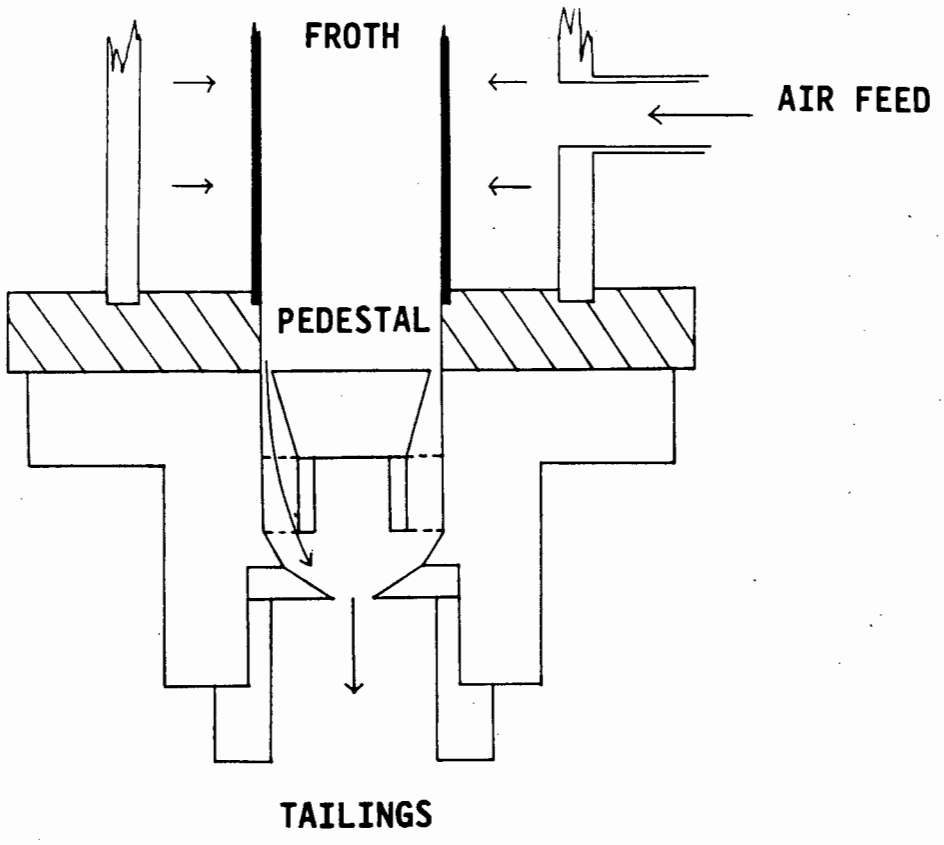

Figure 4.4: Diagrammatic representation of the pedestal and annular opening configuration of ASH II

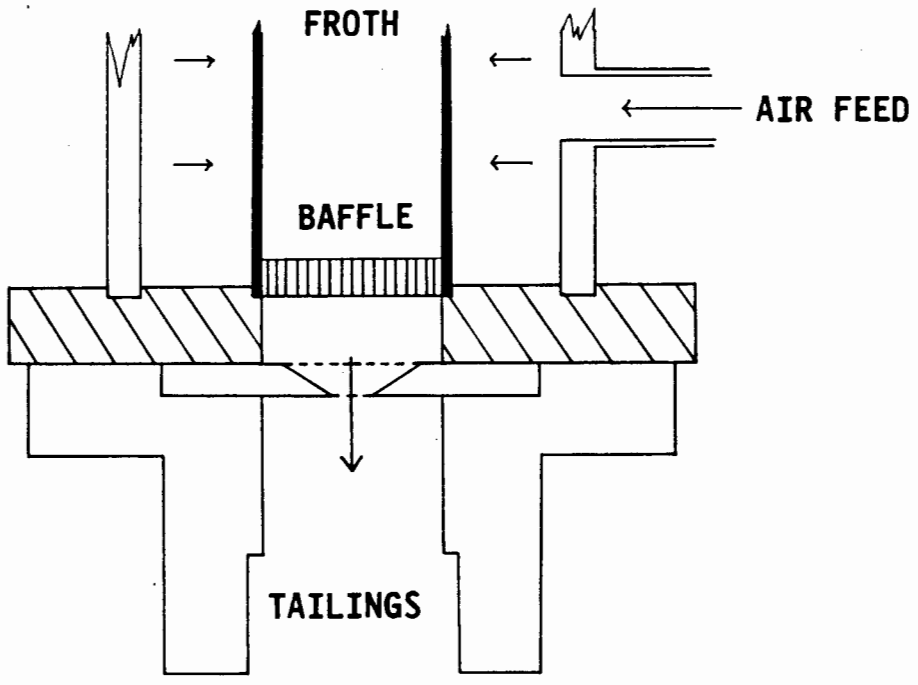

Figure 4.5: Diagrammatic representation of the baffle and orifice underflow configuration of ASH II

The slurry was drawn from the centre of the base of the conditioning tank by a 5.5 kW centrifugal pump. The slurry passed through an in-line screen, with an aperture size of 1x1 mm, before entering the ASH. This screen removed oversize particles which would have resulted in blockages of the annular underflow opening. The size of the pump allowed a recirculating bypass stream, at a flow rate of up to 200 lpm, to be returned to the conditioning tank (this ensured turbulent mixing in the conditioning tank).

The flow rate to the ASH was varied by means of a valve, and monitored by means of a magnetic flowmeter. The splitting of the flow into the feed and bypass streams was accomplished by a Y-shaped splitter. The diameters of the splitter outlets were chosen so that the slurry velocity in each of the outlets was approximately the same. Burger (1986, p27) found that this configuration gave the most consistent feed to the hydrocyclone, with respect to both particle size and pulp density.

The compressed air required by the ASH was supplied by a departmental compressor, at a pressure of 5.6 bar. The air fed to the ASH passed through a water-trap, a pressure gauge and a rotameter. The water-trap prevented any particulates from blocking the pores of the porous cylinder. The pressure gauge and rotameter enabled the results obtained to be quoted at standard conditions, thereby allowing comparison with results obtained by other workers.

In addition to the above equipment, a modified Leeds batch cell (similar to the unit described in Section 4.3.1) was used to disperse the collector and frother prior to adding them to the coal slurry in the conditioning tank.

4.2.1.3 reagents used

Numerous researchers have reported the effect of various collector/frother interactions on the flotation of both minerals and coal. For this reason only one collector and one frother were used.

The collector used was Shellsol A; a commercial grade oil with a 95 % aromatic content (SG=0.88). The frother used was hi-flash triethoxybutane (HTEB), obtained from Senmin.

4.2.2 Experimental methods

Both two-phase (water and air) and three-phase (water, air and coal) testwork was carried out during this investigation. The two-phase testwork was carried out using *ASH I*, and the three-phase testwork using *ASH II*. The three-phase testwork comprised the preliminary work (described in Chapter Five), the factorial design investigation (Chapter Six) and the subsequent investigation into pulp density/air rate and collector dosage effects (later sections of Chapter Six). The sections which follow describe the experimental methods followed when carrying out these tests.

4.2.2.1 definition of run types

In the experimental methods described below, and in the rest of this thesis, the following definitions are used:

i) A **run** is an experiment carried out at a certain ASH configuration# and group of operating conditions.
ii) A **primary run** is the first run carried out at a particular set of conditions.
iii) A **duplicate run** is a run carried out under the same conditions as a primary run, using the same batch of ore (tank of water) and ASH.
iv) A **repeat run** is a run carried out under the same conditions as a primary run, using the same ASH but a different batch of ore (water).
v) A **replicate run** is a run carried out under the same conditions as a primary run, using a different batch of ore (tank of water) and a reassembled ASH.
vi) A **set of runs** are those runs carried out using the same batch of coal slurry (tank of water).

The ASH configuration is the set of design parameter dimensions used, i.e. d_c, L_c, UF type, d_p, d_o, d_{vf}, L_{vf}, A_i, cylinder porosity.

4.2.2.2 two-phase testwork

The two-phase work was carried out using *ASH I* (see Section 4.2.1.1 above). Each set of runs was carried out using the same ASH configuration, but different water feed rates.

A set of two-phase runs was begun by assembling the ASH according to the configuration chosen for the set of runs. The conditioning tank was filled to the 260 l mark, the impeller switched on, and the required amount of HTEB frother added. The water was allowed to condition for 10 minutes while the tank was filled to the 470 l mark.

The air was then adjusted to the required flow rate and the feed pump switched on. The bypass stream flow rate was adjusted to give the required feed rate to the ASH, indicated by the magnetic flowmeter reading.

The residence time of water in the ASH was in the region of 1 second, and therefore the ASH was assumed to have achieved steady state within 3 seconds. Timed samples of the overflow and underflow were taken simultaneously where possible, being collected in buckets. If it was not possible to take the samples simultaneously, the overflow was sampled before the underflow. Once the samples had been taken the run was complete. The bypass valve was adjusted to give a new feed rate to the ASH and another run was carried out.

The above method allowed four to seven different runs, including duplicates, to be carried out per set. Each set was carried out using the same ASH configuration. After each set of runs the conditioning tank was drained and the ASH was dissembled. Replicates of all the runs were carried out. Exclusion of problematic sets of runs ensured that the results were valid, i.e. that the ASH had been correctly assembled, etc.

The results of the two-phase tests were expressed in terms of the mass of water reporting to the overflow and underflow, and the recovery of water to the overflow, as calculated in Section B.3 of Appendix B.

4.2.2.3 three-phase testwork

The three-phase testwork was carried out using *ASH II* (see Section 4.2.1.1 above). The experimental method followed depended on the particular investigation being carried out, i.e. on whether preliminary work, factorial design, pulp density/air rate or collector dosage runs were being performed. In addition, the method employed in the factorial design investigation depended on whether or not the run was a primary (or replicate), duplicate or repeat run.

i) Preliminary work (Chapter Five)

Before a set of preliminary work runs was begun, the conditioning tank and the ASH feed lines were rinsed to ensure that no reagent or coal residue was present from previous runs. Water was then added to the conditioner, to the 260 l mark, and the impeller was switched on. The required amount of wet coal was then added to the conditioning tank and the ASH configuration to be used was assembled. The coal/water slurry was then left to condition overnight (with the impeller still running).

The following day the required amount of Shellsol A collector was added to the modified Leeds batch cell, and water was added to the 3 liter level. The impeller was then switched on, at a speed of 2000 rpm, and the collector was allowed to disperse for 10 minutes. After 10 minutes the required amount of HTEB frother was added to the batch cell, and a further 10 minutes of agitation was allowed.

During the first 10 minutes of collector dispersion, the feed pump to the ASH was switched on. Keeping the feed valve to the ASH closed, the slurry/water mixture was allowed to

circulate back to the conditioning tank through the in-line screen. During the 10 minutes of collector/frother dispersion, the feed pump was switched off, and the screen isolated by means of two valves. This enabled the screen to be removed, cleaned and replaced before commencing with a set of runs, thereby minimising the possibility of a loss in feed pressure caused by screen blockage.

The dispersed collector/frother mixture was drained into a 20 l bucket, the batch cell was rinsed, and the dispersion poured into the 260 liters of coal/water slurry. The slurry was allowed to condition for a further 10 minutes before filling the conditioning tank to the 470 liter mark. Twenty minutes after the addition of the collector/frother mixture, the first run of the set was commenced.

The run was begun by adjusting the air to the required flow rate, switching the feed pump on and adjusting the bypass valve to obtain the required feed rate to the ASH, indicated once again by the magnetic flowmeter. As in the two-phase work, the ASH was assumed to reach steady state after 3 seconds. Timed samples of the overflow and underflow were taken simultaneously where possible, being collected in buckets. If it was not possible to take the samples simultaneously, the overflow was sampled before the underflow. Once the samples had been taken the feed pump was switched off, and the feed valve was closed.

Where duplicate runs were being carried out, the feed pump was switched on again, the feed valve adjusted to give the same feed rate, and the sampling procedure repeated. Tests were carried out at both increasing and decreasing feed rates of consecutive samples.

The above procedures were continued until the level in the conditioning tank reached 200 liters. This made it possible to obtain between four and seven runs per set, some of which were duplicate runs. Below a level of 200 l air was drawn

into the feed pump. Once the level in the conditioning tank reached 200 l the tank was drained and rinsed in preparation for further runs. The ASH was also dissembled and rinsed.

ii) Factorial design investigation (Chapter Six)

In the factorial design investigation the procedure of preparing the slurry, ASH and reagents was as described in (i) above. The sampling procedure followed and the method of obtaining duplicate samples was also the same.

However where subsequent (new primary or replicates of a previous primary) runs were to be performed, it was necessary for the ASH to be dissembled and reassembled according to the configuration required for the following run. Once the ASH had been reassembled the air rate was adjusted to the required flow rate, the feed pump switched on and the feed valve adjusted to give the desired feed rate. Samples were once again taken as described above. The above method allowed between three and seven factorial design runs to be carried out per set, i.e. before the level reached 200 l. The number of runs per set depended on the number of duplicate runs performed. Where a repeat factorial design run was to be performed the ASH was not dismantled between subsequent batches of slurry.

iii) Pulp density/air rate investigation (Chapter Six)

In the investigation into pulp density/air rate effects the procedure of preparing the slurry and the ASH was as described in (i) above. The sampling procedure followed was also the same.

However, in this investigation the collector was added directly to the conditioner. After conditioning for 10 minutes, 5 of which were carried out with the bypass stream in operation, the frother was added to the slurry. The slurry was allowed a further 10 minutes of agitation before being filled as described in (i) above.

The pulp density/air rate runs were all carried out in a single set, using the same ASH configuration. Three runs, using different air flow rates, were carried out at each pulp density. The highest pulp density was tested first. After the first three runs, at the highest pulp density, the slurry was diluted to the next highest density to be tested, and the next three runs were performed. A total of twelve runs at four different pulp densities, between about 10 and 1 %, were carried out.

iv) Collector dosage investigation (Chapter Six)

The method of slurry and ASH preparation followed in this investigation was the same as described in (i) above. In addition the sampling procedure followed and the method of obtaining duplicate samples was the same. However, the method of reagent addition followed was the same as in (iii) above.

As in (iii) above, the collector dosage runs were all carried out in a single set, using the same ASH configuration. The lowest level of collector addition was tested first; frother was only added in the first instance. After each run the amount of coal remaining in the conditioner was calculated, and the amount of additional collector required was added. The coal was allowed 10 minutes to condition at the new collector dosage and then the next run was commenced. This method allowed 6 levels of collector addition to be tested.

v) Analysis of results

In all the three-phase ASH runs, the mass of the overflow and underflow samples was determined by weighing the buckets and samples, and then the empty buckets. The samples were pressure filtered, and then placed in a drying oven, at 80°C, overnight.

The dried samples were allowed to cool to room temperature before being weighed to determine the mass of solids in the overflow and underflow. Each sample was thoroughly mixed

before fractional shovelling# was used to reduce it to subsamples small enough for size and ash analyses. From the above, the yield, coal recovery and water recovery to the overflow were calculated, as set out in Section B.4 of Appendix B.

4.3 Batch Flotation Testwork

Batch flotation testwork was carried out to provide a benchmark against which to compare the results of the ASH investigations. A limited amount of work was done, according to the procedure outlined below.

4.3.1 Batch flotation equipment

The batch flotation testwork was carried out in a 3-litre laboratory Leeds cell which had been modified to enable the impeller speed to be varied (and controlled) and the pulp level to be maintained at a constant froth height. The collector used was Shellsol A and the frother used was hi-flash tri-ethoxybutane (HTEB).

4.3.2 Conventional batch flotation method

The conventional batch flotation experiments were carried out according to the Standard UCT Batch Coal Flotation Method. This is based on the method employed by Fickling (1985) which has been found to produce reproducible results from operator to operator. A detailed description of the method, which involves the removal of the froth at fixed intervals, is given in Section B.2 of Appendix B.

4.3.3 Release float method

In a release float a large number of small concentrates are collected over a long period of time, by varying the flotation conditions so that only the most hydrophobic coal in the slurry at that time is recovered. Initially no reagent is used, and conservative operating conditions are

The method of fractional shovelling is described in Appendix A.

chosen. Once the initial concentrate has been recovered the operating conditions are gradually altered, and incremental (starvation) quantities of reagent are added. This process is continued until as much as possible of the coal has been recovered. In this way the best possible flotation performance at a particular ash, CV, or yield can be obtained.

4.4 Methods of Analysis

4.4.1 Size analyses

Size analyses of the feed, batch flotation concentrate and tails samples, and selected ASH concentrate and tails samples were performed by wet sieving subsamples with a mass of about 40 g. Each sample was first suspended in a beaker, using a laboratory mixer, before being poured onto the largest (425 micron) sieve. The sieves were placed in a laboratory shaker and the water flow rate adjusted to ensure a spray of water. The underflow from the smallest (45 micron) sieve was collected in a bucket. Once the underflow water from the -45 micron sieve was clear, the water was turned off and the shaking stopped. The coal remaining on each sieve was then hand-rinsed to the centre of the sieve, and the process repeated until the underflow was once again clear.

The coal remaining on the various size sieves was filtered, and placed in a drying oven at 80°C overnight. After drying, the samples were allowed to cool to room temperature before being weighed to determine the mass in each size fraction. The ash content of the coal in each size fraction was usually also determined, according to the method outlined below.

4.4.2 Determination of ash content

Ash content determinations were carried out by first weighing the crucible to be used for a particular sample. A representative sample of about 0.7 to 1 g was placed in the crucible, and the mass of the

coal and crucible was determined. The crucible containing the coal was then placed in a muffle furnace. The temperature of the furnace was ramped up to 820°C, over a period of 2 hours. Four hours after the ramp implementation the furnace was ramped down to 80°C, over a period of 6 hours. The crucibles were then removed and placed in a desiccator. Once the crucibles had cooled to room temperature the mass of the crucible and ash was obtained by weighing. This enabled the ash content of the sample to be calculated. The ash contents of the concentrate and tails samples were used to determine the concentrate recovery. They were also used as a check for the material balance, and therefore of steady-state.

4.4.3 Float-and-sink analyses

Float-and-sink analyses were carried out on subsamples of the feed and selected batch and ASH flotation concentrate and tails samples using the centrifugal method developed by Franzidis and Harris (1986). The advantage of this method lies in the fact that it yields reliable results down to particle sizes of 25 micron.

The float-and-sinks analysis was carried out in a Beckman GPR Tabletop Centrifuge, at a speed of 4000 rpm. Use was made of specifically designed centrifuge tubes. Float-sink separations were carried out in the relative density (RD) range 1.30 to 1.80. The dense liquid used consisted of a solution of zinc chloride in water, diluted to the required RD. The RD of the solution was measured with a hydrometer.

CHAPTER FIVE

PRELIMINARY WORK

Before commencing with a detailed experimental programme using the ASH, preliminary work was done to characterise the coal sample to be used in the investigation, and to become familiar with the operation of the ASH. Batch flotation work was also carried out to obtain a benchmark against which the results from the ASH could be compared. This Chapter describes and discusses the results of this preliminary work.

The aim of the coal characterisation work was to provide an indication of:

i) the size distribution of the coal and gangue materials (size and ash-by-size analyses);
ii) the liberation characteristics of the coal (float-and-sink analysis)
iii) the best separation possible using flotation (release flotation analysis); and
iv) the results obtainable in a batch flotation cell (batch floats).

The preliminary ASH testwork was performed in two separate stages; two-phase (water and air) and three-phase (water, coal and air) testwork. The aims of the preliminary work described below were to:

i) become familiar with the operation of the ASH;
ii) determine the collector dosage required to float the coal in the ASH;
iii) determine the optimal volumetric feed rate to the ASH; and
iv) compare the results obtained in the ASH with those obtained in the coal characterisation work

5.1 Coal Sample Characterisation

The coal used in the investigation was characterised by means of size, ash-by-size, petrographic, proximate, float-and-sink and flotation release analyses. In addition, batch flotation experiments were performed on subsamples of the coal to obtain a benchmark against which the ASH results could be evaluated. The results of all these tests are described and discussed in the sections which follow.

5.1.1 Sample collection and preparation

The coal used in the experimental programme was obtained from the Kleinkopje Colliery, near Witbank. The sample was collected in six 42 gallon drums in such a way as to ensure that the coal in each drum was representative of the sample as a whole. The drums were sealed and dispatched by rail to the Department of Metallurgical Engineering at the University of Stellenbosch, where the experimental work was carried out. Once there, fractional shovelling, as recommended by Gy (1982, p299), was carried out on the contents of the individual drums to produce subsamples for further experimental work.

A detailed description of the sample collection and splitting procedures followed, and a statistical analysis of the results obtained, is given in Appendix A. The results of the statistical analysis show that fractional shovelling produced unbiased, representative subsamples for characterisation and flotation testwork.

5.1.2 Petrographic and Proximate Analyses

A subsample of the Kleinkopje coal was sent to the Falcon Research Laboratories in Johannesburg for petrographic analysis. Another sample was sent to Richlab in Johannesburg for proximate analysis and determination of the sulphur content. The results of the petrographic and proximate analyses are given in Table 5.1 below.

Table 5.1: Maceral and proximate analysis of Kleinkopje coal

Vitrinite	27.3 % by volume
Exinite	1.7 % by volume
Inertinite	71.0 % by volume
H_2O	2.3 %
Ash Content	22.9 %
Volatile matter	21.9 %
Fixed Carbon	52.9 %
Sulphur	1.67 %
CV	24.1 MJ/kg

The petrographic analysis classified the Kleinkopje coal as a low rank bituminous coal. As may be seen, the coal consisted chiefly of inertinite (71.0 % by volume), and only a small amount of vitrinite (27.3 % by volume). The petrographic analysis also indicated the presence of large carbominerite (particles rich in mineral matter) and quartz particles, the bulk of which were greater than 100 micron in diameter (Falcon, 1991). It was suggested in the report accompanying the petrographic analysis that the presence of the large carbominerite particles might cause difficulties in any beneficiation process based on surface properties, as these particles would be unlikely to report to the tails (Falcon, 1991). The sample also contained a high proportion of fine inertinite fragments smaller than 30 micron in diameter.

Table 5.1 indicates that the coal sample had an ash content of 22.9 %, a calorific value (CV) of 24.1 MJ/kg and a sulphur content of 1.67 %.

5.1.3 Size and ash-by-size distributions

The mean size distribution and the ash content of each size fraction, at the 95 % confidence level, were obtained during the statistical analysis of the sampling procedure described in Appendix A. The results of the size and ash-by-size distributions of the coal are given in Tables A.9 and A.16 in Appendix A and plotted in Figures 5.1 and 5.2 below.

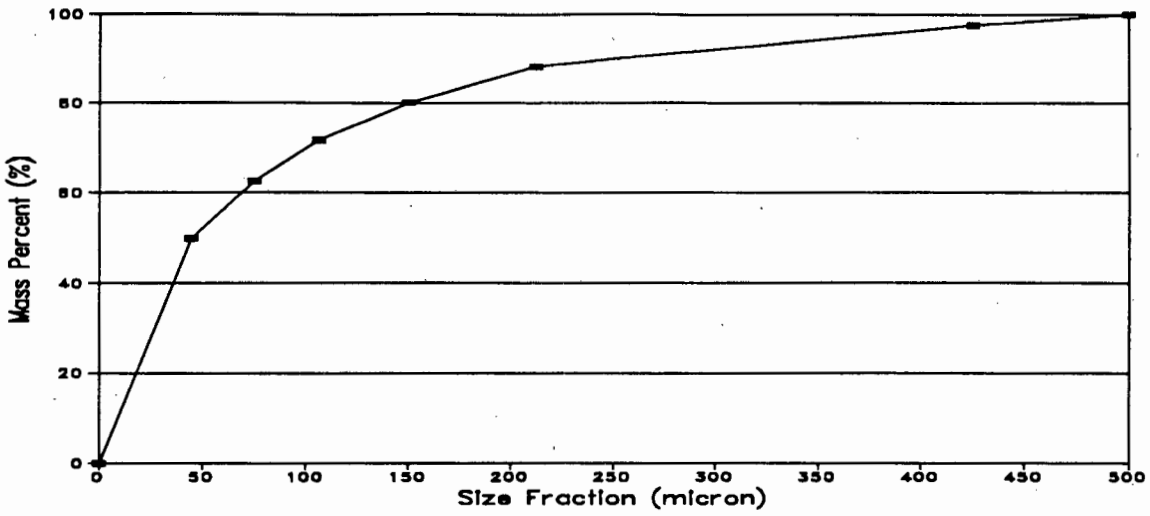

Figure 5.1: Size analysis of Kleinkopje coal

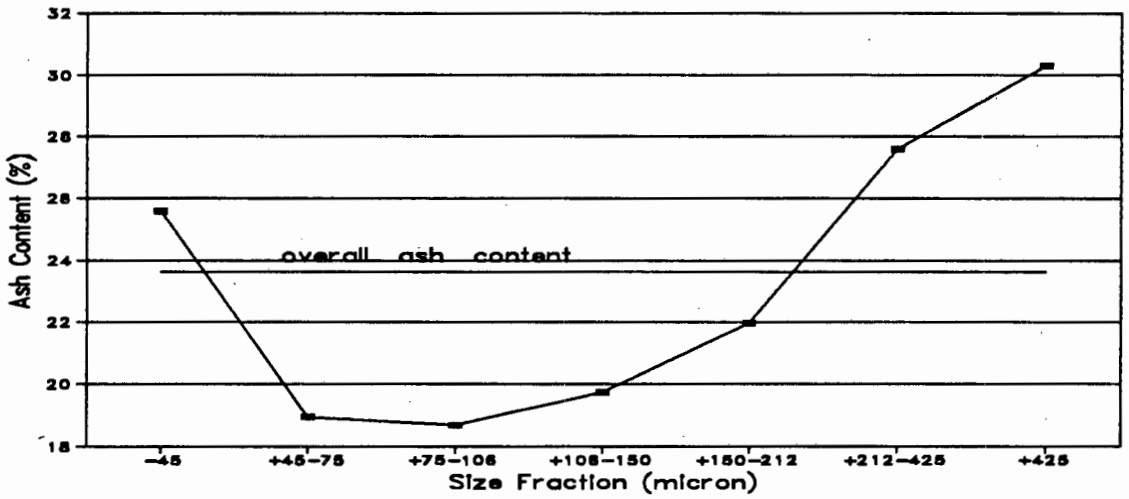

Figure 5.2: Size-ash analysis of Kleinkopje coal

The results indicate that the sample contained a large amount of fine material (50 % passing 45 micron) but that a fair amount of coarse material was also present (20 % greater than 150 micron). The +425 micron fraction had the greatest ash content, 33.3 % ash, followed by the -45 micron fraction, with an ash content of 25.6 %.

5.1.4 Float-and-sink analyses

Float-and-sink analyses were carried out on subsamples produced by fractional shovelling to determine the degree of liberation of the coal, so that an indication of the efficiency of flotation on an absolute basis could be obtained. The results of the float-and-sink analysis are listed in Table 5.2 and plotted in Figure 5.3 below.

Table 5.2: Float-and-sink analysis of Kleinkopje coal

Specific Gravity	% Floats	% Ash Floats	% Ash Sinks
1.30	7.03	2.4	23.6
1.35	17.42	3.5	27.0
1.40	28.80	4.1	30.4
1.45	42.57	5.7	36.2
1.50	59.52	6.4	46.4
1.55	65.92	7.7	52.0
1.60	73.22	9.5	60.0
1.65	75.34	9.2	65.3
1.70	78.82	10.3	68.7
1.75	80.82	11.0	70.7
1.80	82.78	12.2	71.6

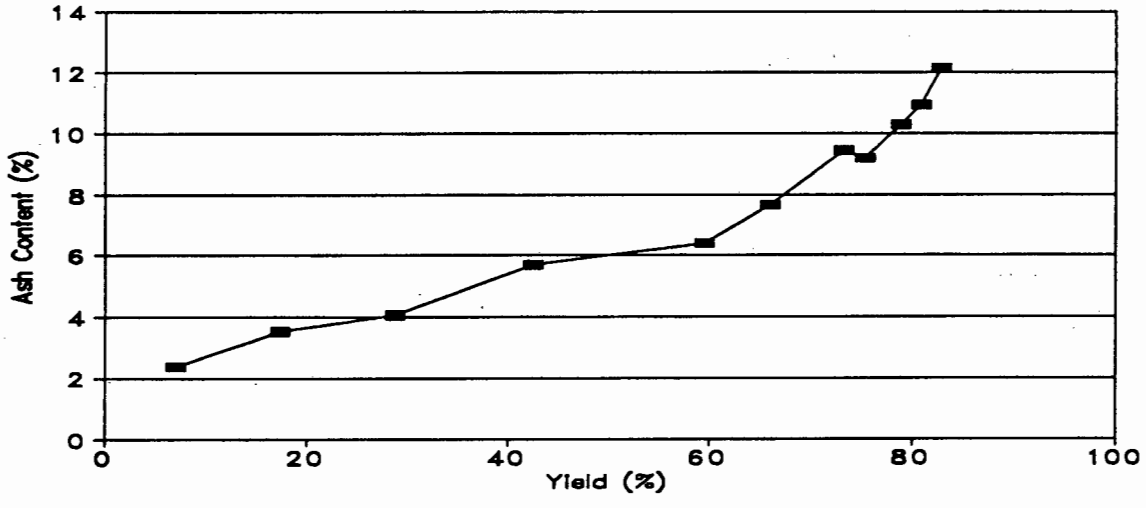

Figure 5.3: Float-and-sink analysis of Kleinkopje coal

The float-and-sink results indicate that the material was fairly evenly distributed in the relative density (R.D.) range between 1.3 and 1.6, with 28.8 % of the material in the relative density range below 1.4. Figure 5.3 indicates a theoretical yield of 65 % at an ash content of 7 %, and 80 % at an ash content of 10 %.

5.1.5 Release flotation analysis

A flotation release analysis was performed on a subsample of the coal to obtain an indication of the optimum performance that could be achieved by flotation. This is because a separation process (at these particle sizes) based on surface properties can never be as selective as one based on density. The release flotation method described in Section 4.3.3 was used. The air rate and impeller speed were maintained at 4 l/min and 1200 rpm respectively. A pulp density of 4.6 % was used. Starvation amounts of both frother (HTEB) and collector (Shellsol A) were added.

Detailed results of the release flotation analysis are given in Section B.1 in Appendix B. The results are plotted in Figure 5.4 below.

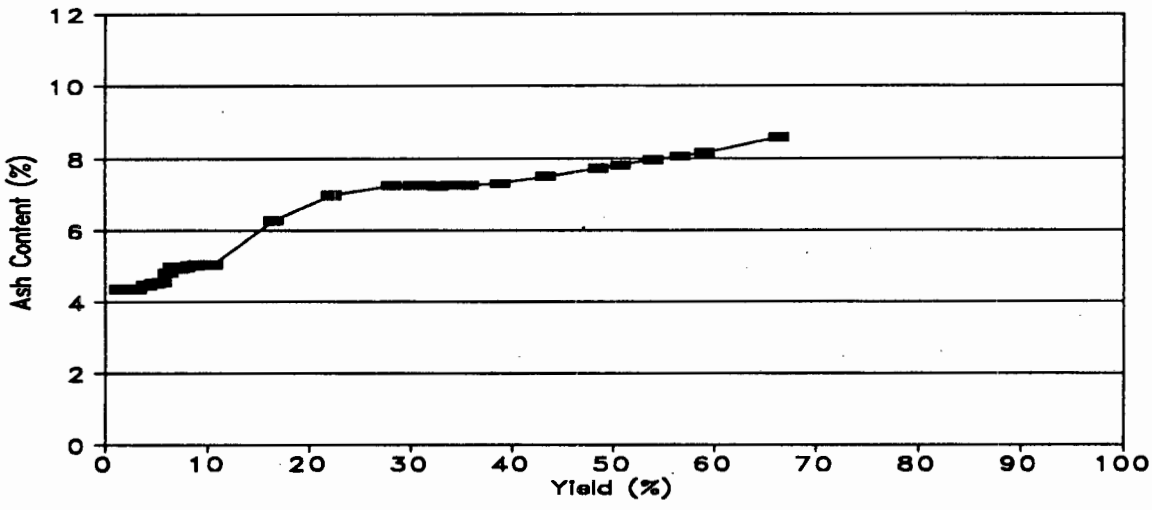

Figure 5.4: Release flotation results using Kleinkopje coal

It can be seen that the material was reasonably floatable in a batch cell, but that the selectivity was poor. The "hump" between yields of

15 and 30 % in Figure 5.4 indicates that the coal consisted of two distinct types of material. This fact was confirmed by on-site testwork carried out at the colliery, where it was found that a "low-ash" metallurgical coal (LAC) and a steam coal product are produced from different regions of the seam, although the fines from both parts of the seam are combined in the thickener. Figure 5.4 indicates a theoretical yield of LAC product, at an ash content of 7 %, of only 25 % by flotation in comparison with the theoretical yield of 65 % obtained in the float-and-sink analysis (Section 5.1.4 above). However, the release flotation analysis indicates a theoretical yield of 75 % at an ash content of 10 % (cf. 80 % from the float-and-sink analysis).

5.1.6 Batch Flotation Results

Batch flotation experiments were carried out on subsamples of the Kleinkopje coal as they provide a standard against which other flotation work can be evaluated. Five runs were carried out according to the method described in Section 4.3.2 in Chapter Four. The frother concentration was maintained at 12 μl/l, while the Shellsol A collector concentration was varied from 0 to 1500 g/ton. The air rate and impeller speed were maintained at 4 l/min and 1200 rpm respectively. A pulp density in the region of 9 % was used.

Detailed results of these experiments appear in Section B.2 in Appendix B. For each run the experimental conditions pertaining to that run are presented, together with the flotation results, and the results of size analyses carried out on the flotation concentrates and tailings. A size and ash-by-size analysis of the reconstituted feed was calculated for each run; these are also tabulated in Section B.2.

The results are presented in graphical form in Figures 5.5 and 5.6 below.

As can be seen from Figure 5.5, a yield of only 8.5 % was obtained in the absence of collector, and a collector dosage of about 1500 g/ton was necessary to achieve a yield of 80 %. The ash contents of the respective products (from Section B.2) were 9.2 and 11.2 %.

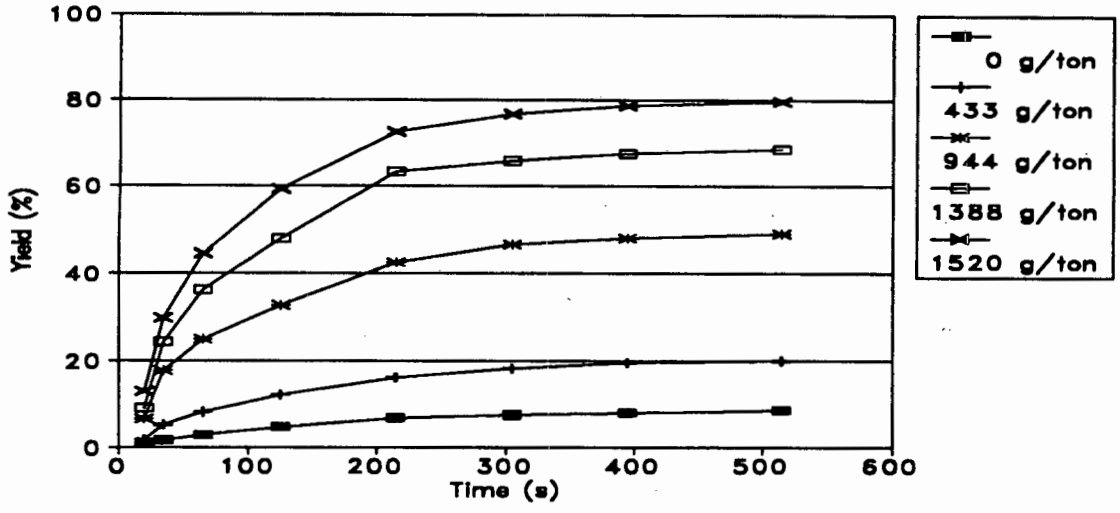

Figure 5.5: Kleinkopje coal batch results at different collector dosages

In Figure 5.6 a separation coefficient defined as:

$$\text{Sep. Coeff.} = \left(1 - \frac{\text{concentrate ash}}{100}\right)\left(\frac{\text{clean coal recovery}}{100}\right)$$

is plotted against the size fraction. This separation coefficient has a value of 1.0 at a recovery of 100 % and a concentrate ash content of 0 %.

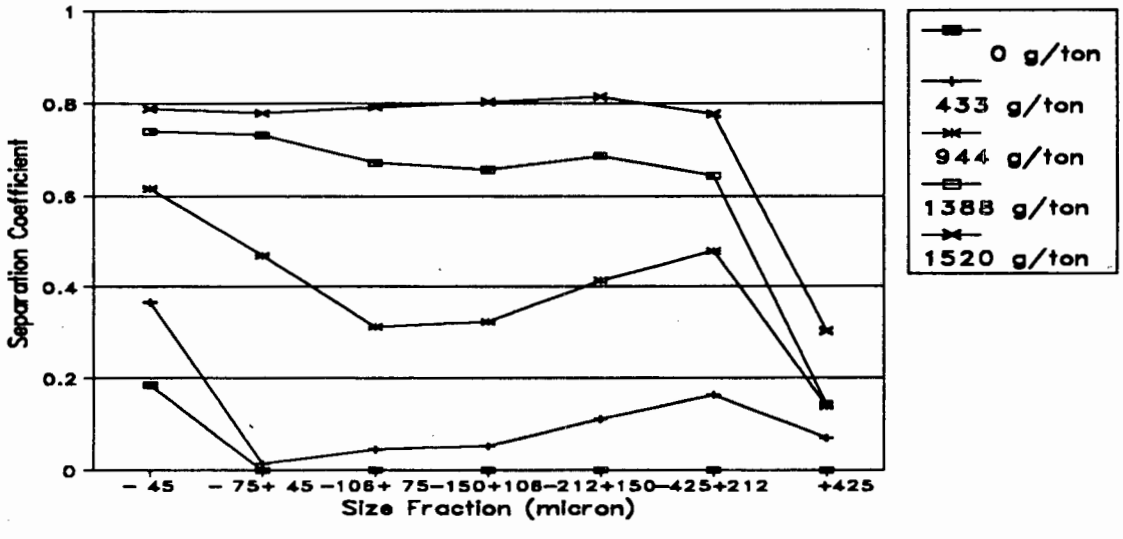

Figure 5.6: Kleinkopje coal batch results for the different size fractions at varying collector dosages

Comparison of Figures 5.5 and 5.6 indicates that at collector dosages below 1000 g/ton (i.e. concentrate yields less than 60 %) the batch cell performed best in the -45 micron and -425+212 micron fractions.

The comparatively high yield obtained in the -45 micron fraction is a result of the high collision efficiency of these particles, as predicted for particles in the region of 30 micron (Dobby and Finch, 1987), and the fact that oils adsorb faster onto finer particles (Anderson, 1988, p207). The poor grade in comparison to that predicted by the float-and-sink results can be attributed to entrainment.

The comparatively good upgrading in the -425+212 micron fraction can be attributed to the higher vitrinite content of this coarser fraction compared with the high inertinite content of the fines, as confirmed by the petrographic analysis (Section 5.1.2 above). Similar results were obtained by Birtek and King (1986).

The poor flotation response of the intermediate, and generally most floatable, size fractions can be attributed to the poorer quality of the material in comparison with that of the coarser fractions, and the "mopping up" effect that the fines have on the collector. Once the collector dosage is increased sufficiently (to 1520 g/ton), the relative performance of the intermediate size fractions improves to being comparable with that of the other size fractions.

In each of Tables B.2.x(c) in Section B.2 of Appendix B, the (calculated) size analysis (i.e. mass percent in each size fraction) and ash-by-size analysis of the reconstituted feed (batch flotation feed) is compared with the 95 % confidence limits for the size analysis and ash-by-size analysis for subsequent representative samples, as calculated in Section A.3.3 of Appendix A#. The above comparison serves to confirm that the batch flotation feed was representative of the sample as a whole.

It should be noted that the limits in the tables in Appendix A were calculated assuming n=3, where n is the number of samples. However, time constraints prevented size analyses from being carried out in

see Tables A.11 and A.18 in Appendix A, as well as Figures A.2 and A.5.

triplicate. Therefore, although some of the results lie outside the calculated confidence limits, such as in batch float 5 (run id. KKB19), no results were discarded on the grounds that the material fed to the batch cell was not a subsample of the population.

A comparison of the results obtained in the float-and-sink, release flotation and batch flotation experiments is shown in Figure 5.7 below. From Figure 5.7 it is apparent that flotation in a batch cell was unable to reproduce the results obtained in the float-and-sink analysis. In addition the difference between the release and batch flotation results indicates the effect of entrainment on the concentrate grade.

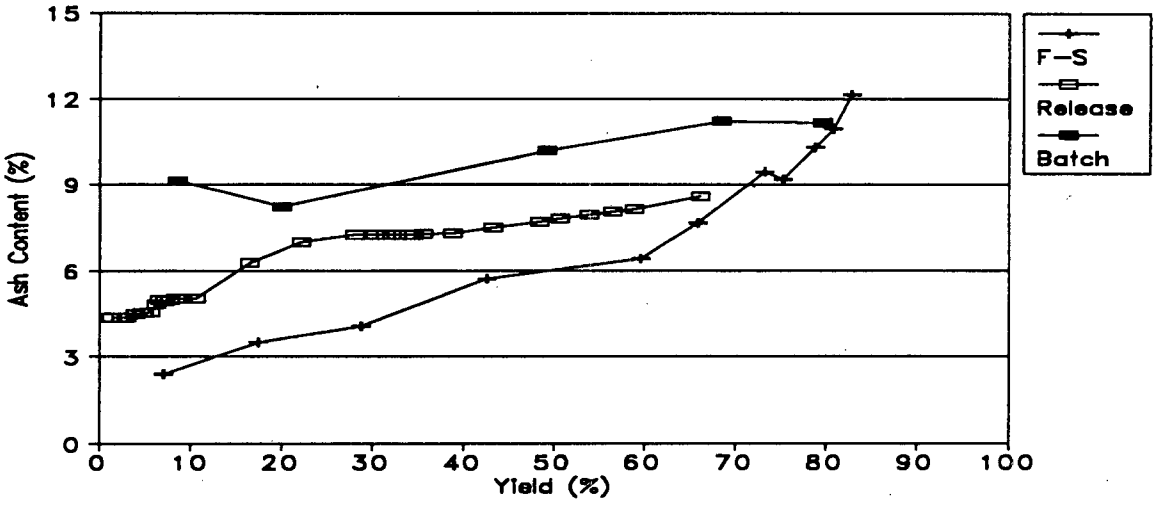

Figure 5.7: Comparison of Kleinkopje coal float-and-sink (F-S), release flotation (RELEASE) and batch flotation results (BATCH)

5.2 Air-Sparged Hydrocyclone Work

This section describes and discusses the results obtained in the two-phase (water and air) and the preliminary three-phase (water, coal and air) ASH testwork. In addition to the above, the results of the three-phase work are compared to the results obtained in the coal characterisation work.

The ASH testwork can be divided into two sections: the two-phase work and the three-phase work.

5.2.1 Two-phase work

Burger (1986, p46) carried out experimental work using a two-phase system, in the absence of frother, to determine the effect of the water feed rate on the performance of the ASH as measured by the water recovery to the overflow (see Section 3.7.1 above). It was decided as part of the preliminary work to investigate the effect of the pedestal and overflow (vortex-finder) diameters at different water feed rates on a two-phase system, in the presence of frother. This work was performed to extend the work carried out by Burger (1986, p46) to a two-phase system with frother and to determine the relative effects of the areas of the overflow (A_{of}) and underflow (A_{uf}) openings on the performance of the ASH. To date numerous workers have reported the ratio (A^*) of the above to be the most important parameter in ASH flotation. In addition, Miller and Ye (1989) recommended operating the ASH at the feed rate at which the recovery of water to the overflow was a minimum. It was expected that two-phase work would provide an indication of the above whilst having the advantage of simpler analysis than three-phase work.

The two-phase testwork was carried out using *ASH II* (ceramic porous cylinder). The ASH configuration and experimental procedure followed are described in Section 4.2 in Chapter Four. The frother concentration used was based on a theoretical pulp density of 3 %, and was maintained at 1000 g/ton. The air rate was maintained at a flow rate of 175 slpm. The effect of the pedestal diameter (at 44.1, 46.0 and 48.2 mm) was investigated at each of the four vortex-finder diameters (10.0, 16.0, 21.5 and 27.5 mm). In addition the water feed rate was varied between 0 and 65 lpm for each of the vortex-finder/pedestal combinations.

The detailed results obtained are given in Section B.3 in Appendix B, and in Figures 5.8(a) to (c) below. In Figures 5.8(a) to (c), the water recovery at each of the different vortex-finder diameters is plotted against the water feed rate, for each of the pedestal

diameters, respectively. The axes in Figures 5.8(a) to (c) are identical to make comparisons between the different pedestal diameters easier.

In each of Figures 5.8(a), (b) and (c) it can be seen that increasing the water feed rate resulted in an initial increase in the water recovery to the overflow, until a maximum recovery was obtained at between 10 and 20 l/min. Further increase in the water feed rate resulted in a decrease in the overflow water recovery, to a minimum at about 35 l/min. Above about 40 l/min, an increase in the feed rate resulted in a slight increase in the water recovery to the overflow. It can also be seen in each of Figures 5.8(a), (b) and (c) that an increase in the diameter of the vortex-finder (at a constant pedestal diameter) increased the overflow water recovery.

Comparison of Figures 5.8(a), (b) and (c) indicates that an increase in the pedestal diameter (at a constant vortex-finder diameter) resulted in an increase in the overflow water recovery at all water flow rates. The results also indicate that the most dramatic increase in the water recovery, with increasing pedestal diameter (d_p), occurs at the point of maximum water recovery, e.g. for d_{vf}=21.5 mm at flow rates in the region of 15 lpm, the overflow water recoveries were 6.51 % (d_p=44.1 mm), 19.30 % (d_p=46.0 mm) and 30.12 % (d_p=48.2).

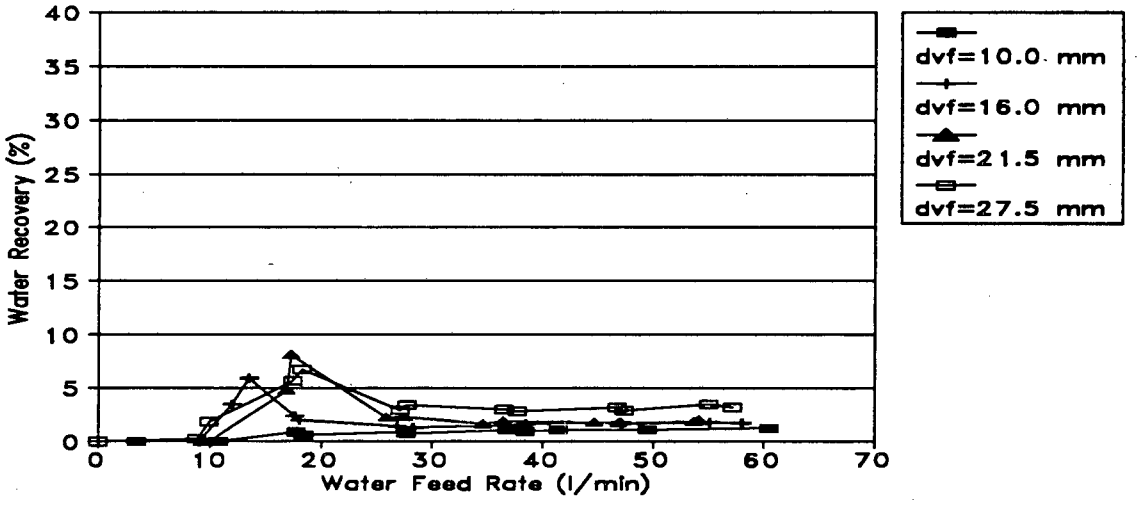

Figure 5.8(a): Water recovery to the overflow for the two-phase system and a pedestal diameter of 44.1 mm (viz. A_{of}/A_{uf}=4 %)

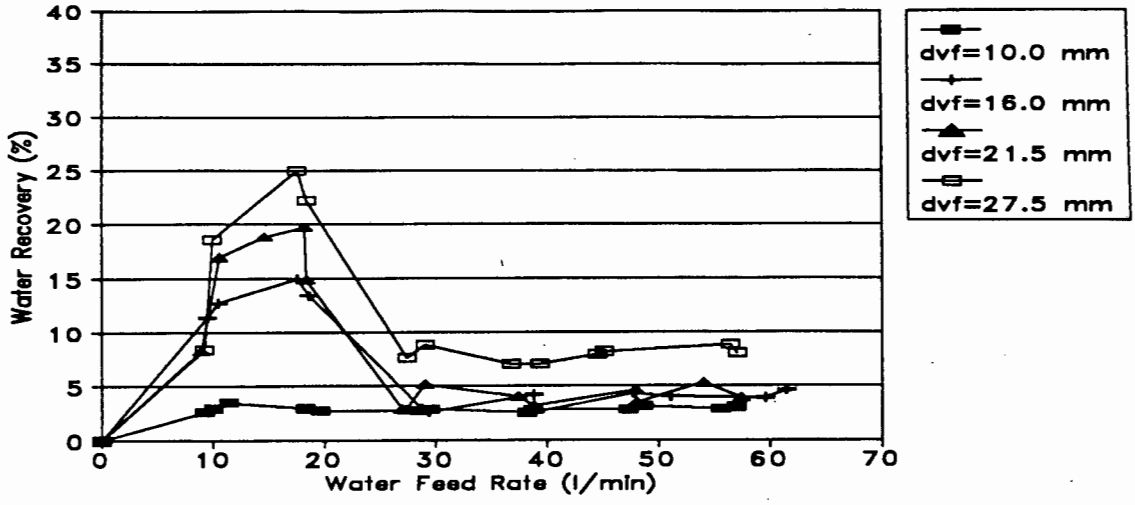

Figure 5.8(b): Water recovery to the overflow for the two-phase system and a pedestal diameter of 46.0 mm (viz. A_{of}/A_{uf}=8 %)

As when operating in the absence of frother (Section 3.7.1 above), the shape of Figures 5(a), (b) and (c) can be explained in terms of the centrifugal force exerted by the liquid, and the radial force of the air acting on the swirl-layer.

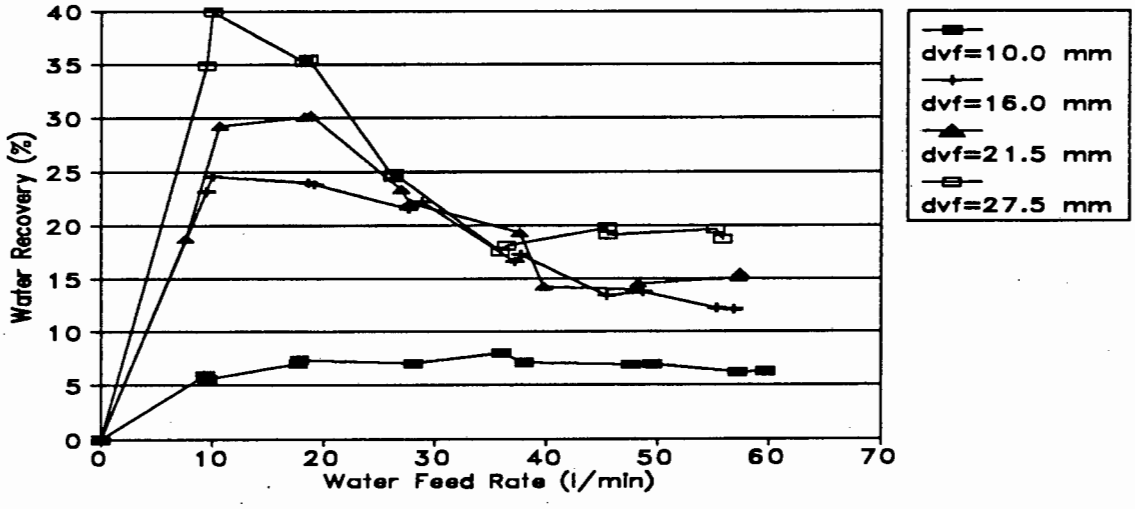

Figure 5.8(c): Water recovery to the overflow for the two-phase system and a pedestal diameter of 48.2 mm (viz. A_{of}/A_{uf}=12 %)

At low feed rates an increase in the centrifugal force associated with an increase in the feed rate is insufficient to counteract the radial

forces acting on the larger volume of liquid present, and hence the water recovery to the overflow increases as more water is carried to the cyclone axis (the radial forces dominate).

However, at a feed rate of between 10 and 20 lpm, an equilibrium between the radial and centrifugal forces is reached, as is indicated by the local maximum.

Further increases in the feed rate result in the increased centrifugal forces dominating, and hence the recovery of water to the overflow decreases to a local minimum.

Increasing the rate even further results in the mass of water entering the cyclone being too great to exit the cyclone via the annular opening. This causes the water to exit the cyclone via the overflow, resulting in the recovery of water to the overflow increasing with increasing water feed rate.

It is apparent from these results that the addition of frother does not change the shape of the curves of the water recovery to the overflow. In addition, the curves obtained above, and by Van Deventer et al (1988) in the flotation of pyrite, suggest that water recovery curves of the same shape are obtained in the flotation of ores in which the mass yield is low. If a similar trend were to occur in the flotation of coal (where the mass yield is generally high), then the results of Miller and Ye (1989) described above (page 99) could be used to determine the optimum slurry feed rate.

Furthermore, the results obtained indicate that a vortex-finder greater than 10 mm in diameter was needed to facilitate froth transport to the overflow, and that the diameter of the vortex-finder and the area of the underflow opening have a significant effect on the performance of the ASH.

5.2.2 Three-phase work

Preliminary three-phase work on the ASH was carried out with the aims of:

i) determining the collector dosage required in the ASH for use in the factorial design experiments described in Chapter Six; and
ii) determining whether or not the ASH was capable of producing concentrate grades comparable with those achieved in batch and column flotation cells.

Six sets of runs were carried out using the *ASH II* unit (see Section 4.2.1.1) and following the procedures outlined in Section 4.2.2.3 in Chapter Four. The HTEB frother concentration was maintained at 1 kg/ton while the Shellsol A collector dosage was varied from 8 to 49 kg/ton. The pulp density used was in the region of 3 % and the air rate was maintained at 175 slpm. Other parameters which were kept constant were: the L_c/d_c ratio (L_c=500 mm, d_c=46.0 mm), the inlet area (A_i=15x9 mm) and the vortex-finder diameter (d_{vf}=21.5 mm).

Vortex-finder lengths (L_{vf}) of 50 and 69 mm were used and both pedestal and orifice type underflow configurations were tested. A 42.0 mm pedestal was used in four of the six sets of runs, and a 40.5 mm pedestal in another. A 14.0 mm orifice (and baffle) was used in the final set. Within each set of runs, the slurry feed rate was varied from about 15 to about 80 l/min.

Detailed results of this work are given in Tables B.4.1 to B.4.6 in Appendix B. Table (a) of each set gives the measured results (sampling times, wet and dry sample masses, and ash contents, of the underflow and overflow samples) and the calculated feed ash content. Table (b) of each set gives the rest of the calculated results (overflow yield, overflow clean coal recovery, separation coefficient, overflow water recovery, slurry feed rate and pulp density). Tables B.4.3(c) and (e) give the results of size analyses carried out on concentrate and tails samples of runs 2 and 7 of set 3, respectively. Tables B.4.3(d) and

(f) give the size and ash-by-size analyses of the (calculated) reconstituted feeds of the respective runs, and (for comparison) the 95 % confidence limits of the size and ash-by-size analyses obtained from Tables A.11 and A.18 of Appendix A.

The results are summarised in Figures 5.9 and 5.10 below. These show, respectively, the variation in the overflow yield and separation coefficient with slurry (feed) flow rate at different collector dosages. From the Figures it is apparent that the highest yields and the best separations were obtained at flow rates in the region of 65 l/min.

At the end of run PWP2 the annular opening at the base of the ASH was found to be *blocked* (this problem was not encountered when using the orifice and baffle underflow configuration). This resulted in run PWP2 having significantly higher water and overall recoveries at low slurry feed rates in comparison with the other runs. In addition it is not correct to use the results obtained during run PWO1 on account of air entrainment by the pump during the run. This resulted in pressure flotation, as described by Nonaka and Uchio (1984), occurring in the conditioning tank, and varying the composition, solids content and flow rate of the feed to the ASH.

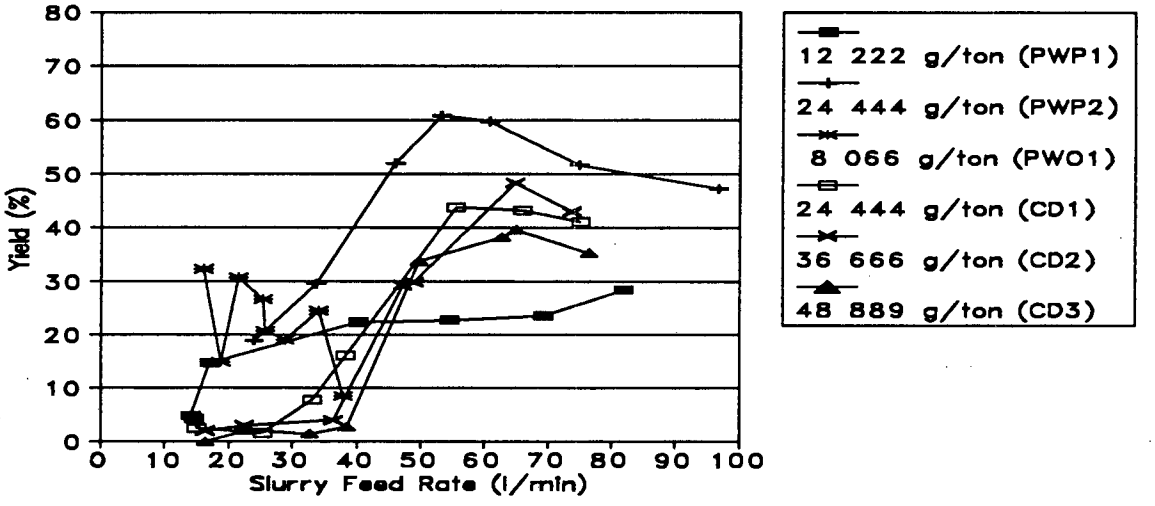

Figure 5.9: Kleinkopje coal ASH results at varying collector dosages and slurry feed rates: overflow yield

In a previous study using the same Kleinkopje coal sample, it was found that the poor flotation response of the coal in a column cell could be attributed to the conditioning phase being the limiting factor (Von Holt, 1992, p123). Von Holt (1992, p123) found that the degree of agitation in a batch cell was an order of magnitude greater than that obtained in conditioning vessels used in conjunction with other flotation machines. For this reason, collector dosages required in the column cell varied between 4 and 12 kg/ton, as opposed to 0.5 to 1 kg/ton in a laboratory batch cell.

Taking the above into consideration, it can be seen from Figure 5.9 that collector dosages in the region of 35 kg/ton were necessary to achieve yields in the region of 50 %. This is an extremely high level of collector addition, and is probably due to inadequate conditioning. In addition, the ASH literature suggests that collector dosages in small diameter ASH's are greater than those required in conventional equipment (Miller and Ye, 1989; Ye et al, 1988; Van Deventer et al, 1988; Cloete et al, 1987). Thus, the collector dosages of between 12.75 and 37.5 kg/ton seem feasible (though probably economically prohibitive).

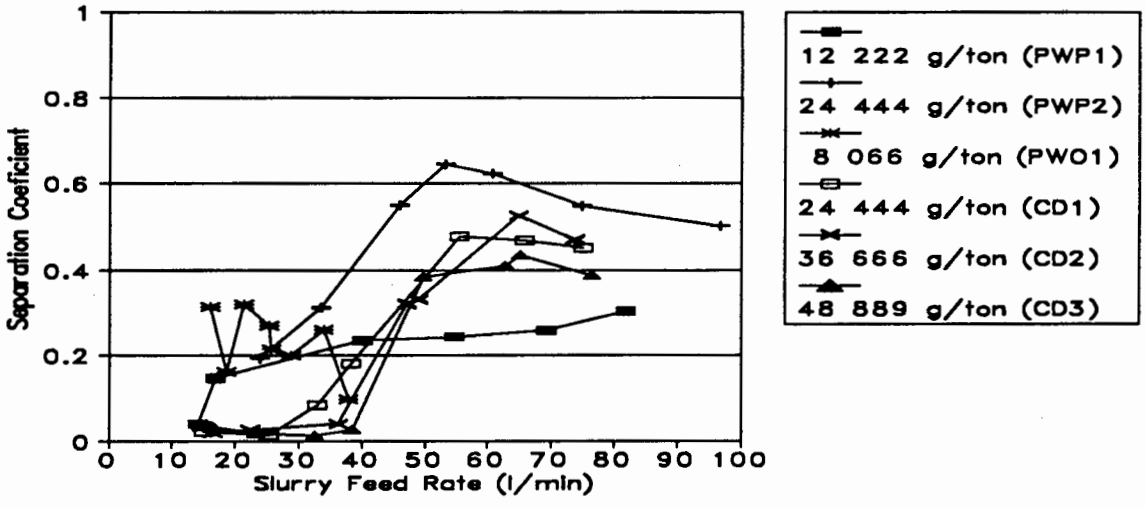

Figure 5.10: Kleinkopje coal ASH results at varying collector dosages and slurry feed rates: separation coefficient

In addition to the above work, the variation of the feed composition to the ASH at different feed rates and feed tank levels was checked by performing size analyses on samples of the concentrate and tails from runs 2 and 7 of the third set of runs (KKCD3). The results of the size and ash-by-size analyses are given in Tables B.4.3(d) and (f) in Appendix B, and summarised in Tables 5.3 and 5.4 below. In both cases the reconstituted feed falls within the 95 % confidence limits calculated for the feed, in terms of the size, ash-by-size and overall ash analyses (see Tables A.11 and A.18 in Appendix A).

Table 5.3: Size analysis of the feed to the ASH at varying slurry feed rate and conditioning tank level

Size Fraction	Reconstituted Feed 2	Reconstituted Feed 7	95 % Confidence Limits
+425	2.87	1.78	1.16 - 4.07
-425+212	10.72	8.88	6.93 - 11.38
-212+150	8.46	7.88	6.42 - 9.04
-150+106	8.39	9.71	7.71 - 9.14
-106+ 75	10.11	9.19	6.92 - 11.19
- 75+ 45	10.85	10.52	10.40 - 14.93
- 45	48.60	52.04	46.34 - 53.35

Table 5.4: Ash-by-size analysis of the feed to the ASH at varying slurry feed rate and conditioning tank level

Size Fraction	Reconstituted Feed 2	Reconstituted Feed 7	95 % Confidence Limits
+425	36.63	28.74	21.33 - 39.27
-425+212	29.23	27.09	21.61 - 33.55
-212+150	25.29	22.47	18.70 - 25.28
-150+106	22.06	18.78	17.77 - 21.73
-106+ 75	18.48	18.92	17.01 - 20.37
- 75+ 45	17.89	18.71	17.94 - 19.98
- 45	25.76	25.21	24.16 - 27.00
Overall	24.42	23.57	21.93 - 25.37

5.3 Comparison of Results

A global representation of all the preliminary ASH results, together with the float-and-sink, release flotation and batch flotation results is given in Figure 5.11 below. Also shown are the results of column cell testwork performed on the same coal sample, using a 5 cm id. laboratory column cell (Von Holt, 1992, p163).

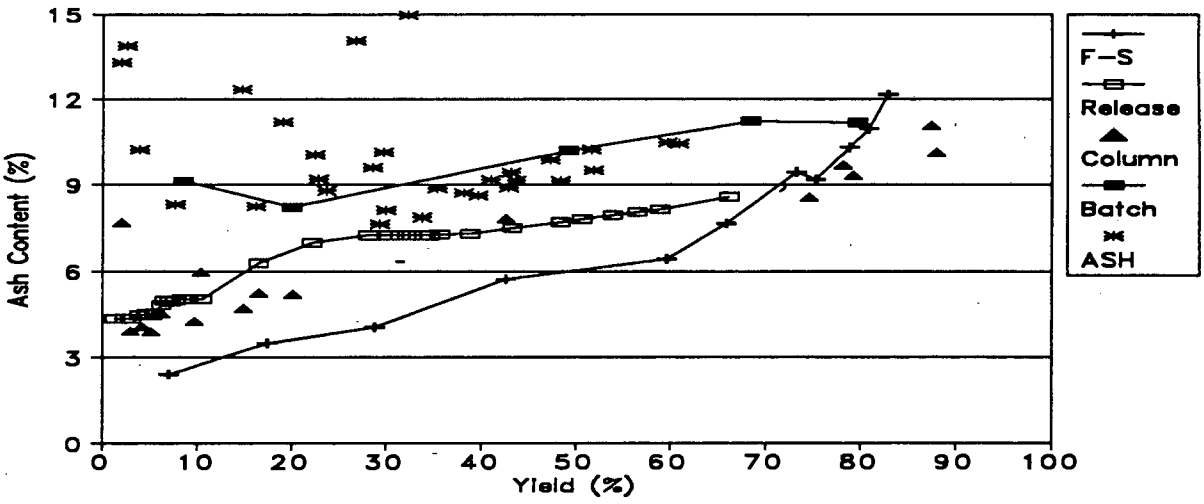

Figure 5.11: Comparison between different types of flotation machines and washability data for Kleinkopje coal

At all yields the column cell produced concentrates of superior grades to those of both the batch cell and the ASH. This can be attributed to the reduction of entrainment (through froth washing) in the column, resulting in the column results approximating those of the release float.

At yields below 30 % the ash contents achieved in the ASH ranged from 8 to over 20 %. This is a result of the variety of conditions (and configurations) tested. It should be stressed that there was no attempt to optimise the performance of the ASH during this work; the aim was rather to examine the performance under a wide range of conditions. At yields between 30 and 60 % the ASH results obtained were generally better than those of the batch cell. In this region the product ash content of both cells increased with increasing yield. From Figure 5.11 it seems as

though the ASH product ash content was increasing at a faster rate than that of the batch cell, with the result that the ASH product ash content may be the same as (or greater than) that of the batch cell at yields above 60 %.

It is of interest to compare the performance of the batch cell and the ASH by size fraction. Size analyses carried out on batch float 2 (KKB2) and ASH run 2 of set KKCD2, both of which gave overall yields in the region of 50 %, are listed in Tables B.2.2(b) and B.2.2(c), and B.4.3(c) and B.4.3(d), respectively, in Appendix B. Figure 5.12 shows the separation coefficients for both runs for each size fraction. It can be seen that the ASH performed better in the finer (-212 micron) size fractions, although the batch cell and the ASH performed equally well in the -45 micron fraction, which contained 50 % of the feed mass. The overall ash content for the batch flotation was 10.2 % while ASH flotation achieved an ash content of 9.1 %.

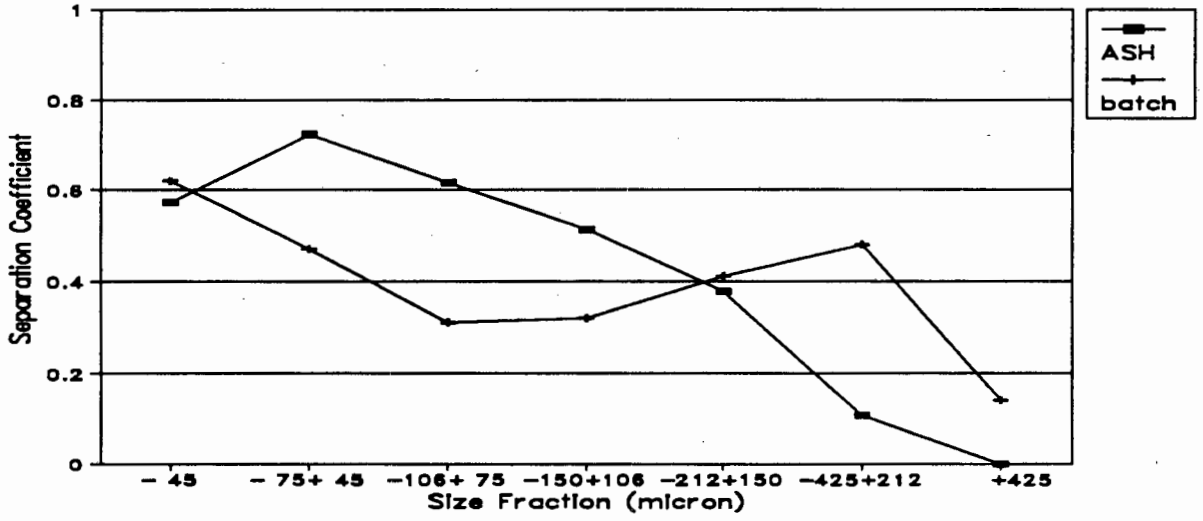

Figure 5.12: Comparison between ASH and batch flotation at an overall yield of 50 %

It should be noted at this stage that the best ASH results were obtained at a flow rate of 65 l/min, or a solids rate of about 2 kg/min. This corresponds to an ASH capacity which is about 48 times greater (cross-

sectional area basis) than the 1.5 t/hr.m^2 obtained using the same material in a column cell (Von Holt, 1992, p168). This difference in capacity is about 576 if the comparison is carried out using a volumetric basis.

5.4 Chapter Summary

Preliminary work carried out involved the characterisation of the coal sample (by size, ash-by-size, float-and-sink and release flotation analyses) and performing batch flotation tests for comparison with the ASH work. In addition two-phase and three-phase ASH work was carried out.

The method of sample preparation used ensured that the samples used throughout the investigation were identical, and representative of the entire sample of Kleinkopje thickener underflow coal.

Petrographic analysis showed that the coal was a low rank bituminous coal with a high inertinite content (≈71.0 %). In addition, a large proportion of the inertinite was concentrated in the -30 micron size fraction. The coal had an ash content of 23.65 % (calculated) and a sulphur content of 1.67 %.

Size and ash-by-size analyses indicated that about 50 % of the material was finer than 45 micron in diameter, and that the coal in this size fraction had the greatest ash content (25.6 %) of the flotation sized particles, i.e. -212 micron fraction. The results indicated that a fair amount of coarse material was also present (20 % greater than 150 micron).

Float-and-sink analyses indicated that the material was evenly distributed in the relative density range between 1.3 and 1.6. The results of the float-and-sink analyses indicated a theoretical yield of 65 % at an ash content of 7 % and 80 % at an ash content of 10 %.

The flotation release analysis showed that the flotation selectivity of the material was poor, and confirmed that two distinct types of material were present. A yield of only 25 % was possible at an ash content of 7 %,

while a yield of 75 % was predicted at an ash content of 10 % (cf. 65 % and 80 % predicted, respectively, by the float-and-sink analysis).

Batch flotation experiments in the absence of collector resulted in a yield of only 8.5 %, at an ash content of 9.2 %: a collector dosage of 1.5 kg/ton was necessary to obtain a yield of 80 %. At low yields (low collector dosages) the best recovery by size fraction was obtained in the +212 and -45 micron size fractions. The above was attributed to the high vitrinite content of the floatable coarse material, the optimum particle size for flotation being in the region of 30 micron, and the "mopping up" effect the fines have on the collector added.

The results of the two-phase ASH work indicated that the recovery of water to the overflow in the presence of frother yielded similar water recovery (to the overflow) curves to those obtained in the absence of frother. In addition, the shapes of these curves were similar to those obtained when floating an ore (pyrite) in which the mass yield is low.

It was found that increasing the feed water flow rate, whilst keeping other factors constant, resulted in an increase in the overflow water recovery. This continued until a maximum overflow was reached, at between 10 and 20 l/min. Further increases in the water feed rate resulted in a decrease in the water recovery, until a minimum water recovery was achieved, at about 40 l/min. Any further increase in the water feed rate resulted in a slow increase in the water recovery to the overflow. The shape of the curves can be described in terms of the comparative strengths of the centrifugal and radial forces acting on the water.

In addition, it was found that a vortex-finder greater than 10 mm in diameter was necessary to facilitate froth transport to the overflow, and that the vortex-finder diameter and the area of the underflow opening have a significant effect on the performance of the ASH.

The three-phase work was carried using a wide range of operating conditions, without any attempt to optimise the performance of the ASH. For all the collector dosages tested the best separations and highest yields were obtained at a slurry feed rate in the region of 65 lpm. It was found that a collector dosage in the region of 35 kg/ton was necessary

to achieve yields of about 50 %. Previous work carried out using the same coal indicated that the conditioning method was a determining factor in the flotation of this particular coal. For this reason and because the literature suggested that ASH flotation generally required increased collector dosages, the high collector dosage was anticipated.

Size and ash-by-size analyses carried out on selected concentrate and tails samples from the ASH showed that the composition of the feed to the ASH did not fluctuate when the feed rate to the ASH, or the level of slurry in the feed tank, varied.

Comparison of the ASH results with those achieved in the batch cell, and with those obtained using the coal sample in a column cell, indicated that neither the batch nor the ASH results were as good as those achieved in the column cell, in terms of grade achieved at a particular yield. At yields of between 30 and 60 % the ASH results were better than those achieved in the batch cell. In this region the product ash content of both cells increased with increasing yield. However, it seemed as though the ASH product ash content was increasing at a faster rate than that of the batch cell, with the result that the ASH product ash content may be the same as (or greater than) that of the batch cell at yields in excess of 60 %.

At yields between 30 and 60 % the ASH concentrate grades were superior to those achieved in the batch flotation cell. Comparing the "performance by size fraction" of the two cells indicated that the ASH performed better in the intermediate sizes (-212+45 micron), the batch cell performed better in the coarse sizes (+212 micron) and both cells performed equally in the fines (-45 micron).

An important result of the work carried out was the determination of the relative capacities of the ASH and the column cell. At a slurry feed rate of 65 l/min, at 3 % solids, the ASH had a capacity in the region of 72 $t/hr.m^2$ or 144 $t/hr.m^3$ compared with the capacity of 1.5 $t/hr.m^2$ or 0.25 $t/hr.m^3$ of the column cell. This resulted in the ASH having a capacity of about 48 (surface area basis) to 576 (volumetric basis) times that of the column cell.

CHAPTER SIX

FACTORIAL DESIGN RESULTS AND DISCUSSION

The results obtained in the preliminary work (reported in Chapter Five) suggested that the ASH could be used to beneficiate "ultrafine" coal. The results further suggested that results comparable to those obtained in conventional batch flotation cells were possible. It was therefore decided to carry out a more thorough investigation into the effect of various design and operating parameters on the performance of the ASH. This Chapter describes and discusses the results of the investigation carried out.

The work carried out in this Chapter can be divided into three main sections:

i) the factorial design investigation;
ii) the pulp density/air rate investigation; and
iii) the collector dosage investigation.

To date numerous researchers, in a wide variety of fields, have recognised the value of statistically designed experiments for obtaining the most valid data from the least number of experiments. For this reason it was decided to use the method of Factorial Design to determine the effects of various parameters, and their relative rank, on the flotation of coal in the ASH. One of the greatest advantages of statistically designed experiments is the reliable estimate of the errors involved, and hence the confidence with which conclusions can be drawn. An excellent review of the method of factorial design is contained in Von Holt (1992).

The parameters investigated in the factorial design were the ASH length to diameter ratio (L_c/d_c), the underflow configuration, the ratio of the overflow area to the underflow area (A^*), the area of the inlet (A_{inlet}), the ratio of the air feed rate to the slurry feed rate (Q^*) and the ratio of the vortex-finder length to the ASH diameter (L_{vf}/d_c). These were the parameters found previously by other researchers to be most significant in affecting the performance of the ASH (see literature review in Chapter Three).

Pulp density was excluded from the factorial design for a very specific reason. If the pulp density had been chosen as a parameter in the factorial design, then the pulp density used for the first run would have had to be used for the entire set of runs (runs carried out using the same tank of slurry). This would have affected the random nature of choosing the run order required when using the method of factorial design. The problem was solved by carrying out a separate pulp density investigation which also enabled the effect of the air rate on the performance of the ASH to be confirmed as the factorial design results proved to be inconclusive for this parameter.

In addition to the factorial design and pulp density investigations, a collector dosage investigation using an ASH configuration which maximised the overflow yield was carried out. This was an attempt to reduce the collector dosage found to be necessary during the preliminary work and used during the factorial design analysis.

This Chapter begins with a description of the factorial design - the levels of the parameters investigated and the design used. This is followed by a statistical analysis of the results obtained. Details of the pulp density/air rate and collector dosage investigations are then presented. The next section contains an analysis of the role of particle size in the ASH. A discussion of the results obtained in the experimental work and how they compare with the results obtained by other researchers follows. Finally a discussion of the use of the ASH for the flotation of coal, with specific reference to the results obtained, is presented.

6.1 Experimental Details

In the factorial design carried out on the ASH, certain parameters were held constant while others were varied. The Kleinkopje coal sample used in the preliminary work (Chapter Five) was also used in this investigation. The aim of the work was to determine the relative importance of various design and operating parameters of the ASH, and their effects on the product yield, clean coal recovery, water recovery and product grade (ash content).

6.1.1 Parameter levels

The levels used for certain parameters were chosen from the literature survey on the use of the ASH on coal and other minerals (Chapter Three), while the levels of other parameters were chosen as a result of the preliminary work (Chapter Five).

The parameters which were held constant during the factorial design are listed in Table 6.1 below, together with the values used in the testwork.

Table 6.1: Parameters held constant during the factorial design investigation

Parameter	Value Used
$d_{cyclone}$	46 mm
Q_{slurry}	65 l/min
pulp density (solids %)	3 %
collector dosage	37 500 g/ton Shellsol A
frother dosage	1000 g/ton HTEB

The parameters varied, and their respective high (+) and low (-) values, are listed in Table 6.2 below.

Table 6.2: Low and high values of the parameters varied during the factorial design investigation

Variable	Parameter	Low (-)	High (+)
A	$A_{overflow}/A_{underflow}$	0.54	1.34
	$d_{vortex-finder}$	16.0 mm	21.7 mm
	$d_{pedestal}$	40.5 mm	42.0 mm
	$d_{orifice}$	21.8 mm	18.8 mm
	% of $d_{cyclone}$	11.95%	8.7 %
B	$L_{cyclone}/d_{cyclone}$	6.52	10.87
	$L_{cyclone}$	300 mm	500 mm
C	A_{inlet}	15x9 mm	15x12 mm
D	underflow configuration	pedestal	orifice
E	Q_{air}/Q_{slurry}	2.69	4.62
	Q_{air}	175 slpm	300 slpm
F	L_{vf}/d_c	1.0	1.5
	L_{vf}	46 mm	69 mm

6.1.2 Structure of the factorial design

The form of the factorial design used was obtained from McLean and Anderson (1984, p251) and is listed below in Table 6.3 below.

This design was chosen as it is a resolution (iv) design. This means that main effects are confounded with 3-factor and higher order interactions, and 2-factor interactions are confounded with 2-factor and higher order interactions.

This type of design allows the main effects to be determined directly, as 3-factor and higher order interactions can be assumed to have no effect. In addition, certain 2-factor interactions can be disregarded, and this allows other 2-factor interactions to be quantified. For example, if two main effects are found to have no effect, then there is a very strong likelihood that any interaction between the two would be negligible.

Table 6.3: Fractional factorial design used (after McLean and Anderson (1984, p251))

Run no	Variable					
	A	B	C	D	E	F
1	-	-	-	-	-	-
2	-	-	+	+	+	+
3	+	+	-	+	-	+
4	+	+	+	-	+	-
5	-	+	-	-	+	+
6	-	+	+	+	-	-
7	+	-	-	+	+	-
8	+	-	+	-	-	+
9	+	+	+	+	+	+
10	+	+	-	-	-	-
11	-	-	+	-	+	-
12	-	-	-	+	-	+
13	+	-	+	+	-	-
14	+	-	-	-	+	+
15	-	+	+	-	-	+
16	-	+	-	+	+	-

In the above design I = ABCE = ABDF = CDEF.

Further information detailing the definitions, calculations and procedures involved in the design and analysis of factorial designs can be obtained from standard statistics textbooks such as Montgomery (1984), Mason et al (1989) and McLean and Anderson (1984). In addition, Von Holt (1992) has reviewed the theory, definitions and calculations pertaining to factorial design, and carried out sample problems and calculations.

6.1.3 Experimental programme

The experimental programme involved carrying out the factorial design runs in a random order. This random order was determined by "flipping a coin". The same method was used to determine whether or not *duplicate* and *repeat* runs were carried out (see Section 4.2.2.1 for definitions). This resulted in the number of runs per set (batch of slurry) varying from set to set.

Sixteen runs were carried out in each of the first (KKFD"A") and second (KKFD"B") factorial designs. KKFD"C" and "D" consisted of runs carried

out as a result of large differences between the results obtained in KKFD"A" and "B". However, the experimental order was always random, and the ASH was dissembled and reassembled between all *replicates*.

The experimental method followed when carrying out a run is described in Section 4.2.2.3.

6.2 Results

A total of 62 factorial design runs were carried out (*primary*, *duplicate*, *repeat* and *replicate*). The experimental results of these runs are listed in Table C.1(a) in Appendix C, and the calculated values (coal yield and recovery, water recovery, separation coefficient, etc.) are listed in Table C.1(b) The results of the *duplicate* and *repeat* runs are listed as KKFD-A_iX(y_i), while *replicate* runs are listed as KKFD-A_iX where:

A_i = *replicate* identifier; A, B, C, D
X = run number; from 1 to 16
y_i = *duplicate* and *repeat* runs.

A major problem in the operation of the ASH rig was found to be the reproducibility of any run carried out on a different day using a reassembled cyclone and a new batch of slurry, viz. reproducibility between *replicates*. However, where *duplicate* and *repeat* runs were carried out, the results were found to be in close agreement with one another.

A statistical analysis carried out on the pulp density and the volumetric feed rate to the ASH during the factorial design experiments showed that the solids feed rate variations could be attributed to random error. The results of this analysis are listed in Section C.1.1.1 in Appendix C. For the above reason the poor reproducibility between *replicates* could be primarily attributed to errors in dissembling and reassembling the ASH. These problems were to be expected as a consequence of the small size of the unit being used (to date no other researchers have reported the results of their reproducibility experiments).

The results obtained in all the factorial design runs listed in Tables C.1(a) and (b) of Appendix C are presented graphically in Figure 6.1 below, together with the float-and-sink, release float and batch flotation results.

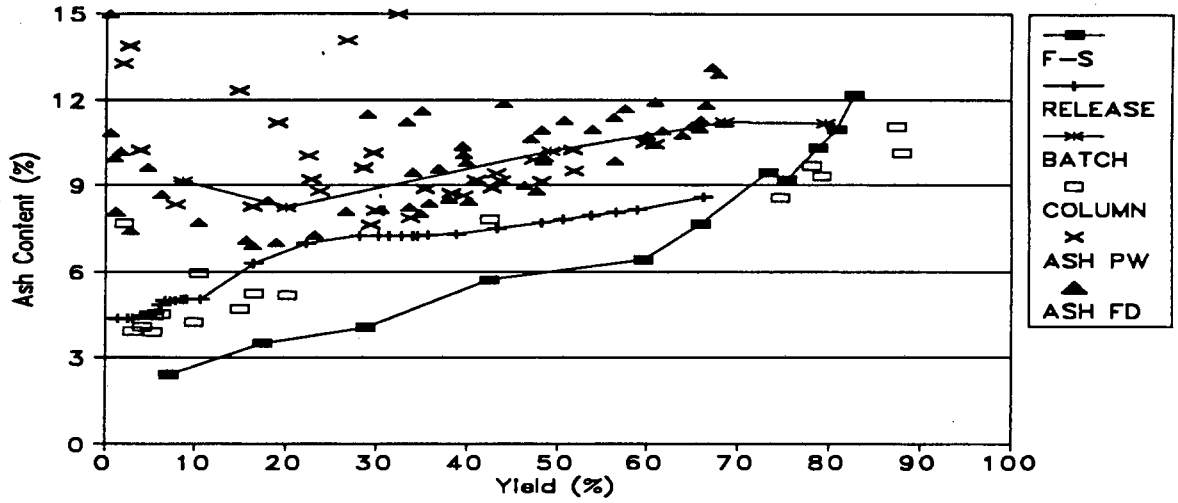

Figure 6.1: Global results obtained during the Kleinkopje factorial design investigation (ASH FD) compared with the results of the float-and-sink (F-S) and release flotation (RELEASE) analyses, and the batch (BATCH), column (COLUMN) and preliminary ASH (ASH PW) flotation results.

From Figure 6.1 it can be seen that the range of ASH conditions investigated produced a wide range of results, some of which were better, and some poorer than those obtained in the batch flotation experiments. However, at yields between 30 and 40 % much better grades were achieved in the ASH than in the batch cell, with some of the ASH results approaching the limits predicted by the release float curve.

6.3 Statistical Analysis

Exclusion of problematic runs (runs in which problems were identified) reduced the number of runs for statistical error analysis from 62 to 50. These 50 runs are designated the "original factorial design"; the experimental results obtained in these runs are listed in Table C.2(a) and the calculated values in Table C.2(b), in Appendix C. Averaging the

results of *duplicate* and *repeat* runs contained in the original factorial design further reduced the number of (*replicate*) runs to 40. The results of these 40 runs were used in the original factorial design *analysis*. The data used in this analysis are summarised in Tables C.2(c_1) and (c_2) in Appendix C, and reproduced in Tables 6.4 and 6.5 below.

Table 6.4: Yield and concentrate ash data used in original Kleinkopje factorial design analysis

Experimental	Yield				Concentrate Ash			
Conditions	A	B	C	D	A	B	C	D
1	15.80	1.18	2.79		7.09	8.06	7.43	
2	56.33	60.68			9.84	10.42		
3		43.96	48.35			11.86	10.93	
4	30.29	10.35	17.91	5.46	8.15	7.72	8.46	9.14
5	0.48	0.85			15.57	16.98		
6		46.32	40.78	47.70		8.97	9.14	8.80
7		56.88		60.82		11.53		11.91
8	66.98		63.86		11.07		10.74	
9	28.08	53.98		33.28	11.49	10.97		11.23
10	36.87	16.22	30.47	40.21	8.44	6.90	8.14	8.43
11	1.77	1.22			10.18	16.28		
12	65.92	64.89			11.28	11.10		
13	67.01	67.76			13.11	12.89		
14	48.47	39.56	34.81		9.89	10.37	8.02	
15	0.66	1.06			10.83	9.95		
16	18.87	23.08			7.01	7.26		

Table 6.5: Recovery and water recovery data used in original Kleinkopje factorial design analysis

Experimental	Clean Coal Recovery				Water Recovery			
Conditions	A	B	C	D	A	B	C	D
1	19.22	1.43	3.36		1.35	0.57	0.42	
2	66.64	71.68			9.33	11.31		
3		50.49	56.34			28.93	24.78	
4	36.55	12.58	22.17	6.50	6.56	2.89	4.72	2.37
5	.54	0.92			0.55	0.67		
6		55.44	47.99	57.31		7.11	9.44	7.77
7		65.7		68.39		29.32		26.32
8	77.72		73.92		11.60		13.35	
9	32.53	62.16		38.52	17.51	21.04		19.16
10	43.97	19.69	36.68	48.93	6.32	2.51	5.37	3.90
11	2.04	1.33			1.09	1.15		
12	77.52	76.86			17.52	15.24		
13	76.85	78.08			30.38	33.97		
14	57.68	46.59	42.52		11.61	6.67	5.56	
15	0.78	1.27			0.50	0.54		
16	23.56	27.62			2.81	4.05		

6.3.1 Original factorial design error analysis

The statistical error analysis was carried out using a spreadsheeting package, QUATTRO PRO, and is given in Tables C.2(d), (e) and (f) in Appendix C. The calculations carried out are described in Section C.1.2 of Appendix C. From statistical tables, the *F*-factors at various significance levels are:

$F_o(.025, 1, 16) = 6.12$
$F_o(.05, 1, 16) = 4.49$
$F_o(.10, 1, 16) = 3.05$
$F_o(.25, 1, 16) = 1.42$

In the determination of the above *F*-factors the number of degrees of freedom used was 16. This was because the factorial design used had 16 runs.

6.3.1.1 yield error analysis

A summary table of the yield error analysis is given in Table 6.6 below. Values in the table were obtained from Tables C.2(d), (e) and (f) in Appendix C. In Table 6.6, and subsequent error analysis tables, lk is the magnitude of the (variable) contrast (viz. the sum of the effects resulting from an increase in the variable under discussion from its low to its high value) and MSlk is the mean square of the contrast. The *F*-ratio term = MSlk/MSe where MSe is the mean square error#.

From Table 6.6 it can be seen that the yield of concentrate from the ASH is affected by three main effects and one interaction term. The significant main effects are:

a) the underflow configuration, at the 2.5 % significance level;
b) the $A_{overflow}/A_{underflow}$ ratio, at the 10 % significance level; and
c) the $L_{cyclone}/d_{cyclone}$ ratio, at the 10 % significance level.

The calculation of these statistics is described in Section C.1.2 of Appendix C.

The interaction term which affects the ASH yield is the AD + BF term, which represents the sum of the interactions between the $A_{overflow}/A_{underflow}$ ratio and the underflow configuration, and between the $L_{cyclone}/d_{cyclone}$ ratio and the $L_{vortex\text{-}finder}/d_{cyclone}$ ratio, at the 25 % significance level.

Table 6.6: Summary table for yield error analysis

Parameter	Yield Contrast lk	Yield Contrast MSlk	Yield *F*-ratio
Main Effects			
A - $A_{overflowf}/A_{underflow}$	164.72	211.97	3.75
B - $L_{cyclone}/d_{cyclone}$	-165.62	214.29	3.79
C - A_{inlet}	22.52	3.96	0.07
D - Underflow configuration	237.73	441.54	7.81
E - Q_{air}/Q_{slurry}	- 91.81	65.84	1.16
F - $L_{vortex\text{-}finder}/d_{cyclone}$	69.23	37.44	0.66
Interactions			
AB + CE + DF	- 36.49	10.40	0.18
AC + BE	- 1.80	0.03	0.00
AD + BF	-122.68	117.59	2.08
AE + BC	- 19.51	2.97	0.05
AF + BD	- 33.65	8.85	0.16
CD + EF	13.25	1.37	0.02
CF + DE	- 2.40	0.04	0.00
ACD + BDE + BCF + AEF	- 30.67	7.35	0.13
ACF + BEF + BCD + ADE	48.74	18.56	0.33
	MSe	56.56	
	se	7.52	

6.3.1.2 concentrate ash error analysis

A summary table of the overflow (concentrate) ash error analysis is given in Table 6.7 below. Values in the table were obtained from Tables C.2(d), (e) and (f) in Appendix C. It is apparent that the overflow ash content is not affected by any of the parameters (main effects) varied, even at the 25 % significance level.

The results indicate that if any of the main effects could be considered to have an effect on the grade then it would be the $L_{vortex\text{-}finder}/d_{cyclone}$ ratio. This possibility is supported by the

interaction terms affecting the grade all containing the $L_{vortex-finder}/d_{cyclone}$ ratio, even though the significance levels are between 10 and 25 %.

Table 6.7: Summary table for concentrate ash error analysis

Parameter	OF Ash Contrast lk	OF Ash Contrast MSlk	OF Ash *F*-ratio
Main Effects			
A - $A_{overflow}/A_{underflow}$	- 0.82	0.01	0.00
B - $L_{cyclone}/d_{cyclone}$	- 5.39	0.23	0.20
C - A_{inlet}	3.58	0.10	0.09
D - Underflow configuration	0.67	0.00	0.00
E - Q_{air}/Q_{slurry}	6.16	0.30	0.25
F - $L_{vortex-finder}/d_{cyclone}$	13.02	1.32	1.17
Interactions			
AB + CE + DF	- 6.78	0.36	0.32
AC + BE	2.39	0.04	0.04
AD + BF	20.67	3.34	2.94
AE + BC	- 11.23	0.98	0.87
AF + BD	- 9.23	0.67	0.59
CD + EF	0.20	0.00	0.00
CF + DE	- 14.84	1.72	1.52
ACD + BDE + BCF + AEF	- 1.71	0.02	0.02
ACF + BEF + BCD + ADE	14.13	1.56	1.37
	MSe	1.13	
	se	1.07	

6.3.1.3 concentrate recovery error analysis

A summary table of the overflow (concentrate) coal recovery error analysis is given in Table 6.8 below. Values in the table were obtained from Tables C.2(d), (e) and (f) in Appendix C. As could be expected from the concentrate yield and ash error analyses discussed in Sections 6.3.1.1 and 6.3.1.2 above, the coal recovery from the ASH is affected by the same main effects, and to the same degree, as the yield, viz.:

a) the underflow configuration, at the 2.5 % significance level;

b) the $A_{overflow}/A_{underflow}$ ratio, at the 10 % significance level; and

c) the $L_{cyclone}/d_{cyclone}$ ratio, at the 10 % significance level.

Table 6.8: Summary table for concentrate recovery error analysis

Parameter	Coal Recovery Contrast lk	Coal Recovery Contrast MSlk	Coal Recovery *F*-ratio
Main Effects			
A - $A_{overflow}/A_{underflow}$	186.92	272.85	3.43
B - $L_{cyclone}/d_{cyclons}$	-189.79	281.40	3.54
C - A_{inlet}	24.37	4.64	0.06
D - Underflow configuration	274.89	590.34	7.42
E - Q_{air}/Q_{slurry}	-106.82	89.15	1.12
F - $L_{vortex-finder}/d_{cyclone}$	80.54	50.67	0.64
Interactions			
AB + CE + DF	- 39.56	12.23	0.15
AC + BE	- 3.51	0.10	0.00
AD + BF	153.27	183.52	2.31
AE + BC	- 21.56	3.63	0.05
AF + BD	- 37.96	11.26	0.14
CD + EF	18.37	2.64	0.03
CF + DE	- 4.08	0.13	0.00
ACD + BDE + BCF + AEF	- 33.60	8.82	0.11
ACF + BEF + BCD + ADE	54.73	23.40	0.29
	MSe	79.52	
	se	8.92	

In addition, the sum of the interactions between the $A_{overflow}/A_{underflow}$ ratio and the underflow configuration, and between the $L_{cyclone}/d_{cyclone}$ ratio and the $L_{vortex-finder}/d_{cyclone}$ ratio, affects the overflow recovery at the 25 % significance level.

6.3.1.4 overflow water recovery error analysis

A summary table of the overflow water recovery error analysis is given in Table 6.9 below. Values in the table were obtained from Tables C.2(d), (e) and (f) in Appendix C. It is apparent from Table 6.9 that the ASH configuration has a marked effect on the water

recovery to the overflow. The main effects and interaction terms affecting the overflow water recovery are the same as those affecting the yield and recovery, viz.:

a) the underflow configuration, at the 2.5 % significance level;
b) the $A_{overflow}/A_{underflow}$ ratio, at the 2.5 % significance level; and
c) $L_{cyclone}/d_{cyclone}$ ratio, at the 10 % significance level.

Table 6.9: Summary table for overflow water recovery error analysis

Parameter	Water Recovery Contrast lk	Water Recovery Contrast MSlk	Water Recovery *F*-ratio
Main Effects			
A - $A_{overflow}/A_{underflow}$	93.90	68.89	21.73
B - $L_{cyclone}/d_{cyclone}$	- 41.60	13.52	4.27
C - A_{inlet}	- 0.26	0.00	0.00
D - Underflow configuration	112.21	98.37	31.04
E - Q_{air}/Q_{slurry}	- 27.20	5.78	1.82
F - $L_{vortex-finder}/d_{cyclone}$	12.25	1.17	0.37
Interactions			
AB + CE + DF	- 9.73	0.74	0.23
AC + BE	2.01	0.03	0.01
AD + BF	41.80	13.65	4.31
AE + BC	- 6.58	0.34	0.11
AF + BD	- 16.54	2.14	0.67
CD + EF	- 9.04	0.64	0.20
CF + DE	- 18.22	2.59	0.82
ACD + BDE + BCF + AEF	- 5.77	0.26	0.08
ACF + BEF + BCD + ADE	4.11	0.13	0.04
	MSe	3.17	
	se	1.78	

In addition the sum of the interactions between the $A_{overflow}/A_{underflow}$ ratio and the underflow configuration, and between the $L_{cyclone}/d_{cyclone}$ ratio and the $L_{vortex-finder}/d_{cyclone}$ ratio, affect the water recovery to the overflow at the 10% significance level.

6.3.2 Modified factorial design

Because of the problems experienced when performing *replicate* runs, the calculated MSe and se values were numerically rather large, e.g. $Yield_{MSe}$ = 56.56 and $Yield_{se}$ = 7.52 (see Table 6.6 above), thus reducing the power of the *F*-tests; i.e. the analysis was only able to detect large effects. For this reason the factorial design analysis was repeated, but this time runs which seemed incorrect were excluded from the analysis, purely on the basis that they were considered to be "outliers".

For example, the yield in run KKFD-B9 was 53.98 %, whereas the yields in runs KKFD-A9 (1) and KKFD-D9 were 28.29 and 33.28 % respectively (see Table 6.4). For this reason run KKFD-B9 was considered to be an "outlier", and excluded from further analysis. Other runs which were excluded were KKFD-B10 and KKFD-A1.

In the case where *replicate* runs produced a scatter of results, as in KKFD-A_i4, where yields of 30.29 (av. for run KKFD-A4), 10.35, 17.91 and 5.46 % (av. for run KKFD-D4) were obtained, all the runs were retained in the analysis. The experimental results of runs used in the statistical analysis of the *modified factorial design* are listed in Table C.3(a) and the calculated values are listed in Table C.3(b) of Appendix C. Averaging the results of the duplicate and repeat runs reduced the number of runs (*replicates*) to 37. These results are summarised in Tables C.3(c_1) and (c_2) in Appendix C, and reproduced in Tables 6.10 and 6.11 below.

A statistical analysis of the modified factorial design was carried out using the QUATTRO.PRO spreadsheeting package; the results of the error analysis appear in Tables C.3(d), (e) and (f) in Appendix C. Exclusion of runs KKFD-A1, KKFD-B9 and KKFD-B10 reduced the MSe and se values as indicated in Table 6.12 below.

Table 6.10: Yield and concentrate ash data used in modified Kleinkopje factorial design analysis

Experimental	Yield				Concentrate Ash			
Conditions	A	B	C	D	A	B	C	D
1		1.18	2.79			8.06	7.43	
2	56.33	60.68			9.84	10.42		
3		43.96	48.35			11.86	10.93	
4	30.29	10.35	17.91	5.46	8.15	7.72	8.46	9.14
5	0.48	0.85			15.57	16.98		
6		46.32	40.78	47.70		8.97	9.14	8.80
7		56.88		60.82		11.53		11.91
8	66.98		63.86		11.07		10.74	
9	28.08			33.28	11.49			11.23
10	36.87		30.47	40.21	8.44		8.14	8.43
11	1.77	1.22			10.18	16.28		
12	65.92	64.89			11.28	11.10		
13	67.01	67.76			13.11	12.89		
14	48.47	39.56	34.81		9.89	10.37	8.02	
15	0.66	1.06			10.83	9.95		
16	18.87	23.08			7.01	7.26		

Table 6.11: Recovery and water recovery data used in modified Kleinkopje factorial design analysis

Experimental	Clean Coal Recovery				Water Recovery			
Conditions	A	B	C	D	A	B	C	D
1		1.43	3.36			0.57	0.42	
2	66.64	71.68			9.33	11.31		
3		50.49	56.34			28.93	24.78	
4	36.55	12.58	22.17	6.5	6.56	2.89	4.72	2.37
5	0.54	0.92			0.55	0.67		
6		55.44	47.99	57.31		7.11	9.44	7.77
7		65.7		68.39		29.32		26.32
8	77.72		73.92		11.60		13.35	
9	32.53			38.52	17.51			19.16
10	43.97		36.68	48.93	6.32		5.37	3.90
11	2.04	1.33			1.09	1.15		
12	77.52	76.86			17.52	15.24		
13	76.85	78.08			30.38	33.97		
14	57.68	46.59	42.52		11.61	6.67	5.56	
15	0.78	1.27			0.50	0.54		
16	23.56	27.62			2.81	4.05		

Table 6.12: MSe and se values for the original and modified Kleinkopje factorial designs

	MSe		se	
	Original	Modified	Original	Modified
Yield	56.56	27.59	7.52	5.25
Concentrate Ash	1.13	1.20	1.07	1.10
Coal Recovery	79.52	39.64	8.92	6.30
Water Recovery	3.17	3.11	1.78	1.76

The modified factorial design analysis did not result in a change in the ranking of the parameters investigated, but it did result in the air rate having a weak effect (at the 25% significance level) on the overflow yield, recovery and water recovery responses.

6.4 Pulp Density / Air Rate Investigation

As described at the beginning of this Chapter, including the pulp density parameter in the factorial design would have affected the random sequence of the runs carried out. For this reason a separate investigation was carried out to determine the effect of pulp density on the performance of the ASH. The uncertainty of the factorial design results with respect to the effect of the air rate on the performance of the ASH led to this parameter also being further investigated.

The configuration of the ASH was chosen in such a way as to maximise the overflow yield. This was because the results of the factorial design indicated that the overflow ash content was not significantly affected by any of the parameters investigated. However, the factorial design results suggested that the L_{vf}/d_c ratio might have a slight effect on the concentrate grade. It was therefore decided to use the larger L_{vf}/d_c ratio to enable the results to be directly compared with those obtained in runs KKFD-13 (in which the smaller L_{vf}/d_c ratio was used) while the other parameters remained constant.

The parameters varied or held constant, and their respective values, are listed in Table 6.13 below. The pulp densities investigated ranged from 9.4 % to 1.6 %, and the air rates investigated were 125, 175 and 300 slpm. The frother addition rate was chosen to be on a g/ton of solids basis, with the result that the frother concentration in the slurry decreased (on a volumetric basis) when water was added to reduce the pulp density.

A total of 12 pulp density runs were carried out according to the method described in Section 4.2.2.3. Four different pulp densities (9.4, 5.3, 3.2 and 1.6 % solids) were each tested at 3 different air rates (125, 175

and 300 slpm). However no *duplicate*, *repeat* or *replicate* runs were performed. The experimental results and the calculated values are listed in Tables C.4(a) and (b) in Appendix C, respectively.

Table 6.13: Parameters used during the pulp density/air rate investigation

Parameter	Values Used
$d_{cyclone}$	46 mm
$L_{cyclone}$	300 mm
underflow configuration	orifice
$d_{orifice}$	18.8 mm
$L_{vortex-finder}$	69 mm
$d_{vortex-finder}$	21.7 mm
A_{inlet}	15x12 mm
collector dosage	37 500 g/ton Shellsol A
frother dosage	1000 g/ton HTEB
Q_{slurry}	65 l/min
Q_{air}	125, 175, 300 slpm
pulp density (solids %)	9.4 % to 1.6 %

6.4.1 Global Results

Before proceeding with a statistical analysis of the results, it is of interest to consider the overall results obtained in the pulp density/air flow rate investigation, compared with those obtained in the previous experiments. These are presented graphically in Figure 6.2 below, together with the coal characterisation results from Chapter Four. From Figure 6.2 it is apparent that the yields obtained were in the region of 60 %, at ash contents of about 12 %.

These results were generally poorer, with respect to ash content (grade), than those obtained during the factorial design. This meant that certain factors do have an effect on the concentrate grade, but that these effects were masked in the factorial design analysis (Section 6.3 above) by the errors incurred in the factorial design. This is investigated in the statistical analysis below.

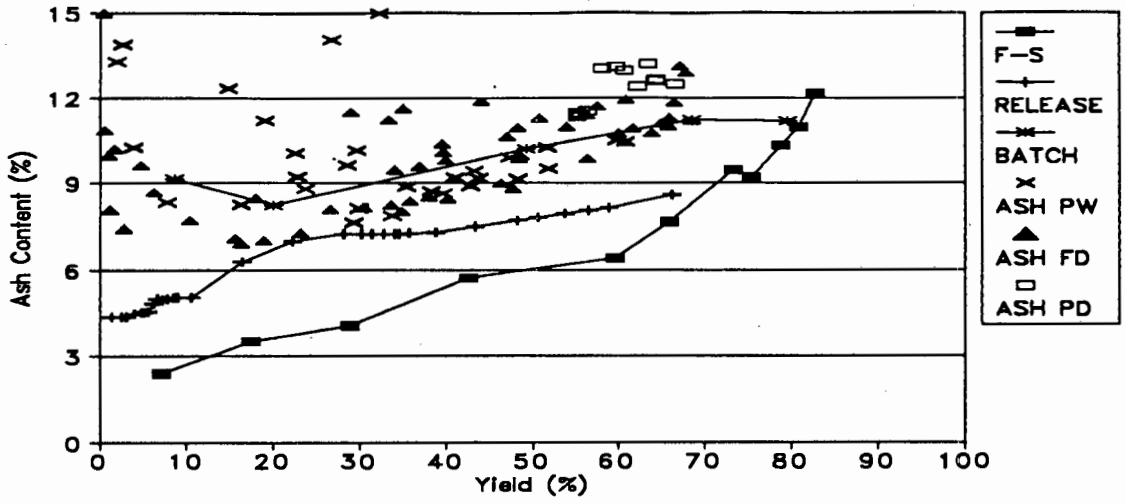

Figure 6.2: Global results obtained during the Kleinkopje pulp density/air rate investigation (ASH PD) compared with the results of the float-and-sink (F-S) and release flotation (RELEASE) analyses, and the batch (BATCH), preliminary ASH (ASH PW) and factorial design (ASH FD) flotation results.

6.4.2 Statistical analysis

No *duplicate*, *repeat* or *replicate* runs were carried out during the pulp density/air rate investigation. The reason for this is as follows. During the factorial design investigation the major source of error was identified as being the dissembling and reassembling of the ASH. However, as the ASH was not dissembled and reassembled between the runs carried out in this investigation, and as a single batch of slurry was used for the investigation, the errors encountered during the factorial design investigation were not expected to be a problem.

It was therefore assumed that it was possible to obtain an estimate of the pulp density/air rate investigation errors from the 10 duplicate and repeat runs (i.e. 20 runs in all) carried out in the factorial design, i.e. when the ASH was not dissembled and reassembled.

The experimental results obtained in the runs used in the error analysis are listed in Table C.5(a) in Appendix C and the calculated values are listed in Table C.5(b). The data used in the error analysis are listed in Tables C.5(c_1) and (c_2) and the error analysis is given in Table C.5(d).

A summary of the calculated errors is given in Table 6.14 below. As expected, the errors were considerably lower than those of the factorial design. For example, the mean yield error in the KKPD investigation could be assumed to be 2.01 %, whereas in the modified factorial design it was 5.25 %.

Table 6.14: MSe and se values for the Kleinkopje factorial design repeat and duplicate runs

	Yield	Ash Content	Recovery	Water Rec.
MSe	4:06	0.08	5.55	1.45
se	2.01	0.28	2.36	1.20
dof	10	10	10	10

From these error estimates, a parameter can be considered to affect the yield if the difference in the yields at different levels of the parameter is greater than 2*2.01 = 4.02 %. Similarly ash content, clean coal recovery and water recovery effects would be indicated by differences of 0.56, 4.72 and 2.40 %, respectively.

6.4.2.1 yield error analysis

The yields (%) obtained at the different pulp densities and air rates are given in Table 6.15 below.

Table 6.15: Yields obtained at different pulp densities and air flow rates

	Air Flow Rate			
Pulp Density (%)	125 slpm	175 slpm	300 slpm	Average (%)
9.4	58.04	66.62	55.22	59.96
5.3	59.74	64.17	55.12	59.68
3.2	63.41	64.37	56.32	61.37
1.6	60.66	62.15	55.63	59.48
Average (%)	60.46	64.33	55.57	

From Table 6.15 it can be seen that the pulp density had no effect on the yield, for pulp densities between 1.6 and 9.4 %. This effect is clearly demonstrated by the average yields at the four different pulp densities being within 2 % (cf. se=2.01 %) of one another.

The above results also indicate that increasing the average air rate from 125 slpm to 175 slpm resulted in an increase in the yield. These results are statistically significant, at each pulp density. The average increase is almost 4 %. A further increase in the average air rate, to 300 slpm, resulted in an average decrease in the yield of about 9 % (i.e. to below the yield at 125 slpm at each pulp density).

6.4.2.2 concentrate ash error analysis

The concentrate ash contents (%) obtained at the different pulp densities and air rates are given in Table 6.16 below.

Table 6.16: Concentrate ash contents obtained at different pulp densities and air flow rates

	Air Flow Rate			
Pulp Density (%)	125 slpm	175 slpm	300 slpm	Average (%)
9.4	13.01	12.48	11.33	12.27
5.3	13.09	12.59	11.45	12.38
3.2	13.19	12.59	11.53	12.46
1.6	12.97	12.39	11.39	12.25
Average (%)	13.07	12.53	11.43	

The results listed above indicate that, as in the case of the concentrate yield, the pulp density of the feed slurry had no effect on the concentrate grade, between pulp densities of 1.6 % and 9.4 %. The difference between the best and worst grades is only 0.21 % and from Table 6.14 the se=0.28 %.

However, increasing the average air rate from 125 slpm to 175 slpm resulted in an average reduction in the ash content of 0.54 %, while

a further increase in the average air rate to 300 slpm resulted in a further 1.1 % reduction in the ash content, which is significant.

6.4.2.3 concentrate recovery error analysis

The concentrate coal recoveries (%) obtained at the different pulp densities and air rates are given in Table 6.17 below. As expected the trend follows that of the yield.

Table 6.17: Concentrate recoveries obtained at different pulp densities and air flow rates

	Air Flow Rate			
Pulp Density (%)	125 slpm	175 slpm	300 slpm	Average (%)
9.4	66.44	76.40	63.64	68.81
5.3	68.44	74.24	63.88	68.85
3.2	72.31	73.68	64.35	70.11
1.6	68.62	70.35	63.55	67.51
Average (%)	68.95	73.79	63.86	

The maximum average concentrate coal recovery, of 70.11 %, was obtained at a pulp density of 3.2 % and the minimum average overflow recovery, of 67.51 %, was obtained at a pulp density of 1.6 %. However, the difference of 2.6 % between them indicates that the feed pulp density had no significant effect on the overflow recovery. This result confirms the results obtained in 6.4.2.1 and 6.4.2.2 above.

The average recovery increased by an average of 4.84 % (cf. se=2.36) with an increase in the average air rate from 125 slpm to 175 slpm, and then decreased by 9.93 % with an increase of the average air rate from 175 slpm to 300 slpm. Although the increase in the recovery with an increase in the average air rate from 125 slpm to 175 slpm is not statistically significant, the results obtained in 6.4.2.1 and 6.4.2.2 suggest that this increase in the air rate does

affect the recovery. The reduction in the recovery when the average air rate is increased from 175 slpm to 300 slpm is of the same order of magnitude as the reduction in the yield under the same conditions, i.e. ≈10 %.

6.4.2.4 overflow water recovery error analysis

The overflow water recoveries (%) obtained at the different pulp densities and air rates are given in Table 6.18 below.

Table 6.18: Overflow water recoveries obtained at different pulp densities and air flow rates

	Air Flow Rate			
Pulp Density (%)	125 slpm	175 slpm	300 slpm	Average (%)
9.4	33.21	23.69	14.99	23.96
5.3	29.89	26.53	16.26	24.23
3.2	29.98	27.46	17.46	24.97
1.6	32.44	26.74	18.91	26.03
Average (%)	31.38	26.11	16.91	

The difference between the maximum average overflow water recovery, at a pulp density of 1.6 %, and the minimum average overflow water recovery, at a pulp density of 9.4 %, was 2.07 %. The se of 1.20 %, from Table 6.14 therefore suggests that the pulp density might have a slight effect on the overflow water recovery. The gradual increase in the water recovery with a reduction in the pulp density supports this possibility.

From the average water recoveries at different air rates it is apparent that increasing the air rate to the ASH resulted in a significant decrease in the water recovery to the overflow.

6.5 Collector Dosage Investigation

In the preliminary work carried out using the ASH it was found that collector dosages in the region of 35 kg/ton were necessary to achieve yields of the order of 50 % (see Section 5.2.2). However, the results of the factorial design investigation indicated that the optimal ASH configuration (viz. the configuration used in the pulp density/air rate investigation) was very different to the one used for the preliminary work. For this reason it was decided to re-examine the effect of collector dosage on the performance of the ASH, using an ASH configuration similar to the one used in the pulp density investigation. The parameters varied or held constant, and their respective values, are listed in Table 6.19 below.

Table 6.19: Parameters used during the collector dosage investigation

Parameter	Values Used
collector dosages	1.0 to 37.5 kg/ton Shellsol A
frother dosage	1000 g/ton HTEB
Q_{slurry}	65 l/min
Q_{air}	175 slpm
pulp density (solids %)	3%
$d_{cyclone}$	46 mm
$L_{cyclone}$	300 mm
underflow configuration	orifice
$d_{orifice}$	18.8 mm
$L_{vortex-finder}$	46 mm
$d_{vortex-finder}$	21.7 mm
A_{inlet}	15x12 mm

The only difference between the ASH described above and the one used in the pulp density/air rate investigation was the vortex-finder length. In the collector dosage investigation a 46 mm vortex-finder was chosen, as the factorial design results indicated that a shorter vortex-finder might result in a slight improvement in the grade (i.e. the ASH used was the same as the one used in KKFD-A_i13, and differed only in L_{vf} from the ASH used in the pulp density/air rate investigation).

A total of 7 runs were carried out in the collector dosage investigation. The experimental method followed is described in Section 4.2.2.3. Each run was carried out at a different collector dosage, with the collector dosages ranging from 1 kg/ton to 35 kg/ton. However no *duplicate*, *repeat* or *replicate* runs were performed. The experimental results and the calculated values are listed in Tables C.6(a) and (b) respectively, in Appendix C.

6.5.1 Global Results

Before proceeding with a statistical analysis of the results, it is of interest to consider the overall results compared with those obtained in the previous experiments. The overall results obtained in the collector dosage investigation are plotted, together with the coal characterisation results from Chapter Four, and the results of the preliminary work, the factorial design, and the pulp density/air rate investigation, in Figure 6.3 below. The yields obtained varied between 15.1 % (1 kg/ton), at an ash content of 18.1 %, and 74.0 % (36.7 kg/ton), at an ash content of 12.8 %. From Figure 6.3 it can be seen that the results obtained in the collector dosage investigation are generally far poorer than those obtained previously, in both the ASH and the batch cell, in terms of ash content at a particular yield.

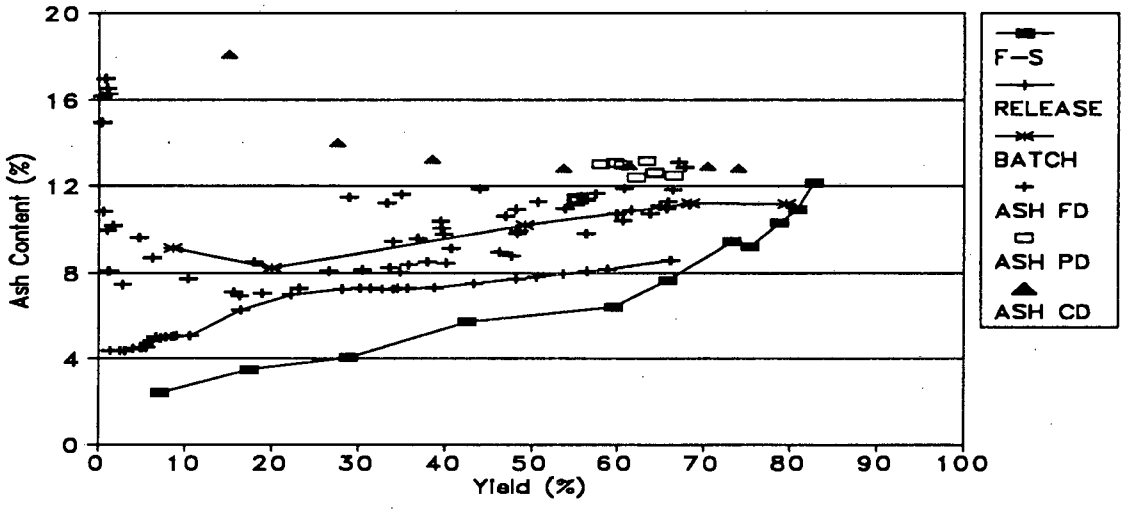

Figure 6.3: Global results obtained during the Kleinkopje collector dosage investigation (ASH CD) compared with the results of the float-and-sink (F-S) and release flotation (RELEASE) analyses, and the batch (BATCH), factorial design (ASH FD) and pulp density/air rate investigation (ASH PD) flotation results.

6.5.2 Error Analysis

As in the pulp density/air rate investigation the errors involved in the collector dosage investigation could be estimated from the repeat and duplicate runs carried out in the factorial design. The yield, concentrate ash, clean coal recovery and water recovery errors used in the error analysis were therefore as calculated in Section C.2.2 in Appendix C, and listed in Table 6.14 above.

The yields, concentrate ash contents, clean coal recoveries and water recoveries obtained at the different collector dosages, and the MSe and se values, are listed in Table 6.20 below.

Table 6.20: Yields, overflow ash contents, clean coal recoveries and water recoveries obtained at various collector dosages

Collector Dosage (kg/ton)	Yield (%)	Overflow Ash (%)	Coal Recovery (%)	Water Recovery (%)
1	15.10	18.07	16.58	28.51
2	27.47	14.01	31.36	28.99
4	38.55	13.21	44.44	30.12
8	53.78	12.81	62.62	31.86
13	61.31	12.95	70.88	31.78
25	70.39	12.92	80.68	33.48
36	73.98	12.81	84.48	33.74
MSe	4.06	0.08	5.55	1.45
se	2.01	0.28	2.36	1.20

The results in Table 6.20 above indicate that at collector dosages below 25 kg/ton, increasing the collector dosage results in a statistically significant increase in the overflow yield. However, above 25 kg/ton increasing the collector dosage has no effect on the overflow yield. A similar trend is observed for the clean coal recovery.

At collector dosages below 4 kg/ton, increasing the collector dosage results in a statistically significant reduction in the concentrate ash content, between subsequent samples. However, at collector dosages above 4 kg/ton the collector dosage has no statistically significant effect on the concentrate ash content.

Increasing the collector dosage has no statistically significant effect on the water recovery to the overflow, but an overall trend (of increasing water recovery with increasing collector dosage) can be observed.

6.6 Particle Size Effects

It has been claimed that the ASH is more effective for the flotation of fine particles than conventional flotation devices. However, few researchers have confirmed the above statement. Consequently, size analyses were carried out on selected subsamples of the concentrate and underflow samples from the batch flotation, factorial design and collector dosage investigations, and float-and-sink analyses were performed on the various size fractions. This enabled an analysis of the "performance by size fraction" of the ASH across a range of results. In addition further comparison with the batch cell was possible.

The float-and-sink analyses were carried out at a single SG for each sample. The SG used was chosen in such a way as to detect the "misplaced" material. For example, in run KKFD-D6 the yield was 47.7 %; from Table 5.2 (in Chapter 5) the SG at a theoretical yield of 47.7 % is between 1.45 and 1.50. Therefore float-and-sink analyses of the concentrate and tails samples were carried out at SG's of 1.50 and 1.45 respectively. This resulted in the concentrate sinks and the tails floats consisting of "misplaced" material. The runs on which size and float-and-sink analyses were carried out, and the SG's used for the concentrate and tails samples, respectively, are listed in Table 6.21 below.

Table 6.21: Runs on which size and float-and-sink analyses were carried out, and the SG's used for the concentrate and tails samples

	SG	
Run id.	Concentrate	Tails
KKCD1	1.35	1.30
KKCD4	1.50	1.45
KKCD6	1.60	1.55
KKFD-A8(2)	1.60	1.55
KKFD-B16	1.45	1.40
KKFD-D6	1.50	1.45
KKB3	1.60	1.55

The first three runs listed in Table 6.21 above were carried out during the collector dosage investigation. In this investigation, the poorest grades were achieved at the lowest yield, i.e. at the lowest collector dosage. This is the reverse of the usual trend. As the collector dosage was increased the yield increased, at a reduced ash content. At collector dosages above 25 kg/ton the yield tended to a limit in the region of 75 %, at a limiting ash content of about 12.8 %. Size and float-and-sink analyses were carried out to determine the nature of the material being recovered at relatively low (KKCD1), intermediate (KKCD4) and high (KKCD6) collector dosages.

Runs KKFD-B16 and KKFD-D6 were carried out during the factorial design. The result (yield at a particular ash content) achieved in run KKFD-B16 was close to the flotation limits predicted by the release flotation analyses. The result obtained in run KKFD-D6 was not as close to the predicted limiting efficiency as run KKFD-B16, but it was superior to those obtained at a similar ash content in the batch cell, and in other ASH runs. Size and float-and-sink analyses were carried out to determine the nature of the material being recovered when the ASH operated efficiently.

Runs KKB3 and KKFD-A8(2) were carried out during the batch and factorial design investigations, respectively. Although the results obtained in these runs were not close to the limits predicted by the release flotation

analysis, approximately the same concentrate yield (68 %) and ash content (11.2 %) were obtained. This enabled a comparison to be made between the performance of the batch cell and the ASH in the different size fractions, at a similar overall performance.

The results of the size analyses and the performance in each size fraction of runs KKCD1, KKCD4 and KKCD6 are listed in Tables C.7(a), (b) and (c) in Appendix C, respectively. The results of the size analyses and the performance in each size fraction of runs KKFD-A8(2), KKFD-B16 and KKFD-D6 are listed in Tables C.9(a), (b) and (c) in Appendix C, respectively. The results of the size analyses and the performance in each size fraction of run KKB3 is listed in Table B.2.3(b) and (c).

The float-and-sink analyses of the above runs are listed in Tables C.8(a) to (g) in Appendix C. These tables list the SG used, the proportion of each size fraction which floated at the SG used, and the ash content of the "floats" and "sinks" fractions, for each of the concentrate and tails samples.

The data in Tables C.8(a) to (g) were used to calculate the "% sinks" in the concentrate samples investigated, i.e. the amount of refuse material that had been "misplaced " to the overflow. These results (except for KKCD1) are indicated in Figure 6.4 below.

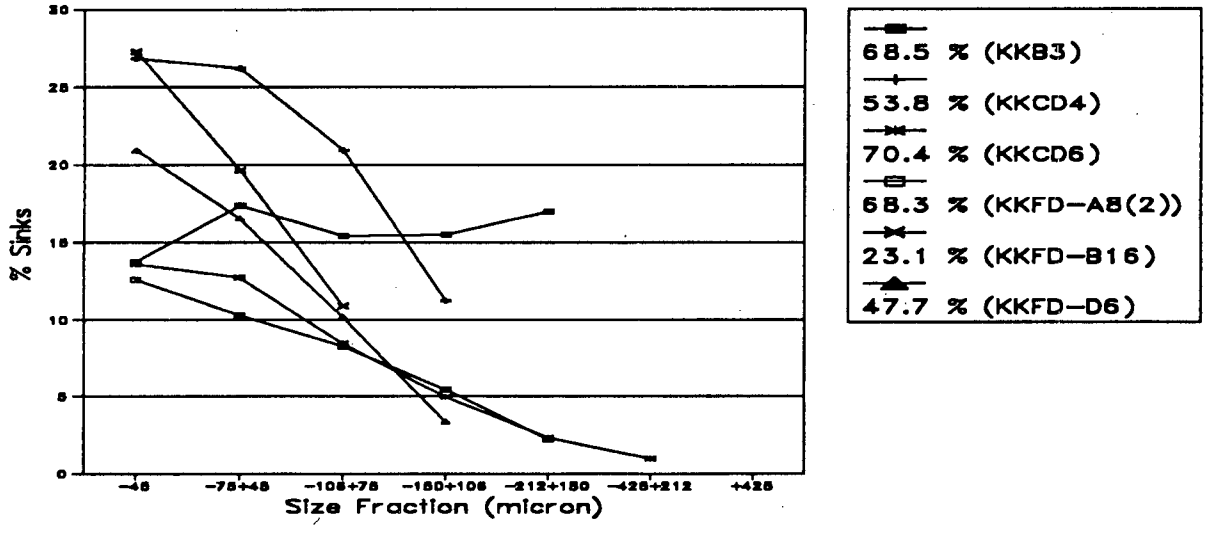

Figure 6.4: Proportion of each size fraction of the concentrate which has been "misplaced" to the concentrate sample, i.e. material which should have reported to the tails

From Figure 6.4 it is apparent that the amount of "misplaced" material in the ASH concentrates decreased linearly as the particle size increased. The results seem to indicate that an increase in the overall product yield in the ASH resulted in a reduction in the fraction of material "misplaced" to the concentrate, but because the ASH runs were carried out at different conditions (design and operating) the above cannot be considered to be conclusive.

However, the amount of "misplaced" material in the batch flotation concentrate was reasonably constant for all the size fractions. Comparing the results of runs KKFD-A8(2) and KKB3 are compared seems to indicate that the ASH concentrate contains less "misplaced" coarse material than the batch cell concentrate, but more "misplaced" fines, i.e more fine particle entrainment occurs in the ASH.

The "% floats" in the various size fractions of the tails samples are listed in Tables C.8(a) to (g) in Appendix C, i.e. the amount of material that had been "misplaced" to the tails. These results are presented graphically in Figure 6.5 below.

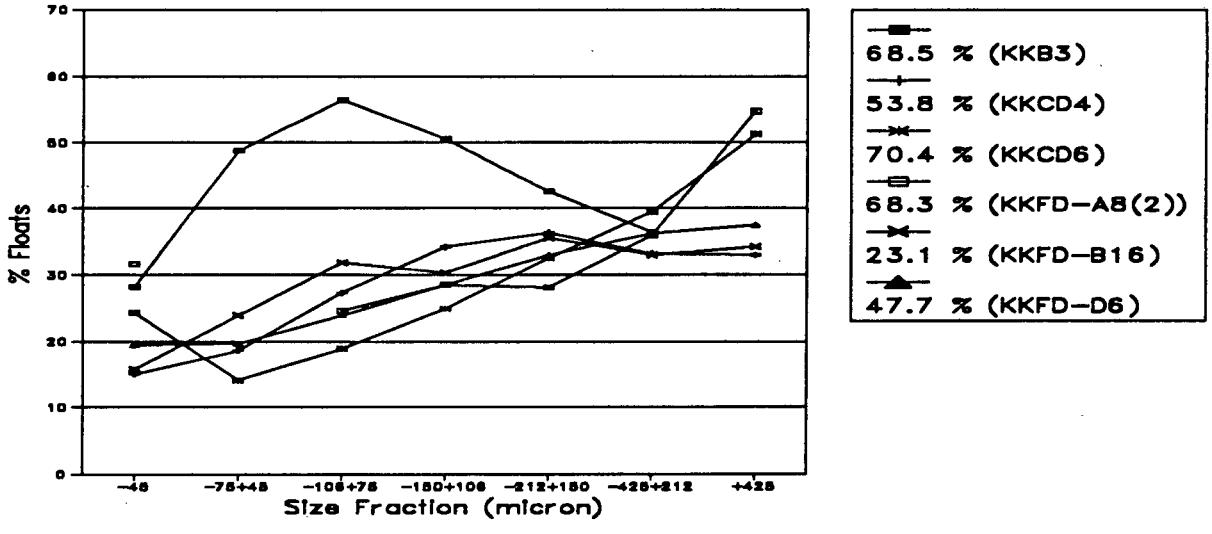

Figure 6.5: Proportion of each size fraction of the tails which has been "misplaced" to the tails sample, i.e. material which should have reported to the concentrate

From Figure 6.5 it is apparent that the amount of "misplaced" material in the ASH tails increases linearly as the particle size increases. However,

it is not possible to determine whether or not an increase in the overall yield affects the proportion of material "misplaced" to the tails.

The amount of "misplaced" material in the batch cell tails is a maximum in the intermediate size fractions, and decreases in the fine and coarse fractions. Comparison of runs KKFD-A8(2) and KKB3 indicates that similar amounts of "misplaced" material in the fine and coarse fractions report to the tails of the ASH and the batch cell. However, the ASH seems to perform better in the intermediate size fractions.

6.7 Discussion and Interpretation of Results

In the sections which follow, an attempt is made to interpret the results of the factorial design experiments and the other investigations reported in previous sections of this Chapter. In this discussion, comparisons are made between the average responses achieved for the different parameters. These average high (+) and low (-) responses were obtained by calculating the average response (yield, concentrate ash content, coal recovery and water recovery) at the low and high value of each of the parameters investigated (A^*, L_c/d_c, A_i, UF type, Q^*, L_{vf}/d_c). The average responses of the various parameters at their respective high and low values are listed in Table 6.22 below. It should be noted that the difference between a parameter's average response at its respective high and low values is the parameter contrast (as defined in 6.3.1.1 above) divided by 8.

Table 6.22: Average factorial design response values of the different parameters at their respective high (+) and low (-) values

	$Yield_{av}$		$Concentrate\ Ash_{av}$		$Clean\ Coal\ Recovery_{av}$		$Water\ Recur_{av}$	
Parameter	(+)	(-)	(+)	(-)	(+)	(-)	(+)	(-)
A_{of}/A_{uf}	45.52	24.93	10.50	10.61	52.98	29.62	16.90	5.16
L_c/d_c	24.87	45.57	10.22	10.89	29.44	53.16	8.43	13.63
A_{inlet}	36.63	33.82	10.78	10.33	42.82	39.78	11.01	11.04
UF type	50.08	20.37	10.60	10.51	58.48	24.12	18.04	4.01
Air	29.49	40.96	10.94	10.17	34.62	47.98	9.33	12.73
L_{vf}/d_c	39.55	30.90	11.37	9.74	46.33	36.27	11.79	10.26

6.7.1 Underflow Configuration

Most researchers investigating flotation in the ASH have not examined the effect of different underflow configurations. Exceptions are Van Deventer et al (1988) and Nieuwoudt et al (1990) (see Section 3.6.2); in both instances not using a conventional ASH underflow design did not result in poorer flotation results. Instead the results obtained by Nieuwoudt et al (1990) suggested that a pedestal was not necessary.

In the factorial design carried out on the Kleinkopje sample (Section 6.3.1 above) the underflow configuration was found to have the greatest effect on the performance of the ASH in terms of yield and clean coal recovery. This fact is clearly illustrated by the "UF type" contrast having a magnitude almost one-and-a-half times that of the second most important parameter, the A_{of}/A_{uf} ratio, (in Tables 6.6, 6.8 and 6.9 above). The average yield using the underflow configuration consisting of an orifice with a baffle located above it was almost 30 % greater than that obtained using a pedestal and an annular opening (the average yield increased from 20.37 to 50.08 %). The factorial design results also indicate that the increase in the yield occurred without a corresponding reduction in the concentrate grade; hence the average clean coal recovery increased by about 34 % (from 24.12 to 58.48 %) when an orifice was used in the place of a pedestal.

These results can be largely attributed to the 14 % increase in the average water recovery associated with the use of an orifice and baffle in place of a pedestal (from 4.01 to 18.04 %). The orifice/baffle configuration restricts the flow of the tails stream to a greater extent than an annular opening of the same area. This is because the centrally located underflow opening forces the slurry to migrate from the porous tube wall to the axis of the cyclone in order to exit through the orifice (underflow) of the ASH. This has the effect of facilitating froth transport to the overflow.

The above results in an increase in the concentrate water recovery and in the recovery of coal associated with the water. As the greatest restriction occurs on the axis of the cyclone one would expect the froth/water containing the most hydrophobic material to be most

strongly prevented from reporting to the tails. This would result in the yield increasing, without a corresponding reduction in the grade.

For the same reason similar results would be obtained if the pedestal diameter was increased. This would reduce the width of the annular opening thereby increasing the water, and the associated coal, recovery to the overflow. However, at the greater A_{of}/A_{uf} ratio used, blockages were a problem. For this reason no runs were carried out with an annular opening width that was less than 8.7 % of the cyclone diameter.

6.7.2 $A_{overflow}/A_{underflow}$ Ratio (A*)

Miller et al (1988) found that the flotation response at a constant Q^* (Q_{air}/Q_{slurry}) was independent of the absolute overflow and underflow values, but dependent on the A_{of}/A_{uf} ratio; and that the A_{of}/A_{uf} ratio was the most important parameter in the flotation of coal in the ASH. In the factorial design carried out above, the A_{of}/A_{uf} ratio was found to be the second most important parameter. The larger A_{of}/A_{uf} ratio resulted in an average yield response which was 20 % greater than at the lower A_{of}/A_{uf} ratio (from 24.93 to 45.52 %), without a corresponding reduction in the grade.

This result contradicts those of numerous workers, including Ye et al (1988), Baker et al (1987), Stoessner et al (1990), Miller et al (1988) and Nieuwoudt et al (1990) all of whom found that increasing the A_{of}/A_{uf} ratio resulted in an increase in the recovery but a *reduction* in the concentrate grade (see Section 3.6.3). In the case of Nieuwoudt et al (1990), the results were obtained using a baffle and orifice instead of a pedestal.

The results obtained in the factorial design of the Kleinkopje coal can be explained as follows: as in the case of the "UF Type" parameter, the increase in the yield can be attributed to the increase in the water recovery to the overflow (from 5.16 to 16.90 %). A larger A_{of}/A_{uf} ratio facilitates the withdrawal of a larger cross-sectional area of the froth phase, and hence results in an increased water recovery and an associated increase in the coal yield. As in Section 6.7.1 above the cross-section of the froth phase which is recovered when using a larger

A_{of}/A_{uf} ratio contains little "extra" gangue. This results in the increased average yield not being accompanied by a reduction in the grade of the coal. The net result was a 23 % increase in the average clean coal recovery when a larger A_{of}/A_{uf} ratio was used (from 29.62 to 52.98 %) with no change in the average concentrate ash content.

6.7.3 $L_{cyclone}/d_{cyclone}$ Ratio

In the factorial design carried out, the L_c/d_c ratio was found to have the third greatest effect on the flotation performance of the ASH. Reducing the cyclone length from 500 mm (L_c/d_c=10.87) to 300 mm (L_c/d_c=6.52) resulted in a 20 % increase in the overflow yield (from 45.57 to 24.87 %). As in 6.7.1 and 6.7.2 above, this increase in yield was not associated with a reduction in the concentrate grade, with the result that the clean coal recovery increased by about 23 % (from 29.44 to 53.16 %). As would be expected from the preceding results, the water recovery to the overflow was also greater for the shorter ASH than for the longer ASH (13.63 vs 8.43 %).

However, the magnitude of the water recovery *F*-ratio was considerably lower than that of the A_{of}/A_{uf} (4.27 vs 21.73 %), although the yield *F*-ratios were the same (3.79 vs 3.75 %). This suggests that the increase in the yield when using the shorter ASH cannot be solely attributed to the increase in the water recovery. Therefore a smaller (shorter) ASH need not act primarily as a splitter, as postulated by Nieuwoudt et al (1990) (see Section 3.6.1).

The above results are also in disagreement with those reported by Miller and Van Camp (1982), Miller and Kinneberg (1984), Baker et al (1987) and Stoessner (1990). These researchers all found that increasing the cyclone length resulted in an increase in the yield and a reduction in the concentrate grade. The above contradiction can probably be attributed to each mineral, and possibly each size fraction, having its own optimum L_c/d_c ratio. This postulate is supported by the results of Nieuwoudt et al (1990) for pyritic ores A and B (see Section 3.6.1). They found that increasing the L_c/d_c had a less marked effect on the recovery of a finer pyritic ore.

It is further suggested that where "true flotation" is the principal means of product recovery, increasing the L_c/d_c ratio (to the optimum for the particular mineral) results in an increase in the recovery (and possibly the grade) as a result of the increase in the residence time (as found by Miller and Van Camp (1982)). However increasing the L_c/d_c ratio beyond the optimum would increase the recovery of coarse particles, as found by Miller and Kinneberg (1984), but result in a reduction in the overall grade as a result of the increased water recovery.

However, the coal used in this project was poorly floatable (low inherent hydrophobicity). Therefore the process whereby the product reported to the overflow could be considered to be a combination of "flotation" and "using a water only cyclone". For the above reason facilitating froth migration to the overflow was the most important consideration. During "normal" operation of the ASH about 50 % of the ASH is filled with slurry (Baker, 1987), with a cone shaped froth region on the axis of the ASH. During "choked" flow up to 70 % of the ASH can be filled with slurry. Therefore decreasing the length of the ASH raises the height of the base of the "froth cone", facilitating its transport to the overflow.

6.7.4 Q_{air}/Q_{slurry} Ratio (Q*)

In the original factorial design, the air rate was found to have no effect on the performance of the ASH, even at the 25% significance level. This result contradicts results obtained in other flotation equipment and was one of the reasons for the *modified factorial design* analysis being carried out (Section 6.3.2 above). In the modified factorial design analysis, the air rate was found to affect the yield, clean coal recovery and water recovery, all at the 25 % significance level. However the analysis indicated that increasing the Q^* from 2.69 to 4.62 (i.e. increasing the air rate from 175 to 300 slpm) caused the yield, coal recovery and water recovery to decrease, while the ash content remained constant. Once again this result seemed to contradict those obtained by workers using both the ASH and other flotation machines (Miller and Van Camp, 1982; Miller et al, 1988; Cloete et al, 1988; Ye et al, 1988).

For this reason the effect of air rate, at a constant slurry rate, was investigated during the pulp density investigation (Section 6.4). The results are summarised in Figure 6.6 below. The results obtained indicate that an optimum air rate exists at a constant slurry rate. Increasing the air rate to the optimum results in an increase in the recovery at a constant grade, as found by Miller and Van Camp (1982). Further increases result in an increase in the yield but a reduction in the grade, as found by Ye et al (1988).

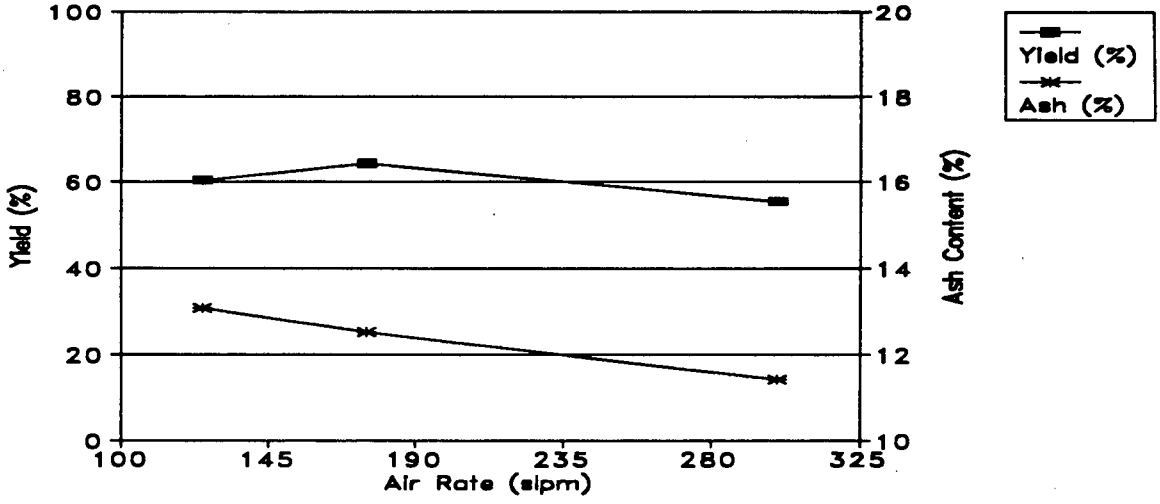

Figure 6.6: Effect of air rate on (average) overflow yield and ash content of Kleinkopje coal

A possible reason for the reduction in the yield and water recovery with a further increase in the air rate, as found in the pulp density investigation, could be that the increased volumetric air flow rate results in the diameter of the vortex-finder becoming a limiting factor. This postulate is supported by Miller et al (1985) and Miller and Kinneberg (1984) who found that the air split to the overflow was in the region of 85% for most air rates. In this instance the grade would therefore be expected to improve as a result of the reduced hydrophilic gangue carry over.

6.7.5 L_{vf}/d_c Ratio

In both the original and modified factorial designs the L_{vf}/d_c parameter was statistically insignificant. However, in both designs the L_{vf}/d_c concentrate ash *F*-ratios were almost an order of magnitude greater than those of the other parameters tested. In addition, the interaction terms resulting in the greatest concentrate ash *F*-ratios all contained the L_{vf}/d_c parameter. These facts suggest that the L_{vf}/d_c parameter may have a slight effect on the concentrate ash content, with a larger L_{vf}/d_c (viz. a longer vortex-finder) resulting in a poorer concentrate grade. This result would agree with those reported by Van Deventer et al (1988) and Nieuwoudt et al (1990).

In the pulp density/air rate investigation the L_{vf}/d_c ratio was chosen as the larger of the values used in the factorial design (viz. 1.5). For the reasons stated above it was expected that the ash contents of the concentrates obtained in the pulp density/air rate investigation would be greater than those obtained in the factorial design. The above was expected to be most apparent when the results of KKPD-X_ib were compared to those of KKFD-(A_i)13(y_i) and KKCD-7. In these runs only the L_{vf}/d_c ratio was different. The average results of runs KKFD-(A_i)13(y_i) and KKCD-7, runs KKPD-X_ib and the se's from the modified factorial design are listed in Table 6.23 below.

Table 6.23: Average results of runs KKFD-(A_i)13(y_i), KKCD-7 and KKPD-X_ib together with the se's from the modified factorial design

	KKFD-A_i13	KKCD-7	KKPD-X_ib	se
Yield (%)	67.47	73.98	64.33	5.25
OF Ash (%)	13.00	12.81	12.53	1.10
Recovery (%)	77.50	84.48	73.79	6.30
Water Recovery (%)	32.64	33.74	26.11	1.76

The results listed in Table 6.23 indicate that the L_{vf}/d_c ratio had a statistically significant effect on the water recovery to the overflow, but had no effect on the yield, concentrate ash or clean coal recovery,

for the range of L_{vf}/d_c ratios investigated. These results agree with those of Van Deventer et al (1988) who found that the vortex-finder length did not have a significant effect on the performance of the ASH.

However, Nieuwoudt et al (1990) reported that increasing the vortex-finder length resulted in a reduction in the concentrate recovery (once a minimum vortex-finder length had been exceeded) and a deterioration in the concentrate grade. In addition Miller et al (1985) found that the axial and tangential swirl-layer velocities went through a local minimum just below the slurry inlet and hence a vortex-finder of a similar length would be expected to result in a greater recovery at poorer grade. This phenomenon is further discussed in Section 6.7.7 below.

6.7.6 A_{inlet}

The area of the slurry inlet was found to have no effect on the performance of the ASH, in both the original and modified factorial designs. Most workers have operated the ASH using a fixed inlet area. However, Nieuwoudt et al (1990), who investigated the effect of the inlet area, found it had no effect on the recovery of sulphur at a constant slurry feed rate, but that the point of maximum sulphur grade shifted to higher feed rates at larger inlet areas. This result can be attributed to the effect of a larger inlet area on the pressure drop across the ASH.

6.7.7 Interaction terms

6.7.7.1 two-factor interactions

The only two-factor interaction term found to have an effect on the overflow yield, ash content, clean coal recovery (all at the 25 % significance level) and water recovery (at the 10 % significance level) was the sum of the A^*/UF type and the L_{vf}/L_c interactions. In the factorial design analysis it was found that the A^* and UF type both had strong effects on the yield, recovery and water recovery, but none on the overflow ash content. It therefore seems likely

that the concentrate yield, ash content, clean coal recovery and water recovery are subject to an interactive effect between the A^* and UF type parameters while the L_{vf}/L_c interaction affects the concentrate grade.

The L_{vf}/L_c interaction term once again suggests that the L_{vf} had a slight effect on the concentrate grade. This interaction could be attributed to the relative positions of the vortex-finder inlet and the region of reduced tangential and axial slurry velocity below the slurry inlet.

In addition to the above, the sum of the L_{vf}/A_{inlet} and UF type/Q^* interactions may have had a slight effect on the concentrate grade (at the 25% significance level). It seems unlikely that the effect on the ash content is a result of a UF type/Q^* interaction, as an interaction between these parameters would also be expected to affect the yield, recovery and water recovery of the ASH. It can therefore be assumed that the L_{vf}/A_{inlet} interaction is the one which had an effect on the concentrate grade. This assumption is supported by results obtained by Nieuwoudt et al (1990) which indicated that below a certain vortex-finder length a poor grade results from turbulence at the inlet. Miller et al (1985) also found that short circuiting across the roof of the ASH to the vortex-finder was visible when using a specially constructed ASH with plexiglass windows; this could contribute to a reduced concentrate grade.

Most previous researchers, including Gopalakrishnan et al (1990), using coal in the ASH have found that there is an interactive effect between A^* and Q^* parameters. These workers found that at a fixed value of A^* or Q^* the performance of the ASH could be described simply by Q^* or A^* respectively. However, this interaction was not apparent from the results obtained in the factorial design carried out on the Kleinkopje coal but could possibly have been masked by the use of different underflow configurations.

6.7.7.2 three-factor interactions

Even though the sum of the $A^*/A_{inlet}/L_{vf}$, the $L_c/Q^*/_{Lv}f$, the L_c/A_{inlet}/UF type and the A^*/UF type/Q^* interaction terms showed an effect on the overflow ash content at a significance level of less than 25%, the fact that its *F*-ratio was almost an order of magnitude greater than the other interactions suggested that it should be considered. From the discussions of the preceding sections it seems unlikely that the L_c/A_{inlet}/UF type or the A^*/UF type/Q^* interactions would effect the concentrate grade. However, because the $A^*/A_{inlet}/L_{vf}$ and $L_c/Q^*/L_{vf}$ could be expected to affect the flow regimes in the region of the vortex-finder either, or both, could affect the grade of the overflow product, as discussed in Section 6.7.7.1 above.

6.7.8 Pulp density

In the pulp density investigation it was found that the pulp density had no effect on the performance of the ASH, between pulp densities of 1.6 and 9.4 %. This is clearly visible from Figure 6.7 below.

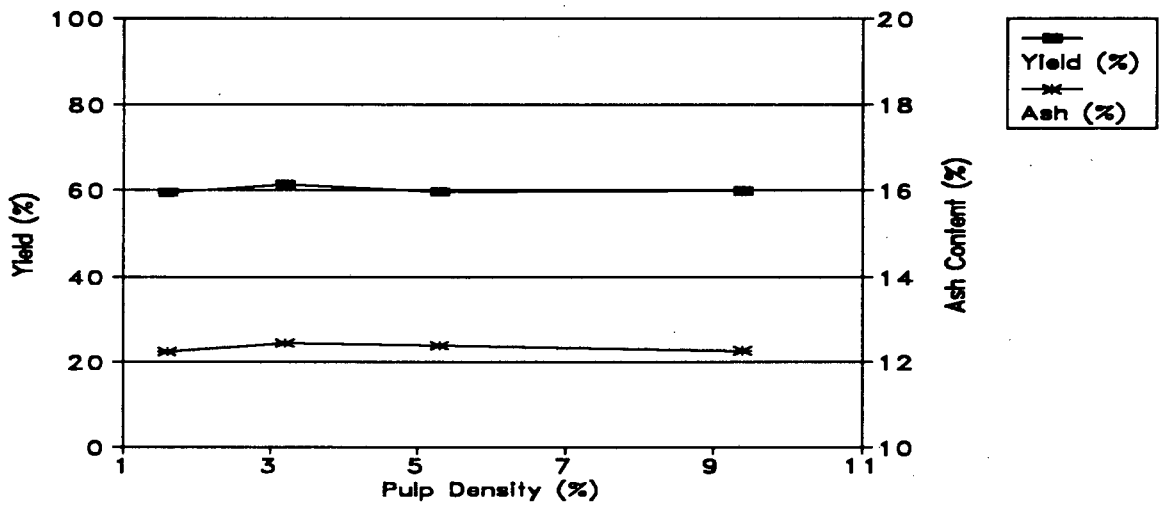

Figure 6.7: Effect of feed pulp density on overflow yield and ash content of Kleinkopje coal

This result is in contrast to those obtained by Miller and Kinneberg (1984) and Miller et al (1985) in the flotation of copper porphyry ore, Nieuwoudt et al (1990) and Cloete et al (1987) in the flotation of a

pyrite ore and Stoessner (1990) in the flotation of coal. The above researchers all found that increasing the pulp density of the feed slurry resulted in an increase in the water recovery and hence a reduction in the concentrate grade, but that the increase in the recovery was either small (Cloete et al, 1987) or negligible (Miller et al, 1985). The contradictory result obtained in the factorial design carried out on the Kleinkopje coal may be as a result of the limiting point with respect to recovery being above a pulp density of 10 % for the coal being investigated. It may also be that the slurry feed rate was sufficiently high to prevent a reduction in the grade with an increase in the pulp density, as found by Nieuwoudt et al (1990).

Being able to operate the ASH at increased pulp densities without affecting the concentrate grade or recovery has far reaching implications when comparisons are made between the specific capacities of the ASH and other flotation devices.

Numerous workers, including Miller and Van Camp (1982), Cloete et al and Stoessner et al (1990) have found that the specific volumetric capacity of the ASH is between 100 and 300 times that of conventional flotation devices. Miller et al (1988) postulated that the ASH had a specific capacity in the region of 3 500 t/d.m^3 (dry feed). This value compares well with the capacity of 144 t/hr.m^3 obtained in Section 5.3 and is up to 100 times the 35 to 70 t/d.m^3 of conventional cells (Miller and Ye, 1989).

Increasing the pulp density by a factor of 3, to about 9.5 % solids would further increase the specific capacity of the ASH to about 10 500 t/d.m^3. This results in the capacity of the ASH being about 300 times that of conventional cells. Furthermore, comparison of the above with the column cell capacity of 1.5 t/hr.m^2 obtained by Von Holt (1992, p 168), for the same feed, indicates that the ASH (operating at 9.5 % solids) has a specific capacity in excess of 140 times that of the column cell on a cross-sectional area basis, and in excess of 1 700 times that of the column cell on a volumetric basis.

The increased capacity of the ASH as a result of the increase in the feed pulp density would play a major role in the size of the equipment required for a given throughput, and in the amount of space required for the equipment. This space saving would be an even greater advantage where the retrofitting of a plant was being carried out.

6.7.9 Collector dosage

The collector dosage found to be necessary in the ASH preliminary work, and used in the subsequent factorial design work, was significantly higher than the collector dosage found to be needed to produce similar yields (in the region of 50 %) using the optimal ASH configuration. However, the ash contents at these yields were poor, with the best separations, as defined by the Separation Coefficient (see Chapter Five), being at the highest yields. The collector dosages used in the runs, the yields and concentrate ash contents obtained and the Separation Coefficients calculated are listed in Table 6.24 below.

Table 6.24: Separation Coefficients for collector dosage investigation runs

Run Number	Collector Dosage (kg/ton)	Concentrate Ash (%)	Coal Recovery (%)	Separation Coefficient
KKCD1	1	18.07	16.58	0.14
KKCD2	2	14.01	31.36	0.27
KKCD3	4	13.21	44.44	0.39
KKCD4	8	12.81	62.62	0.55
KKCD5	13	12.95	70.88	0.62
KKCD6	25	12.92	80.68	0.70
KKCD7	36	12.81	84.48	0.74

In ASH flotation, increasing the collector dosage increases the number of particles with sufficient hydrophobicity to enable them to overcome the centrifugal forces and thus report to the overflow. This results in an increase in the overflow yield and recovery. But, in turn, the increase in the number of particles reporting to the overflow results in a reduction in the grade.

However, as discussed in Section 6.7.3 above, the factor governing the flotation recovery of the Kleinkopje coal is the facilitation of froth transport to the overflow; and the ASH configuration used in the collector dosage investigation was chosen on this basis. The above is evident from the amount of water reporting to the overflow, even at the lowest collector dosage (Table 6.20 above). This water recovery to the overflow results in the entrainment of fine hydrophilic gangue. The above was confirmed by the size analyses carried out on concentrates KKCD1, KKCD4 and KKCD6, the results of which are listed in Tables C.7(a) to (c), and reproduced in Table 6.25 below.

Table 6.25: Size analysis of concentrates KKCD1, KKCD2 and KKCD6

Size Fraction (micron)	KKCD1 1 kg/ton (Yield=15.1 %)	KKCD4 8 kg/ton (Yield=53.78 %)	KKCD6 25 kg/ton (Yield=70.39 %)
+425	0.04	0.09	0.04
-425+212	0.87	0.57	2.69
-212+150	0.76	2.54	5.77
-150+106	1.46	5.83	8.37
-106+ 75	2.15	9.50	11.15
- 75+ 45	3.84	13.33	8.51
- 45	90.88	68.15	63.47

The results indicate that at all collector dosages the ASH concentrate consists chiefly of -45 micron material. Although this result indicates a classification effect may be occurring within the ASH, on its own it is inconclusive as 50 % of the feed material is in this size fraction. However, the results listed in Table C.8(a) in Appendix C indicate that in concentrate KKCD1 90 % of the material was in fact "misplaced" to the concentrate (for a theoretical yield of 15 %). Similar data for runs KKCD4 and KKCD6 are listed in Tables C.8(b) and (c) in Appendix C, and the amount of "misplaced" material in the various size fractions is plotted in Figures 6.4 and 6.5 above (see Section 6.6 above).

It may therefore be concluded that the classification effect of the ASH, resulting from the proportion of water reporting to the overflow,

plays an important role in determining the grade of the concentrate as a result of fine particle entrainment; as found by numerous previous workers (see Chapter Three) and indicated in Figure 6.8 below#. However, the errors in the factorial design resulted in the effect of parameters on the concentrate ash content not being detected, even though the associated increase in the water recovery was detected.

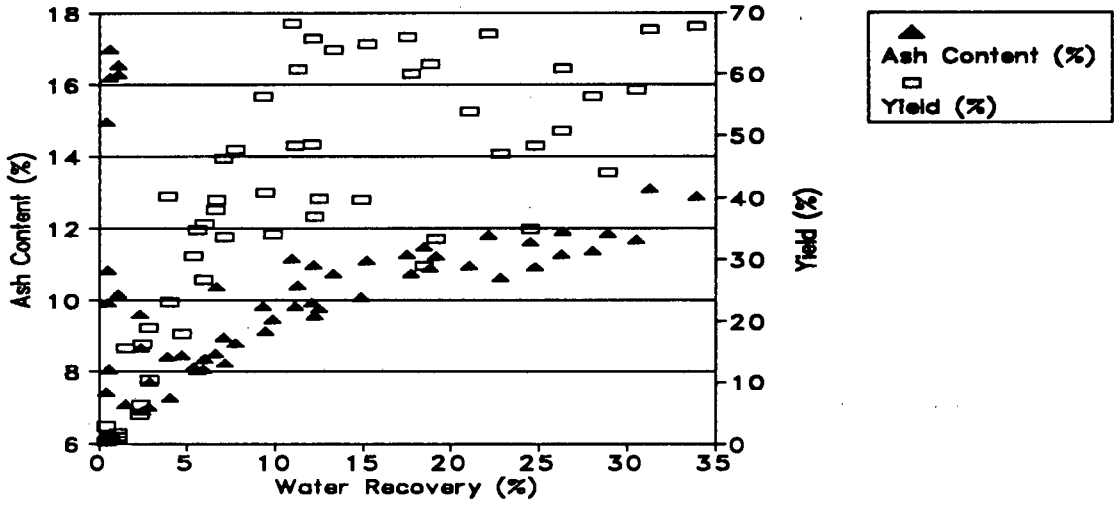

Figure 6.8 Effect of water recovery to the concentrate on the yield and concentrate ash content of Kleinkopje coal

Figure 6.8 also indicates that the yield is not as affected by the water recovery as the concentrate ash. This once again confirms that the ASH does not simply act as a splitter, as postulated by Nieuwoudt et al (1990) (see Section 3.6.1).

However, the results in Table 6.25 above also indicate that increasing the collector dosage results in a reduction in the proportion of -45 micron material in the concentrate with increasing overflow yield. This suggests that classification is not the only mechanism by which material is recovered to the overflow. The above is confirmed by the improvement in the grade, from 18.1 (KKCD1) to 12.8 % (KKCD4), with a corresponding increase in yield from 15.1 to 53.8 %. Further confirmation is apparent in the increase in the yield (with increasing collector dosage), from 53.8 (KKCD4) to 70.4 % (KKCD6) without a

Figure 6.8 was plotted using the data from the factorial design analysis (see Table C.1(b) in Appendix C).

corresponding reduction in the concentrate grade. The above are graphically illustrated in Figure 6.9 below which indicates the increasing proportion of coarse material reporting to the concentrate with increasing collector dosage. It should be stressed that increasing the collector dosage increased the recovery of *coarse particles* (as expected from the results of previous workers) at the *same grade*.

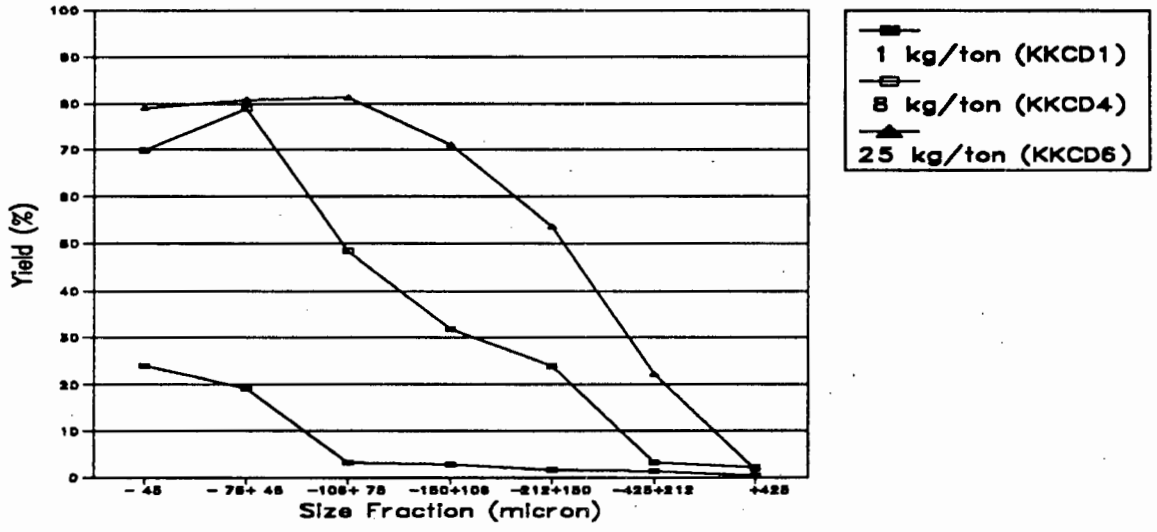

Figure 6.9: Effect of collector dosage on the size of the particles reporting to the overflow (concentrate)

From the discussion above it is apparent that the amount of water reporting to the overflow is primarily determined by the ASH configuration. The water recovery increases very little with increasing collector dosage. Thus the increasing yield is a result of *flotation* and the increased water recovery is a result of the increased coal recovery and not vice versa. This results in the amount of entrained mineral matter remaining constant (*classification*), with a resulting overall improvement in the flotation grade and recovery (separation coefficient) with increasing collector dosage.

It is also of significance that a yield in the region of 50 % was obtained at a collector dosage of about 25 kg/ton using the optimal ASH configuration, compared with the dosage of 36 kg/ton found to be

necessary in the preliminary work. This is a reduction of about 30 % in collector addition.

In addition, it is of importance to take into account the nature of the material being floated. As discussed previously (Section 5.2.2), Von Holt (1992, p168) found that conditioning was a critical factor in the flotation of the coal used in this work. Von Holt found that the flotation of this coal (Kleinkopje) in a column cell required between 5 and 12 kg/ton of collector compared with the 0.1 to 1.5 kg/ton required for other South African coals (Greenside, Durnacol, Zululand Anthracite).

If this fact is considered together with the results of previous researchers, who found that the ASH needed three times the collector dosage required in batch cells (see Section 3.7.4.2), then the collector dosages used for the ASH work are understandable. It can therefore be expected that collector dosages using more floatable coals in the ASH will be about an order of magnitude lower than those used in this work.

6.7.10 Particle size effects

The results plotted in Figures 5.12 (Chapter Five), and 6.4 and 6.5 above indicate that the ASH achieves better separation efficiencies in the intermediate size fractions (-150+75 micron), while the batch cell performs better in the coarse (+150 micron) and fine (-45 micron) size fractions. The better performance of the batch cell in the -45 micron size fraction contradicts the alleged advantage of the ASH with respect to the flotation of fine particles. In addition to the fine particle anomaly, the poor performance of the batch cell in the -150+45 micron fraction, compared with that of the ASH, requires further examination. These anomalies are discussed below.

6.7.10.1 fine and coarse particle size effects

Although numerous workers have claimed that the ASH recovers fine particles more efficiently than conventional (batch) flotation cells, few workers have reported results which support this alleged

advantage. Among the exceptions are Miller and Van Camp (1982) (coal), Miller et al (1986) (gold) and Misra et al (1983) (oil shale). In contrast to the above, Van Deventer (1988) reported "similar" results (pyrite) and Cloete et al (1987) found that batch flotation was more efficient than the ASH in the flotation of fine pyrite.

In general, researchers have referred to the performance of the ASH as "being comparable to that of batch flotation". However, all workers have reported the reduced recovery of coarse particles in the ASH in comparison to those achieved in conventional (batch) flotation cells.

The results obtained in the analysis of particle size effects (Section 6.6 above) and in the collector dosage investigation (Sections 6.5 and 6.7.9 above) show that the ASH displays some of the characteristics of a conventional cyclone. This results in the entrainment of fine particles into the overflow (i.e. fine material "misplaced" to the overflow; see Figure 6.4 above), and the loss of coarse particles to the underflow (i.e. coarse material "misplaced" to the underflow ; see Figure 6.5 above). These results confirm similar results obtained by Kinneberg and Miller (1983) (copper sulphide), Miller et al (1988) (coal) and Miller et al (1985) (hydrophilic particles). This results in the yield of fine particles being large, even when the overall yield is low, and the coarse particle yield being low, even when the overall recovery is high. This is indicated in Figure 6.10 below.

A similar trend is not as apparent in the batch cell results. The recovery of +425 micron particles is low, but the recovery of the -425 micron particles is similar for yields above 50 %. This is shown in Figure 6.11 below. Comparison of Figures 6.10 and 6.11 indicate that the ASH and batch cells achieve similar yields in the finer sizes (-106 micron), but that the ASH concentrate yield declines rapidly with increasing particle size in comparison with the batch cell. These results compare well with those of Miller et al (1988), who suggested that the upper limit to flotation in an ASH (d_c=5 cm) was in the region of 100 micron.

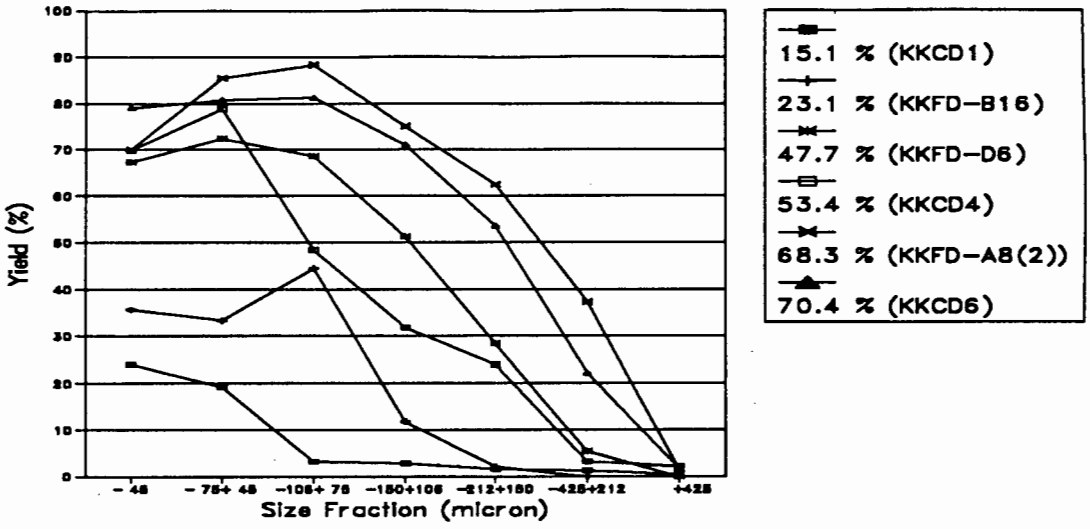

Figure 6.10: ASH concentrate yields in each size fraction at a variety of operating conditions

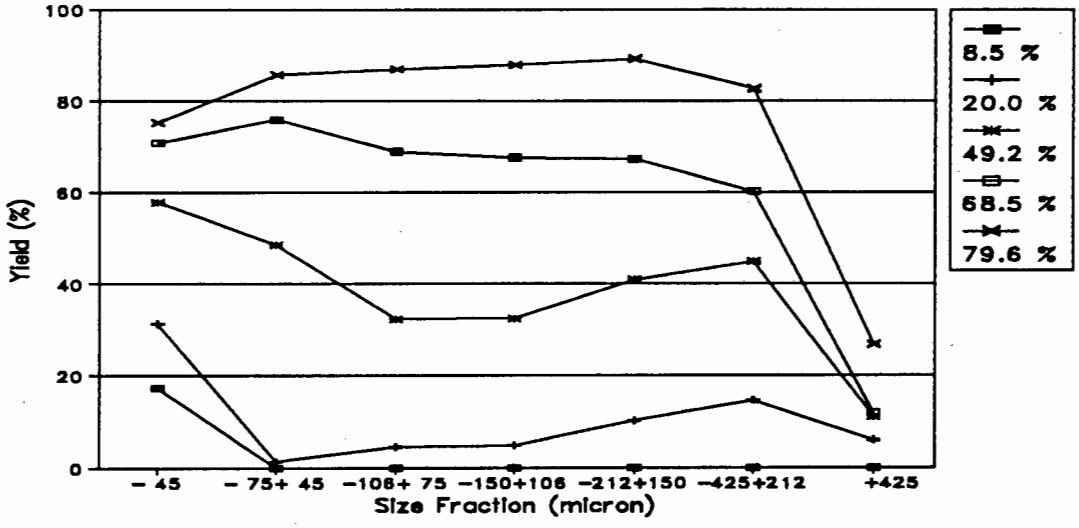

Figure 6.11: Batch cell concentrate yields in each size fraction at a variety of operating conditions

6.7.10.2 intermediate particle size effects

The poor performance of the batch cell in the intermediate sizes indicated in Figure 6.5 above contradicts the results obtained by numerous workers, including Harris et al (1992). Harris et al investigated the flotation of coal in various flotation devices, including batch cells, and found the -150+75 micron fraction to be the most amenable to flotation.

The reduced recovery of particles in these intermediate sizes (in run KKB3 - 1388 g/ton Shellsol A), in which the overall yield was about 50 %, can be attributed to two interacting factors; namely the nature of the coal being floated, and the resulting collector starvation of the intermediate sizes.

As described in Section 5.1.5, the coal used in the testwork consisted of two distinct types of material, from which a low-ash metallurgical (LAC) and a steam coal product are produced on the mine. These different types of coal are mined from different regions of the seam, but their fines and discard streams are handled together.

The petrographic analysis (Section 5.1.2) indicated that the inertinite was concentrated in the fines fraction, and the vitrinite was concentrated in the coarser sizes. Vitrinite needs very little collector to float (see Section 2.5.2), hence the comparatively good upgrading of the coarser size fraction (see Figure 5.6), even at low collector dosages.

However, almost 50 % of the Kleinkopje coal sample is located in the fines (-45 micron) fraction, and (as found by numerous workers) the fines require large quantities of reagent. In addition, Anderson (1988, p207) found that oils adsorb faster onto fine particles. The above results in the fines effectively removing large quantities of collector from the slurry. This results in insufficient collector being available for the flotation of the particles in the intermediate sizes, i.e. collector starvation.

The above is supported by the results obtained in KKB5, at 1.5 kg/ton (see Figure 5.6). In this run the flotation recovery of the intermediate particle sizes increased as a result of the increase in the collector dosage. Further confirmation of the above is apparent in Figure 6.12 below, in which the concentrate yield in each size fraction of runs KKB2 and KKCD3-2 (overall yields≈50 %); runs KKB3 and KKFD-A8(2) (overall yields≈68 %) and run KKB5 are shown.

Increasing the collector dosage from runs KKB3 to KKB5 has the same effect as increasing the collector dosage from runs KKCD4 to KKCD6: the overall yield is increased without a corresponding reduction in the concentrate grade.

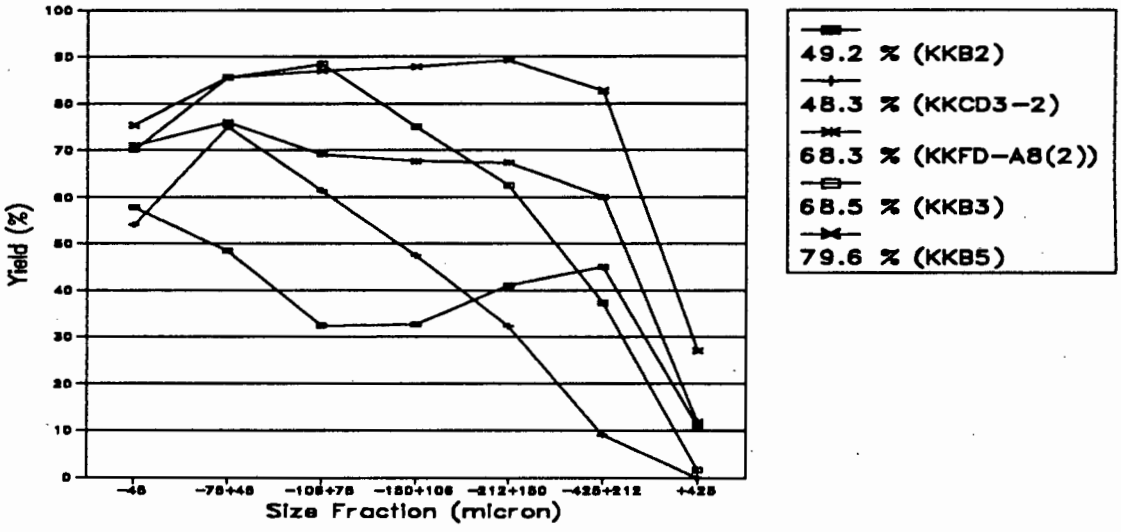

Figure 6.12: Comparison of the concentrate yield in each size fraction at similar overall yields in the ASH and batch cell

From Figure 6.12 it is clear that at similar overall yields the ASH recovers more intermediate size material. It is apparent that this can be attributed to the fact that some of the coarse material is very floatable in the batch cell (but not in the ASH) while the fines adsorb the available collector. This results in the performance of the batch cell being retarded by the lack of available collector, rather than the ASH performing better in these size fractions.

6.7.10.3 summary of particle size effects

From the results presented in Section 6.6, and the discussion in 6.7.10 above, it is apparent that the performance of the ASH in the -106 micron fraction is comparable with that of the batch cell. However, the performance of the batch cell is superior to that of the ASH in the +106 micron fraction, if the collector addition is not a limiting factor to the batch cell flotation. It can therefore

be said that, in this particular application, the small diameter ASH used is *not a more efficient device for the flotation of fine particles*, but *a less efficient device for the flotation of coarse particles* in terms of product grades attainable at a particular yield.

6.8 Chapter Summary and Conclusions

The experimental work described in this Chapter can be divided into three main sections; the factorial design analysis, the pulp density/air rate investigation and the collector dosage investigation. In addition to the above, an analysis of the performance of the ASH on the basis of particle size was carried out.

A resolution (iv) fractional factorial design was carried out to determine the relative effects of the ASH length to diameter ratio (L_c/d_c), the underflow configuration, the ratio of the overflow area to the underflow area (A^*), the area of the inlet (A_{inlet}), the ratio of the air feed rate to the slurry feed rate (Q^*) and the ratio of the vortex-finder length to the ASH diameter (L_{vf}/d_c). These parameters were investigated at a high (+) and a low (-) value. The high and low values of the parameters were chosen on the basis of the literature survey on the use of the ASH on coal and other minerals.

The variables that were kept constant, and the values used, were the collector dosage (≈36 kg/ton), the frother dosage (≈1 kg/ton), the ASH diameter (d_c=46 mm), the feed pulp density (≈3 % solids) and the slurry feed rate (Q_{slurry}≈65 lpm). The frother and collector dosages and the slurry feed rate used were chosen as a result of the preliminary work carried out, while the pulp density was as recommended by previous workers for the flotation of coal; the effect of the pulp density was determined in a separate investigation to allow the sequence of factorial design runs to be carried out in a completely random order.

A total of 62 factorial design runs were carried out. Identification of problematic runs resulted in 50 runs being included in the statistical analysis of the *original factorial design*. A statistical analysis on the

variation of the feed to the ASH during the runs determined that the errors involved were chiefly as a result of the dissembling and reassembling of the ASH. Because the MSe and se values calculated during the statistical analysis were numerically rather large, thus reducing the power of the *F*-tests, runs considered to be "outliers" were discarded and the statistical analysis was repeated.

A total of 37 runs were included in the statistical analysis of the *modified factorial design*. The modified factorial design analysis did not change the ranking of the parameters investigated, but it did confirm that the air rate had a weak effect on the overflow yield, coal recovery and water recovery.

In addition both the original and the modified factorial designs found that the parameters that had a major effect on the performance of the ASH, in decreasing order were, the underflow configuration (UF type), the ratio of the overflow to underflow areas (A^*) and the ASH length to diameter ratio (L_c/d_c). The above parameters affected the overflow (concentrate) yield, coal recovery and water recovery, but none had a statistically significant effect on the overflow grade.

The factorial design results indicated that an ASH with a baffle and orifice underflow configuration was more effective than one with a pedestal and an annular opening. The former gave an average yield in the region of 30 % more than the latter configuration. Increasing the A^* ratio from 0.5 to 1.34 resulted in an increase in the average overflow yield in the region of 20 %. This fact confirmed the results of previous workers who found that a larger A^* ratio increased the average yield, but disagreed with the associated reduction in the concentrate grade found by most researchers. An ASH 300 mm long achieved an average yield in the region of 20 % more than in an ASH 500 mm in length. This result was also in disagreement with the results of previous workers using the ASH, who found that increasing the ASH length increased the yield (especially of coarse particles) as a result of the reduced turbulence at the base of the cyclone and the increased slurry residence time.

The results obtained and the conclusions drawn, from the above results can be considered to be largely a function of the material being floated. Kleinkopje coal has been found to be poorly floatable, both in laboratory (Von Holt, 1992) and plant trial experimental work (Von Holt, 1991). In these circumstances the factor which determines the performance of the ASH is facilitation of froth transport to the overflow. The above is accomplished by a shorter ASH and restricting the slurry phase at the base of the ASH, forcing it to migrate to the axis of the ASH in order to exit the ASH via the orifice. The above facilitate froth withdrawal by increasing the pressure gradient across the ASH length, while a larger A^* facilitates froth removal.

In the factorial design the ratio of the air to slurry flow rates (Q^*) was found to have a minor effect on the performance of the ASH.

Increasing the air rate, from 175 to 300 slpm, resulted in a reduction in the yield, coal recovery and water recovery, at the same product grade. This result contradicts the results of previous workers, who found that increasing Q^* increased the yield but reduced the grade. Experiments carried out at three different air rates (in the pulp density/air rate investigation) confirmed the factorial design results, and showed that the reduced yield was accompanied by an improvement in the concentrate grade. The reduced yield and improved grade may be a result of the increased volume of air reporting to the underflow as a result of overflow opening limitations.

The factorial design results also indicated that the length of the vortex-finder (L_{vf}/d_c) may have an effect on the performance of the ASH. This parameter was also evident in interaction terms containing the A_{inlet} and L_c/d_c. Comparison with the fluid flow regimes at the top of the ASH suggest that the location of the vortex-finder inlet (i.e. length) with respect to the point of minimum fluid (slurry) velocity may affect the performance of the ASH to a degree. Similar results have been reported by other workers.

The inlet area (A_{inlet}) was found to have no effect on the performance of the ASH. This confirmed the work of previous workers.

The pulp density/air rate investigation was carried out using the ASH configuration which the factorial design showed to be optimal in terms of the concentrate yield to the overflow. These results indicated that the pulp density of the feed to the ASH could be increased to 9.4 % solids without having an adverse effect on the performance of the ASH. Previous workers have found that the optimum % solids for coal flotation was in the region of 3 %, but up to 50 % solids has been used in the flotation of other mineral ores.

The collector dosage investigation indicated that using an ASH configuration which maximised the concentrate (overflow) yield allowed the collector dosage to be reduced by about 30 % (to 25 kg/ton) and still achieve a yield in the region of 50 %. In addition, size analyses carried out on certain concentrate and tails samples indicated that the ASH configuration was the determining factor with respect to the concentrate grade. The configuration used was chosen so as to maximise the yield. This resulted in a comparatively large water recovery to the overflow, and hence a high ash content, even at low overall yields (collector dosages)#. As the collector dosage was increased the proportion of entrained material was reduced, causing a reduction in the overall ash content with a corresponding increase in the yield (collector dosage). The above was apparent in the increased flotation of the coarser size fractions with increasing collector dosage, i.e. the recovery of material is the result of both classification and flotation.

Particle size analyses carried out on selected concentrate and tails samples indicated that more entrainment of fine mineral matter occurred in the ASH than in the batch cell. At the same time the ASH lost a greater proportion of coarse material to the tails (underflow) than the batch cell did. In addition it seemed as though the amount of material "misplaced" to the underflow increased linearly with increasing particle size. The results showed that the performance of the ASH in the -106 micron fraction is comparable with that of the batch cell. However, the performance of the batch cell is superior to that of the ASH in the +106 micron fraction,

The errors involved in the factorial design prevented the detection of factors affecting the concentrate grade even though the associated increases in the water recovery were detected.

if the collector addition is not a limiting factor to the batch cell flotation. It can therefore be said that, in this particular application, the ASH is *not a more efficient device for the flotation of fine particles*, but that it *is a less efficient device for the flotation of coarse particles* in terms of product grades attainable at a particular yield.

Overall, it can be seen from the results obtained that the ASH is capable of achieving separations which are comparable to those achieved in batch cells, for the coal used. In addition, it seems as though the ASH is capable of producing better concentrate grades at yields between 30 and 50 %; Miller et al (1988) achieved similar results for the ASH and batch cells at overall yields between 30 and 50 %. At yields below 50 % the ASH is capable of producing a concentrate with a grade in the region of 9 %. However, at yields in excess of 60 % grades in the region of 13 % are obtained.

An important factor is that these results were obtained at capacities in the region of 100 times those achievable in conventional cells, and over 500 times those achieved in a column cell. Furthermore, the pulp density/air rate investigation results demonstrated that the feed % solids could be increased to 9.4 % without a corresponding reduction in the concentrate grade or recovery. This increases the capacity of the ASH relative to conventional and column cells to 300:1 and 1500:1, respectively. These results indicate that an ASH circuit would require far smaller ancillary equipment, thus reducing the cost in comparison to that of a conventional circuit. Where retrofitting a plant to include a flotation circuit the above would have important space saving implications.

The major disadvantage of the ASH was found to be the high collector dosage required for flotation. However, work carried out using the same coal determined that the conditioning step was critical in the flotation of this coal. Inadequate conditioning in comparison with that in batch cells resulted in collector dosages of between 5 and 12 kg/ton being required in the column cell. This problem should not be encountered in the flotation of more floatable coals.

The results obtained above suggest that it might be possible to use the ASH as a rougher, producing final concentrate in the case of a steam quality product, or cleaner (column cell) feed in the case of a metallurgical coal (7 % LAC) product. However the use of the ASH as a scavenger seems unlikely to succeed as a result of the material needing to be strongly hydrophobic for it to report to the concentrate; if it has not floated in other devices then it is unlikely to be recovered in the ASH, except by classification.

In the event of the former circuit being employed (i.e. rougher producing steam quality product) the ASH could be used to produce a product at a yield of between 30 and 50 %. The ASH tails, consisting chiefly of the coarser material could be scavenged in conventional cells, to produce a similar product for blending with the ASH concentrate product. The tails from the scavengers would report to final tails. Use of this circuit would greatly reduce the size of the conventional cells required, and in certain cases scavengers may not be necessary. Two options that would not appear to be feasible are: the returning of the scavenger concentrate to the ASH (for the same reason that would prevent the ASH from acting as a scavenger), and scavenging the ASH tails in a column cell (the material would be expected to be too coarse).

CHAPTER SEVEN

CONCLUSIONS AND RECOMMENDATIONS

The principal aims of this thesis were to investigate the use of an ASH in the flotation of South African coal *ultrafines*, and to determine the effect of various design and operating parameters on the performance of the process, in terms of the product yields and grades obtainable. The coal chosen for the testwork was a typical Witbank coal, from the Kleinkopje Colliery, which had been used by other students in the Department of Chemical Engineering at the University of Cape Town for flotation testwork, including column flotation studies.

The results described and discussed in the preceding chapters show that it was possible to use the ASH to beneficiate this coal at capacities of up to 300 times greater than those possible in conventional (batch) flotation, and in the region of 1500 times those achieved using the same coal in a column cell. The ASH was able to produce product grades and yields which were comparable with those achieved in batch flotation tests. However, neither the ASH nor the batch cell were able to produce results comparable with those achieved in the column cell.

At concentrate yields between 30 and 50 % the grades achieved at a particular yield were generally better in the ASH than those achieved in the batch cell. However, at yields in excess of 60 % the grades achieved in the batch cell seemed to surpass those of the ASH.

The nature of the material being floated resulted in collector dosages in the region of 36 kg/ton being necessary to achieve concentrate yields in the region of 50 %. However, use of the optimal ASH configuration reduced this collector dosage requirement to about 25 kg/ton. From the results

achieved by Von Holt (1992) in column cell testwork using the same coal it is expected that the above collector dosage would not be necessary in the flotation of a more "floatable" coal. A frother dosage of 1 kg/ton was found to be sufficient.

The concentrate coal yield was found to be largely dependent on the water recovery to the overflow. In order to increase the coal recovery it was necessary to facilitate froth transport to the overflow by either increasing the overflow area or restricting the underflow outlet. The latter was most significantly effected by altering the ASH configuration, i.e. by replacing the conventional pedestal and annular opening underflow configuration with a flow limiting orifice and horizontal baffle.

Facilitating froth removal resulted in the entrainment of both fine hydrophilic and hydrophobic material into the concentrate product. This resulted in the proportion of fines in the concentrate being high. The net result was that material was recovered to the overflow as a result of both classification and flotation. This resulted in the efficiency of the ASH with respect to fine particles being comparable with that of the batch cell. However the batch cell was found to be more efficient in the recovery of coarse particles (+106 micron).

For the above reasons, in this particular application, the ASH cannot be considered to be a *more efficient device for the flotation of fine particles*, but rather a *less efficient device for the recovery of coarse particles*. Although the ASH proved to be less efficient in the coarse particle fractions the aim of the thesis was to beneficiate *ultrafine* coal, i.e. -150 micron coal, and in these sizes the results of the ASH and the batch cell were comparable.

The parameters found to have the greatest influence on the performance of the ASH, in descending order of magnitude, were: the underflow configuration, the ratio of the overflow to underflow openings (A^*), the ASH length to diameter ratio (L_c/d_c) and the ratio of the air to slurry feed rates (Q^*). The effects of these parameters are described below.

i) The use of a pedestal and annular opening underflow configuration was not necessary for the flotation of this coal; higher yields at similar ash contents were achieved using a flow restricting orifice with a horizontal baffle located above it. In addition the latter configuration reduced the possibility of blockages. (When the annular opening became blocked it was necessary to dissemble, unblock and reassemble the ASH, before repeating the run.)

ii) Increasing the area of the overflow opening relative to that of the underflow increased the concentrate yield, at a similar grade, as a result of the removal of the froth phase being facilitated.

iii) Reducing the length of the ASH resulted in an increase in the concentrate yield, without an associated reduction in the concentrate grade. This is because the reduction in the ASH length causes the base of the froth cone to be raised, facilitating its transport to the overflow.

iv) At a given slurry rate, an air rate exists at which the concentrate recovery is a maximum. At air rates above this optimum the yield is reduced as a result of overflow area limitations. At air rates below this optimum the bubble swarm density is too low to achieve maximum recovery. Increasing the air rate resulted in a reduction in the concentrate ash content, as a consequence of only the most hydrophobic particles being able to attach to air bubbles.

It was found that the length of the vortex-finder may have an effect on the concentrate grade, if its length coincides with the region of reduced axial and tangential velocity below the slurry inlet, or as a result of short-circuiting of the slurry across the roof of the cyclone.

The parameters which were found to have no effect on the performance of the ASH, at the levels tested, were the pulp density and the A_{inlet}. The pulp density was increased from the 3 % to 9.4 % with no adverse effect on the performance of the ASH. This increased the volumetric capacity of the ASH threefold; this would significantly reduce the costs of an ASH circuit.

From all the results obtained in this investigation, and the conclusions drawn therefrom, a few recommendations can be made as to the direction in which future research into the flotation of coal in an Air-Sparged Hydrocyclone should take.

Most importantly, research should focus on the collector dosage requirements of the ASH when floating South African coals. The major drawback in the application of the ASH to the flotation of the Kleinkopje coal lies in the collector dosage required being economically prohibitive. As this problem also affected the performance of the column cell in which the same material was floated, and as other South African coals (which consist predominantly of inertinite) are likely to present similar problems, this area warrants substantial research energy. Scope for improvement in this field lies in the use of more selective collectors and (especially) in the use of different conditioning equipment and/or methods.

Irrespective of the outcome of the above, the most obvious question to be answered is, "what results could be achieved using a more floatable coal in the ASH?". This is a question which should be answered as soon as possible, as it would present an entire series of avenues for the flotation at very great throughputs of large quantities of *ultrafine* coal which at present are being discarded.

In addition, the work carried out in the pulp density/air rate investigation should be extended to determine the limiting pulp density, i.e. the pulp density at which the performance of the ASH deteriorates to the extent that any subsequent increase in capacity is counteracted by either reduced recovery, or an increase in the ash content of the concentrate product.

A further avenue for research is the determination of the scale-up factors governing the ASH, as most research has been limited to small diameter units as a result of the high capacity of the device.

REFERENCE APPENDIX

Alberts, B.C., The Planning for the Utilisation of South Africa's Mineral Reserves with Specific Reference to Coal" Journal of the South African Institute of Mining and Metallurgy, Vol 87, November 1987, pp 371-395.

Amcoal, 1987 as cited by Horsfall, D.W., "Cost Effective Routes in Fine Coal Beneficiation ", Presented at AIME Conference - Industrial Practice of Fine Coal Processing, Hidden Valley, Somerset PA, Sept. 1988, Ch 34, pp 365-374.

Anderson, G. V. M., "The Role of Hydrocarbon Oils in Coal Flotation: An Investigation into some Pulp-Phase Sub-processes", PhD Thesis submitted to University of Cape Town, June 1988.

Aplan, F. F., 1987 as cited by Von Holt, S., "An Investigation of Column Flotation at Kleinkopje Colliery", Report prepared for the Anglo American Corporation, University of Cape Town, March 1991.

Aplan, F. F., "How the nature of raw coal influences its cleaning ", Presented at AIME Conference - Industrial Practice of Fine Coal Processing, Hidden Valley, Somerset PA, Sept. 1988, Ch13, pp 99-111.

Baker, M.W., "High Speed Fine Coal Cleaning with the Air-Sparged Hydrocyclone", Proceedings of the Fifth Australian Coal Preparation Conference - Preparation in the 1990's, Newcastle, Australia, 13-16 May 1991, pp 122-134.

Baker, M.W., Gopalakrishnan, S., Rogovin, Z. and Miller ,J.D., "Hold-up Volume and Mean Residence Time Measurements in the Air-sparged Hydrocyclone", Particulate Science and Technology, Vol 5, 1987, pp 409-420.

Bennet, A.J.R., Chapman, N.R. and Dell, C.C., 1958 as cited by Fickling, R.S., "An Investigation into the Froth Flotation of Four South African Coals", M.Sc. Thesis, University of Cape Town, 1985.

Birtek, N. and King, R.P., 1986 as cited by Harris, M.C., "The Liberation Characteristics of Greenside No. Two Seam Coal", M.Sc Thesis, University of Cape Town, 1987.

Botha, P.H., "An Investigation of the Flotation of Three South African Coals", Journal of the South African Institute of Mining and Metallurgy, November 1980, pp 395-400.

Breed, A.W. and Inglis, K.E., "The Reduction of Entrainment by Column Flotation", Final Year Project, University of Cape Town, 1989.

Breed, A.W., Harris, M.C., Franzidis, J-P. and O'Connor, C.T. "Column Flotation Pilot Plant Trials at Koornfontein Colliery", Report prepared for GENMIN, University of Cape Town, April 1991.

Brown, D. J., Gray, V. R. and Jackson A. W., "The Spreading of Oil on Wet Coal", J. appl. Chem., 8, 1958, pp 752-759.

Burdon, R.G., 1962 as cited by Fickling, R.S., "An Investigation into the Froth Flotation of Four South African Coals", M.Sc. Thesis, University of Cape Town, 1985.

Burger, A.J., "Flotasie van 'n Growwe Pirieterts in 'n Luggeborrerelde Hidrosikloon", M.Eng. Thesis, University of Stellenbosch, 1986.

Burkin , A.R. and Bramley, J.V., "Flotation with Insoluble Reagents I. Collision and Spreading Behaviour in the Coal-Oil-Water System", Journal of Applied Chemistry, vol 11, August 1961, pp 300-309.

Burkin , A.R. and Bramley, J.V., "Flotation with Insoluble Reagents II. Effectsof Surface-Active Reagents on the Spreading of Oil at Coal-Water Interfaces", Journal of Applied Chemistry, vol 13, October 1963, pp 417-422.

Buys, I. E., "A Comparison of Froth Flotation and Oil Agglomeration for fine and Ultrafine Coal Beneficiation", B.Sc (Hons) Project, University of Cape Town, 1987.

Buys, I. E., "A Liberation Study on Ultrafine South African Coals", M.Sc Thesis, University of Cape Town, 1989.

Campbell, J.A.L. and Sun, S.C., "Anthracite Coal Electrokinetics", Transactions of the Society of Mining Engineers, vol 247, June 1970, pp 120-122.

Chironis,.N.P., "Advanced Techniques Clean Ultrafine Coal at Homer City", Coal Age, December 1987, pp 68-69.

Cloete, F.L.D., Burger ,A.J. and Van Deventer, J.S.J., "Flotation of Pyritic Ore in an Air-sparged Hydrocyclone", 3rd International Conference on Hydrocyclones, Oxford, England, 1987, pp 215-220.

Collins, G.L. and Jameson, G.J., "Experiments on the Flotation of Fine Particles - The Influence of Particle Size and Charge", Chemical Engineering Science, vol 31, 1976, pp 985-991.

Collins, G.L. and Jameson, G.J., "Double-Layer Effects in the Flotation of Fine Particles", Chemical Engineering Science, vol 32, 1977, pp 239-246.

Department of Mineral and Energy Affairs, "South African Discard and Duff Coal : National Inventory", 1985.

Dobby, G.S. and Finch, J.A., "Particle Size Dependence in Flotation Devised from a Fundamental Model of the Capture Process", International Journal of Mineral Processing, vol 21, 1987, pp 241-260.

Edwards, D., "Better Prospects Ahead for Coal", S.A. Mining, Coal, Gold and Base Minerals, December 1988, pp 11-14.

Engel, M.D. and Smitham, J.B., "The Relationship Between Coal Particle Size and Hydrophobicity in the Formation of Particle Stabilised Froths", The AusIMM Bulletin and Proceedings, Vol 293, 1988, pp 63-66.

Evans, L.F., "Bubble-Mineral Attachment in Flotation", Industrial and Engineering Chemistry, Vol 46, 1954, pp 2420-2424.

Falcon, R.M.S., "Coal in South Africa - Part 1 : The Quality of South African Coal in Relation to its Uses and World Energy", Minerals Science Engineering, Vol 9, no 4, October 1978, pp 198-217.

Falcon, R.M.S., "Coal in South Africa - Part 2 : The Application of Petrography to the Characterisation of Coal", Minerals Science Engineering, Vol 10, no 1, January 1978, pp 28-52.

Falcon, R.M.S., "Coal in South Africa - Part 3 : Summary and Proposals - The Fundamental Approach to the Characterisation and Rationalisation of South Africa's Coal", Minerals Science Engineering, Volume 10, no 21, April 1978, pp 130-153.

Falcon, R.M.S. and Snyman, C.P., "An Introduction to Coal Petrography : Atlas of Petrographic Constituents in the Bituminous Coals of Southern Africa", Review Paper No 2, The Geological Society of South Africa, 1986.

Falcon, R.M.S., personal communication

Fickling, R.S., "An Investigation into the Froth Flotation of Four South African Coals", M.Sc. Thesis, University of Cape Town, 1985.

Flint, L.R. and Howarth, W.J., "The Collision Efficiency of Small Particles With Spherical Air Bubbles", Chemical Engineering Science, vol 26, 1971, pp 1155-1168.

Franzidis, J-P., "Developments in Fine Coal Beneficiation in South Africa", Coal Preparation, Vol. 11, 1992, pp 103-114.

Franzidis, J-P. and Harris, M.C., "A New Method for the Rapid Float-Sink Analysis of Coal Fines", Journal of the South African Institute of Mining and Metallurgy, vol 86, no 10, October 1986, pp 409-414.

Gan, H., Nandi, S.P., and Walker, P.L.Jnr., 1972 as cited by Aplan, F. F., "How the nature of raw coal influences its cleaning ", Presented at AIME Conference - Industrial Practice of Fine Coal Processing, Hidden Valley, Somerset PA, Sept. 1988, Ch13, pp 99-111.

Gaudin, A.M., Groh, J.O. and Henderson, H.B., 1931 as cited by Trahar, W.J. and Warren, L.J., "The Flotability of Very Fine Particles - A Review", International Journal of Mineral Processing, vol 3, 1976, pp 103-131.

Gopalakrishnan, S., Ye, Y. and Miller, J.D., "Dimensionless Analysis of Process Variables in Air-Sparged Hydrocyclone Flotation of Fine Coal", Coal Preparation, 1991, Vol. 9, pp 169-184.

Gray, R.J., Rhoades, A.H. and King, D.T., "Detection of Oxidised Coal and the Effect of Oxidation on the Technological Properties", Transactions of the Society of Mining Engineers, vol 260, December 1976, pp 334-341.

Grobbelaar, C.J., "Colliery Discards Worldwide with Reference to its Utilisation", S.A. Mining World, October 1988, pp 104-125.

Gy, M., "Sampling of Particulate Solids : Theory and Practice", Elsevier Scientific Publishing Company, New York, 1982.

Guy, T.W., 1937 as cited by Aplan, F. F., "How the nature of raw coal influences its cleaning ", Presented at AIME Conference - Industrial Practice of Fine Coal Processing, Hidden Valley, Somerset PA, Sept. 1988, Ch13, pp 99-111.

Harris, M.C., "The Liberation Characteristics of Greenside No. Two Seam Coal", M.Sc Thesis, University of Cape Town, 1987.

Harris, M.C., Franzidis, J-P., O'Connor, C.T. and Stonestreet, P., "An Evaluation of the Role of Particle Size in the Flotation of Coal using Different Cell Technologies", Proceedings of Minerals Engineering '92, Vancouver, Canada, 14-16 April 1992, pp 1225-1238

Hemmings, C.E., "On the Significance of Flotation Froth Liquid Lamellae Thickness", Transactions of the Institution of Mining and Metallurgy, vol 90, September 1981, pp C96-C102.

Horsfall, D.W., "A General Review of Coal Preparation in South Africa", Journal of the South African Institute of Mining and Metallurgy, August 1980, pp 257-268.

Horsfall, D.W. (ed), "Coal Preparation for Plant Operators", The South African Coal Processing Society, Cape Town, 1980.

Horsfall, D.W., "The Treatment of Fine Coal : Upgrading -0.5mm Coal to Obtain a Low-Ash Product", ChemSA, July 1976, pp 124-129.

Horsfall, D.W., "Cost Effective Routes in Fine Coal Beneficiation ", Presented at AIME Conference - Industrial Practice of Fine Coal Processing, Hidden Valley, Somerset PA, Sept. 1988, Ch 34, pp 365-374.

Horsfall, D.W. and Franzidis, J-P., "Beneficiation of South African Coal Fines", in Proceedings of the 5th Annual International Pittsburgh Coal Conference, Pittsburgh, PA, September 12-16, 1988, pp 311-325.

Jameson, G. J., "Physical Factors Affecting Recovery Rates in Flotation", Minerals Sci. Engng, 1977, vol. 9, no 3., pp 103-118.

Kelly, E.G., Spottiswood, D.J., Spiller, D.E. and Robinson, C.N., "Performance of Compound Trough Profile Spiral Cleaning Fine Coal", Transactions of the Society of Mining Engineers of AIME, 1984, Vol. 276, pp 1943-1949.

Kinneberg, D.J. and Miller, J.D., 1983 as cited by Miller, J.D. and Kinneberg, D.J., "Fast Flotation with an Air-sparged Hydrocyclone", Prceedings of Mintek 50 : International Conference on Recent Advances in Mineral Science and Technology, Johannesburg, South Africa, March 1984, pp 373-383.

Kirchberg, H. and Topfer, E., 1965 as cited in Jameson, G. J., "Physical Factors Affecting Recovery Rates in Flotation", Minerals Sci. Engng, 1977, vol. 9, no 3., pp 103-118.

Klaasen, V.I. and Mokrousov, V.A., 1963 as cited in Jameson, G. J., "Physical Factors Affecting Recovery Rates in Flotation", Minerals Sci. Engng, 1977, vol. 9, no 3., pp 103-118.

Lai, R.W., Wen, W-W. and Okoh, J.M., "Effect of Humic Substances on the Flotation Response of Coal", Coal Preparation, Vol 7, 1989, pp 69-83.

Laskowski, J.S., Sirois, L.L. and Moon, K.S., "Effect of Humic Acids on Coal Flotation Part 1. Coal Flotation Selectivity in the Presence of Humic Acids", Coal Preparation, Vol 3, 1986, pp 133-154.

Leys, J.L., "Recovery of Ultra-Fine Coal from Washery Underflow by the Oil Agglomeration Process", S.A. Mining World, September 1988, pp 77-83.

MacKenzie, J.M.W., 1969 as cited in Anderson, G. V. M., "The Role of Hydrocarbon Oils in Coal Flotation: An Investigation into some Pulp-Phase Sub-processes", PhD Thesis submitted to University of Cape Town, June 1988.

Mason, R.L., Gunst, F.G., and Hess, J.L, "Statistical Design and Analysis of Experiments - With Applications to Engineering and Science", John Wiley and Sons, New York, 1989.

McLean, R.A. and Anderson, V.L., "Applied Factorial and Fractional Designs", Marcel Dekker, Inc., New York, 1984.

Mehrotra, S.P. and Kupar, P.C., "The Effects of Aeration Rate, Particle Size and Pulp Density on the Flotation Rate Distributions", Powder Technology, vol 9, 1974, pp 213-219.

Miller, J.D. and Kinneberg, D.J., "Fast Flotation with an Air-sparged Hydrocyclone", Prceedings of Mintek 50 : International Conference on Recent Advances in Mineral Science and Technology, Johannesburg, South Africa, March 1984, pp373-383.

Miller, J.D., Mistra, M. and Gopalakrishnan, S., "Gold Flotation from Colorado River Sand using the Air-sparged Hydrocyclone", Minerals and Mineral Processing, August 1986, pp 145-148.

Miller, J.D., Upadrashta, K.R., Kinneberg, D.J. and Gopalakrishnan, S., "Fluid Flow in the Air-sparged Hydrocyclone", Proceedings of the XVth International Mineral Processing Congress, Cannes, June 2-9, 1985, pp87-99.

Miller, J.D. and Van Camp, M.C., "Fine Coal Flotation in a Centrifugal Field With an Air Sparged Hydrocyclone", Mining Engineering, November 1982, pp 1575-1580.

Miller, J.D. and Ye, Y., "Froth Characteristics in Air-sparged Hydrocyclone Flotation", Mineral Processing and Extractive Metallurgy Review, Vol 5, 1989, pp 307-329.

Miller, J.D., Ye, Y., Lin, C.L. and Cortes, A.B., 1989 as cited by Miller, J.D. and Ye, Y., "Froth Characteristics in Air-sparged Hydrocyclone Flotation", Mineral Processing and Extractive Metallurgy Review, Vol 5, 1989, pp 307-329.

Miller, J.D., Ye, Y., Pacquet, E., and Baker, M.W., "The Air Sparged Hydrocyclone for Fine Coal Flotation", Proceedings of the 1988 American Mining Congress, Chicago, April 24 - 28, 1988, pp 1-15.

Miller, J.D., Ye ,Y., Pacquet, E., Baker, M.W. and Gopalakrishnan, S., "Design and Operating Variables with the Air-sparged Hydrocyclone" Proceedings of the 16th International Mineral Processing Congress, Stockholm, June 5 - 10, 1988, pp 87-99.

Miller, K.J., "Novel Flotation Equipment : A Survey of Equipment and Processes", Presented at AIME Conference - Industrial Practice of Fine Coal Processing, Hidden Valley, Somerset PA, Sept. 1988, Ch 13, pp 347-363.

Mishra, S.K., 1987 as cited in Anderson, G. V. M., "The Role of Hydrocarbon Oils in Coal Flotation: An Investigation into some Pulp-Phase Sub-processes", PhD Thesis submitted to University of Cape Town, June 1988.

Misra, M. and Anzia, I., "Ultrafine coal flotation by gas phase transport of atomised reagents", I. Miner. Metall Process, v4, n4, Nov. 1987, pp 233-236.

Montgomery,D.C. Design and Anaysis of Experiments. John Wiley and Sons. New York. 1987.

Ng, F.L., 1982 as cited in Anderson, G. V. M., "The Role of Hydrocarbon Oils in Coal Flotation: An Investigation into some Pulp-Phase Sub-processes", PhD Thesis submitted to University of Cape Town, June 1988.

Nieuwoudt, D.J., Van Deventer, J.S.J., Reuter, M.A. and Ross, V.E., "The Influence of Design Variables on the Flotation of Pyrite in an Air-Sparged Hydrocyclone", Minerals Engineering, Vol 3 no 5, 1990, pp 483-499.

Nimerick, K.H. and Scott, B.E., 1980 as cited in Fickling, R.S., "An Investigation into the Froth Flotation of Four South African Coals", M.Sc. Thesis, University of Cape Town, 1985.

Nonaka, M. and Uchio, T., "Pressure Flotation in Hydrocyclone", Proceedings of the 2nd International Conference on Hydrocyclones, Bath, England, 19 - 21 September 1984, pp 381-392.

Onlin, T.J. and Aplan, F.F., as cited in Aplan, F. F., "How the nature of raw coal influences its cleaning ", Presented at AIME Conference - Industrial Practice of Fine Coal Processing, Hidden Valley, Somerset PA, Sept. 1988, Ch13, pp 99-111.

Panopoulos, G. and King, R.P., "Flotation of Fine and Ultrafine Coal", Batch Flotation Tests Report No CSPCOAL 3, June 1984.

Park, G.A., 1970 as cited in Wen, W.W. and Sun, S.C., "An Electrokinetic Study on the Amine Flotation of Oxidised Coal", Transactions of the Society of Mining Engineers, vol 262, June 1977, pp 174-180.

Reay, D. and Ratcliff, G.A., "Removal of Fine Particles from Water by Dispersed Air Flotation : Effects of Bubble Size and Particle Size on Collection Efficiency", The Canadian Journal of Chemical Engineering, Vol 51, April 1973, pp 178-185.

Rhodes, N. and Pericleous, K.A., "Use of Computational Fluid Dynamics in Analysis and Design", 1986.

Sanders, G.J. and Brookes, G.F., 1986 as cited in Franzidis, J-P., "Developments in Fine Coal Beneficiation in South Africa", Coal Preparation, Vol. 11, 1992, pp 103-114.

Sachs, L., "Applied Statistics - A Handbook of Techniques", Springer-Verlag, New York, 1982.

Stoessner, R.D., Shirey, G.A., Zawadski, E.A., Welsh, C.E., Miller, J.D. and Shell, W.P., 1990 as cited by Baker, M.W., "High Speed Fine Coal Cleaning with the Air-Sparged Hydrocyclone", pp 122-134

Stoessner, R.D., Shirey, G.A., Gopalakrishnan, S., "Optimising the Air-Sparged Hydrocyclone for Fine Coal Cleaning : A Progress Report", Advances in Coal and Mineral Processing using Flotation, Chapter 12, Eng. Foundation and SME, Dec. 1988, pp 107-112.

Sun, S.C., "Flotation Theory", in Part 3. Froth Flotation in Coal Preparation, The American Institute of Mining, Metallurgical and Petroleum Engineers, Inc., New York, 1968, pp 10-66 - 10-90.

Swanson, A.R., Firth, B.A. and Roberts, T., "The Interaction Between Pulp Density and Frother Addition in Coal Flotation", Proceedings of the Australasian Institute of Mining and Metallurgy, No. 289, February, 1984, pp 45-50.

Szatkowski, M and Freyberger, W.L., "Kinetics of Flotation with Fine Bubbles", Transactions of the Institution of Mining and Metallurgy, vol 94, June 1984, pp C61-C70.

Szczypa, j., Neczaja-Hruzewicz, J. and Sablik, J., "Some Properties of Slime Coatings in Coal-Gangue Systems", Transactions of the Institution of Mining and Metallurgy, vol 82, 1973, pp C167-C169.

Taylor, G.I., 1948 as cited by Miller, J.D. and Kinneberg, D.J., "Fast Flotation with an Air-sparged Hydrocyclone", Prceedings of Mintek 50 : International Conference on Recent Advances in Mineral Science and Technology, Johannesburg, South Africa, March 1984, pp 373-383.

Trahar, W.J., 1981 as cited by Fickling, R.S., "An Investigation into the Froth Flotation of Four South African Coals", M.Sc. Thesis, University of Cape Town, 1985.

Trahar, W.J. and Warren, L.J., "The Flotability of Very Fine Particles - A Review", International Journal of Mineral Processing, vol 3, 1976, pp 103-131.

Tsai, S.C., "Coal Science and Technology 2 - Fundamentals of Coal Beneficiation and Utilisation", Elsevier Scientific Publishing Company, New York, 1982.

Van Camp, M.C., as cited in Miller, J.D. and Van Camp, M.C., "Fine Coal Flotation in a Centrifugal Field With an Air Sparged Hydrocyclone", Mining Engineering, November 1982, pp 1575-1580.

Van Deventer, J.S.J., Burger, A.J. and Cloete, F.L.D., "Intensification of Flotation with an Air-sparged Hydrocyclone", Journal of the South African Institute of Mining and Metallurgy, Vol 88, No 10, 1988, pp 325-332.

Voges, H. C., "Development in Coal Fine Beneficiation", Journal of the South African Institute of Mining and Metallurgy, 91(2), pp 41-50.

Von Holt, S., "An Investigation of Column Flotation at Kleinkopje Colliery", Report prepared for the Anglo American Corporation, University of Cape Town, March 1991.

Von Holt, S., "An Investigation into Column Flotation of South African Coals, M.Sc. Thesis submitted to University of Cape Town, April, 1992.

Walker, S., "The Future for Hydrocyclones", International Mining, May 1988, pp 26-30.

Ward, R.C.(ed), "Coal Geology and Coal Technology", Blackwell Scientific Publications, London, 1984.

Wen, W.W. and Sun, S.C., "An Electrokinetic Study on the Amine Flotation of Oxidised Coal", Transactions of the Society of Mining Engineers, vol 262, June 1977, pp 174-180.

Wen, W.W. and Sun, S.C., 1981 as cited in Fickling, R.S., "An Investigation into the Froth Flotation of Four South African Coals", M.Sc. Thesis, University of Cape Town, 1985.

Ye, Y., Gopalakrishnan, S., Pacquet, E. and Miller, J.D., "Development of the Air-sparged Hydrocyclone - A Swirl-flow Flotation Column", Proceedings of the International Symposium on Column Flotation, Phoenix, January 25 - 28, 1988, pp 305-313.

Ye, Y., Khandrika, S.M. and Miller, J.D. "Induction-Time Measurements at a Particle Bed", International Journal of Mineral Processing, Vol 25, 1988, pp 221-240.

Ye, Y. and Miller, J.D. "The Significance of Bubble/Particle Contact Time During Collision in the Analysis of Flotation Phenomena", International Journal of Mineral Processing, Vol 25, 1989, pp 199-219.

Ye, Y and Miller, J.D., "Bubble/Particle Contact Time in the Analysis of Coal Flotation", Coal Preparation, Vol 5, 1988, pp 147-166.

APPENDIX A

ANALYSIS OF SAMPLING METHOD

A.1 Sample Collection

The coal used in the experimental testwork described in this thesis was obtained from the Kleinkopje Colliery near Witbank. The slurry sample was collected in six 42 gallon drums. The material consisted of the underflow from a multiweave linear screen (supplied by Delkor), with an average aperture size of 150 micron, over which the washing plant thickener underflow was passed. To ensure that each drum contained similar material a bucket of screen underflow slurry was added sequentially to each of the six drums. This was continued until the drums were full. The solids were allowed to settle before the water was decanted. This process was then repeated until each drum contained about 150 kg of wet coal, i.e. coal with a moisture content in the region of 28 %. The drums were then sealed and railed to the Department of Metallurgical Engineering at the University of Stellenbosch.

The underlying assumption of the subsequent testwork and statistical analyses is that the composition of the coal in any single drum was representative of that of the coal in all of the other drums.

A.2 Sampling Theory

The sampling method used was the method of fractional shovelling. This method is recommended by Gy (1982, p299) for the sampling of wet, sticky solids. Fractional shovelling is easier, quicker and more reliable than

coning and quartering (Gy, 1982, p299). Fractional shovelling by hand can be used for particles with a maximum diameter (d_p) of 100 mm and for samples of up to a few tons in mass. In this way the lot can be reduced to between 2 and 20 equivalent samples (Gy, 1982, p299).

Fractional shovelling involves moving the entire batch and in the process it is split into equivalent samples. The shovels used should contain less than $M_1/30n$ of the lot, where M_1 is the mass of the lot and n is the number of equivalent samples. This ensures that each potential sample contains at least 30 shovelfuls (Gy, 1982, p299) in order to satisfy assumptions of normality. To ensure that accuracy is not reduced the sample mass (in grams) should always be greater than 125 000 d_p^3 (d_p in cm) (Gy, 1982, p299). In true fractional shovelling the shovelfuls are taken from the lot and deposited in n distinct heaps, thus reducing the lot to n equivalent samples and achieving a splitting ratio of $\tau=1/n$.

A.3 Statistical Methods Employed

Once a sample has been reduced to the required number of equivalent subsamples, the sampling technique employed can be tested for bias. A sampling technique can be considered to be unbiased if differences in sample values are due only to random error. This would be indicated by the sample values, and the residuals, following a normal $N(\mu,\sigma^2)$ distribution. In addition the residual values should have a mean $\mu_{res}=0$.

The normality of a distribution can be tested by carrying out goodness-of-fit tests. Once sample values have been found to follow a normal distribution the sample can be tested for bias, using the Students-t distribution. If $\mu_{res}=0$ then the sample values can be assumed to be unbiased. The population properties, μ and σ, can then be estimated from the sample mean, y_m, and the sample standard deviation, s, using the Students-t and Chi-squared (χ^2) distributions.

A.3.1 Tests for normality

The Shapiro-Wilk (S-W) test for normality, and the Kolmogorov-Smirnov (K-S) goodness-of-fit test were used to check whether or not the sample data fitted the normal distribution. The S-W test is generally regarded as the most powerful test for normality, and is therefore recommended for use when sample sizes are small (n<50) (Mason et al, 1989, p534). When sample sizes are large (n>10) the K-S test can be used. In the work done both the S-W and the K-S tests were used.

The algorithm for the Shapiro-Wilk test was obtained from Mason et al (1989, p533) and is outlined below.

i) Rearrange the n response values, y_i, in ascending order.

ii) Calculate the sample mean, y_m, according to:

$$y_m = \frac{\sum_{i=1}^{i=n} y_i}{n}$$

iii) Calculate the mean residual, r_m, and the numerator of the variance, c^2, according to:

$$r_i = y_i - y_m$$

$$r_m = \frac{\sum_{i=1}^{i=n} r_i}{n}$$

$$c^2 = \sum_{i=1}^{i=n} (r_i - r_m)^2$$

iii) obtain the values of $a_i = f(n)$ from Appendix 28 of Mason et al (1989, p674-676).

iv) calculate b as shown below:

$$b = \sum_{i=1}^{i=n} r_i a_i$$

v) calculate the S-W test statistic as shown below:

$$W = \frac{b^2}{c^2}$$

vi) obtain the value of W_o from Appendix 29 of Mason et al (1989, p677) at the desired significance level, α.

vii) test the hypotheses
H_0 : data is not normally distributed
H_1 : data is normally distributed
using W and W_o.

viii) If $W < W_o$ then accept H_0, data is not normally distributed. If $W > W_o$ then reject H_0 and accept H_1, data is normally distributed.

W_o increases with increasing α, making it easier to accept the null hypothesis. Therefore the greater the value of α which still results in the rejection of the null hypothesis, the more normally the data is distributed.

The K-S goodness-of-fit test tests how well a sample distribution fits a theoretical distribution. The null hypothesis (H_0) is that the sample distribution comes from the theoretical distribution. The alternative hypothesis (H_1) is that the sample does not come from the theoretical distribution. Theoretically the test requires that the distribution is continuous, but it is applicable to discrete data, especially where n is large.

The algorithm for the Kolmogorov-Smirnov test as given in Applied Statistics : A Handbook of Techniques (Sachs, 1982, p330-332) is outlined below.

i) The n sample values are divided into k classes, where $n \geq 10$ and $k \geq 5$.

ii) Calculate the observed and expected frequencies in each of the k classes.

iii) Calculate the observed, F_o, and expected, F_e, cumulative frequencies.

iv) Calculate the test statistic D_{max}, where

$$D_{max} = \frac{\max|F_{oi}-F_{ei}|}{n}$$

v) Obtain the theoretical D, where $D=f(\alpha,n)$, from tables

vi) Test the hypotheses
H_0 : data is normally distributed
H_1 : data is not normally distributed
using D_{max} and D.

vii) If $D_{max} < D$ then accept H_0, data is normally distributed
If $D_{max} > D$ then reject H_0 and accept H_1, data is not normally distributed.

D decreases with increasing α, making it more difficult to accept the null hypothesis. Therefore the greater the value of α which still results in the accepting of the null hypothesis, the more normally the data is distributed.

A computational procedure using the K-S one sample goodness-of-fit test is included in the software package STATGRAPHICS available in the UCT Chemical Engineering Department. It was this routine that was used to perform the K-S goodness-of-fit tests. The output from the routine is:

DPLUS = $\max(F_o-F_e)$
DMINUS = $|\min(F_o-F_e)|$
DN = larger of DPLUS and DMINUS
significance level = α (the significance level is calculated automatically, and for any $\alpha>0.1$ accept H_0).

A.3.2 Tests for bias

A normal distribution can be considered to be unbiased if the mean of the sample, y_m, differs only randomly from the population mean, μ_0. If the above is true then the residuals should have a mean, $\mu_{res}=0$. This hypothesis can be checked using a 2-sided Students-*t* test.

The algorithm for the 2-sided Students-*t* test, as given in Applied Statistics : A Handbook of Techniques (Sachs, 1982, p255-258) is outlined below.

i) Calculate the sample mean, y_m, the sample standard deviation, s, and the degrees of freedom, ν as shown below:

$$y_m = \frac{\sum_{i=1}^{i=n} y_i}{n}$$

$$s^2 = \frac{\sum_{i=1}^{i=n} (y_m - y_i)^2}{n-1}$$

$$\nu = n-1.$$

ii) Calculate the Students-t test statistic using:

$$t = \frac{|y_m - \mu_0|}{\frac{s}{\sqrt{n}}}$$

iii) Obtain $t_{\nu;\alpha/2}$ from tables

iv) Test the hypotheses

$H_0 : \mu_{res} = \mu_0$

$H_1 : \mu_{res} \neq \mu_0$

using t and $t_{\nu;\alpha/2}$.

v) If $t < t_{\nu;\alpha/2}$ then accept H_0, $\mu_{res} = \mu_0$.

If $t > t_{\nu;\alpha/2}$ then reject H_0 and accept H_1, $\mu_{res} \neq \mu_0$.

A routine for performing 2-sided Students-t tests on single samples is included in the software package STATGRAPHICS. The package allows the user to enter the required confidence interval and the test to be performed. The output from the routine is:

the number of degrees of freedom, ν
the computed t statistic
the significance level
whether H_0 should be accepted or rejected

A.3.3 Confidence intervals

If the mean of a normally distributed population is unknown then a confidence interval for the mean, at a specified significance level, can be computed using the mean and standard deviation of a normally distributed random sample from the population. This is done using the Students-t test. The method followed is described below.

i) calculate the sample average, y_m, standard deviation, s, and degrees of freedom, ν

ii) obtain $t_{\nu;\alpha/2}$ from statistical tables

iii) calculate the confidence interval using:

$$y_m - \frac{t_{\nu;\alpha/2}s}{\sqrt{n}} \leq \mu \leq y_m + \frac{t_{\nu;\alpha/2}s}{\sqrt{n}}$$

A similar method can be used to calculate a confidence interval at a chosen significance level, α, for the standard deviation of a normally distributed population using the sample variance and the Chi-squared (χ^2) distribution. In a normal distribution the variance, s^2, follows the χ^2 distribution. Like the Students-*t* distribution the χ^2 distribution has *n*-1 degrees of freedom. The procedure followed is described below.

i) calculate the sample variance, s^2 and degrees of freedom, ν

ii) obtain $\chi^2_{\nu;\alpha/2}$ and $\chi^2_{\nu;1-\alpha/2}$ from statistical tables

iii) calculate the confidence interval using:

$$\frac{s^2\nu}{\chi^2_{\nu;\alpha/2}} \leq \sigma^2 \leq \frac{s^2\nu}{\chi^2_{\nu;1-\alpha/2}}$$

The calculated values of μ and σ can then be used to test, at a chosen significance level, whether or not any subsequent samples belong to the same population. The sample average is compared to the population mean at a chosen significance level, α, using the Students-*t* test, as shown in Section A.3.2. The sample variance is compared to the population variance, using the χ^2 distribution, as indicated below.

i) calculate the sample variance, s^2, and the degrees of freedom, ν

ii) calculate the χ^2 test statistic using:

$$\chi^2 = \frac{\nu s^2}{\sigma^2}$$

iii) obtain $\chi^2_{\nu;\alpha/2}$ and $\chi^2_{\nu;1-\alpha/2}$ from statistical tables

iv) test the hypotheses

$H_0 : \sigma = \sigma_0$

$H_1 : \sigma \neq \sigma_0$

using χ^2, $\chi^2_{\nu;\alpha/2}$ and $\chi^2_{\nu;1-\alpha/2}$

v) if $\chi^2 < \chi^2_{\nu;1-\alpha/2}$ or $\chi^2 > \chi^2_{\nu;\alpha/2}$ then reject H_0 ($\sigma = \sigma_0$) and accept H_1 ($\sigma \neq \sigma_0$).

A.4 Fractional Shovelling Results

A.4.1 Fractional shovelling on a drum of coal slurry

A drum of coal slurry was chosen at random, by flipping a coin, and the water was siphoned off. The coal was removed from the drum, mixed, broken into small pieces and placed in a conical heap. Fractional shovelling with a 300 g shovel was then used to produce 15 equivalent samples, each with a mass of approximately 10 kg. These samples were stored (wet) in sealed buckets. The distribution of the masses of the 15 samples and the calculations for the K-S goodness-of-fit test, the S-W test for normality and the Students-*t* test for bias are shown in Table A.1 below. The results of the statistical tests are summarised in Table A.2 below.

Table A.1: Distribution of sample masses from fractional shovelling on a drum of wet coal and the calculations for the S-W, K-S and Students-t test

sample mass (kg)	Shapiro-Wilk test a_i	r_i	$(r_i-r_m)^2$	$a_i r_i$	K-S test mass (kg)	t test r_i
9.75	-0.52	-0.67	0.45	0.35	9.75	-0.67
9.90	-0.33	-0.52	0.27	0.17	9.90	-0.52
10.20	-0.25	-0.22	0.05	0.06	10.20	-0.22
10.20	-0.19	-0.22	0.05	0.04	10.20	-0.22
10.30	-0.14	-0.12	0.02	0.02	10.30	-0.12
10.40	-0.09	-0.02	0.00	0.00	10.40	-0.02
10.40	-0.04	-0.02	0.00	0.00	10.40	-0.02
10.40	0.00	-0.02	0.00	0.00	10.40	-0.02
10.40	0.04	-0.02	0.00	-0.00	10.40	-0.02
10.45	0.09	0.02	0.00	0.00	10.45	0.03
10.60	0.14	0.18	0.03	0.02	10.60	0.18
10.60	0.19	0.18	0.03	0.03	10.60	0.18
10.75	0.25	0.33	0.11	0.08	10.75	0.33
10.80	0.33	0.38	0.14	0.12	10.80	0.38
11.20	0.52	0.78	0.60	0.40	11.20	0.78
n= 15 y_m= 10.42 s= 0.35		n= 15 r_m= 0.00 s= 0.35 c^2= 1.76 b= 1.30 W= 0.96			Statgraf file FRACTSHO.var1 y_m= 10.42 s= 0.35 DPLUS= 0.14 DMINUS= 0.14 DN= 0.14 α= 0.93	Statgraf file FRACTSHO.var2 r_m= 0.00 s= 0.36 t= 5.15E-15 α= 1.00

The results obtained indicate that the fractional shovelling carried out on the drum of coal was unbiased. The average mass of the samples produced was 10.42 kg, with a sample standard deviation of 0.354 kg.

Table A.2: Results of statistical tests on the masses of the samples produced during the fractional shovelling of a drum of wet coal

test	test statistics	α	H_0	result
S-W	W =0.96 W_o=0.95	50 %	reject	normal
K-S	DN=0.14	0.93	accept	
t	*t* =5.15E-15	0.05	accept	unbiased

A.4.2 Fractional shovelling on a bucket of wet coal

A bucket of wet coal was randomly chosen and the coal was pressure filtered to remove the excess water. The filter cake was then broken up, by passing it through a 4 mm screen, and placed in a cone. Fractional shovelling, using a 30 g shovel, was used to produce ten 1 kg subsamples. Water was added to these subsamples and they were stored in sealed packets. The distribution of the masses of the 10 subsamples and the calculations for the K-S goodness-of-fit test, the S-W test for normality and the Students-*t* test for bias are shown in Table A.3, and are summarised in Table A.4 below.

Table A.3: Distribution of sample masses from fractional shovelling on a bucket of wet coal and the calculations for the S-W, K-S and Students-t test

sample mass (g)	Shapiro-Wilk test a_i	r_i	$(r_i-r_m)^2$	$a_i r_i$	K-S test mass (g)	t test r_i
1018.9	-0.57	-5.57	31.02	3.20	1018.9	-5.57
1020.0	-0.33	-4.47	19.98	1.47	1020.0	-4.47
1022.0	-0.21	-2.47	6.10	0.53	1022.0	-2.47
1023.5	-0.12	-0.97	0.94	0.12	1023.5	-0.97
1024.6	-0.04	0.13	0.02	-0.01	1024.6	0.13
1024.7	0.04	0.23	0.05	0.01	1024.7	0.23
1024.8	0.12	0.33	0.11	0.04	1024.8	0.33
1026.6	0.21	2.13	4.54	0.46	1026.6	2.13
1026.7	0.33	2.23	4.97	0.73	1026.7	2.23
1032.9	0.57	8.43	71.06	4.84	1032.9	8.43
n= 10 y_m= 1024.47 s= 3.92		n= 10 r_m= -0.00 s= 3.93 c^2= 138.80 b= 11.39 W= 0.93			Statgraf file FRACTSHO.var3 y_m= 1024.47 s= 3.93 DPLUS= 0.19 DMINUS= 0.11 DN= 0.19 α= 0.88	Statgraf file FRACTSHO.var4 r_m= -3.41E-14 s= 3.927 t= 2.75E-14 α= 1.00

The results obtained show that the fractional shovelling carried out on the bucket of wet coal was unbiased. The average mass of the samples produced was 1024.5 g, with a sample standard deviation of 3.927 g.

Table A.4: Results of statistical tests on the masses of the samples produced during the fractional shovelling of a bucket of wet coal

test	test statistics	α	H_0	result
S-W	W =0.93 W_o=0.94	10-50 %	reject	**normal**
K-S	DN=0.19	0.88	accept	
t	*t* =2.75E-14	0.05	accept	unbiased

A.4.3 Fractional shovelling on a packet of dry coal

A packet of wet coal was randomly chosen and the coal was dried overnight in a drying oven (at 80°C). The dried coal was broken up by passing it through a 1 mm screen. Fractional shovelling, using a spatula as a 1 g shovel, was then used to produce 15 subsamples, each with a mass of about 40 g, for size and ash-by-size analyses. The distribution of the masses of the 15 samples and the calculations for the K-S goodness-of-fit test, the S-W test for normality and the Students-*t* test for bias are shown in Table A.5 below. The results of the statistical tests are summarised in Table A.6 below.

The results obtained show that the fractional shovelling carried out on the dried coal samples was unbiased. The average mass of the subsamples produced was 43.85 g, with a sample standard deviation of 0.354 g.

Table A.5: Distribution of sample masses from fractional shovelling on a packet of dry coal and the calculations for the S-W, K-S and Students-t test

sample mass (g)	Shapiro-Wilk test a_i	r_i	$(r_i-r_m)^2$	$a_i r_i$	K-S test mass (g)	t test r_i
40.19	-0.52	-3.66	13.40	1.89	40.19	-3.66
40.72	-0.33	-3.13	9.80	1.04	40.72	-3.13
42.75	-0.25	-1.10	1.21	0.27	42.75	-1.10
42.82	-0.19	-1.03	1.06	0.19	42.82	-1.03
42.83	-0.14	-1.02	1.04	0.14	42.83	-1.02
43.56	-0.09	-0.29	0.08	0.03	43.56	-0.29
43.65	-0.04	-0.20	0.04	0.01	43.65	-0.20
43.79	0.00	-0.06	0.00	0.00	43.79	-0.06
44.19	0.04	0.34	0.12	0.01	44.19	0.34
44.33	0.09	0.48	0.23	0.04	44.33	0.48
44.65	0.14	0.80	0.64	0.11	44.65	0.80
44.94	0.19	1.09	1.19	0.20	44.94	1.09
44.97	0.25	1.12	1.25	0.28	44.97	1.12
47.12	0.33	3.27	10.69	1.08	47.12	3.27
47.25	0.52	3.40	11.56	1.75	47.25	3.40
n= 15 y_m= 43.85 s= 0.35	n= 15 r_m= 0.00 s= 1.93 c^2= 52.31 b= 7.04 W= 0.95				Statgraf file FRACTSHO.var5 y_m= 43.85 s= 1.93 DPLUS= 0.15 DMINUS= 0.15 DN= 0.15 α= 0.88	Statgraf file FRACTSHO.var6 r_m= -3.34E-15 s= 1.93 t= 6.69E-15 α= 1.00

Table A.6: Results of statistical tests on the masses of the samples produced during the fractional shovelling of a packet of dry coal

test	test statistics	α	H_0	result
S-W	W =0.95 W_o=0.95	50 %	reject	normal
K-S	DN=0.15	0.88	accept	
t	t =6.69E-15	0.05	accept	unbiased

A.4.4 Size, ash-by-size and ash analyses

The 15 samples obtained above were subjected to size, ash-by-size and ash analyses as detailed in Section 4.4 of Chapter Four.

A.4.4.1 size analyses

The distribution of the masses in the different size fractions (j=1,..,7) for each of the 15 samples (i=1,..,15) and the calculations for the K-S goodness-of-fit tests, the S-W tests for normality and the Students-t tests for bias are shown in Tables A.7(a) to A.7(g) below. The results of these tests are summarised in Table A.8 below.

Table A.7(a): Distribution of masses in the +425 micron size fraction (j=1) of the 15 samples generated by fractional shovelling on a packet of dry coal and the calculations for the K-S, S-W and Students-t tests

mass in fraction (g)	Shapiro-Wilk test a_i	r_i	$(r_i-r_m)^2$	$a_i r_i$	K-S test mass (g)	t test r_i
1.54	-0.52	-1.08	1.16	0.56	1.54	-1.08
1.86	-0.33	-0.76	0.57	0.25	1.86	-0.76
2.19	-0.25	-0.43	0.18	0.11	2.19	-0.43
2.26	-0.19	-0.36	0.13	0.07	2.26	-0.36
2.32	-0.14	-0.30	0.09	0.04	2.32	-0.30
2.38	-0.09	-0.24	0.06	0.02	2.38	-0.24
2.76	-0.04	0.14	0.02	-0.01	2.76	0.14
2.79	0.00	0.17	0.03	0.00	2.79	0.17
2.85	0.04	0.23	0.05	0.01	2.85	0.23
2.89	0.09	0.27	0.07	0.02	2.89	0.27
2.93	0.14	0.31	0.10	0.04	2.93	0.31
2.95	0.19	0.33	0.11	0.06	2.95	0.33
2.98	0.25	0.36	0.13	0.09	2.98	0.36
3.24	0.33	0.62	0.39	0.21	3.24	0.62
3.33	0.52	0.71	0.51	0.37	3.33	0.71
n= 15 y_m= 2.62 s= 0.51	n= 15 r_m= 0.00 s= 0.51 c^2= 3.60 b= 1.84 W= 0.94				Statgraf file SAMPSIZE.var1 y_m= 2.62 s= 0.51 DPLUS= 0.10 DMINUS= 0.21 DN= 0.21 α= 0.52	Statgraf file SAMPSIZE.var2 r_m= 0.00 s= 0.51 t= 0.00 α= 1.00

Table A.7(b): Distribution of masses in the -425+212 micron size fraction (j=2) of the 15 samples generated by fractional shovelling on a packet of dry coal and the calculations for the K-S, S-W and Students-t tests

mass in fraction (g)	Shapiro-Wilk test a_i	r_i	$(r_i-r_m)^2$	$a_i r_i$	K-S test mass (g)	t test r_i
7.99	-0.52	-1.17	1.37	0.60	7.99	-1.17
8.09	-0.33	-1.07	0.57	0.35	8.09	-0.77
8.13	-0.25	-1.03	0.18	0.26	8.13	-0.43
8.68	-0.19	-0.50	0.13	0.09	8.68	-0.36
8.69	-0.14	-0.47	0.09	0.06	8.69	-0.30
8.72	-0.09	-0.44	0.06	0.04	8.72	-0.24
9.09	-0.04	-0.07	0.02	0.00	9.09	0.14
9.18	0.00	0.02	0.03	0.00	9.18	0.17
9.46	0.04	0.30	0.05	0.01	9.46	0.23
9.49	0.09	0.33	0.07	0.03	9.49	0.27
9.54	0.14	0.38	0.10	0.05	9.54	0.31
9.68	0.19	0.52	0.11	0.10	9.68	0.33
9.94	0.25	0.78	0.13	0.19	9.94	0.36
10.17	0.33	1.01	0.39	0.33	10.17	0.62
10.55	0.52	1.39	0.51	0.72	10.55	0.71
n= 15 y_m= 9.16 s= 0.78	n= 15 r_m= -0.00 s= 0.78 c^2= 8.42 b= 2.85 W= 0.96				Statgraf file SAMPSIZE.var3 y_m= 9.16 s= 0.78 DPLUS= 0.10 DMINUS= 0.12 DN= 0.12 α= 0.99	Statgraf file SAMPSIZE.var4 r_m= -2.35E-16 s= 0.78 t= 1.18E-15 α= 1.00

Table A.7(c): Distribution of masses in the -212+150 micron size fraction (j=3) of the 15 samples generated by fractional shovelling on a packet of dry coal and the calculations for the K-S, S-W and Students-t tests

mass in fraction (g)	Shapiro-Wilk test a_i	r_i	$(r_i-r_m)^2$	$a_i r_i$	K-S test mass (g)	t test r_i
7.77	-0.52	-0.46	0.21	0.24	7.77	-0.46
7.80	-0.33	-0.43	0.18	0.14	7.80	-0.43
8.00	-0.25	-0.23	0.05	0.06	8.00	-0.23
8.03	-0.19	-0.20	0.04	0.04	8.03	-0.20
8.06	-0.14	-0.17	0.03	0.02	8.06	-0.17
8.12	-0.09	-0.11	0.01	0.01	8.12	-0.11
8.19	-0.04	-0.04	0.00	0.00	8.19	-0.04
8.19	0.00	-0.04	0.00	0.00	8.19	-0.04
8.27	0.04	0.04	0.00	0.00	8.27	0.04
8.34	0.09	0.11	0.01	0.01	8.34	0.11
8.38	0.14	0.15	0.02	0.02	8.38	0.15
8.41	0.19	0.18	0.03	0.03	8.41	0.18
8.47	0.25	0.24	0.06	0.06	8.47	0.24
8.69	0.33	0.46	0.21	0.15	8.69	0.46
8.72	0.52	0.49	0.24	0.25	8.72	0.49
n= 15 y_m= 8.23 s= 0.28	n= 15 r_m= 0.00 s= 0.28 c^2= 1.11 b= 1.04 W= 0.97				Statgraf file SAMPSIZE.var5 y_m= 8.23 s= 0.28 DPLUS= 0.09 DMINUS= 0.08 DN= 0.09 α= 1.00	Statgraf file SAMPSIZE.var6 r_m= 2.93E-18 s= 0.28 t= 4.03E-15 α= 1.00

Table A.7(d): Distribution of masses in the -150+106 micron size fraction (j=4) of the 15 samples generated by fractional shovelling on a packet of dry coal and the calculations for the K-S, S-W and Students-t tests

mass in fraction (g)	Shapiro-Wilk test a_i	r_i	$(r_i-r_m)^2$	$a_i r_i$	K-S test mass (g)	t test r_i
7.94	-0.52	-0.49	0.24	0.25	7.94	-0.49
8.07	-0.33	-0.36	0.13	0.12	8.07	-0.36
8.13	-0.25	-0.30	0.09	0.07	8.13	-0.30
8.17	-0.19	-0.26	0.07	0.05	8.17	-0.26
8.40	-0.14	-0.03	0.00	0.00	8.40	-0.03
8.46	-0.09	0.03	0.00	-0.00	8.46	0.03
8.47	-0.04	0.04	0.00	-0.00	8.47	0.04
8.49	0.00	0.06	0.00	0.00	8.49	0.06
8.50	0.04	0.07	0.01	0.00	8.50	0.07
8.51	0.09	0.08	0.01	0.01	8.51	0.08
8.54	0.14	0.11	0.01	0.02	8.54	0.11
8.55	0.19	0.12	0.02	0.02	8.55	0.12
8.61	0.25	0.18	0.03	0.05	8.61	0.18
8.68	0.33	0.25	0.06	0.08	8.68	0.25
8.87	0.52	0.44	0.20	0.23	8.87	0.44
n= 15 y_m= 8.43 s= 0.25	n= 15 r_m= -0.00 s= 0.25 c^2= 0.86 b= 0.90 W= 0.93				Statgraf file SAMPSIZE.var7 y_m= 8.43 s= 0.25 DPLUS= 0.12 DMINUS= 0.22 DN= 0.22 α= 0.46	Statgraf file SAMPSIZE.var8 r_m= -5.70E-17 s= 0.25 t= 8.91E-16 α= 1.00

Table A.7(e): Distribution of masses in the -106+75 micron size fraction (j=5) of the 15 samples generated by fractional shovelling on a packet of dry coal and the calculations for the K-S, S-W and Students-t tests

mass in fraction (g)	Shapiro-Wilk test a_i	r_i	$(r_i-r_m)^2$	$a_i r_i$	K-S test mass (g)	t test r_i
7.28	-0.52	-1.77	3.15	0.91	7.28	-1.77
8.22	-0.33	-0.83	0.70	0.28	8.22	-0.83
8.35	-0.25	-0.70	0.50	0.18	8.35	-0.70
8.82	-0.19	-0.23	0.06	0.04	8.82	-0.23
8.87	-0.14	-0.18	0.03	0.02	8.87	-0.18
8.96	-0.09	-0.09	0.01	0.01	8.96	-0.09
8.96	-0.04	-0.09	0.01	0.00	8.96	-0.09
8.99	0.00	-0.06	0.00	0.00	8.99	-0.06
9.17	0.04	0.12	0.01	0.00	9.17	0.12
9.27	0.09	0.22	0.05	0.02	9.27	0.22
9.30	0.14	0.25	0.06	0.03	9.30	0.25
9.59	0.19	0.54	0.29	0.10	9.59	0.54
9.78	0.25	0.73	0.53	0.18	9.78	0.73
9.94	0.33	0.89	0.78	0.29	9.94	0.89
10.32	0.52	1.27	1.60	0.65	10.32	1.27
n= 15 y_m= 9.05 s= 0.75	n= 15 r_m= 0.00 s= 0.75 c^2= 7.77 b= 2.73 W= 0.96				Statgraf file SAMPSIZE.var9 y_m= 9.05 s= 0.75 DPLUS= 0.10 DMINUS= 0.18 DN= 0.18 α= 0.74	Statgraf file SAMPSIZE.var10 r_m= 7.55E-16 s= 0.75 t= 3.92E-15 α= 1.00

Table A.7(f): Distribution of masses in the -75+45 micron size fraction (j=6) of the 15 samples generated by fractional shovelling on a packet of dry coal and the calculations for the K-S, S-W and Students-t tests

mass in fraction (g)	Shapiro-Wilk test a_i	r_i	$(r_i-r_m)^2$	$a_i r_i$	K-S test mass (g)	t test r_i
11.40	-0.52	-1.27	1.60	0.65	11.40	-1.27
11.42	-0.33	-1.25	1.55	0.41	11.42	-1.25
11.92	-0.25	-0.75	0.56	0.19	11.92	-0.75
12.02	-0.19	-0.65	0.42	0.12	12.02	-0.65
12.23	-0.14	-0.44	0.19	0.06	12.23	-0.44
12.23	-0.09	-0.44	0.19	0.04	12.23	-0.44
12.36	-0.04	-0.31	0.09	0.01	12.36	-0.31
12.72	0.00	0.05	0.00	0.00	12.72	0.05
13.01	0.04	0.34	0.12	0.01	13.01	0.34
13.11	0.09	0.44	0.20	0.04	13.11	0.44
13.26	0.14	0.59	0.35	0.08	13.26	0.59
13.33	0.19	0.66	0.44	0.12	13.33	0.66
13.52	0.25	0.85	0.73	0.21	13.52	0.85
13.60	0.33	0.93	0.87	0.31	13.60	0.93
13.85	0.52	1.18	1.40	0.61	13.85	1.18
n= 15 y_m = 12.67 s= 0.79	n= 15 r_m= 0.00 s= 0.79 c^2= 8.72 b= 2.87 W= 0.95				Statgraf file SAMPSIZE.var11 y_m= 12.67 s= 0.79 DPLUS= 0.12 DMINUS= 0.14 DN= 0.14 α= 0.95	Statgraf file SAMPSIZE.var12 r_m= 3.65E-16 s= 0.79 t= 1.79E-15 α= 1.00

Table A.7(g): Distribution of masses in the -45 micron size fraction (j=7) of the 15 samples generated by fractional shovelling on a packet of dry coal and the calculations for the K-S, S-W and Students-t tests

mass in fraction (g)	Shapiro-Wilk test a_i	r_i	$(r_i-r_m)^2$	$a_i r_i$	K-S test mass (g)	t test r_i
47.82	-0.52	-2.03	4.11	1.04	47.82	-2.03
48.51	-0.33	-1.34	1.79	0.44	48.51	-1.34
48.86	-0.25	-0.99	0.97	0.25	48.86	-0.99
49.11	-0.19	-0.74	0.54	0.14	49.11	-0.74
49.38	-0.14	-0.47	0.22	0.06	49.38	-0.47
49.45	-0.09	-0.40	0.16	0.03	49.45	-0.40
49.51	-0.04	-0.34	0.11	0.01	49.51	-0.34
49.90	0.00	0.05	0.00	0.00	49.90	0.05
49.97	0.04	0.12	0.02	0.01	49.97	0.12
50.03	0.09	0.18	0.03	0.02	50.03	0.18
50.20	0.14	0.35	0.12	0.05	50.20	0.35
50.34	0.19	0.49	0.24	0.09	50.34	0.49
50.72	0.25	0.87	0.76	0.22	50.72	0.87
50.74	0.33	0.89	0.80	0.30	50.74	0.89
53.17	0.52	3.32	11.04	1.71	53.17	3.32
n= 15 y_m= 49.85 s= 1.22	n= 15 r_m= 0.00 s= 1.22 c^2= 20.92 b= 4.37 W= 0.91				Statgraf file SAMPSIZE.var13 y_m= 49.85 s= 1.22 DPLUS= 0.17 DMINUS= 0.08 DN= 0.17 α= 0.80	Statgraf file SAMPSIZE.var14 r_m= 2.36E-15 s= 1.23 t= 7.46E-15 α= 1.00

Table A.8: Results of statistical tests on the size analysis of the samples produced during the fractional shovelling of a packet of dry coal

size fraction (micron)	test	test statistics	α	H_0	result
+425	S-W K-S t	W =0.94 W_o=0.95 DN=0.21 t =9.67E-16	10-50 % 0.52 0.05	reject accept accept	normal unbiased
-425+212	S-W K-S t	W =0.96 W_o=0.95 DN=0.12 t =1.18E-15	50 % 0.99 0.05	reject accept accept	normal unbiased
-212+150	S-W K-S t	W =0.97 W_o=0.95 DN=0.09 t =4.03E-15	50 % 1.00 0.05	reject accept accept	normal unbiased
-150+106	S-W K-S t	W =0.93 W_o=0.95 DN=0.22 t =8.91E-16	10-50 % 0.46 0.05	reject accept accept	normal unbiased
-106+ 75	S-W K-S t	W =0.96 W_o=0.95 DN=0.18 t =3.92E-15	50 % 0.74 0.05	reject accept accept	normal unbiased
- 75+ 45	S-W K-S t	W =0.95 W_o=0.95 DN=0.14 t =1.79E-15	50 % 0.95 0.05	reject accept accept	normal unbiased
- 45	S-W K-S t	W =0.91 W_o=0.95 DN=0.17 t =7.46E-15	10-50 % 0.80 0.05	reject accept accept	normal unbiased

The above results show that the mass of coal in each of the size fractions of the 15 samples was normally distributed and unbiased. These results confirm that the fractional shovelling and wet sieving methods employed were unbiased.

The average size analysis of the coal samples is given in Table A.9 below. The average size analysis data listed in Table A.9 can be used to calculate a confidence interval within which the population mean and standard deviation lie (i.e. the coal in all the drums), according to the method outlined in Section A.3.3 above. The 95 % confidence intervals for the population mean and standard deviation are listed in Table A.10 below and are shown in Figure A.1 below.

Table A.9: Average size analysis of Kleinkopje coal

size fraction (micron)	mass (%) $y_{m,j}$	mass (%) $s_{m,j}$	cumulative % passing
+425	2.62	0.51	100.00
-425+212	9.16	0.78	97.38
-212+150	8.23	0.28	88.22
-150+106	8.43	0.25	79.99
-106+ 75	9.05	0.75	71.57
- 75+ 45	12.67	0.791	62.51
- 45	49.85	1.22	49.85

Table A.10: Calculated for the 95 % confidence intervals for the population means and standard deviations of the different size fractions

size fraction (micron)	$y_{m,j}$ (% mass)	$s_{m,j}$ (% mass)	95 % conf. int for μ_o (% mass)	95 % conf. int for σ_o (% mass)
+425	2.62	0.51	2.39 - 2.85	0.37 - 0.80
-425+212	9.16	0.78	8.81 - 9.51	0.57 - 1.22
-212+150	8.23	0.28	8.10 - 8.36	0.21 - 0.44
-150+106	8.43	0.25	8.31 - 8.54	0.18 - 0.39
-106+ 75	9.05	0.75	8.72 - 9.39	0.55 - 1.17
- 75+ 45	12.67	0.79	12.31 - 13.02	0.58 - 1.24
- 45	49.85	1.22	49.29 - 50.40	0.90 - 1.93

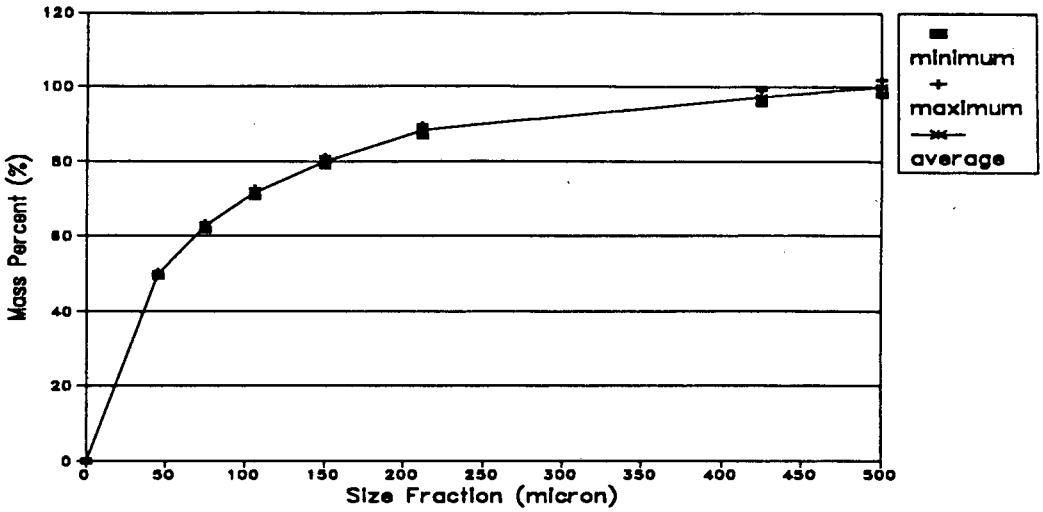

Figure A.1: Plot of the 95 % confidence intervals for the population mean size analysis of the coal

It is possible to use the statistical methods described in Section A.3 to calculate a confidence interval within which the size distribution of the population mean and that of all subsequent representative samples should lie. The confidence interval of 95 % for the mean size distribution for subsequent samples, using n=3, is calculated in Table A.11 below, and plotted in Figure A.2 below.

In Table A.11 the average population standard deviation ($[\sigma_{max}+\sigma_{min}]/2$) was used to calculate the confidence interval for the mean of all subsequent samples. From Table A.11 it can be seen that using small samples results in a very large confidence interval for the hypothesis that $\sigma^2=\sigma_0^2$. Therefore, in the case of small samples, using the 95 % confidence interval for the population mean would give the test more power.

Table A.11: Calculated 95 % confidence intervals for subsequent samples, assuming n=3

size fraction (micron)	$\mu_{o,j}$ (% mass)	$\sigma_{o,j}$ (% mass)	95 % conf. int for H_o:$\mu=\mu_o$	95 % conf. int for H_o:$\sigma=\sigma_o$
+425	2.62	0.59	1.16 - 4.07	0.30 - 3.70
-425+212	9.16	0.90	6.93 - 11.38	0.47 - 5.66
-212+150	8.23	0.33	7.42 - 9.04	0.17 - 2.06
-150+106	8.43	0.29	7.71 - 9.14	0.15 - 1.81
-106+ 75	9.05	0.86	6.92 - 11.19	0.45 - 5.44
- 75+ 45	12.67	0.91	10.40 - 14.93	0.47 - 5.76
- 45	49.85	1.41	46.34 - 53.35	0.73 - 6.93

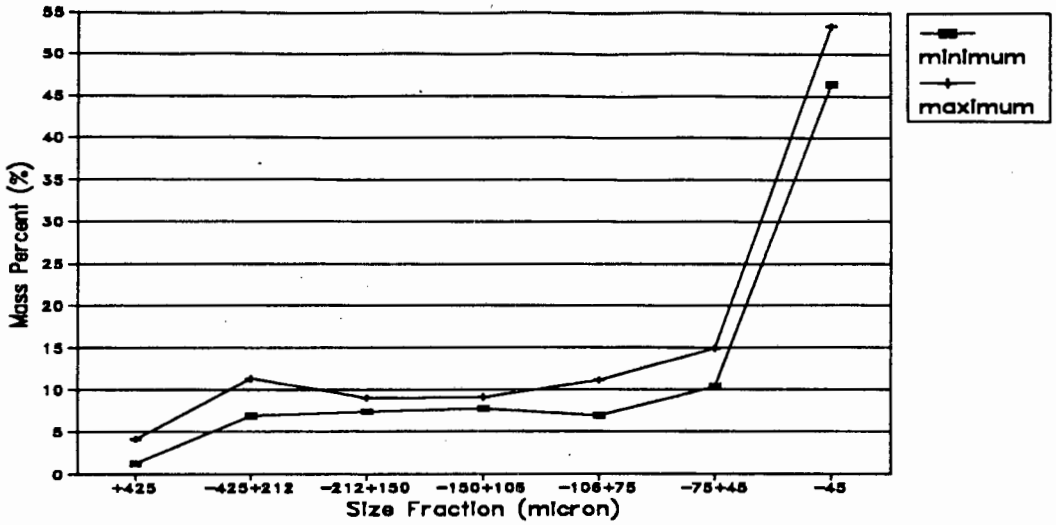

Figure A.2: Plot of the 95 % confidence intervals for the mean size analysis of subsequent coal samples, for n=3

A.4.4.2 ash-by-size analyses

The distribution of the ash contents in the different size fractions for each of the 15 samples and the calculations for the K-S goodness-of-fit tests, the S-W tests for normality and the Students-*t* tests for bias are shown in Tables A.12(a) to A.12(g). The results of these tests are summarised in Table A.13 below.

Table A.12(a): Distribution of ashes in the +425 micron size fraction of the 15 samples generated by fractional shovelling on a packet of dry coal and the calculations for the K-S, S-W and Students-t tests

ash in fraction (%)	Shapiro-Wilk test a_i	r_i	$(r_i-r_{m.})^2$	$a_i r_i$	K-S test ash (%)	t test r_i
24.18	-0.52	-6.12	37.44	3.15	24.18	-6.12
27.13	-0.33	-3.17	10.04	1.05	27.13	-3.17
27.28	-0.25	-3.02	9.11	0.75	27.28	-3.02
27.31	-0.19	-2.99	8.93	0.56	27.31	-2.99
27.77	-0.14	-2.53	6.39	0.34	27.77	-2.53
27.97	-0.09	-2.33	5.42	0.20	27.97	-2.33
30.42	-0.04	0.12	0.01	-0.01	30.42	0.12
31.19	0.00	0.89	0.79	0.00	31.19	0.89
31.69	0.04	1.39	1.94	0.06	31.69	1.39
31.84	0.09	1.54	2.38	0.14	31.84	1.54
33.06	0.14	2.76	7.62	0.37	33.06	2.76
33.22	0.19	2.92	8.53	0.55	33.22	2.92
33.25	0.25	2.95	8.71	0.74	33.25	2.95
33.36	0.33	3.06	9.37	1.01	33.36	3.06
34.81	0.52	4.51	20.35	2.32	34.81	4.51
n= 15 y_m= 30.30 s= 3.13	n= 15 r_m= 0.00 s= 3.13 c^2= 137.05 b= 11.24 W= 0.92				Statgraf file SAMPASH.var1 y_m= 30.30 s= 3.13 DPLUS= 0.17 DMINUS= 0.15 DN= 0.17 α= 0.77	Statgraf file SAMPASH.var2 r_m= 1.20E-15 s= 3.13 t= 1.49E-15 α= 1.00

Table A.12(b): Distribution of ashes in the -425+212 micron size fraction of the 15 samples generated by fractional shovelling on a packet of dry coal and the calculations for the K-S, S-W and Students-t tests

ash in fraction (%)	Shapiro-Wilk test a_i	r_i	$(r_i-r_m)^2$	$a_i r_i$	K-S test ash (%)	t test r_i
23.87	-0.52	-3.71	13.74	1.91	23.87	-3.71
24.62	-0.33	-2.96	8.74	0.98	24.62	-2.96
25.22	-0.25	-2.36	5.55	0.59	25.22	-2.36
25.94	-0.19	-1.64	2.68	0.31	25.94	-1.64
26.33	-0.14	-1.25	1.55	0.17	26.33	-1.25
26.73	-0.09	-0.85	0.72	0.07	26.73	-0.85
26.94	-0.04	-0.64	0.41	0.03	26.94	-0.64
27.85	0.00	0.27	0.07	0.00	27.85	0.27
28.88	0.04	1.30	1.70	0.06	28.88	1.30
28.92	0.09	1.34	1.80	0.12	28.92	1.34
28.98	0.14	1.40	1.97	0.19	28.98	1.40
29.42	0.19	1.84	3.40	0.35	29.42	1.84
29.56	0.25	1.98	3.93	0.49	29.56	1.98
29.62	0.33	2.04	4.18	0.68	29.62	2.04
30.77	0.52	3.19	10.20	1.64	30.77	3.19
n= 15 y_m= 27.58 s= 2.08	n= 15 r_m= -0.00 s= 2.08 c^2= 60.64 b= 7.58 W= 0.95				Statgraf file SAMPASH.var3 y_m= 27.58 s= 2.08 DPLUS= 0.10 DMINUS= 0.20 DN= 0.20 α= 0.58	Statgraf file SAMPASH.var4 r_m= -9.85E-16 s= 2.08 t= 1.83E-15 α= 1.00

Table A.12(c): Distribution of ashes in the +150-212 micron size fraction of the 15 samples generated by fractional shovelling on a packet of dry coal and the calculations for the K-S, S-W and Students-t tests

ash in fraction (%)	Shapiro-Wilk test a_i	r_i	$(r_i-r_m)^2$	a_ir_i	K-S test ash (%)	t test r_i
20.26	-0.52	-1.73	2.99	0.89	20.26	-1.73
20.74	-0.33	-1.25	1.56	0.41	20.74	-1.25
20.78	-0.25	-1.21	1.46	0.30	20.78	-1.21
20.86	-0.19	-1.13	1.27	0.21	20.86	-1.13
21.01	-0.14	-0.98	0.96	0.13	21.01	-0.98
21.44	-0.09	-0.55	0.30	0.05	21.44	-0.55
21.67	-0.04	-0.32	0.10	0.01	21.67	-0.32
22.07	0.00	0.08	0.01	0.00	22.07	0.08
22.36	0.04	0.37	0.14	0.02	22.36	0.37
22.37	0.09	0.38	0.15	0.03	22.37	0.38
22.53	0.14	0.54	0.29	0.07	22.53	0.54
22.67	0.19	0.68	0.47	0.13	22.67	0.68
23.49	0.25	1.50	2.26	0.37	23.49	1.50
23.61	0.33	1.62	2.83	0.54	23.61	1.62
23.96	0.52	1.97	3.89	1.02	23.96	1.97
n= 15 y_m= 21.99 s= 1.15	n= 15 r_m= 0.00 s= 1.15 c^2= 18.46 b= 4.19 W= 0.95				Statgraf file SAMPASH.var5 y_m= 21.99 s= 1.15 DPLUS= 0.14 DMINUS= 0.10 DN= 0.14 α= 0.94	Statgraf file SAMPASH.var6 r_m= 9.50E-16 s= 1.15 t= 3.20E-15 α= 1.00

Table A.12(d): Distribution of ashes in the -150+106 micron size fraction of the 15 samples generated by fractional shovelling on a packet of dry coal and the calculations for the K-S, S-W and Students-t tests

ash in fraction (%)	Shapiro-Wilk test a_i	r_i	$(r_i-r_m)^2$	a_ir_i	K-S test ash (%)	t test r_i
19.00	-0.52	-0.75	0.56	0.39	19.00	-0.75
19.00	-0.33	-0.75	0.56	0.25	19.00	-0.75
19.01	-0.25	-0.74	0.55	0.18	19.01	-0.74
19.06	-0.19	-0.69	0.48	0.13	19.06	-0.69
19.16	-0.14	-0.59	0.35	0.08	19.16	-0.59
19.22	-0.09	-0.53	0.28	0.05	19.22	-0.53
19.54	-0.04	-0.21	0.04	0.01	19.54	-0.21
19.76	0.00	0.01	0.00	0.00	19.76	0.01
19.98	0.04	0.23	0.05	0.01	19.98	0.23
19.99	0.09	0.24	0.06	0.02	19.99	0.24
20.09	0.14	0.34	0.12	0.05	20.09	0.34
20.20	0.19	0.45	0.20	0.08	20.20	0.45
20.37	0.25	0.62	0.39	0.15	20.37	0.62
20.59	0.33	0.84	0.71	0.28	20.59	0.84
21.27	0.52	1.52	2.31	0.78	21.27	1.52
n= 15 y_m= 19.75 s= 0.69	n= 15 r_m= 0.00 s= 0.69 c^2= 6.65 b= 2.46 W= 0.91				Statgraf file SAMPASH.var7 y_m= 19.75 s= 0.69 DPLUS= 0.18 DMINUS= 0.14 DN= 0.18 α= 0.72	Statgraf file SAMPASH.var8 r_m= 6.99E-16 s= 0.69 t= 3.03E-15 α= 1.00

Table A.12(e): Distribution of ashes in the -106+75 micron size fraction of the 15 samples generated by fractional shovelling on a packet of dry coal and the calculations for the K-S, S-W and Students-t tests

ash in fraction (%)	Shapiro-Wilk test a_i	r_i	$(r_i-r_m)^2$	a_ir_i	K-S test ash (%)	t test r_i
17.97	-0.52	-0.72	0.52	0.37	17.97	-0.72
18.07	-0.33	-0.62	0.38	0.20	18.07	-0.62
18.11	-0.25	-0.58	0.33	0.14	18.11	-0.58
18.15	-0.19	-0.54	0.29	0.10	18.15	-0.54
18.21	-0.14	-0.48	0.23	0.06	18.21	-0.48
18.28	-0.09	-0.41	0.17	0.04	18.28	-0.41
18.48	-0.04	-0.21	0.04	0.01	18.48	-0.21
18.71	0.00	0.02	0.00	0.00	18.71	0.02
18.74	0.04	0.05	0.00	0.00	18.74	0.05
18.89	0.09	0.20	0.04	0.02	18.89	0.20
18.92	0.14	0.23	0.05	0.03	18.92	0.23
18.93	0.19	0.24	0.06	0.05	18.93	0.24
18.49	0.25	0.80	0.64	0.20	18.49	0.80
19.55	0.33	0.86	0.74	0.28	19.55	0.86
19.83	0.52	1.14	1.30	0.59	19.83	1.14
n= 15 y_m= 18.69 s= 0.59	n= 15 r_m= 0.00 s= 0.59 c^2= 4.81 b= 2.10 W= 0.92				Statgraf file SAMPASH.var9 y_m= 18.69 s= 0.59 DPLUS= 0.16 DMINUS= 0.11 DN= 0.16 α= 0.85	Statgraf file SAMPASH.var10 r_m= 2.37E-16 s= 0.59 t= 1.57E-15 α= 1.00

Table A.12(f): Distribution of ashes in the -75+45 micron size fraction of the 15 samples generated by fractional shovelling on a packet of dry coal and the calculations for the K-S, S-W and Students-t tests

ash in fraction (%)	Shapiro-Wilk test a_i	r_i	$(r_i-r_m)^2$	a_ir_i	K-S test ash (%)	t test r_i
18.57	-0.52	-0.39	0.15	0.20	18.57	-0.39
18.62	-0.33	-0.34	0.12	0.11	18.62	-0.34
18.66	-0.25	-0.30	0.09	0.08	18.66	-0.30
18.75	-0.19	-0.21	0.05	0.04	18.75	-0.21
18.76	-0.14	-0.20	0.04	0.03	18.76	-0.20
18.77	-0.09	-0.19	0.04	0.02	18.77	-0.19
18.83	-0.04	-0.13	0.02	0.01	18.83	-0.13
18.83	0.00	-0.13	0.02	0.00	18.83	-0.13
18.94	0.04	-0.02	0.00	-0.00	18.94	-0.02
18.94	0.09	-0.02	0.00	-0.00	18.94	-0.02
19.07	0.14	0.11	0.01	0.01	19.07	0.11
19.10	0.19	0.14	0.02	0.03	19.10	0.14
19.27	0.25	0.31	0.09	0.08	19.27	0.31
19.40	0.33	0.44	0.19	0.14	19.40	0.44
19.93	0.52	0.97	0.94	0.50	19.93	0.97
n= 15 y_m= 18.96 s= 0.36	n= 15 r_m= -0.00 s= 0.36 c^2= 1.77 b= 1.24 W= 0.86				Statgraf file SAMPASH.var11 y_m= 18.96 s= 0.36 DPLUS= 0.19 DMINUS= 0.14 DN= 0.19 α= 0.64	Statgraf file SAMPASH.var12 r_m= -4.73E-16 s= 0.36 t= 5.15 α= 1.00

Table A.12(q): Distribution of ashes in the -45 micron size fraction of the 15 samples generated by fractional shovelling on a packet of dry coal and the calculations for the K-S, S-W and Students-t tests

ash in fraction (%)	Shapiro-Wilk test a_i	r_i	$(r_i-r_m)^2$	$a_i r_i$	K-S test ash (%)	t test r_i
24.92	-0.52	-0.86	0.43	0.34	24.92	-0.86
25.01	-0.33	-0.57	0.32	0.19	25.01	-0.57
25.16	-0.25	-0.42	0.17	0.10	25.16	-0.42
25.17	-0.19	-0.41	0.16	0.08	25.17	-0.41
25.19	-0.14	-0.39	0.15	0.05	25.19	-0.39
25.34	-0.09	-0.24	0.06	0.02	25.34	-0.24
25.44	-0.04	-0.14	0.02	0.01	25.44	-0.14
26.47	0.00	-0.11	0.01	0.00	26.47	-0.11
25.52	0.04	-0.06	0.00	-0.00	25.52	-0.06
25.69	0.09	0.11	0.01	0.01	25.69	0.11
25.74	0.14	0.16	0.03	0.02	25.74	0.16
25.78	0.19	0.20	0.04	0.04	25.78	0.20
26.33	0.25	0.75	0.57	0.19	26.33	0.75
26.41	0.33	0.83	0.70	0.28	26.41	0.83
26.46	0.52	0.88	0.78	0.46	26.46	0.88
n= 15 y_m= 25.58 s= 0.50	n= 15 r_m= 0.00 s= 0.50 c^2= 3.45 b= 1.77 W= 0.91				Statgraf file SAMPASH.var13 y_m= 25.58 s= 0.50 DPLUS= 0.14 DMINUS= 0.14 DN= 0.14 α= 0.91	Statgraf file SAMPASH.var14 r_m= -1.87E-03 s= 0.50 t= 1.46E-02 α= 0.99

Table A.13: Results of statistical tests on the size-ash analysis of the samples produced during the fractional shovelling of a packet of dry coal

size fraction (micron)	test	test statistics	α	H_0	result
+425	S-W K-S t	W =0.92 W_o=0.95 DN=0.17 t =1.49E-15	10-50 % 0.77 0.05	reject accept accept	normal unbiased
-425+212	S-W K-S t	W =0.95 W_o=0.95 DN=0.20 t =1.83E-15	50 % 0.58 0.05	reject accept accept	normal unbiased
-212+150	S-W K-S t	W =0.95 W_o=0.95 DN=0.14 t =3.20E-15	50 % 0.94 0.05	reject accept accept	normal unbiased
-150+106	S-W K-S t	W =0.91 W_o=0.95 DN=0.18 t =3.93E-15	10-50 % 0.72 0.05	reject accept accept	normal unbiased
-106+ 75	S-W K-S t	W =0.92 W_o=0.95 DN=0.16 t =1.57E-15	10-50 % 0.85 0.05	reject accept accept	normal unbiased
- 75+ 45	S-W K-S t	W =0.86 W_o=0.95 DN=0.19 t =5.15E-15	2-5 % 0.64 0.05	accept accept accept	? unbiased
- 45	S-W K-S t	W =0.91 W_o=0.95 DN=0.14 t =3.70E-15	10-50 % 0.92 0.05	reject accept accept	normal unbiased

The above results indicate that the ash contents of the different size fractions of the 15 samples, except possibly the -75+45 micron fraction, were normally distributed. The -75 + 45 micron fraction failed the S-W test for normality at α=5 %, but passed the K-S test at α=0.64. Mason et al (1989, p534) recommend that the S-W test be used together with statistical plots, as large samples may lead to rejections in the assumption of normality as a result of relatively few outliers.

A log-probability plot was used to detect outliers, and after rejection of a single point, the log-probability plot given in Figure A.3 below was obtained, and the α obtained in the K-S test improved to a value of α=0.78. Both of the above indicate that the sample is in fact normally distributed.

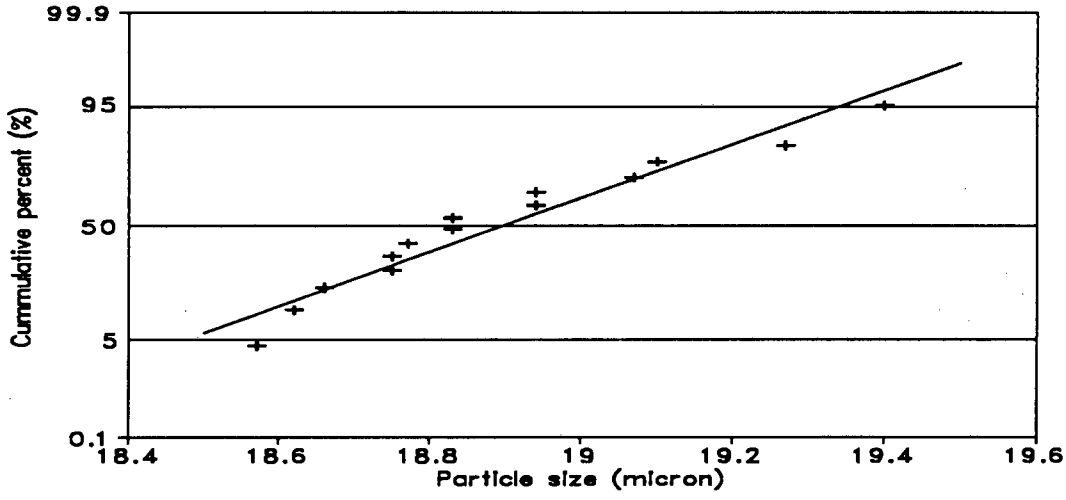

Figure A.3: Normal probability plot of the ash content of the -75+45 micron size fraction after removal of a single point (outlier)

A.4.4.3 overall ash contents

The distribution of the calculated overall ash contents (reconstituted by size fraction) of the 15 samples and the calculations for the K-S goodness-of-fit tests, the S-W tests for normality and the Students-*t* tests for bias are shown in Table A.14. The results of these tests are given in Table A.15 below.

Table A.14: Distribution of overall ashes of the 15 samples generated by fractional shovelling on a packet of dry coal and the calculations for the K-S, S-W and Students-t tests

sample ash (%)	Shapiro-Wilk test a_i	r_i	$(r_i-r_m)^2$	$a_i r_i$	K-S test ash (%)	t test r_i
22.81	-0.52	-0.84	0.71	0.44	22.81	-0.84
22.92	-0.33	-0.73	0.54	0.24	22.92	-0.73
22.98	-0.25	-0.67	0.46	0.17	22.98	-0.67
23.03	-0.19	-0.62	0.39	0.12	23.03	-0.62
23.32	-0.14	-0.33	0.11	0.05	23.32	-0.33
23.39	-0.09	-0.26	0.07	0.02	23.39	-0.26
23.43	-0.04	-0.22	0.05	0.01	23.43	-0.22
23.71	0.00	0.06	0.00	0.00	23.71	0.06
23.76	0.04	0.11	0.01	0.00	23.76	0.11
23.87	0.09	0.22	0.05	0.02	23.87	0.22
23.89	0.14	0.24	0.06	0.03	23.89	0.24
24.14	0.19	0.49	0.24	0.09	24.14	0.49
24.36	0.25	0.71	0.50	0.18	24.36	0.71
24.45	0.33	0.80	0.63	0.26	24.45	0.80
24.76	0.52	1.11	1.22	0.57	24.76	1.11
n= 15 y_m= 23.65 s= 0.60	n= 15 r_m= -0.00 s= 0.60 c^2= 5.03 b= 2.20 W= 0.96				Statgraf file SAMPASH.var15 y_m= 23.65 s= 0.60 DPLUS= 0.12 DMINUS= 0.08 DN= 0.12 α= 0.99	Statgraf file SAMPASH.var16 r_m= -2.27E-15 s= 0.60 t= 1.47E-15 α= 1.00

Table A.15: Results of statistical tests on the overall ash contents of the samples produced during the fractional shovelling of a packet of dry coal

test	test statistics	α	H_0	result
S-W	W =0.96 W_o=0.95	50 %	reject	normal
K-S	DN=0.12	0.99	accept	
t	t =1.47E-15	0.05	accept	unbiased

The results calculated in Table A.14 clearly indicate that the overall ashes of the 15 samples were normally distributed.

The results of the ash analyses gave the average ash-by-size and overall ash contents listed in Table A.16 below.

Table A.16: Average ash-by-size analysis of Kleinkopje coal

size fraction (micron)	ash content (%) $y_{m,j}$	ash % $s_{m,j}$
+425	30.30	3.13
-425+212	27.58	2.08
-212+150	21.99	1.15
-150+106	19.75	0.69
-106+ 75	18.69	0.59
- 75+ 45	18.96	0.36
- 45	25.58	0.60
overall	23.65	0.60

Once again the statistical analyses carried out in the preceding sections can be used to infer that the average ash-by-size analysis data listed above is the same as that of the population (i.e. the coal in all the drums). It is therefore possible to use the statistical methods described in Section A.3 to calculate a confidence interval within which the population mean ash-by-size and overall ash lies. These calculations are given in Table A.17 below and the 95 % confidence intervals for the ash-by-size distribution is indicated in Figure A.5 below.

Table A.17: Calculations for the 95 % confidence intervals for the population means and standard deviations of the ash-by-size distribution of the coal

size fraction (micron)	$y_{m,j}$ (% ash)	$s_{m,j}$ (% ash)	95 % conf. int for μ_o (% ash)	95 % conf. int for σ_o(% ash) (% ash)
+425	30.30	3.13	28.88 - 31.72	2.30 - 4.93
-425+212	27.58	2.08	26.63 - 28.53	1.52 - 3.28
-212+150	21.99	1.15	21.47 - 22.51	0.84 - 1.81
-150+106	19.75	0.69	19.44 - 20.06	0.50 - 1.09
-106+ 75	18.69	0.59	18.42 - 18.96	0.43 - 0.92
- 75+ 45	18.96	0.36	18.80 - 19.12	0.26 - 0.56
- 45	25.58	0.50	25.35 - 25.81	0.36 - 0.78
overall	23.65	0.60	23.38 - 23.92	0.44 - 0.95

APPENDIX B

PRELIMINARY WORK - DETAILED RESULTS

B.1 Release Flotation Results

A release flotation analysis was carried out in a batch flotation cell, on a sample of Kleinkopje coal, according to the method outlined in Section 4.3.3. The method involves using starvation quantities of reagents; concentrates are collected in small quantities over a long period of time. The conditions used were as follows:

Operating conditions

Run id.	: KKRF
Aeration Rate	: 4 l/min
Impeller Speed	: 1200 revs/min
Froth Height	: 3 cm
Collector Dosage	: Starvation amounts of SSOLA
Frother Dosage	: Starvation amounts of HTEB
Pulp Density	: 4.63 %

In Table B.1.1 below the values in the various columns signify the following:

i) The **sample mass**, in column 2, is the measured mass of each concentrate, $m_{s,i}$. The final value in the column is the mass of the tails M_t. The feed sample mass is calculated as shown below:

$$M_f = \sum_{i=1}^{i=n} m_{s,i} + M_t$$

ii) The **sample ash**, in column 3, is the measured ash content (%) of each concentrate ($a_{s,i}$) and of the tails sample (A_t). The feed sample ash content is calculated as shown below:

$$A_f = \frac{\sum_{i=i}^{i=n} m_{s,i}a_{s,i} + M_tA_t}{M_f}$$

iii) The **cum. mass** ($M_{s,i}$), in column 4, is the cumulative mass of the concentrates from i=1 to i=i. It is calculated as shown below:

$$M_{s,i} = \sum_{i=1}^{i=i} m_{s,i}$$

iv The **mass ash** ($m_{a,i}$), in column 5, is the mass of ash in each concentrate (i). It is calculated as shown below:

$$m_{a,i} = \frac{m_{s,i}a_{s,i}}{100}$$

v) The **cum. mass ash** ($M_{a,i}$), in column 6, is the cumulative mass of ash in the concentrates from i=1 to i=i. It is calculated as shown below:

$$M_{a,i} = \sum_{i=1}^{i=i} m_{a,i}$$

vi) The **cum. yield** (Y_i), in column 7, is the cumulative process yield (%) from i=1 to i=i. It is calculated as shown below:

$$Y_i = \frac{M_{s,i}}{M_f}$$

vii) The **cum. ash** (A_i), in column 8, is the cumulative ash content (%) of samples i=1 to i=i. It is calculated as shown below:

$$A_i = \frac{M_{a,i}}{M_{s,i}}$$

Table B.1.1: Release float results

sample id	sample mass (g)	sample ash (%)	cum mass (g)	mass ash (g)	cum mass ash (g)	cum yield (%)	cum ash (%)
KK R1.	2.00	4.35	2.00	0.09	0.09	1.44	4.35
KK R2.	1.47	4.35	3.46	0.06	0.15	2.49	4.35
KK R4.	0.80	4.35	4.26	0.03	0.19	3.06	4.35
KK R5.	1.36	4.79	5.61	0.06	0.25	4.04	4.46
KK R6.	1.09	4.79	6.70	0.05	0.30	4.82	4.51
KK R8.	0.23	4.70	6.92	0.01	0.31	4.98	4.52

Table B.1.1: continued

sample id	sample mass (g)	sample ash (%)	cum mass (g)	mass ash (g)	cum mass ash (g)	cum yield (%)	cum ash (%)
KK R2.3	0.86	4.70	7.78	0.04	0.35	5.59	4.54
KK R2.5	0.86	7.37	8.63	0.06	0.42	6.21	4.82
KK R2.7	0.58	7.37	9.21	0.04	0.46	6.62	4.98
KKRI 3.1	0.89	4.66	10.09	0.04	0.50	7.26	4.95
KKRI 3.3	0.75	5.43	10.84	0.04	0.54	7.80	4.98
KKRI 3.5	0.95	5.43	11.78	0.05	0.59	8.48	5.02
KKRI 4.1	0.40	5.26	12.18	0.02	0.61	8.76	5.03
KKRI 4.3	0.40	5.26	12.57	0.02	0.63	9.05	5.03
KKRI 4.5	2.04	5.09	14.61	0.10	0.74	10.51	5.04
KKRI 6.1	8.27	8.44	22.87	0.70	1.43	16.46	6.27
KKRI 6.2	7.89	9.07	30.76	0.72	2.15	22.13	6.99
KKRI 6.3	8.27	8.17	39.02	0.68	2.82	28.08	7.24
KKRI 6.4	2.96	7.36	41.98	0.22	3.04	30.21	7.25
KKRI 6.5	1.71	7.21	43.68	0.12	3.16	31.43	7.25
KKRI 6.6	1.77	7.03	45.45	0.12	3.29	32.70	7.24
KKRI 6.7	1.71	7.35	47.15	0.13	3.41	33.93	7.24
KKRI 6.8	0.89	7.65	48.04	0.07	3.48	34.57	7.25
KKRI 7.1	1.44	7.52	49.47	0.11	3.59	35.60	7.26
KKRI 7.2	4.46	7.81	53.93	0.35	3.94	38.80	7.30
KKRI 7.3	6.22	9.12	60.14	0.57	4.50	43.28	7.49
KKRI 7.4	7.01	9.67	67.15	0.68	5.18	48.32	7.72
KKRI 7.5	3.27	9.86	70.41	0.32	5.50	50.67	7.82
KKRI 7.6	4.42	10.06	74.83	0.44	5.95	53.84	7.95
KKRI 8.1	3.73	10.06	78.55	0.37	6.32	56.53	8.05
KKRI 9.1	3.21	10.73	81.76	0.34	6.67	58.83	8.15
KKRI 9.2	10.21	12.06	91.96	1.23	7.90	66.17	8.59
KKRI T	47.01	39.75					
feed	138.97	19.13	(calculated)				

B.2 Batch Flotation Results

The batch flotation method followed was the UCT standard batch flotation procedure. The method involves froth removal, with a scraper, at set intervals. This method has been found to give reproducible results (Fickling, 1985, p50). The UCT batch flotation procedure is outlined below.

i) Add 2 l of Cape Town tap water to a modified 3 l Leeds cell.

ii) Set the impeller to a speed of 1200 rpm.

iii) Add the required quantity of coal solids.

iv) Fill the cell to 3 l with tap water. This gives a froth height of 3 cm.

v) Allow the pulp to condition for 10 minutes.

vi) Add the desired quantity of collector, using a micropipette, below the pulp surface.

vii) Allow the pulp to condition for a further 3 minutes

viii) Add the required quantity of frother, using a microsyringe, below the pulp surface.

ix) Allow 55 seconds for frother dispersion before turning on the air to a flowrate of 4 l/min.

x) Let time zero, t=0 be 55 seconds after the time at which the frother was added. Starting at t=5 seconds remove concentrates at regular intervals as described below in Table B.2:

Table B.2: Concentrate removal times during UCT standard batch flotation procedure

Concentrate number	Time period (s)	Scraping intervals (s)
C1	t= 5 to 20	5
C2	t= 20 to 35	5
C3	t= 35 to 65	10
C4	t= 65 to 125	10
C5	t= 125 to 215	10
C6	t= 215 to 305	10
C7	t= 305 to 495	10
C8	t= 425 to 515	10

xi) Once the final concentrate has been collected turn the air and the impeller off.

xii) Drain the cell. The remaining pulp is the tails sample.

xiii) Analyse the concentrate and tails samples as described in Chapter 4 (Section 4.4)

The results of the 5 batch flotation experiments carried out are listed in Tables **B.2.x_k(a)** below, where x_k is the batch float number; the results of

the size analyses performed on *subsamples* of the concentrate and tails are listed in **Tables B.2.x_k(b)**, and the size analysis of the mathematically reconstituted feed is given in **Tables B.2.x_k(c)**.

In Tables B.2.x_k(a) below the values in the various columns signify the following:

i) The **elapsed time** (column 2) is the time elapsed from t=0 to the end of the sampling period (i).

ii) The **sample mass**, in column 3, is the measured mass of solids in the concentrates ($m_{s,i}$) and tails (M_t). The feed sample mass (M_f) is calculated as shown below:

$$M_f = \sum_{i=1}^{i=8} m_{s,i} + M_t$$

iii) The **sample ash**, in column 4, is the measured ash content of each concentrate ($a_{s,i}$) and of the tails (A_t). The feed sample ash content is calculated as shown below:

$$A_f = \frac{\sum_{i=1}^{i=8} m_{s,i}a_{s,i} + M_tA_t}{M_f}$$

iv) The **cum. yield** (Y_i), in column 5, is the cumulative process yield (%) at the end of sampling period (i), i.e. from i=1 to i=i. It is calculated as shown below:

$$Y_i = \frac{\sum_{i=1}^{i=i} m_{s,i}}{M_f}$$

v) The **cum. ash** (A_i), in column 6, is the cumulative ash content (%) at the end of sampling period (i), i.e. for samples i=1 to i=i. It is calculated as shown below:

$$A_i = \frac{\sum_{i=1}^{i=i} m_{s,i}a_{i,s}}{\sum_{i=1}^{i=i} m_{s,i}}$$

In Tables B.2.x_k(b) below the values in the various columns signify the following:

i) The **sample mass** is the mass of concentrate ($c_{m,j}$), in column 2, or tails ($t_{m,j}$), in column 5, remaining in each of the size fractions (j) after sieving a sample of the concentrate or tailings. Fractional shovelling (as described in Appendix A) was used to produce concentrate and tails samples small enough for size analysis. Hence, the **overall sample mass** of concentrate ($c_{m,o}$) and tails ($t_{m,o}$) is the mass of the subsamples actually sieved. These masses are generally not the same as the masses reported in Table B.2.x_k(a). $c_{m,o}$ and $t_{m,o}$ were calculated as shown below:

$$c_{m,o} = \sum_{j=1}^{j=7} c_{m,j}$$

$$t_{m,o} = \sum_{j=1}^{j=7} t_{m,j}$$

ii) The **sample ash** is the measured ash content of the concentrate ($c_{a,j}$), in column 3, or tails ($t_{a,j}$), in column 6, remaining in each of the size fractions (j) after sieving of the samples. The **overall** sample ash of the concentrate ($c_{a,o}$) and tails ($t_{a,o}$) is the calculated ash content of the subsamples sieved. $c_{a,o}$ and $t_{a,o}$ were calculated as shown below:

$$c_{a,o} = \frac{\sum_{j=1}^{j=7} c_{m,j}c_{a,j}}{c_{m,o}}$$

$$t_{a,o} = \frac{\sum_{j=1}^{j=7} t_{m,j}t_{a,j}}{t_{m,o}}$$

iii) The **% in size fraction** is the mass percent of the concentrate ($c_{s,j}$), in column 4, or tails ($t_{s,j}$), in column 7, in each of the size fractions (j). The mass percent in each size fraction is calculated as shown below:

$$c_{s,j} = \frac{100c_{m,j}}{c_{m,o}}$$

$$t_{s,j} = \frac{100t_{m,j}}{t_{m,o}}$$

The reconstituted feed results were calculated from the values in Tables B.2.x_k(a) and (b) and are shown in Table B.2.x_k(c) below. The results in columns 7, 8 and 9 represent an analysis of the performance of the batch flotation by size fraction. The values in the various columns were calculated as described below.

i) The **sample mass** ($f_{m,j}$), in column 2, is the mass of reconstituted feed in each of the size fractions (j). The **overall** ($f_{m,o}$) sample mass is the same as the feed mass of Table B.2.x_k(a). The calculation used was:

$$f_{m,j} = \frac{c_{s,j}(M_f - M_t)}{100} + \frac{t_{s,j}M_t}{100}$$

$$f_{m,o} = \sum_{j=1}^{j=7} f_{m,j}$$

ii) The **sample ash** ($f_{a,j}$), in column 3, is the ash content (%) of the reconstituted feed in each of the size fractions (j). The **overall** ($f_{a,o}$) ash content is the ash content of the reconstituted feed, calculated by size fraction (this can be compared with the feed ash content listed in Table B.2.x_k(a) which was calculated for the flotation concentrate and tailings). The calculations used were:

$$f_{a,j} = \frac{c_{a,j}c_{s,j}(M_f - M_t) + t_{a,j}t_{s,j}M_t}{100 f_{m,j}}$$

$$f_{a,o} = \frac{\sum_{j=1}^{j=7} f_{m,j}f_{a,j}}{f_{m,o}}$$

iii) The **95% ash confidence limits**, in column 4, are the ranges within which the ash content of the material in each size fraction (j) should lie, if the sample were truly representative. The method of calculating these limits is described in Section A.3.3, and the limits are calculated in Sections A.4.4.3, of Appendix A.

iv) The **% in size fraction** ($f_{s,j}$), in column 4, is the mass percent of the reconsituted feed in each of the size fractions (j). The values are calculated as shown below:

$$f_{s,j} = \frac{100 f_{m,j}}{f_{m,o}}$$

v) The **95% size anal. confidence limits**, in column 6, are the ranges within which the amount of material in each size fracction (j) should lie, if the sample were truly representative. The method of calculating these limits is described in Section A.3.3, and the limits are calculated in Section A.4.4.1, of Appendix A.

vi) The **coal yield** (Y_j), in column 7, is the mass recovery in each size fraction (j), calculated as shown below:

$$Y_j = \frac{c_{s,j}(M_f - M_t)}{f_{m,j}}$$

vii) The **coal rec.** (R_j), in column 8, is the recovery (%) of "clean coal" to the concentrate in each size fraction (j). The values were calculated as shown below:

$$R_j = \frac{Y_j f_{m,j}(1 - \frac{c_{a,j}}{100})}{f_{m,j}(1 - \frac{f_{a,j}}{100})}$$

viii) The **Sep. Coef.** (S_j), in column 9, is the separation coefficient (a measure of the efficiency of separation of the feed into clean coal and gangue) in each size fraction (j). The separation coefficient has a value of 1.0 at a coal recovery of 100 % and a concentrate ash of 0 %. The values were calculated as shown below:

$$S_j = \frac{R_j}{100} \left(1 - \frac{c_{a,j}}{100} \right)$$

B.2.1 Batch float 1

Operating conditions

Run id. : KKB1
Aeration Rate : 4 l/min
Impeller Speed : 1200 revs/min
Froth Height : 3 cm
Collector Dosage : SSOLA - 0 g/ton
Frother Dosage : HTEB 12 µl/l
Pulp Density : 9.40 %

Table B.2.1(a): Batch float 1 results

concentrate	elapsed time (s)	sample mass (g)	sample ash (%)	cum. yield (%)	cum. ash (%)
C1	20	2.20	9.41	0.78	9.41
C2	35	2.21	8.58	1.56	8.99
C3	65	3.50	7.99	2.80	8.55
C4	125	5.42	7.56	4.73	8.15
C5	215	6.15	7.21	6.91	7.85
C6	305	1.91	6.14	7.58	7.70
C7	395	1.45	6.09	8.10	7.60
C8	515	1.19	5.82	8.52	7.51
tails		258.04	24.37	(measured)	
feed		282.07	22.93	(calculated)	

Table B.2.1(b): Size analyses of batch float 1 concentrate and tails

	concentrate			tails		
size fraction (micron)	sample mass (g)	sample ash (%)	% in size fraction	sample mass (g)	sample ash (%)	% in size fraction
+425	0.00	0.00	0.00	1.22	22.16	2.21
-425+212	0.00	0.00	0.00	4.56	21.10	8.27
-212+150	0.00	0.00	0.00	4.89	17.79	8.87
-150+106	0.00	0.00	0.00	5.50	17.23	9.97
-106+ 75	0.00	0.00	0.00	5.53	17.63	10.03
- 75+ 45	0.00	0.00	0.00	8.75	19.21	15.86
- 45	24.03	10.78	100.00	24.71	29.29	44.80
overall	24.03	10.78	100.00	55.16	23.47	100.00

Table B.2.1(c): Size analysis of reconstituted feed for batch float 1

	reconstituted feed					results		
size sraction (micron)	sample mass (g)	sample ash (%)	95% ash % confidence limits	% in size fraction	95% size anal. confidence limits	coal yield (%)	coal rec. (%)	sep coef
+425	5.71	22.16	21.33 - 39.27	2.02	1.16 - 4.07	0.00	0.00	0.00
-425+212	21.33	21.10	21.61 - 33.55	7.56	6.93 - 11.38	0.00	0.00	0.00
-212+150	22.88	17.79	18.70 - 25.28	8.11	6.42 - 9.04	0.00	0.00	0.00
-150+106	25.73	17.23	17.77 - 21.73	9.12	7.71 - 9.14	0.00	0.00	0.00
-106+ 75	25.87	17.63	17.01 - 20.37	9.17	9.17 - 11.19	0.00	0.00	0.00
- 75+ 45	40.93	19.21	17.94 - 19.98	14.51	10.40 - 14.93	0.00	0.00	0.00
- 45	139.62	26.10	24.16 - 27.00	49.50	46.34 - 53.35	17.21	20.78	0.19
overall	282.07	23.65	21.93 - 25.37	100.00		8.52	10.22	

B.2.2 Batch Float 2

Operating conditions

Run id. : KKB2
Aeration Rate : 4 l/min
Impeller Speed : 1200 revs/min
Froth Height : 3 cm
Collector Dosage : SSOLA - 944 g/ton
Frother Dosage : HTEB 12 μl/l
Pulp Density : 9.16 %

Table B.2.2(a): Batch float 2 results

concentrate	elapsed time (s)	sample mass (g)	sample ash (%)	cum. yield (%)	cum. ash (%)
C1	20	18.33	10.53	6.67	10.53
C2	35	30.33	10.33	17.70	10.41
C3	65	19.75	9.23	24.89	10.07
C4	125	21.57	9.10	32.74	9.83
C5	215	26.68	9.99	42.44	9.87
C6	305	11.28	9.96	46.55	9.88
C7	395	4.18	9.85	48.07	9.88
C8	515	3.09	10.33	49.19	9.89
tails		139.66	35.57	(measured)	
feed		274.87	22.94	(calculated)	

Table B.2.2(b): Size analyses of batch float 2 concentrate and tails

	concentrate			tails		
size fraction (micron)	sample mass (g)	sample ash (%)	% in size fraction	sample mass (g)	sample ash (%)	% in size fraction
+425	0.15	6.82	0.36	1.26	33.73	2.80
-425+212	3.08	10.68	7.33	3.93	37.42	8.72
-212+150	2.51	10.10	5.98	3.76	26.85	8.34
-150+106	2.33	9.32	5.55	5.03	21.74	11.16
-106+ 75	2.68	10.47	6.38	5.82	20.14	12.91
- 75+ 45	4.58	10.44	10.90	5.07	24.09	11.25
- 45	26.67	10.68	63.50	20.20	44.82	44.82
overall	42.00	10.52	100.00	45.07	34.27	100.00

Table B.2.2(c): Size analysis of reconstituted feed for batch float 2

	reconstituted feed					results		
size fraction (micron)	sample mass (g)	sample ash (%)	95% ash % confidence limits	% in size fraction	95% size anal. confidence limits	coal yield (%)	coal rec. (%)	sep coef
+425	4.39	30.77	21.33 - 39.27	1.60	1.16 - 4.07	11.01	14.81	0.14
-425+212	22.09	25.42	21.61 - 33.55	8.04	6.93 - 11.38	44.88	53.75	0.48
-212+150	19.73	19.99	18.70 - 25.28	7.18	6.42 - 9.04	40.95	46.01	0.41
-150+106	23.09	17.70	17.77 - 21.73	8.40	7.71 - 9.14	32.49	35.80	0.32
-106+ 75	26.66	17.01	17.01 - 20.37	9.70	9.17 - 11.19	32.36	34.91	0.31
- 75+ 45	30.45	17.48	17.94 - 19.98	11.08	10.40 - 14.93	48.41	52.54	0.47
- 45	148.45	25.07	24.16 - 27.00	54.01	46.34 - 53.35	57.84	68.95	0.62
overall	274.87	22.59	21.93 - 25.37	100.00		49.19	57.19	

B.2.3 Batch Float 3

Operating conditions

Run id. : KKB3
Aeration Rate : 4 l/min
Impeller Speed : 1200 revs/min
Froth Height : 3 cm
Collector Dosage : SSOLA - 1388 g/ton
Frother Dosage : HTEB 12 µl/l
Pulp Density : 8.96 %

Table B.2.3(a): Batch float 3 results

concentrate	elapsed time (s)	sample mass (g)	sample ash (%)	cum. yield (%)	cum. ash (%)
C1	20	24.54	10.87	9.13	10.87
C2	35	40.89	11.01	24.33	10.96
C3	65	31.86	10.10	36.16	10.68
C4	125	31.46	10.10	47.88	10.54
C5	215	41.50	12.12	63.32	10.92
C6	305	7.11	12.97	65.96	11.00
C7	395	4.29	14.03	67.56	11.08
C8	515	2.49	14.09	68.48	11.12
tails		84.79	48.66	(measured)	
feed		268.93	22.95	(calculated)	

Table B.2.3(b): Size analyses of batch float 3 concentrate and tails

	concentrate			tails		
size fraction (micron)	sample mass (g)	sample ash (%)	% in size fraction	sample mass (g)	sample ash (%)	% in size fraction
+425	0.14	11.73	0.33	2.11	38.74	5.30
-425+212	3.44	11.32	8.00	4.59	49.36	11.53
-212+150	3.37	11.19	7.84	3.30	46.14	8.29
-150+106	3.46	10.85	8.04	3.33	33.43	8.36
-106+ 75	4.32	10.81	10.04	3.91	34.73	9.82
- 75+ 45	4.23	11.25	9.83	2.70	40.52	66.78
- 45	24.05	11.55	55.92	19.87	57.55	49.91
overall	43.01	11.34	100.00	39.81	49.25	100.00

Table B.2.3(c): Size analysis of reconstituted feed for batch float 3

	reconstituted Feed					results		
size fraction (micron)	sample mass (g)	sample ash (%)	95% ash % confidence limits	% in size fraction	95% size anal. confidence limits	coal yield (%)	coal rec. (%)	sep coef
+425	5.09	35.56	21.33 - 39.27	1.89	1.16 - 4.07	11.77	16.13	0.14
-425+212	24.50	26.49	21.61 - 33.55	9.11	6.93 - 11.38	60.12	72.53	0.64
-212+150	21.45	22.63	18.70 - 25.28	7.98	6.42 - 9.04	67.26	77.20	0.69
-150+106	21.90	18.16	17.77 - 21.73	8.15	7.71 - 9.14	67.64	73.68	0.66
-106+ 75	26.82	18.23	17.01 - 20.37	9.97	9.17 - 11.19	68.97	75.23	0.67
- 75+ 45	23.86	18.30	17.94 - 19.98	8.87	10.40 - 14.93	75.91	82.46	0.73
- 45	145.26	24.94	24.16 - 27.00	54.02	46.34 - 53.35	70.88	83.53	0.74
overall	268.88	23.29	21.93 - 25.37	100.00		68.48	79.07	

B.2.4 Batch Float 4

Operating conditions

Run id. : KKB4
Aeration Rate : 4 l/min
Impeller Speed : 1200 revs/min
Froth Height : 3 cm
Collector Dosage : SSOLA - 433 g/ton
Frother Dosage : HTEB 12 µl/l
Pulp Density : 9.88 %

Table B.2.4(a): Batch float 4 results

concentrate	elapsed time (s)	sample mass (g)	sample ash (%)	cum. yield (%)	cum. ash (%)
C1	20	5.50	9.11	1.86	9.11
C2	35	10.06	9.07	5.25	9.08
C3	65	9.09	8.51	8.32	8.87
C4	125	11.65	7.88	12.25	8.55
C5	215	11.51	7.66	16.13	8.34
C6	305	6.34	7.40	18.27	8.23
C7	395	3.47	7.29	19.44	8.17
C8	515	1.59	6.77	19.98	8.13
tails		237.21	29.58	(measured)	
feed		296.42	25.30	(calculated)	

Table B.2.4(b): Size analyses of batch float 4 concentrate and tails

	concentrate			tails		
size fraction (micron)	sample mass (g)	sample ash (%)	% in size fraction	sample mass (g)	sample ash (%)	% in size fraction
+425	0.30	9.11	0.93	1.95	31.85	3.67
-425+212	2.38	9.66	7.40	5.76	30.09	10.84
-212+150	1.34	8.76	4.17	4.86	24.92	9.14
-150+106	0.71	8.14	2.21	5.73	21.88	10.78
-106+ 75	0.65	9.03	2.02	5.80	19.13	10.91
- 75+ 45	0.16	9.94	0.50	5.04	20.32	9.48
- 45	26.62	8.17	82.77	24.01	36.63	45.17
overall	32.16	8.34	100.00	53.15	29.63	100.00

Table B.2.4(c): Size analysis of reconstituted feed for batch float 4

	reconstituted feed					results		
size fraction (micron)	sample mass (g)	sample ash (%)	95% ash % confidence limits	% in size fraction	95% size anal. confidence limits	coal yield (%)	coal rec. (%)	sep coef
+425	9.26	30.49	21.33 - 39.27	3.12	1.16 - 4.07	5.97	7.80	0.07
-425+212	30.09	27.11	21.61 - 33.55	10.15	6.93 - 11.38	14.56	18.05	0.16
-212+150	24.16	23.27	18.70 - 25.28	8.15	6.42 - 9.04	10.21	12.14	0.11
-150+106	26.88	21.21	17.77 - 21.73	9.07	7.71 - 9.14	4.86	5.67	0.05
-106+ 75	27.08	18.68	17.01 - 20.37	9.14	9.17 - 11.19	4.42	4.94	0.04
- 75+ 45	22.79	20.19	17.94 - 19.98	7.69	10.40 - 14.93	1.29	1.46	0.01
- 45	156.17	27.70	24.16 - 27.00	52.68	46.34 - 53.35	31.38	39.86	0.37
overall	296.42	25.38	21.93 - 25.37	100.00		19.98	24.55	

B.2.5 Batch Float 5

Operating conditions

Run id. : KKB19
Aeration Rate : 4 l/min
Impeller Speed : 1200 revs/min
Froth Height : 3 cm
Collector Dosage : SSOLA - 1520 g/ton
Frother Dosage : HTEB 12 µl/l
Pulp Density : 7.60%

Table B.2.5(a): Batch float 5 results

concentrate	elapsed time (s)	sample mass (g)	sample ash (%)	cum. yield (%)	cum. ash (%)
C1	20	29.40	10.23	12.89	10.23
C2	35	38.57	10.45	29.79	10.35
C3	65	33.61	10.14	44.53	10.28
C4	125	33.82	10.26	59.35	10.28
C5	215	30.16	12.16	72.57	10.62
C6	305	9.24	13.45	76.62	10.77
C7	395	4.65	14.38	78.66	10.86
C8	515	2.13	14.65	79.59	10.91
tails		46.55	52.06	(measured)	
feed		228.13	19.31	(calculated)	

Table B.2.5(b): Size analyses of batch float 5 concentrate and tails

	concentrate			tails		
size fraction (micron)	sample mass (g)	sample ash (%)	% in size fraction	sample mass (g)	sample ash (%)	% in size fraction
+425	0.19	8.06	0.50	2.11	30.98	5.27
-425+212	3.14	11.45	8.21	2.68	40.88	6.69
-212+150	3.29	10.65	8.60	1.63	28.13	4.07
-150+106	3.64	10.20	9.51	2.06	22.36	5.14
-106+ 75	4.22	10.85	11.03	2.59	25.24	6.46
- 75+ 45	4.49	12.68	11.74	3.09	36.59	7.71
- 45	19.29	11.65	50.42	25.92	67.45	64.67
overall	38.26	11.42	100.00	40.08	54.73	100.00

Table B.2.5(c): Size analysis of reconstituted feed for batch float 5

	reconstituted feed					results		
size fraction (micron)	sample mass (g)	sample ash (%)	95% ash % confidence limits	% in size fraction	95% size anal. confidence limits	coal yield (%)	coal rec. (%)	sep coef
+425	3.35	24.82	21.33 - 39.27	1.47	1.16 - 4.07	26.89	32.88	0.30
-425+212	18.01	16.53	21.61 - 33.55	7.90	6.93 - 11.38	82.72	87.76	0.78
-212+150	17.51	12.54	18.70 - 25.28	7.67	6.42 - 9.04	89.19	91.11	0.81
-150+106	19.67	11.68	17.77 - 21.73	8.62	7.71 - 9.14	87.84	89.31	0.80
-106+ 75	23.04	12.73	17.01 - 20.37	10.10	9.17 - 11.19	86.94	88.81	0.79
- 75+ 45	24.90	16.13	17.94 - 19.98	10.91	10.40 - 14.93	85.59	89.10	0.78
- 45	121.65	25.46	24.16 - 27.00	53.33	46.34 - 53.35	75.25	89.19	0.79
overall	228.13	20.26	21.93 - 25.37	100.00		79.59	88.14	

B.3 Two-Phase ASH Results

A total of 24 sets of two-phase runs were carried out. Three different diameter pedestals, and four different size diameter vortex-finders were used, and all vortex-finder/pedestal diameter permutations were tested, in duplicate. The method used is outlined in Section 4.2.2.2 in Chapter Four.

Details of the results obtained are listed in **Tables B.3.x_k** below, where each x_k represents the results obtained using a particular vortex-finder diameter. In each table the values in the various columns were calculated as described below:

i) The **run set no.**, in column 1, represents the set of runs carried out on a particular batch (tank) of water. The A, B, etc represent the replicate run sets. Each set of runs consisted of between 5 and 8 runs, i.e. runs at different water feed rates.

ii) The d_p, in column 2, is the diameter (mm) of the pedestal used in the set of runs.

iii) The **flow reading** (i), in column 3, is the signal (mV) indicated on the magnetic flowmeter at the feed (water) flow rate used.

iv) The **of** ($t_{of,i}$) and **uf** ($t_{uf,i}$) **sampling times** (s), in columns 4 and 5 respectively, are the times in seconds for which the respective overflow and underflow water samples were collected at a flow reading (i).

v) The **of** ($m_{of,i}$) and **uf** ($m_{uf,i}$) **water mass** (kg), in columns 6 and 7 respectively, are the masses of the overflow and underflow water samples collected, over the respective sampling times.

vi) The **feed** ($q_{f,i}$), **of** ($q_{of,i}$) and **uf** ($q_{uf,i}$) **water rates** (l/min), in columns 8, 9 and 10 respectively, are the calculated flowrates of the feed, overflow and underflow streams, respectively. These flowrates were calculated as shown below:

$$q_{of,i} = \frac{60m_{of,i}}{t_{of,i}}$$

$$q_{uf,i} = \frac{60m_{uf,i}}{t_{uf,i}}$$

$$q_{f,i} = q_{of,i} + q_{uf,i}$$

vii) The **water rec. to of** (W_i), in column 11, is the percentage of the water fed to the ASH that reported to the overflow, and was calculated as shown below:

$$W_i = \frac{100q_{of,i}}{q_{f,i}}$$

B.3.1 10.0 mm vortex-finder

Operating conditions

HTEB Dosage : 15 ml/470 l
Air Rate : 150 lpm
Inlet Area : 15x9 mm
Vortex finder length : 37 mm
Vortex finder diameter : 10 mm

Table B.3.1: Two-phase ASH results with d_{vf}=10.0 mm

			sampling time (s)		water mass (kg)		water rate (l/min)			water rec.
run set no.	d_p (mm)	flow reading	of	uf	of	uf	feed	of	uf	to of (%)
1A	44.1	5	60	30	0.00	1.72	3.44	0.00	3.44	0.00
		6	60	30	0.11	9.17	18.45	0.11	18.34	0.60
		7	60	15	0.24	6.85	27.64	0.24	27.40	0.87
		8	60	15	0.39	9.12	36.87	0.39	36.48	1.06
		8.5	60	10	0.44	6.83	41.42	0.44	40.98	1.06
1B	44.1	5	30	10	0.00	1.80	10.80	0.00	10.80	0.00
		6	30	10	0.08	2.93	17.74	0.16	17.58	0.90
		7	30	11	0.10	5.03	27.64	0.20	27.44	0.72
		8	30	10	0.18	6.34	38.40	0.36	38.04	0.94
		9	30	5	0.27	4.08	49.50	0.54	48.96	1.09
		10	30	5	0.36	4.98	60.48	0.72	59.76	1.19
2B	46	5	30	10	0.15	1.63	10.08	0.30	9.78	2.98
		6	30	10	0.28	3.05	18.86	0.56	18.30	2.97
		7	30	10	0.39	4.62	28.50	0.78	27.72	2.74
		8	30	10	0.54	6.27	38.70	1.08	37.62	2.79
		9	30	10	0.67	7.67	47.36	1.34	46.02	2.83
		10	30	5	0.81	4.50	55.62	1.62	54.00	2.91
2C	46	4.5	30	10	0.12	1.51	9.30	0.24	9.06	2.58
		5	30	10	0.20	1.84	11.44	0.40	11.04	3.50
		6	30	10	0.27	3.18	19.62	0.54	19.08	2.75
		7	30	10	0.42	4.77	29.46	0.84	28.62	2.85
		8	30	10	0.48	6.20	38.16	0.96	37.20	2.52
		9	30	5	0.76	3.93	48.68	1.52	47.16	3.12
		10	30	5	0.88	4.60	56.96	1.76	55.20	3.09
3C	48.2	5	30	10	0.27	1.52	9.66	0.54	9.12	5.59
		6	30	10	0.63	2.76	17.82	1.26	16.56	7.07
		7	30	10	0.99	4.35	28.08	1.98	26.10	7.05
		8	30	10	1.36	5.90	38.12	2.72	35.40	7.14
		9	30	5	1.65	3.70	47.70	3.30	44.40	6.92
		10	30	5	1.78	4.47	57.20	3.56	53.64	6.22
3D	48.2	5	30	10	0.28	1.48	9.44	0.56	8.88	5.93
		6	30	10	0.66	2.76	17.88	1.32	16.56	7.38
		7	30	10	0.99	4.35	28.08	1.98	26.10	7.05
		8	30	10	1.44	5.52	36.00	2.88	33.12	8.00
		9	30	5	1.73	3.85	49.66	3.46	46.20	6.97
		10	30	5	1.87	4.67	59.78	3.74	56.04	6.26

B.3.2 21.5 mm vortex-finder

Operating Conditions

HTEB Dosage : 15 ml/470 l
Air Rate : 150 lpm
Inlet Area : 15x9 mm
Vortex finder length : 37 mm
Vortx finder diameter : 21.5 mm

Table B.3.2: Two-phase ASH results with d_{vf}=21.5 mm

			sampling time (s)		water mass (kg)		water rate (l/min)			water rec.
run set no.	d_p (mm)	flow reading	of	uf	of	uf	feed	of	uf	to of (%)
4C	48.2	5	10	10	0.24	1.04	7.68	1.44	6.24	18.75
		6	10	10	0.92	2.14	18.36	5.52	12.84	30.07
		7	10	10	1.05	3.45	27.00	6.30	20.70	23.33
		8	10	10	1.21	5.06	37.62	7.26	30.36	19.30
		9	10	10	1.17	6.88	48.30	7.02	41.28	14.53
		10	10	10	1.44	8.11	57.30	8.64	48.66	15.08
4D	48.2	5	10	10	0.52	1.26	10.68	3.12	7.56	29.21
		6	10	10	0.95	2.20	18.90	5.70	13.20	30.16
		7	10	10	1.02	3.60	27.72	6.12	21.60	22.08
		8	10	10	0.95	5.71	39.96	5.70	34.26	14.26
		9	10	10	1.12	6.88	48.00	6.72	41.28	14.00
		10	10	10	1.48	8.09	57.42	8.88	48.54	15.47
5B	46	5	30	10	0.37	1.37	8.96	0.74	8.22	8.26
		6	30	10	1.80	2.44	18.24	3.60	14.64	19.74
		7	30	10	0.75	4.59	29.04	1.50	27.54	5.17
		8	30	10	0.76	5.99	37.46	1.52	35.94	4.06
		9	30	10	1.11	7.63	48.00	2.22	45.78	4.63
		10	30	10	1.44	8.53	54.06	2.88	51.18	5.33
5C	46	5	30	10	0.90	1.47	10.62	1.80	8.82	16.95
		5.5	20	10	0.92	1.98	14.64	2.76	11.88	18.85
		6	30	10	1.37	2.62	18.46	2.74	15.72	14.84
		6.5	20	10	0.26	4.37	27.00	0.78	26.22	2.89
		7	30	10	0.38	4.43	27.34	0.76	26.58	2.78
		8	30	10	0.63	6.26	38.82	1.26	37.56	3.25
		9	20	5	0.56	3.87	48.12	1.68	46.44	3.49
		10	20	5	0.75	4.60	57.45	2.25	55.20	3.92
6B	44.1	5	30	10	0.00	1.54	9.24	0.00	9.24	0.00
		6	30	10	0.71	2.66	17.38	1.42	15.96	8.17
		7	30	10	0.29	4.23	25.96	0.58	25.38	2.23
		8	30	10	0.28	5.67	34.58	0.56	34.02	1.62
		9	30	10	0.39	7.33	44.76	0.78	43.98	1.74
		10	30	8	0.53	7.09	54.24	1.06	53.18	1.95
6C	44.1	5	30	10	0.00	1.66	9.96	0.00	9.96	0.00
		6	30	10	0.41	2.68	16.90	0.82	16.08	4.85
		7	30	10	0.32	4.49	27.58	0.64	26.94	2.32
		8	30	10	0.35	5.96	36.46	0.70	35.76	1.92
		9	30	10	0.40	7.68	46.88	0.80	46.08	1.71
		10	30	5	0.50	4.40	53.80	1.00	52.80	1.86

B.3.3 16.0 mm vortex-finder

Operating Conditions

HTEB Dosage : 15 ml/470 l
Air Rate : 150 lpm
Inlet Area : 15x9 mm
Vortex finder length : 37 mm
Vortx finder diameter : 16 mm

Table B.3.3: Two-phase ASH results with d_{vf}=16.0 mm

			sampling time (s)		water mass (kg)		water rate (l/min)			water rec.
run set no.	d_p (mm)	flow reading	of	uf	of	uf	feed	of	uf	to of (%)
7B	44.1	5	30	10	0.00	1.52	9.12	0.00	9.12	0.00
		6	30	10	0.55	2.76	17.66	1.10	16.56	6.23
		7	30	10	0.32	4.38	26.92	0.64	26.28	2.38
		8	30	10	0.27	6.33	38.52	0.54	37.98	1.40
		9	30	10	0.38	7.73	47.14	0.76	46.38	1.61
		10	30	10	0.49	9.03	55.16	0.98	54.18	1.78
7C	44.1	5	30	10	0.21	1.93	12.00	0.42	11.58	3.50
		5.5	30	10	0.40	2.12	13.52	0.80	12.72	5.92
		6	30	10	0.18	2.96	18.12	0.36	17.76	1.99
		7	20	10	0.12	4.66	28.32	0.36	27.96	1.27
		8	20	10	0.20	6.29	38.34	0.60	37.74	1.57
		9	20	5	0.26	3.87	47.22	0.78	46.44	1.65
		10	20	5	0.33	4.76	58.11	0.99	57.12	1.70
8E	46	5	30	10	0.54	1.40	9.48	1.08	8.40	11.39
		6	30	10	1.31	2.48	17.50	2.62	14.88	14.97
		7	30	10	0.38	4.77	29.38	0.76	28.62	2.59
		8	30	10	0.50	6.33	38.98	1.00	37.98	2.57
		9	30	5	1.03	3.81	47.78	2.06	45.72	4.31
		10	30	5	1.17	4.77	59.58	2.34	57.24	3.93
8F	46	5	30	10	0.67	1.53	10.52	1.34	9.18	12.74
		6	30	10	1.25	2.69	18.64	2.50	16.14	13.41
		7	30	10	0.42	4.66	28.80	0.84	27.96	2.92
		8	30	10	0.82	6.21	38.90	1.64	37.26	4.22
		9	30	5	1.04	4.09	51.16	2.08	49.08	4.07
		10	10	5	0.47	4.89	61.50	2.82	58.68	4.59
9C	48.2	5	30	10	1.10	1.22	9.52	2.20	7.32	23.11
		6	30	10	2.23	2.36	18.62	4.46	14.16	23.95
		7	30	10	2.98	3.62	27.68	5.96	21.72	21.53
		8	30	10	3.26	5.20	37.72	6.52	31.20	17.29
		9	30	5	3.05	3.28	45.46	6.10	39.36	13.42
		10	10	10	1.13	8.10	55.38	6.78	48.60	12.24
9D	48.2	5	30	10	1.23	1.26	10.02	2.46	7.56	24.55
		6	10	10	0.76	2.43	19.14	4.56	14.58	23.82
		7	10	10	1.07	3.74	28.86	6.42	22.44	22.25
		8	10	10	1.03	5.18	37.26	6.18	31.08	16.59
		9	10	5	1.12	3.50	48.72	6.72	42.00	13.79
		10	10	5	1.15	4.17	56.94	6.90	50.04	12.12

B.3.4 29.0 mm vortex-finder

Operating Conditions

HTEB Dosage : 15 ml/470 l
Air Rate : 150 lpm
Inlet Area : 15x9 mm
Vortex finder length : 37 mm
Vortex finder diameter : 29 mm

Table B.3.4: Two-phase ASH results with d_{vf}=29.0 mm

			sampling time (s)		water mass (kg)		water rate (l/min)			water rec.
run set no.	d_p (mm)	flow reading	of	uf	of	uf	feed	of	uf	to of (%)
10A	48.2	5	10	10	0.67	1.01	10.08	4.02	6.06	39.88
		6	10	10	1.10	2.00	18.60	6.60	12.00	35.48
		7	10	10	1.07	3.30	26.22	6.42	19.80	24.49
		8	10	10	1.05	4.93	35.88	6.30	29.58	17.56
		9	10	10	1.45	6.15	45.60	8.70	36.90	19.08
		10	10	10	1.74	7.58	55.92	10.44	45.48	18.67
10B	48.2	5	10	10	0.55	1.03	9.48	3.30	6.18	34.81
		6	10	10	1.07	1.97	18.24	6.42	11.82	35.20
		7	10	10	1.09	3.31	26.40	6.54	19.86	24.77
		8	10	10	1.10	4.97	36.42	6.60	29.82	18.12
		9	10	10	1.50	6.09	45.54	9.00	36.54	19.76
		10	10	10	1.81	7.41	55.32	10.86	44.46	19.63
11A	46	5	10	10	0.13	1.42	9.30	0.78	8.52	8.39
		6	10	10	0.73	2.19	17.52	4.38	13.14	25.00
		7	10	10	0.35	4.23	27.48	2.10	25.38	7.64
		8	10	10	0.43	5.70	36.78	2.58	34.20	7.02
		9	10	10	0.59	6.83	44.52	3.54	40.98	7.95
		10	10	10	0.83	8.58	56.46	4.98	51.48	8.82
11C	46	5	30	10	0.92	1.35	9.94	1.84	8.10	18.51
		6	30	10	2.05	2.39	18.44	4.10	14.34	22.23
		7	30	10	1.28	4.21	27.82	2.56	25.26	9.20
		8	30	10	1.39	6.10	39.38	2.78	36.60	7.06
		9	30	10	1.85	6.91	45.16	3.70	41.46	8.19
		10	30	10	2.3	8.76	57.16	4.60	52.56	8.05
12B	44.1	5	30	10	0.09	1.63	9.96	0.18	9.78	1.81
		6	30	10	0.50	2.74	17.44	1.00	16.44	5.73
		7	30	10	0.40	4.39	27.14	0.80	26.34	2.95
		8	30	10	0.53	6.12	37.78	1.06	36.72	2.81
		9	30	10	0.69	7.67	47.40	1.38	46.02	2.91
		10	30	8	0.92	7.38	57.19	1.84	55.35	3.22
12C	44.1	5	30	10	0.01	1.48	8.90	0.02	8.88	0.23
		6	30	10	0.62	2.85	18.34	1.24	17.10	6.76
		7	30	10	0.48	4.46	27.72	0.96	26.76	3.46
		8	30	10	0.55	5.92	36.62	1.10	35.52	3.00
		9	30	10	0.75	7.55	46.80	1.50	45.30	3.21
		10	30	8	0.96	7.09	55.09	1.92	53.17	3.49

B.4 Three-Phase ASH Results

A total of 6 sets of three-phase runs were carried out. Each set of runs was carried out using either a different collector dosage or a different ASH configuration. Within each set of runs, the slurry feed rate was varied from about 15 to about 80 l/min. The method used is outlined in Section 4.2.2.3 of Chapter Four.

The experimental results obtained are listed in **Tables B.4.x_k(a)** where x_k is the number of the run set. The calculated values indicating the performance of the ASH are listed in **Tables B.4.x_k(b)**. The size analyses of the concentrate and tails samples (where carried out) are listed in **Tables B.4.x_k(c)** and the size analysis of the reconstituted feed (where calculated) is given in **Tables B.2.x_k(d)**.

In Tables B.4.x_k(a) below the values in the various columns signify the following:

i) The **sample** number (i), in column 1, is the number of the run within the set.

ii) The **of** ($t_{of,i}$) and **uf** ($t_{uf,i}$) **sampling times** (s), in columns 2 and 3 respectively, are the times (in seconds) for which the respective overflow and underflow slurry samples (i) were collected.

iii) The **of** ($wm_{of,i}$) and **uf** ($wm_{uf,i}$) **wet sample mass** (kg), in columns 4 and 5 respectively, are the masses of the respective overflow and underflow slurry samples (i), respectively, collected over the respective sampling times.

iv) The **of** ($dm_{of,i}$) and **uf** ($dm_{uf,i}$) **dry sample mass** (kg), in columns 6 and 7 respectively, are the mass of solids in the overflow and underflow slurry samples (i), respectively, obtained after filtering the wet samples and drying the solids.

v) The measured **of** ($a_{of,i}$) and **uf** ($a_{uf,i}$) and the calculated **feed** ($a_{f,i}$) **ash content** (%) are listed in columns 8, 9 and 10 respectively. The feed ash content was calculated in the following way:

$$a_{f,i} = \frac{\frac{a_{of,i}dm_{of,i}}{t_{of,i}} + \frac{a_{uf,i}dm_{uf,i}}{t_{uf,i}}}{\frac{dm_{of,i}}{t_{of,i}} + \frac{dm_{uf,i}}{t_{uf,i}}}$$

In Tables B.4.x_k(b) below the values in the various columns were calculated as described below.

i) The **coal yield** (Y_i), in column 2 is the concentrate yield (%) achieved in each run (sample) (i), and is calculated as shown below:

$$Y_i = \frac{\frac{dm_{of,i}}{t_{of,i}}}{\frac{dm_{of,i}}{t_{of,i}} + \frac{dm_{uf,i}}{t_{uf,i}}} 100$$

ii) The **coal recovery** (R_i), in column 3, is the recovery (%) of "clean coal" to the concentrate (i). The values were calculated as shown below:

$$R_i = \frac{Y_i(100-a_{of,i})}{100-a_{f,i}}$$

iii) The **sep. coef.** (S_i), in column 4, is the separation coefficient (a measure of the efficiency of separation of the feed into clean coal and gangue). The separation coefficient has a value of 1.0 at a coal recovery of 100 % and a concentrate ash of 0 %. The values were calculated as shown below:

$$S_i = \frac{R_i}{100} \left(1 - \frac{a_{of,i}}{100} \right)$$

iv) The **water recovery** (W_i), in column 5, is the fraction (%) of water in the feed slurry that reported to the overflow during run (i), and was calculated as shown below:

$$W_i = \frac{\dfrac{wm_{of,i} - \dfrac{dm_{of,i}}{1000}}{t_{of,i}}}{\dfrac{wm_{of,i} - \dfrac{dm_{of,i}}{1000}}{t_{of,i}} + \dfrac{wm_{uf,i} - \dfrac{dm_{uf,i}}{1000}}{t_{uf,i}}} (100)$$

v) The slurry rate ($Q_{f,i}$), in column 6, is the slurry feed rate used during run (i), and was calculated as shown below (the SG of the feed coal was found to be 1.6147 and the SG of water was assumed to be 1.0):

$$Q_{f,i} = (60) \frac{wm_{of,i} - \dfrac{dm_{of,i}}{1000}}{t_{of,i}} + \frac{wm_{uf,i} - \dfrac{dm_{uf,i}}{1000}}{t_{uf,i}} + \frac{\dfrac{dm_{of,i}}{t_{of,i}} + \dfrac{dm_{uf,i}}{t_{uf,i}}}{1000\ (1.6147)}$$

vi) The **pulp density** ($\rho_{p,i}$), in column 7, is the calculated feed pulp density on a mass/volume basis. The calculation used is shown below:

$$\rho_{p,i} = \frac{60\ \left(\dfrac{dm_{of,i}}{t_{of,i}} + \dfrac{dm_{uf,i}}{t_{uf,i}} \right)}{1000\ Q_{f,i}} (100)$$

In Tables B.4.3(c) and (e) below the values in the various columns were calculated in the same way as for Tables B.2.x_k(b), as described in Section B.2. The values refer to runs 2 and 7, respectively, of set 3.

The values in the various columns of Tables B.4.3(d) and (f) also refer to runs 2 and 7, respectively, of set 3. They were calculated as described below.

i) The **sample mass** ($f_{m,j}$), in column 2, is the mass of reconstituted feed in each of the size fractions (j), over a nominal 10 second sampling period. The **overall** ($f_{m,o}$) sample mass is the total mass

of reconstituted feed fed over the 10 second sampling period during run (i). The calculations used were:

$$f_{m,j} = \left(\frac{c_{s,j} dm_{of,i}}{100 t_{of,i}} + \frac{t_{s,j} dm_{uf,i}}{100 t_{uf,i}} \right) 10$$

$$f_{m,o} = \sum_{j=1}^{j=7} f_{m,j}$$

ii) The **sample ash** ($f_{a,j}$), in column 3, is the calculated ash content (%) in each of the size fractions (j) of the reconstituted feed. The calculation used was:

$$f_{a,j} = \frac{\left(\frac{c_{a,j} c_{s,j} dm_{of,i}}{100 t_{of,i}} + \frac{t_{a,j} t_{s,j} dm_{uf,i}}{100 t_{uf,i}} \right) 10}{f_{m,j}}$$

The **overall** ($f_{a,o}$) ash content, which can be compared to the feed ash content of Table B.4.3(a), was calculated acccording to the formula:

$$f_{a,o} = \frac{\sum_{j=1}^{j=7} f_{m,j} f_{a,j}}{f_{m,o}}$$

iii) The **95% ash confidence limits**, in column 4, are the ranges within which the ash content of the material in each size fraction (j) should lie, if the sample were truly representative. The method of calculating these limits is described in Section A.3.3, and the limits are calculated in Sections A.4.4.3, of Appendix A.

iv) The **% in size fraction** ($f_{s,j}$), in column 4, is the calculated mass percent of the reconsituted feed in each of the size fractions (j). The values were calculated as shown below:

$$f_{s,j} = \frac{100 f_{m,j}}{f_{m,o}}$$

v) The **95% size anal. confidence limits**, in column 6, are the ranges within which the amount of material in each size fraction (j) should lie, if the sample were truly representative. The method of calculating these limits is described in Section A.3.3, and the limits are calculated in Section A.4.4.1, of Appendix A.

vi) The **coal yield** (Y_j), in column 7, is the mass recovery in each size fraction (j), and is calculated as shown below:

$$Y_j = \frac{\frac{c_{s,j} dm_{of,i}}{100 t_{of,i}}}{f_{m,j}}$$

vii) The **coal rec.** (R_j), in column 8, is the recovery (%) of "clean coal" to the concentrate in each size fraction (j). The values were calculated as shown below:

$$R_j = \frac{Y_j f_{m,j}(1 - \frac{c_{a,j}}{100})}{f_{m,j}(1 - \frac{f_{a,j}}{100})}$$

viii) The **Sep. Coef.** (S_j), in column 9, is the separation coefficient (a measure of the efficiency of separation of the feed into clean coal and gangue) in each size fraction (j). The separation coefficient has a value of 1.0 at a coal recovery of 100 % and a concentrate ash of 0 %. The values were calculated as shown below:

$$S_j = \frac{R_j}{100} \left(1 - \frac{c_{a,j}}{100} \right)$$

B.4.1 ASH preliminary work set 1

Operating conditions

Set id. : KKPWP1
Air Rate : 175 l/min
Inlet Area : 15x9 mm
Vortex finder length : 50 mm
Vortex finder diameter : 21.7 mm
Pedestal diameter : 40.5 mm
Collector Dosage : SSOLA 12 222 g/ton
Frother Dosage : HTEB 13 ml

Table B.4.1(a): Results of ASH three-phase set 1

	sampling time (s)		wet sample mass (kg)		dry sample mass (g)		ash content (%)		
samp.	of	uf	of	uf	of	uf	of	uf	feed
1	30	10	0.16	2.43	11.22	84.98	19.30	22.64	22.50
5	30	10	0.21	2.31	12.24	80.58	19.67	22.30	22.17
7	30	10	0.58	2.66	43.38	83.56	12.34	24.66	22.84
2	30	10	1.45	6.29	146.75	169.27	10.05	26.10	22.50
3	30	10	1.85	8.60	201.03	227.05	9.21	27.07	23.00
4	30	10	2.40	10.88	264.49	284.48	8.80	28.60	23.92
6	30	10	4.03	12.46	378.70	316.55	9.60	29.20	23.61

Table B.4.1(b): Calculated results of ASH three-phase set 1

sample	coal yield (%)	coal recovery (%)	sep. coef.	water recovery (%)	slurry rate (l/min)	pulp density (%)
1	4.22	4.39	0.04	2.07	14.70	3.62
5	4.82	4.97	0.04	2.87	14.09	3.61
7	14.75	16.76	0.15	6.49	16.90	3.48
2	22.42	26.02	0.23	6.63	40.14	3.26
3	22.79	26.87	0.24	6.16	54.63	3.23
4	23.66	28.36	0.26	6.30	69.23	3.23
6	28.51	33.74	0.31	9.11	81.81	3.25

B.4.2 ASH preliminary work set 2

Operating conditions

Set id. : KKCD1
Air Rate : 175 l/min
Inlet Area : 15x9 mm
Vortex finder length : 69 mm
Vortex finder diameter : 21.7 mm
Pedestal diameter : 42 mm
Collector Dosage : SSOLA 24 444 g/ton
Frother Dosage : HTEB 13 ml

Table B.4.2(a): Results of ASH three-phase set 2

	sampling time (s)		wet sample mass (kg)		dry sample mass (g)		ash content (%)		
samp.	of	uf	of	uf	of	uf	of	uf	feed
1	10	10	1.67	10.98	157.55	226.28	9.18	35.9	24.93
2	10	10	1.17	9.94	145.12	190.84	9.42	35.82	24.42
3	20	10	1.28	8.72	250.89	161.44	9.17	36.16	24.36
4	20	10	0.39	6.28	67.83	175.32	8.25	27.45	24.34
5	20	10	0.25	5.46	30.06	177.68	8.33	23	21.86
6	30	10	0.24	4.19	6.7	132.93	16.4	23.77	23.65
7	40	10	0.28	2.46	7.5	75.59	17.94	23.6	23.46

Table B.4.2(b): Calculated results of ASH 3-Phase set 2

sample	coal yield (%)	coal recovery (%)	sep. coef.	water recovery (%)	slurry rate (l/min)	pulp density (%)
1	41.05	49.66	0.45	12.33	75.02	3.07
2	43.20	51.77	0.47	9.51	65.89	3.06
3	43.73	52.51	0.48	5.67	55.50	3.10
4	16.21	19.66	0.18	2.57	38.37	3.27
5	7.80	9.15	0.08	2.04	33.07	3.50
6	1.65	1.81	0.02	1.88	25.31	3.20
7	2.42	2.56	0.02	2.78	15.00	3.10

B.4.3 ASH preliminary work set 3

Operating conditions

Set id. : KKCD2
Air Rate : 175 l/min
Inlet Area : 15x9 mm
Vortex finder length : 69 mm
Vortex finder diameter : 21.5 mm
Pedestal diameter : 42 mm
Collector Dosage : SSOLA 36 666 g/ton
Frother Dosage : HTEB 13 ml

Table B.4.3(a): Results of ASH 3-Phase set 3

	sampling time (s)		wet sample mass (kg)		dry sample mass (g)		ash content (%)		
samp.	of	uf	of	uf	of	uf	of	uf	feed
1	10	10	1.29	11.14	175.43	233.93	8.91	36	24.39
2	10	10	1.06	9.88	178.16	190.52	9.14	38.28	24.20
3	10	10	0.39	7.88	88.17	206.88	8.12	30.48	23.80
4	10	10	0.41	7.56	84.77	204.25	7.62	28.37	22.28
5	20	10	0.24	6.03	17.29	212.57	10.23	23.02	22.52
6	20	10	0.15	3.7	8.01	129.82	16.58	23.08	22.89
7	20	10	0.04	2.74	3.88	93.81	13.26	23.78	23.57

Table B.4.3(b): Calculated results of ASH 3-Phase set 3

sample	coal yield (%)	coal recovery (%)	sep. coef.	water recovery (%)	slurry rate (l/min)	pulp density (%)
1	42.85	51.63	0.47	9.27	73.64	3.34
2	48.32	57.92	0.53	8.34	64.80	3.41
3	29.88	36.03	0.33	3.78	48.95	3.62
4	29.33	34.86	0.32	4.23	47.16	3.68
5	3.91	4.53	0.04	1.88	36.39	3.65
6	2.99	3.24	0.03	1.95	22.34	3.59
7	2.03	2.30	0.02	0.68	16.34	3.52

Table B.4.3(c): Size analyses of ASH three-phase set 3, run 2 concentrate and tails samples

	concentrate			tails		
size fraction (micron)	sample mass (g)	sample ash (%)	% in size fraction	sample mass (g)	sample ash (%)	% in size fraction
+425	0.00	0.00	0.00	2.19	36.63	5.56
-425+212	0.74	7.02	2.00	7.43	31.44	18.87
-212+150	2.13	6.46	5.77	4.32	34.54	10.97
-150+106	3.04	7.70	8.23	3.36	35.02	8.53
-106+ 75	4.75	9.31	12.86	2.97	33.10	7.54
- 75+ 45	6.22	10.94	16.84	2.07	38.69	5.26
- 45	20.06	10.64	54.30	17.04	43.16	43.27
overall	36.94	9.96	100.00	39.38	37.95	100.00

Table B.4.3(d): Size analyses of reconstituted feed for ASH three-phase set 3, run 2 concentrate and tails samples

	reconstituted Feed					results		
size fraction (micron)	sample mass (g)	sample ash (%)	95% ash % confidence limits	% in size fraction	95% size anal. confidence limits	coal yield (%)	coal rec. (%)	sep coef
+425	10.60	36.63	21.33 - 39.27	2.87	1.16 - 4.07	0.00	0.00	0.00
-425+212	39.52	29.23	21.61 - 33.55	10.72	6.93 - 11.38	9.03	11.87	0.11
-212+150	31.17	25.29	18.70 - 25.28	8.46	6.42 - 9.04	32.95	41.26	0.39
-150+106	30.92	22.06	17.77 - 21.73	8.39	7.71 - 9.14	47.42	56.16	0.52
-106+ 75	37.28	18.48	17.01 - 20.37	10.11	9.17 - 11.19	61.45	68.37	0.62
- 75+ 45	40.01	17.89	17.94 - 19.98	10.85	10.40 - 14.93	74.97	81.31	0.72
- 45	179.19	25.76	24.16 - 27.00	48.60	46.34 - 53.35	53.99	64.77	0.58
overall	368.68	24.42	21.93 - 25.37	100.00		48.32	57.57	

Table B.4.3(e): Size analyses of ASH three-phase set 3 run 7 concentrate and tails samples

	concentrate			tails		
size fraction (micron)	sample mass (g)	sample ash (%)	% in size fraction	sample mass (g)	sample ash (%)	% in size fraction
+425	0.00	0.00	0.00	0.71	28.74	1.80
-425+212	0.00	0.00	0.00	3.54	27.09	8.99
-212+150	0.00	0.00	0.00	3.14	22.47	7.97
-150+106	0.00	0.00	0.00	3.87	18.78	9.83
-106+ 75	0.00	0.00	0.00	3.66	18.92	9.29
- 75+ 45	0.00	0.00	0.00	4.19	18.71	10.64
- 45	3.88	13.26	100.00	25.69	50.61	
overall	3.88	13.26		39.04	23.78	

Table B.4.3(f): Size analyses of reconstituted feed for ASH three-phase set 3 run 7 concentrate and tails samples

	reconstituted Feed					results		
size fraction (micron)	sample mass (g)	sample ash (%)	95% ash % confidence limits	% in size fraction	95% size anal. confidence limits	coal yield (%)	coal rec. (%)	sep coef
+425	1.71	28.74	21.33 - 39.27	1.78	1.16 - 4.07	0.00	0.00	0.00
-425+212	8.51	27.09	21.61 - 33.55	8.88	6.93 - 11.38	0.00	0.00	0.00
-212+150	7.55	22.47	18.70 - 25.28	7.88	6.42 - 9.04	0.00	0.00	0.00
-150+106	9.30	18.78	17.77 - 21.73	9.71	7.71 - 9.14	0.00	0.00	0.00
-106+ 75	8.79	18.92	17.01 - 20.37	9.19	9.17 - 11.19	0.00	0.00	0.00
- 75+ 45	10.07	18.71	17.94 - 19.98	10.52	10.40 - 14.93	0.00	0.00	0.00
- 45	49.83	25.21	24.16 - 27.00	52.04	46.34 - 53.35	3.89	4.52	0.04
overall	95.75	23.57	21.93 - 25.37	100.00		2.03	2.30	

B.4.4 ASH preliminary work set 4

Operating conditions

Set id. : KKPWP2
Air Rate : 175 l/min
Inlet Area : 15x9 mm
Vortex finder length : 69 mm
Vortex finder diameter : 21.5 mm
Pedestal diameter : 42 mm
Collector Dosage : SSOLA 24 444 g/ton
Frother Dosage : HTEB 13 ml

Table B.4.4(a): Results of ASH three-phase set 4

	sampling time (s)		wet sample mass (kg)		dry sample mass (g)		ash content (%)		
samp.	of	uf	of	uf	of	uf	of	uf	feed
1	20	10	4.71	13.93	379.37	211.64	9.89	35.92	23.62
2	20	10	4.27	10.48	355.82	166.45	10.24	38.87	24.08
3	20	10	3.06	8.71	329.78	111.42	10.49	42.15	23.26
4	20	10	2.28	7.81	273.26	87.91	10.45	46.01	24.37
5	20	10	1.77	6.87	210.17	97.35	9.49	37.15	22.79
6	40	10	1.78	5.22	175.63	104.20	10.14	28.80	23.27
7	40	10	1.38	3.68	74.43	79.38	11.18	25.04	22.41

Table B.4.4(b): Calculated results of ASH three-phase set 4

sample	coal yield (%)	coal recovery (%)	sep. coef.	water recovery (%)	slurry rate (l/min)	pulp density (%)
1	47.26	55.76	0.50	13.63	96.79	2.49
2	51.66	61.08	0.55	15.9	74.90	2.76
3	59.68	69.60	0.62	13.70	60.81	2.73
4	60.85	72.05	0.65	11.50	53.19	2.53
5	51.91	60.85	0.55	10.30	46.06	2.64
6	29.65	34.72	0.31	7.27	33.65	2.64
7	18.99	21.74	0.19	8.31	23.93	2.46

B.4.5 ASH preliminary work run 5

Operating conditions

Set id. : KKPW01
Air Rate : 175 l/min
Inlet Area : 15x9 mm
Vortex finder length : 50 mm
Vortex finder diameter : 21.5 mm
Orifice diameter : 14 mm
Collector Dosage : SSOLA 8 066 g/ton
Frother Dosage : HTEB 13 ml

Table B.4.5(a): Results of ASH three-phase set 5

	sampling time (s)		wet sample mass (kg)		dry sample mass (g)		ash content (%)		
samp.	of	uf	of	uf	of	uf	of	uf	feed
1	10	10	0.53	2.16	24.34	51.20	14.95	31.27	26.01
2	10	10	0.61	3.63	27.09	74.27	14.06	31.56	26.88
3	10	10	0.55	3.75	10.76	41.32	22.09	46.59	41.53
4	10	10	0.62	4.20	12.70	54.14	21.49	46.37	41.64
5	10	10	0.26	2.87	6.54	37.24	21.54	46.73	42.97
6	10	10	1.10	5.23	24.48	70.14	19.64	46.28	44.01
7	10	10	0.98	4.72	26.97	74.82	17.45	41.31	35.43
8	10	10	0.47	3.13	20.86	60.79	15.71	38.83	31.72

Table B.4.5(b): Calculated results of ASH three-phase set 5

sample	coal yield (%)	coal recovery (%)	sep. coef.	water recovery (%)	slurry rate (l/min)	pulp density (%)
1	32.22	37.04	0.32	19.34	15.97	2.84
2	26.73	31.41	0.27	14.08	25.21	2.41
3	20.66	27.53	0.21	12.69	25.68	1.22
4	19.00	25.56	0.20	12.78	28.77	1.39
5	14.94	20.55	0.16	8.21	18.68	1.41
6	8.53	12.24	0.10	17.49	37.80	1.22
7	24.65	31.52	0.26	17.06	33.97	1.75
8	30.73	37.94	0.32	12.61	21.40	2.46

B.4.6 ASH preliminary work set 6

Operating conditions

Set id. : KKCD3
Air Rate : 175 l/min
Inlet Area : 15x9 mm
Vortex finder length : 69 mm
Vortex finder diameter : 21.5 mm
Pedestal diameter : 42 mm
Collector Dosage : SSOLA 48 888 g/ton
Frother Dosage : HTEB 13 ml

Table B.4.6(a): Results of ASH three-phase set 6

	sampling time (s)		wet sample mass (kg)		dry sample mass (g)		ash content (%)		
samp.	of	uf	of	uf	of	uf	of	uf	feed
1	10	10	1.50	11.38	135.00	247.37	8.87	32.69	24.28
2	10	10	1.04	9.53	124.47	201.37	8.71	30.83	22.38
3	10	10	0.41	7.95	79.83	156.77	7.87	34.18	25.30
4	10	10	0.17	6.33	5.23	190.02	13.86	24.00	23.73
5	20	10	0.22	5.39	4.95	168.04	20.00	25.76	25.68
6	20	10	0.17	3.80	4.23	115.34	18.84	24.83	24.70
7	20	10	-	2.77	-	84.30	-	28.99	28.28
8	10	10	1.09	9.95	127.33	194.07	8.64	33.78	33.78

Table B.4.6(b): Calculated results of ASH three-phase set 6

sample	coal yield (%)	coal recovery (%)	sep. coef.	water recovery (%)	slurry rate (l/min)	pulp density (%)
1	35.31	42.49	0.39	10.92	76.41	3.00
2	38.20	44.93	0.41	8.94	62.68	3.12
3	33.74	41.61	0.38	4.06	49.62	2.86
4	2.68	3.03	0.03	2.61	38.55	3.04
5	1.45	1.56	0.01	2.02	32.61	3.14
6	2.10	2.26	0.02	2.19	23.04	3.07
7	0.00	3.41	0.03	-0.08	16.42	3.16
8	39.62	47.51	0.43	8.98	65.03	1.79

APPENDIX C

DETAILED RESULTS

C.1 Kleinkopje Factorial Design

C.1.1 Overall Results

The results of the factorial design runs carried out on the Kleinkopje coal are listed in **Table C.1(a)** below. The calculated values indicating the performance of the ASH are listed in **Table C.1(b)**. The calculated values listed in Table C.1(a) and C.1(b) were obtained in the same way as those for Tables B.4.x_k(a) and B.4.x_k(b), respectively (see Appendix B). The calculations used are detailed in Section B.4 of Appendix B.

Each set of values contained in Tables C.1(a) and (b) between solid horizontal lines represents the results of duplicate, repeat or replicate runs carried out at a particular set of parameter levels, as part of the factorial design. The structure of the factorial design, the parameter levels used, and the significance of the sample nomenclature are given in Sections 6.1 and 6.2 in Chapter Six.

Table C.1(a): Results obtained during the factorial design (all runs carried out)

	sampling time (s)		wet sample mass (kg)		dry sample mass (g)		ash content (%)		
sample	of	uf	of	uf	of	uf	of	uf	feed
KKFD-A1 (1)	20	10	0.37	11.24	108.00	lost	7.09	lost	
KFD-A1 (2)	20	10	0.43	10.74	103.79	282.21	7.09	26.74	23.69
KFD-B1 (1)	20	10	0.13	11.07	7.54	337.31	8.07	24.92	24.73
KFD-B1 (2)	20	10	0.13	10.80	8.34	329.17	8.05	24.08	23.88
KFD-C1	20	10	0.11	11.00	18.86	327.97	7.43	23.55	23.10

Table C.1(a): continued

	sampling time (s)		wet sample mass (kg)		dry sample mass (g)		ash content (%)		
sample	of	uf	of	uf	of	uf	of	uf	feed
KKFD-A2	20	10	2.25	9.24	379.53	147.12	9.84	41.79	23.79
KKFD-B2	20	10	2.84	9.64	414.66	134.36	10.42	45.40	24.17
KKFD-A3 (1)	10	10	2.70	8.15	120.77	224.99	11.62	28.21	22.42
KKFD-A3 (2)	10	10	1.69	9.10	135.36	206.48	10.08	31.56	23.05
KKFD-A3 (3)	10	10	1.45	9.39	133.69	201.73	9.78	32.08	23.19
KKFD-B3	10	10	3.15	7.56	151.04	192.55	11.86	32.21	23.26
KKFD-C3	10	10	2.79	8.13	171.94	183.70	10.93	35.39	23.56
KKFD-A4 (1)	10	10	0.71	10.11	83.14	229.16	8.06	30.39	24.45
KKFD-A4 (2)	10	10	0.89	10.28	115.82	228.79	8.24	31.09	23.41
KKFD-B4	20	10	0.66	10.25	68.56	296.95	7.72	25.97	24.08
KKFD-C4	20	10	1.13	10.47	119.62	274.08	8.46	29.88	26.04
KKFD-D4 (1)	20	10	0.56	10.71	43.21	326.43	8.67	24.65	23.66
KKFD-D4 (2)	20	10	0.53	10.82	33.68	339.16	9.61	24.45	23.75
KKFD-A5 (1)	20	10	0.10	11.02	3.10	348.39	14.95	24.01	23.97
KKFD-A5 (2)	20	10	0.13	9.84	3.24	312.16	16.18	25.54	25.49
KKFD-B5	20	10	0.15	11.03	5.26	308.57	16.98	24.14	24.08
KKFD-A6	10	10	1.15	9.64	115.49	223.96	9.455	31.39	23.93
KKFD-B6	20	10	1.75	9.54	317.23	183.83	8.97	36.87	23.95
KKFD-C6	10	10	1.10	9.46	134.27	194.97	9.14	32.19	22.79
KKFD-D6	10	10	0.99	10.06	156.48	171.60	8.80	38.05	24.10
KKFD-A7 (1)	10	10	2.45	7.93	159.34	179.58	10.63	35.39	23.75
KKFD-A7 (2)	10	10	2.88	7.75	175.57	170.26	11.28	39.26	25.06
KKFD-B7 (1)	10	10	3.36	7.33	200.94	148.91	11.68	40.16	23.80
KKFD-B7 (2)	10	10	3.07	7.52	192.45	149.30	11.38	37.99	23.01
KKFD-C7 (1)	10	10	2.09	8.88	200.12	133.50	10.73	45.54	24.66
KKFD-C7 (2)	10	10	2.20	8.75	203.55	126.83	10.90	45.46	24.17
KKFD-D7	10	10	3.02	8.02	201.05	129.53	11.91	36.81	21.67
KKFD-A8 (1)	10	10	1.50	9.34	217.59	113.56	10.98	47.14	23.38
KKFD-A8 (2)	10	10	1.33	9.13	217.81	101.10	11.16	49.42	23.29
KKFD-B8	10	10	2.45	7.99	205.93	104.00	11.82	51.18	25.03
KKFD-C8	10	10	1.61	9.22	207.41	117.37	10.74	44.36	22.89
KKFD-A9 (1)	10	10	2.04	8.80	94.97	233.05	11.49	28.29	23.42
KKFD-A9 (2)	10	10	1.78	-	87.10	-	11.49	-	11.49
KKFD-B9	10	10	2.34	8.26	179.15	152.76	10.97	36.45	22.70
KKFD-C9	10	10	1.48	9.92	128.52	219.65	9.57	33.61	24.74
KKFD-D9	10	10	2.07	8.5	104.63	209.79	11.23	29.33	23.31
KKFD-A10 (1)	10	10	0.75	10.08	117.37	211.18	8.36	31.25	23.07
KKFD-A10 (2)	10	10	0.82	9.98	127.89	208.75	8.51	32.44	23.35
KKFD-B10	20	10	0.63	10.46	105.65	272.92	6.90	26.50	23.32
KKFD-C10	20	10	1.36	10.39	208.83	238.23	8.14	30.39	23.61
KKFD-D10	20	10	1.04	9.98	245.55	182.59	8.43	35.73	24.75
KKFD-A11 (1)	20	10	0.23	10.23	11.67	323.82	10.18	22.31	22.10
KKFD-A11 (2)	20	10	0.20	8.85	5.99	284.63	16.53	22.32	22.26
KKFD-B11	20	10	0.25	10.75	8.47	342.80	16.28	23.09	23.01
KKFD-A12	10	10	2.00	8.47	225.53	116.59	11.28	50.24	24.56
KKFD-B12	10	10	1.84	9.21	203.71	110.21	11.10	50.52	24.94
KKFD-A13 (1)	10	10	3.62	7.54	236.52	115.60	13.11	46.85	24.19
KKFD-A13 (2)	10	10	3.33	7.54	233.08	lost	lost	46.85	
KKFD-B13	10	10	3.79	7.05	216.61	103.06	12.89	48.60	24.40
KKFD-A14 (1)	10	10	1.47	9.66	167.36	177.24	9.94	36.85	23.78
KKFD-A14 (2)	10	10	1.36	9.71	164.87	175.97	9.83	38.75	24.76
KKFD-B14	10	10	0.85	10.29	128.69	196.62	10.37	32.74	23.89
KKFD-C14	10	10	0.71	10.30	116.03	217.28	8.02	33.60	24.70
KKFD-A15	20	10	0.11	10.79	4.64	350.24	10.83	24.46	24.37
KKFD-B15	20	10	0.12	10.83	6.56	306.65	9.95	24.85	24.69
KKFD-A16	20	10	0.68	9.89	122.63	263.66	7.01	30.15	25.78
KKFD-B16	20	10	0.95	9.81	142.18	236.91	7.26	27.07	22.50

Table C.1(b): Calculated results obtained during the factorial design (all runs carried out)

sample	coal yield (%)	coal recovery (%)	sep. coef.	water recovery (%)	slurry rate (l/min)	pulp density (%)
KKFD-A1 (1)	100.00	100.00	0.93	1.15	68.43	0.47
KKFD-A1 (2)	15.53	18.91	0.18	1.54	64.97	3.09
KKFD-B1 (1)	1.11	1.35	0.01	0.57	66.03	3.10
KKFD-B1 (2)	1.25	1.51	0.01	0.58	64.43	3.10
KKFD-C1	2.79	3.36	0.03	0.42	65.86	3.07
KKFD-A2	56.33	66.64	0.60	9.33	61.42	3.29
KKFD-B2	60.68	71.68	0.64	11.31	65.58	3.13
KKFD-A3 (1)	34.93	39.79	0.35	24.55	64.31	3.23
KKFD-A3 (2)	39.60	46.27	0.42	14.88	63.96	3.21
KKFD-A3 (3)	39.86	46.82	0.42	12.53	64.27	3.13
KKFD-B3	43.96	50.49	0.45	28.93	63.48	3.25
KKFD-C3	48.35	56.34	0.50	24.78	64.71	3.30
KKFD-A4 (1)	26.62	32.40	0.30	5.97	64.21	2.92
KKFD-A4 (2)	33.61	40.27	0.37	7.15	66.23	3.12
KKFD-B4	10.35	12.58	0.12	2.89	62.72	3.17
KKFD-C4	17.91	22.17	0.20	4.72	65.45	3.06
KKFD-D4 (1)	6.21	7.43	0.07	2.43	65.15	3.21
KKFD-D4 (2)	4.73	5.61	0.05	2.31	65.70	3.25
KKFD-A5 (1)	0.44	0.50	0.00	0.45	65.62	3.20
KKFD-A5 (2)	0.52	0.58	0.00	0.66	58.71	3.21
KKFD-B5	0.85	0.92	0.01	0.67	65.92	2.83
KKFD-A6	34.02	40.50	0.37	9.90	63.96	3.18
KKFD-B6	46.32	55.44	0.50	7.11	61.71	3.33
KKFD-C6	40.78	47.99	0.44	9.44	62.61	3.16
KKFD-D6	47.70	57.31	0.52	7.77	65.55	3.00
KKFD-A7 (1)	47.01	55.10	0.49	22.81	61.51	3.31
KKFD-A7 (2)	50.77	60.10	0.53	26.30	62.99	3.29
KKFD-B7 (1)	57.44	66.57	0.59	30.55	63.34	3.31
KKFD-B7 (2)	56.31	64.82	0.57	28.08	62.76	3.27
KKFD-C7 (1)	59.98	71.07	0.63	17.77	65.06	3.08
KKFD-C7 (2)	61.61	72.39	0.64	18.80	64.95	3.05
KKFD-D7	60.82	68.39	0.60	26.32	65.48	3.03
KKFD-A8 (1)	65.71	76.34	0.68	12.20	64.28	3.09
KKFD-A8 (2)	68.30	79.10	0.70	10.97	62.03	3.08
KKFD-B8	66.44	78.15	0.69	22.15	61.93	3.00
KKFD-C8	63.86	73.92	0.66	13.35	64.24	3.03
KKFD-A9 (1)	28.95	33.46	0.30	18.50	64.29	3.06
KKFD-A9 (2)	100.00	100.00	0.89	100.00	10.48	4.99
KKFD-B9	53.98	62.16	0.55	21.04	62.84	3.17
KKFD-C9	36.91	44.35	0.40	12.23	67.60	3.09
KKFD-D9	33.28	38.00	0.34	19.16	62.70	3.01
KKFD-A10 (1)	35.72	42.56	0.39	6.02	64.23	3.07
KKFD-A10 (2)	37.99	45.34	0.41	6.61	64.03	3.15
KKFD-B10	16.22	19.69	0.18	2.51	63.91	3.06
KKFD-C10	30.47	36.64	0.34	5.37	65.64	3.13
KKFD-D10	40.21	48.93	0.45	3.90	62.30	2.94
KKFD-A11 (1)	1.77	2.04	0.02	1.09	61.32	3.23
KKFD-A11 (2)	1.04	1.12	0.01	1.12	53.04	3.25
KKFD-B11	1.22	1.33	0.01	1.15	64.46	3.23
KKFD-A12	65.92	77.52	0.69	17.52	62.04	3.31
KKFD-B12	64.89	76.86	0.68	15.24	65.58	2.87

Table C.1(b): continued

sample	coal yield (%)	coal recovery (%)	sep. coef.	water recovery (%)	slurry rate (l/min)	pulp density (%)
KKFD-A13 (1)	67.17	76.98	0.67	31.31	66.16	3.19
KKFD-A13 (2)	100.00	100.00	1.00	29.11	64.69	2.16
KKFD-B13	67.76	78.08	0.68	33.97	64.31	2.98
KKFD-A14 (1)	48.57	57.39	0.52	12.08	65.99	3.13
KKFD-A14 (2)	48.37	57.97	0.52	11.14	65.64	3.12
KKFD-B14	39.56	46.59	0.42	6.67	66.10	2.95
KKFD-C14	34.81	42.52	0.39	5.56	65.30	3.06
KKFD-A15	0.66	0.78	0.01	0.50	64.26	3.29
KKFD-B15	1.06	1.27	0.01	0.54	64.63	2.88
KKFD-A16	18.87	23.64	0.22	2.81	60.64	3.22
KKFD-B16	23.08	27.62	0.26	4.05	61.01	3.03

C.1.1.1 statistical analysis of solids feed rate to the ASH

Before carrying out a statistical analysis of the results obtained in the factorial design runs, the random nature of the solids feed rate to the ASH during the factorial design runs was checked.

The feed rate to the ASH was controlled by opening a valve to achieve a slurry flow which corresponded to a predetermined signal reading on the magnetic flowmeter. However, this method resulted in slight variations in the volumetric flow rate to the ASH. In addition to the above, adding slightly different masses of wet coal to the conditioning tank resulted in variations in the pulp density.

The work described below was carried out to determine whether or not the solids feed rate to the ASH was subject only to random variation, i.e. normally distributed. This was done by statistical analyses on the random nature (i.e. normality) of the volumetric feed rate and feed pulp density to the ASH. Statistical analyses on the above allowed the nature of the solids to be inferred.

The statistical method employed was the Kolmogorov-Smirnov test (see Section A.3.1 of Appendix A). The results of the tests performed are listed in Table C.1(c) below. In addition normal probability curves are graphically presented in Figures C.1(a) (volumetric feed

rate) and (b) below (feed pulp density). The volumetric feed rate and feed pulp density data used in the analyses was from Table C.1(a) above. The only runs to be excluded from the analyses were KKFD-A9(2), in which the tails sample was "lost" and run KKFD-A11(2), which was obviously erroneous.

The results obtained show that the volumetric feed rates and pulp densities used were normally distributed, i.e. subject only to random variation. As the assumption of normality was true for this "worst case", it was possible to assume that it would hold if further "outliers" were excluded. This is also apparent from the data plotted in Figures C.1(a) and (b) below. The results listed in Table C.1(c) and presented in Figures C.1(a) and (b) indicated that the distribution of solids feed rates to the ASH, during the factorial design runs, was also normally distributed.

Table C.1(c): Results of the K-S tests on the feed pulp density and volumetric feed rate distributions to the ASH

	volumetric slurry rate (lpm)	feed pulp density (% solids)
DPLUS	0.09	0.10
DMINUS	0.14	0.14
DN	0.14	0.14
α	0.20	0.22
x_m	64.08	3.11
s	1.71	0.17

C.1.2 Statistical analysis

The *original factorial design* results are the results obtained in the factorial design runs excluding those which had been identified as being "problematic". The *modified factorial design* results are the results obtained in the factorial design runs excluding those which had been identified as being either "problematic" or "outliers". The original factorial design consisted of 50 runs (of which 10 were duplicates or repeats) and the modified factorial design consisted of 47 runs (of which 10 were duplicates or repeats).

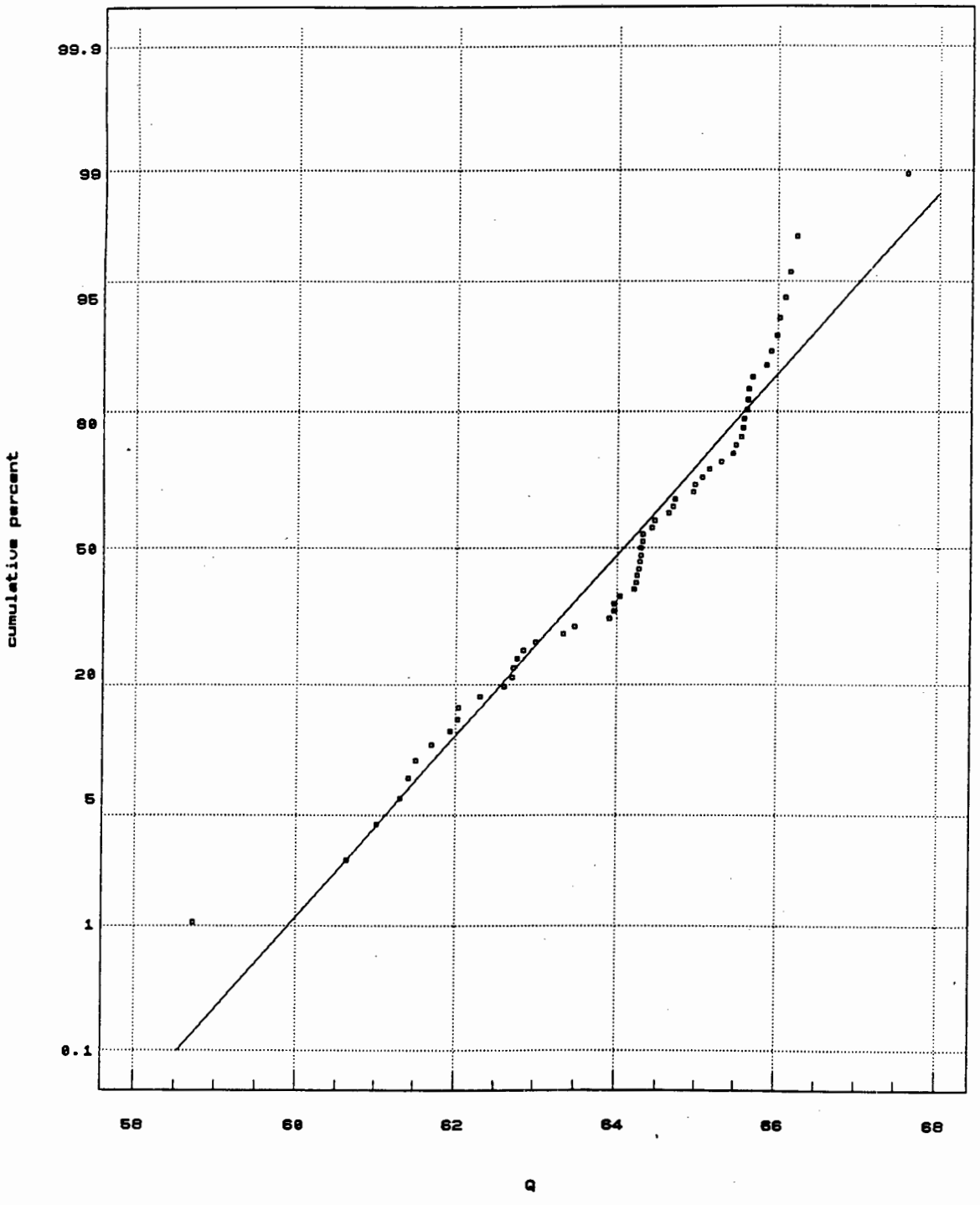

Figure C.1(a): Normal probability plot of the distribution of volumetric feed rates used during the factorial design

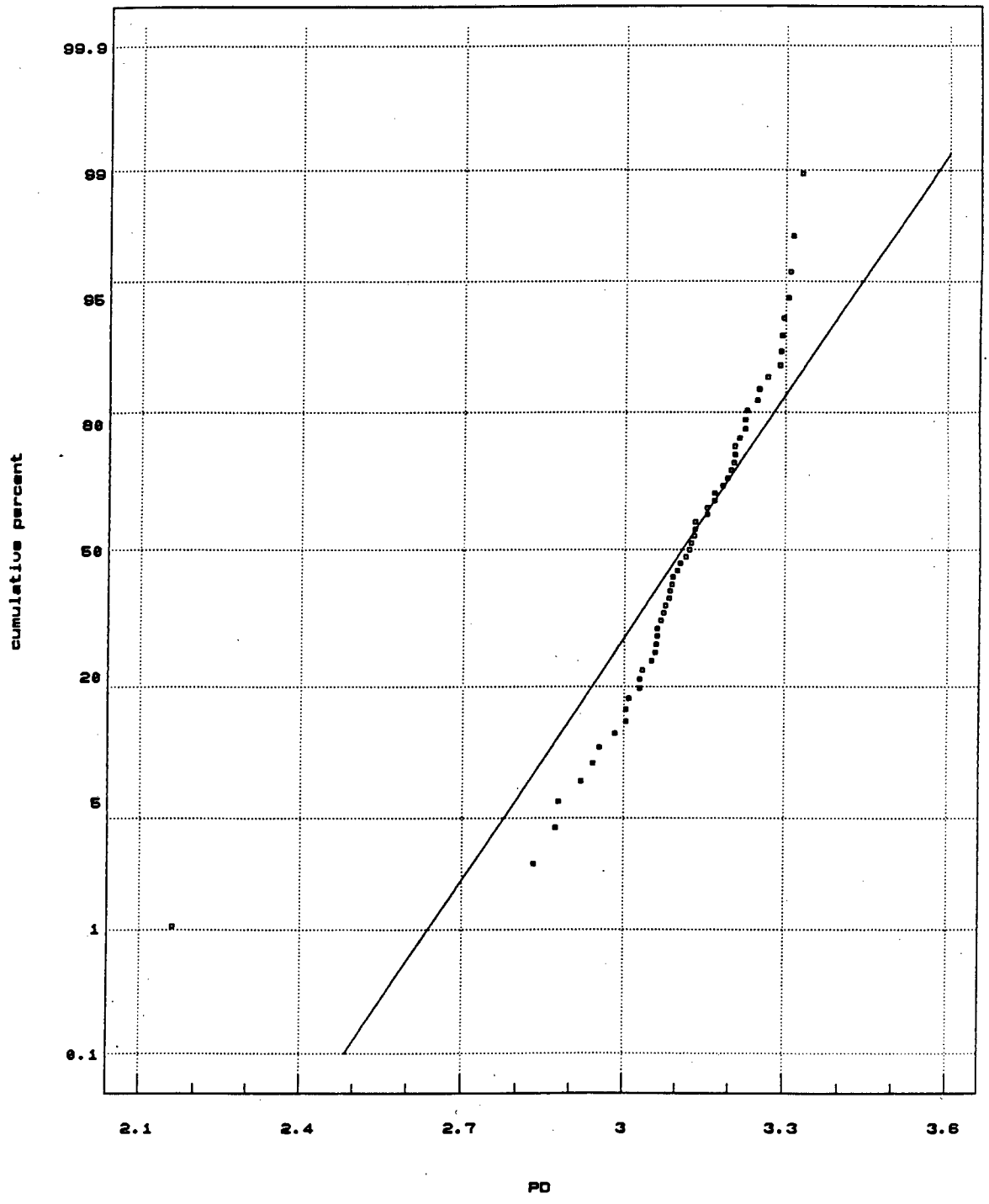

Figure C.1(b): Normal probability plot of the distribution of feed pulp densities used during the factorial design

The experimental results of these runs are listed in **Table C.x_i(a)** where x_i=2 for the *original factorial design* and x_i=3 for the *modified factorial design*. The calculated values indicating the performance of the ASH are listed in **Tables C.x_i(b)**. The data used in the statistical analysis of the factorial designs is given in **Tables C.x_i(c_1)** and **(c_2)**. The average response (yield, concentrate ash content, clean coal recovery and water recovery) values and their respective variances are listed in **Tables C.x_i(d)**. The main effect and interaction term contrasts for the responses are given in **Tables C.x_i(e_1)** and **(e_2)** respectively, and the *F*-ratios for the main effect and interaction term contrasts for the responses are given in **Tables C.x_i(f_1)** and **(f_2)** respectively.

The values listed in Tables C.x_i(a) and C.x_i(b) were taken from Tables C.1(a) and (b), respectively, omitting runs in which problems had been experienced. The problems encountered including blockages of the annular opening of the ASH, incorrect feed rate setting on the magnetic flowmetere, etc..

The values listed in Tables C.x_i(c_1) and (c_2) signify the following:

i) The **experimental condition** (j), in column 1, represents the 16 different sets of conditions tested during the factorial design.

ii) **Yield A** ($Y_{A,j}$), in column 2, is the concentrate yield of the replicates at the 16 (j) different sets of conditions (already listed in Tables C.x_i(a) and (b)); where replicates consisted of one or more duplicates and/or repeats, the values listed are the averages, e.g. run KKFD-B1 has yields of 1.11 % (1) and 1.25 % (2). The yield in Tables C.x_i(c_1) is $Y_{B,j}$=1.18 %

iv) The **concentrate ash** (Table C.x_i(c_1)) and **clean coal** and **water recoveries** (Table C.x_i(c_2)) are similarly defined, as in (i) above.

The values listed in Tables C.x_i(d) signify the following:

i) The **experimental condition** (j), in column 1, represents the 16 different sets of conditions tested during the factorial design.

ii) The **yield av** ($Y_{av,j}$), in column 3, represents the average concentrate yield achieved, in replicates A, B, C and D (where these exist), under the experimental conditions (j) and is calculated from the results in Tables C.x_i(c_1) as shown below:

$$Y_{av,j} = \frac{\sum_{a=A}^{a=D} Y_{a,j}}{\sum_{a=A}^{a=D} a}$$

iv) The **concentrate ash av** ($A_{av,j}$), in column 5, the **clean coal recovery av** ($R_{av,j}$), in column 7, and the **water recovery av** ($W_{av,j}$), in column 9, are similarly defined, as in (ii) above.

v) The **yield** s^2 ($Y_{s,j}$), in column 2, is the variance in the average results of replicates A, B, C and D (where these exist), under the experimental conditions (j) and is calculated as shown below:

$$Y_{s,j} = \sum_{a=A}^{a=D} (Y_{av,j} - Y_{av,j})^2$$

The **total yield** s^2 (Y_s) is the sum of the yield variances and is calculated as shown below:

$$Y_s = \sum_{j=1}^{j=16} Y_{s,j}$$

vi) The **concentrate ash** s^2 ($A_{s,j}$), in column 4, and **clean coal recovery** s^2 ($R_{s,j}$), in column 6, and the **water recovery** s^2 ($W_{s,j}$), in column 8, and the **total concentrate ash** s^2 (A_s), in column 4, etc. are similarly defined, as in (v) above.

vii) The **dof**, in columns 3, 5, 7 and 9 are calculated in the following way; if a run and a replicate of the run are carried out there is one degree of freedom (i.e. one estimate of the error). Therefore, the 16 runs and their replicates (32 runs at 16 sets of conditions) introduced 16 degrees of freedom; each of the

other 8 replicates added a further degree of freedom (a total of 40 replicates appear in Tables C.3(c_1) and (c_2)). Hence the error analysis carried out had 24 degrees of freedom#. However, as only 16 different sets of conditions were investigated, the degrees of freedom used to determine the effect of various parameters (i.e. to calculate the *F*-ratios) was 16.

viii) The **yield MSe** (Y_{MSe}), in column 3, is the yield mean square error and is an average "square of the error" in the yield for all the experimental conditions investigated. It is calculated as shown below:

$$Y_{MSe} = \frac{Y_s}{dof}$$

ix) The **concentrate ash MSe** (A_{MSe}), in column 5, **clean coal recovery MSe** (R_{MSe}), in column 7, and the **water recovery MSe** (W_{MSe}), in column 9 are similarly defined, as in (viii) above.

x) The **yield se** (Y_{se}), in column 3, is the yield mean error and is an average error in the yield for all the experimental conditions investigated. It is calculated as shown below:

$$Y_{se} = \sqrt{Y_{MSe}}$$

xi) The **concentrate ash se** (A_{se}), in column 5, **clean coal recovery se** (R_{se}), in column 7, and the **water recovery se** (W_{Se}), in column 9 are similarly defined, as in (x) above.

The values listed in Tables C.x_i(e_1) and (e_2) signify the following:

i) The **parameter**, in column 1, is the parameter (main effect or interactions) investigated at the upper (+) and lower (-) level values to determine its effect on the responses, i.e. the yield, concentrate ash, recovery and water recovery.

i) The **yield contrast lk** (Y_{lk}), in column 2, is the sum of the average yields of the runs carried out at the lower (-) parameter level value subtracted from the sum of the average yields at the

The modified factorial design had only 21 degrees of freedom as a result of 3 runs being excluded.

upper (+) parameter level value, and is calculated using the data from Tables C.x_i(d) as indicated below:

$$Y_{1k} = \sum_{j=1}^{j=16} Y_{av,j} k_i$$

where k_i=+1 if the parameter is at its high value (+)
k_i=-1 if the parameter is at its low value (-)

The values of k_i may be obtained from Tables 6.3 in Chapter Six.

ii) The **concentrate ash contrast 1k** (A_{1k}), in column 4, **clean coal recovery contrast 1k** (R_{1k}), in column 6, and the **water recovery contrast 1k** (W_{1k}), in column 8 are similarly defined, as in (i) above.

iii) The **yield contrast MS1k** (Y_{MS1k}), in column 3, is the mean square of the yield contrasts and is calculated as indicated below:

$$Y_{MS1k} = \frac{Y_{1k}^2}{n \sum_{i=1}^{i=16} k_i^2}$$

where k_i is as defined in (i) above
n= number of observations (runs) at each level, (+) and (-)

iv) The **concentrate ash contrast MS1k** (A_{MS1k}), in column 5, **clean coal recovery contrast MS1k** (R_{MS1k}), in column 7, and the **water recovery contrast MS1k** (W_{MS1k}), in column 9 are similarly defined, as in (iii) above.

The values listed in Tables C.x_i(f_1) and (f_2) signify the following:

i) The **yield *F*-ratio** (Y_F), in column 2, is the ratio of the mean square of the yield contrast (Y_{MS1k}) in Tables C.x_i(e_1) and (e_2) to the mean square of the yield error (Y_{MSe}) in Tables C.x_i(d), and is calculated as shown below:

$$Y_F = \frac{Y_{MS1k}}{Y_{MSe}}$$

iv) The **concentrate ash *F*-ratio** (A_F), in column 3, **clean coal recovery *F*-ratio** (R_F), in column 4, and the **water recovery *F*-ratio** (W_F), in column 5 are similarly defined, as in (iii) above.

C.1.2.1 original factorial design

Table C.2(a): Results obtained during the original factorial design (excluding runs with identified problems)

	sampling time (s)		wet sample mass (kg)		dry sample mass (g)		ash content (%)		
sample	of	uf	of	uf	of	uf	of	uf	feed
KKFD-A1	20	10	0.40	10.99	105.90	282.21	7.09	26.74	23.64
KKFD-B1 (1)	20	10	0.13	11.07	7.54	337.31	8.07	24.92	24.73
KKFD-B1 (2)	20	10	0.13	10.80	8.34	329.17	8.05	24.08	23.88
KKFD-C1	20	10	0.11	11.05	18.86	327.97	7.43	23.55	23.10
KKFD-A2	20	10	2.25	9.24	379.53	147.12	9.84	41.79	23.79
KKFD-B2	20	10	2.84	9.64	414.66	134.36	10.42	45.40	24.17
KKFD-B3	10	10	3.15	7.56	151.04	192.55	11.86	32.21	23.26
KKFD-C3	10	10	2.79	8.13	171.94	183.70	10.93	35.39	23.56
KKFD-A4 (1)	10	10	0.71	10.11	83.14	229.16	8.06	30.39	24.45
KKFD-A4 (2)	10	10	0.89	10.28	115.82	228.79	8.24	31.09	23.41
KKFD-B4	20	10	0.66	10.25	68.56	296.95	7.72	25.97	24.08
KKFD-C4	20	10	1.13	10.47	119.62	274.08	8.46	29.88	26.04
KKFD-D4 (1)	20	10	0.56	10.71	43.21	326.43	8.67	24.65	23.66
KKFD-D4 (2)	20	10	0.53	10.82	33.68	339.16	9.61	24.45	23.75
KKFD-A5 (1)	20	10	0.10	11.02	3.10	348.39	14.95	24.01	23.97
KKFD-A5 (2)	20	10	0.13	9.84	3.24	312.16	16.18	25.54	25.49
KKFD-B5	20	10	0.15	11.03	5.26	308.57	16.98	24.14	24.08
KKFD-B6	20	10	1.75	9.54	317.23	183.83	8.97	36.87	23.95
KKFD-C6	10	10	1.10	9.46	134.27	194.97	9.14	32.19	22.79
KKFD-D6	10	10	0.99	10.06	156.48	171.60	8.80	38.05	24.10
KKFD-B7 (1)	10	10	3.36	7.33	200.94	148.91	11.68	40.16	23.80
KKFD-B7 (2)	10	10	3.07	7.52	192.45	149.30	11.38	37.99	23.01
KKFD-D7	10	10	3.02	8.02	201.05	129.53	11.91	36.81	21.67
KKFD-A8 (1)	10	10	1.5	9.34	217.59	113.56	10.98	47.14	23.38
KKFD-A8 (2)	10	10	1.33	9.13	217.81	101.10	11.16	49.42	23.29
KKFD-C8	10	10	1.61	9.22	207.41	117.37	10.74	44.36	22.89
KKFD-A9 (1)	10	10	2.04	8.80	94.97	233.05	11.49	28.29	23.42
KKFD-A9 (2)	10	10	1.78	-	87.10	-	11.49	-	11.49
KKFD-B9	10	10	2.34	8.26	179.15	152.76	10.97	36.45	22.70
KKFD-D9	10	10	2.07	8.50	104.63	209.79	11.23	29.33	23.30
KKFD-A10 (1)	10	10	0.75	10.08	117.37	211.18	8.36	31.25	23.07
KKFD-A10 (2)	10	10	0.82	9.98	127.89	208.75	8.51	32.44	23.35
KKFD-B10	20	10	0.63	10.46	105.65	272.92	6.90	26.50	23.32
KKFD-C10	20	10	1.36	10.39	208.83	238.23	8.14	30.49	23.68
KKFD-D10	20	10	1.04	9.98	245.55	182.59	8.43	35.73	24.75
KKFD-A11 (1)	20	10	0.23	10.23	11.67	323.82	10.18	22.31	22.10
KKFD-B11	20	10	0.25	10.75	8.47	342.80	16.28	23.09	23.01
KKFD-A12	10	10	2.00	8.47	225.53	116.59	11.28	50.24	24.56
KKFD-B12	10	10	1.84	9.21	203.71	110.21	11.10	50.52	24.94
KKFD-A13 (1)	10	10	3.62	7.54	236.52	115.60	13.11	46.85	24.19
KKFD-A13 (2)	10	10	3.33	7.54	233.08	-	-	46.85	-
KKFD-B13	10	10	3.79	7.05	216.61	103.06	12.89	48.60	24.40
KKFD-A14 (1)	10	10	1.47	9.66	167.36	177.24	9.94	36.85	23.78
KKFD-A14 (2)	10	10	1.36	9.71	164.87	175.97	9.83	38.75	24.76
KKFD-B14	10	10	0.85	10.29	128.69	196.62	10.37	32.74	23.89
KKFD-C14	10	10	0.71	10.3	116.03	217.28	8.02	33.60	24.70
KKFD-A15	20	10	0.11	10.79	4.64	350.24	10.83	24.46	24.37
KKFD-B15	20	10	0.12	10.83	6.56	306.65	9.95	24.85	24.69
KKFD-A16	20	10	0.68	9.89	122.63	263.66	7.01	30.15	25.78
KKFD-B16	20	10	0.95	9.81	142.18	236.91	7.26	27.07	22.50

Table C.2(b): Calculated results obtained during the original factorial design (excluding runs with identified problems)

sample	coal yield (%)	coal recovery (%)	sep. coef.	water recovery (%)	slurry rate (l/min)	pulp density (%)
KKFD-A1	15.80	19.22	0.18	1.35	66.37	3.03
KKFD-B1 (1)	1.11	1.35	0.01	0.57	66.03	3.10
KKFD-B1 (2)	1.25	1.51	0.01	0.58	64.43	3.10
KKFD-C1	2.79	3.36	0.03	0.42	65.86	3.07
KKFD-A2	56.33	66.64	0.60	9.33	61.42	3.29
KKFD-B2	60.68	71.68	0.64	11.31	65.58	3.13
KKFD-B3	43.96	50.49	0.45	28.93	63.48	3.25
KKFD-C3	48.35	56.34	0.50	24.78	64.71	3.30
KKFD-A4 (1)	26.62	32.40	0.30	5.97	64.21	2.92
KKFD-A4 (2)	33.61	40.27	0.37	7.15	66.23	3.12
KKFD-B4	10.35	12.58	0.12	2.89	62.72	3.17
KKFD-C4	17.91	22.17	0.20	4.72	65.45	3.06
KKFD-D4 (1)	6.21	7.43	0.07	2.43	65.15	3.21
KKFD-D4 (2)	4.73	5.61	0.05	2.31	65.70	3.25
KKFD-A5 (1)	0.44	0.50	0.00	0.45	65.62	3.20
KKFD-A5 (2)	0.52	0.58	0.00	0.66	58.71	3.21
KKFD-B5	0.85	0.92	0.01	0.67	65.92	2.83
KKFD-B6	46.32	55.44	0.50	7.11	61.71	3.33
KKFD-C6	40.78	47.99	0.44	9.44	62.61	3.16
KKFD-D6	47.70	57.31	0.52	7.77	65.55	3.00
KKFD-B7 (1)	57.44	66.57	0.59	30.55	63.34	3.31
KKFD-B7 (2)	56.31	64.82	0.57	28.08	62.76	3.27
KKFD-D7	60.82	68.39	0.60	26.32	65.48	3.03
KKFD-A8 (1)	65.71	76.34	0.68	12.20	64.28	3.09
KKFD-A8 (2)	68.30	79.10	0.70	10.97	62.03	3.08
KKFD-C8	63.86	73.92	0.66	13.35	64.24	3.03
KKFD-A9 (1)	28.95	33.46	0.30	18.50	64.29	3.06
KKFD-A9 (2)	-	-	-	-	-	-
KKFD-B9	53.98	62.16	0.55	21.04	62.84	3.17
KKFD-D9	33.28	38.52	0.34	19.16	62.70	3.01
KKFD-A10 (1)	35.72	42.56	0.39	6.02	64.23	3.07
KKFD-A10 (2)	37.99	45.34	0.41	6.61	64.03	3.15
KKFD-B10	16.22	19.69	0.18	2.51	63.91	3.06
KKFD-C10	30.47	36.68	0.34	5.37	65.64	3.13
KKFD-D10	40.21	48.93	0.45	3.90	62.30	2.94
KKFD-A11 (1)	1.77	2.04	0.02	1.09	61.32	3.23
KKFD-B11	1.22	1.33	0.01	1.15	64.46	3.23
KKFD-A12	65.92	77.52	0.69	17.52	62.04	3.31
KKFD-B12	64.89	76.87	0.68	15.24	65.58	2.87
KKFD-A13 (1)	67.17	76.98	0.67	31.31	66.16	3.19
KKFD-A13 (2)	-	-	-	-	-	-
KKFD-B13	67.76	78.08	0.68	33.97	64.31	2.98
KKFD-A14 (1)	48.57	57.39	0.52	12.08	65.99	3.13
KKFD-A14 (2)	48.37	57.97	0.52	11.14	65.64	3.12
KKFD-B14	39.56	46.59	0.42	6.67	66.10	2.95
KKFD-C14	34.81	42.52	0.39	5.56	65.30	3.06
KKFD-A15	0.66	0.78	0.01	0.50	64.26	3.29
KKFD-B15	1.06	1.27	0.01	0.54	64.63	2.88
KKFD-A16	18.87	23.64	0.22	2.81	60.64	3.22
KKFD-B16	23.08	27.62	0.26	4.05	61.01	3.03

Table C.2(c_1): Yield and concentrate ash data used in original Kleinkopje factorial design analysis

experimental	yield				concentrate ash			
conditions	A	B	C	D	A	B	C	D
1	15.80	1.18	2.79		7.09	8.06	7.43	
2	56.33	60.68			9.84	10.42		
3		43.96	48.35			11.86	10.93	
4	30.29	10.35	17.91	5.46	8.15	7.72	8.46	9.14
5	0.48	0.85			15.57	16.98		
6		46.32	40.78	47.70		8.97	9.14	8.80
7		56.88		60.82		11.53		11.91
8	66.98		63.86		11.07		10.74	
9	28.08	53.98		33.28	11.49	10.97		11.23
10	36.87	16.22	30.47	40.21	8.44	6.90	8.14	8.43
11	1.77	1.22			10.18	16.28		
12	65.92	64.89			11.28	11.10		
13	67.01	67.76			13.11	12.89		
14	48.47	39.56	34.81		9.89	10.37	8.02	
15	0.66	1.06			10.83	9.95		
16	18.87	23.08			7.01	7.26		

Table C.2(c_2): Recovery and water recovery data used in Kleinkopje factorial design analysis

experimental	clean coal recovery				water recovery			
conditions	A	B	C	D	A	B	C	D
1	19.22	1.43	3.36		1.35	0.57	0.42	
2	66.64	71.68			9.33	11.31		
3		50.49	56.34			28.93	24.78	
4	36.55	12.58	22.17	6.50	6.56	2.89	4.72	2.37
5	0.92			0.55	0.67			
6		55.44	47.99	57.31		7.11	9.44	7.77
7		65.7		68.39		29.32		26.32
8	77.72		73.92		11.60		13.35	
9	32.53	62.16		38.52	17.51	21.04		19.16
10	43.97	19.69	36.68	48.93	6.32	2.51	5.37	3.90
11	2.04	1.33			1.09	1.15		
12	77.52	76.86			17.52	15.24		
13	76.85	78.08			30.38	33.97		
14	57.68	46.59	42.52		11.61	6.67	5.56	
15	0.78	1.27			0.50	0.54		
16	23.56	27.62			2.81	4.05		

Table C.2(d): Original Kleinkopje factorial design error analysis

experimental conditions	yield (%)		concentrate ash (%)		clean coal recovery (%)		water recovery (%)	
	s^2	av	s^2	av	s^2	av	s^2	av
1	128.53	6.59	0.48	7.53	190.58	8.00	0.50	0.78
2	9.46	58.51	0.17	10.13	12.70	69.16	1.96	10.32
3	9.64	46.16	0.43	11.40	17.11	53.42	8.61	26.86
4	350.87	16.00	1.07	8.37	514.71	19.45	10.89	4.14
5	0.07	0.67	0.99	16.28	0.07	0.73	0.01	0.61
6	26.83	44.93	0.06	8.97	48.62	53.58	2.88	8.11
7	7.76	58.85	0.07	11.72	3.62	67.05	4.50	27.82
8	4.87	65.42	0.05	10.91	7.22	75.82	1.53	12.48
9	375.45	38.45	0.14	11.23	490.89	44.40	6.24	19.24
10	338.00	30.94	1.61	7.98	490.24	37.32	8.39	4.53
11	0.15	1.50	18.61	13.23	0.25	1.69	0.00	1.12
12	0.53	65.41	0.02	11.19	0.22	77.19	2.60	16.38
13	0.28	67.39	0.02	13.00	0.76	77.47	6.44	32.18
14	96.18	40.95	3.08	9.43	123.13	48.93	20.75	7.95
15	0.08	0.86	0.39	10.39	0.12	1.03	0.00	0.52
16	8.86	20.98	0.03	7.14	8.24	25.59	0.77	3.43
total	1357.55		27.22		1908.48		76.07	
dof		24		24		24		24
MSe		56.56		1.13		79.52		3.17
se		7.52		1.06		8.92		1.78

Table C.2(e_1): Contrasts for original Kleinkopje factorial design main effects

	yield contrast		concentrate ash contrast		clean coal recovery contrast		water recovery contrast	
parameter	lk	MS lk	lk	MS lk	lk	MS lk	lk	MS lk
Ao/Au	164.72	211.97	-0.82	0.01	186.88	272.85	93.90	68.89
Lc/dc	-165.62	214.29	-5.39	0.23	-189.79	281.40	-41.60	13.52
Ainlet	22.52	3.96	3.58	0.10	24.37	4.64	-0.26	0.00
UF	237.73	441.54	0.67	0.00	274.89	590.34	112.21	98.37
Air	-91.81	65.84	6.16	0.30	-106.82	89.15	-27.20	5.78
Lvf/dc	69.23	37.44	13.02	1.32	80.54	50.67	12.25	1.17

Table C.2(e_2): Contrasts for original Kleinkopje factorial design interaction terms

	yield contrast		concentrate ash contrast		clean coal recovery contrast		water recovery contrast	
parameter	lk	MS lk	lk	MS lk	lk	MS lk	lk	MS lk
AB+CE+DF	-36.49	10.40	-6.775	0.36	-39.56	12.23	-9.73	0.74
AC+BE	-1.80	0.03	2.39	0.04	-3.51	0.10	2.01	0.03
AD+BF	-122.68	117.59	20.67	3.34	-153.27	183.52	41.80	13.65
AE+BC	-19.51	2.97	-11.23	0.98	-21.56	3.63	-6.59	0.34
AF+BD	-33.65	8.85	-9.23	0.67	-37.96	11.26	-16.54	2.14
CD+EF	13.25	1.37	0.20	0.00	18.37	2.64	-9.04	0.64
CF+DE	-2.40	0.04	-14.84	1.72	-4.08	0.13	-18.22	2.59
ACD+BDE+BCF+AEF	-30.67	7.35	-1.71	0.02	-33.60	8.82	-5.77	0.26
ACF+BEF+BCD+ADE	48.74	18.56	14.13	1.56	54.73	23.40	4.11	0.13

Table C.2(f_1): F-Ratios for original Kleinkopje factorial design main effects

parameter	yield F-ratio	concentrate ash F-ratio	clean coal recovery F-ratio	water recovery F-ratio
Ao/Au	3.75	0.00	3.43	21.73
Lc/dc	3.79	0.20	3.54	4.27
Ainlet	0.07	0.09	0.06	0.00
UF	7.81	0.00	7.42	31.04
Air	1.16	0.26	1.12	1.82
Lvf/dc	0.66	1.17	0.64	0.37

Table C.2(f_2): F-Ratios for original Kleinkopje factorial design interaction terms

parameter	yield F-ratio	concentrate ash F-ratio	clean coal recovery F-ratio	water recovery F-ratio
AB+CE+DF	0.18	0.32	0.15	0.23
AC+BE	0.00	0.04	0.00	0.01
AD+BF	2.08	2.94	2.31	4.31
AE+BC	0.05	0.87	0.05	0.11
AF+BD	0.16	0.59	0.14	0.67
CD+EF	0.02	0.00	0.03	0.20
CF+DE	0.00	1.52	0.00	0.82
ACD+BDE+BCF+AEF	0.13	0.02	0.11	0.08
ACF+BEF+BCD+ADE	0.33	1.37	0.29	0.04

C.1.2.2 modified factorial design

Table C.3(a): Results used during the modified factorial design

	sampling time (s)		wet sample mass (kg)		dry sample mass (g)		ash content (%)		
sample	of	uf	of	uf	of	uf	of	uf	feed
KKFD-B1 (1)	20	10	0.13	11.07	7.54	337.31	8.07	24.92	24.73
KKFD-B1 (2)	20	10	0.13	10.80	8.34	329.17	8.05	24.08	23.88
KKFD-C1	20	10	0.11	11.05	18.86	327.97	7.43	23.55	23.10
KKFD-A2	20	10	2.25	9.24	379.53	147.12	9.84	41.79	23.79
KKFD-B2	20	10	2.84	9.64	414.66	134.36	10.42	45.40	24.17
KKFD-B3	10	10	3.15	7.56	151.04	192.55	11.86	32.21	23.26
KKFD-C3	10	10	2.79	8.13	171.94	183.70	10.93	35.39	23.56
KKFD-A4 (1)	10	10	0.71	10.11	83.14	229.16	8.06	30.39	24.45
KKFD-A4 (2)	10	10	0.89	10.28	115.82	228.79	8.24	31.09	23.41
KKFD-B4	20	10	0.66	10.25	68.56	296.95	7.72	25.97	24.08
KKFD-C4	20	10	1.13	10.47	119.62	274.08	8.46	29.88	26.04
KKFD-D4 (1)	20	10	0.56	10.71	43.21	326.43	8.67	24.65	23.66
KKFD-D4 (2)	20	10	0.53	10.82	33.68	339.16	9.61	24.45	23.75
KKFD-A5 (1)	20	10	0.10	11.02	3.10	348.39	14.95	24.01	23.97
KKFD-A5 (2)	20	10	0.13	9.84	3.24	312.16	16.18	25.54	25.49
KKFD-B5	20	10	0.15	11.03	5.26	308.57	16.98	24.14	24.08
KKFD-B6	20	10	1.75	9.54	317.23	183.83	8.97	36.87	23.95
KKFD-C6	10	10	1.10	9.46	134.27	194.97	9.14	32.19	22.79
KKFD-D6	10	10	0.99	10.06	156.48	171.60	8.80	38.05	24.10
KKFD-B7 (1)	10	10	3.36	7.33	200.94	148.91	11.68	40.16	23.80
KKFD-B7 (2)	10	10	3.07	7.52	192.45	149.30	11.38	37.99	23.01
KKFD-D7	10	10	3.02	8.02	201.05	129.53	11.91	36.81	21.67
KKFD-A8 (1)	10	10	1.50	9.34	217.59	113.56	10.98	47.14	23.38
KKFD-A8 (2)	10	10	1.33	9.13	217.81	101.10	11.16	49.42	23.29
KKFD-C8	10	10	1.61	9.22	207.41	117.37	10.74	44.36	22.89
KKFD-A9 (1)	10	10	2.04	8.80	94.97	233.05	11.49	28.29	23.43
KKFD-A9 (2)	10	10	1.78	-	87.10	-	11.49	-	11.49
KKFD-D9	10	10	2.07	8.50	104.63	209.79	11.23	29.33	23.31
KKFD-A10 (1)	10	10	0.75	10.08	117.37	211.18	8.36	31.25	23.07
KKFD-A10 (2)	10	10	0.82	9.98	127.89	208.75	8.51	32.44	23.35
KKFD-C10	20	10	1.36	10.39	208.83	238.23	8.14	30.49	23.68
KKFD-D10	20	10	1.04	9.98	245.55	182.59	8.43	35.73	24.75
KKFD-A11 (1)	20	10	0.23	10.23	11.67	323.82	10.18	22.31	22.10
KKFD-B11	20	10	0.25	10.75	8.47	342.80	16.28	23.09	23.01
KKFD-A12	10	10	2.00	8.47	225.53	116.59	11.28	50.24	24.56
KKFD-B12	10	10	1.84	9.21	203.71	110.21	11.10	50.52	24.94
KKFD-A13 (1)	10	10	3.62	7.54	236.52	115.60	13.11	46.85	24.19
KKFD-A13 (2)	10	10	3.33	7.54	233.08	-	-	46.85	-
KKFD-B13	10	10	3.79	7.05	216.61	103.06	12.89	48.60	24.40
KKFD-A14 (1)	10	10	1.47	9.66	167.36	177.24	9.94	36.85	23.78
KKFD-A14 (2)	10	10	1.36	9.71	164.87	175.97	9.83	38.75	24.76
KKFD-B14	10	10	0.85	10.29	128.69	196.62	10.37	32.74	23.89
KKFD-C14	10	10	0.71	10.30	116.03	217.28	8.02	33.60	24.70
KKFD-A15	20	10	0.11	10.79	4.64	350.24	10.83	24.46	24.37
KKFD-B15	20	10	0.12	10.83	6.56	306.65	9.95	24.85	24.69
KKFD-A16	20	10	0.68	9.89	122.63	263.66	7.01	30.15	25.78
KKFD-B16	20	10	0.95	9.81	142.18	236.91	7.26	27.07	22.50

Table C.3(b): Calculated results obtained from the modified factorial design

sample	coal yield (%)	coal recovery (%)	sep. coef.	water recovery (%)	slurry rate (l/min)	pulp density (%)
KKFD-B1 (1)	1.11	1.35	0.01	0.57	66.03	3.10
KKFD-B1 (2)	1.25	1.51	0.01	0.58	64.43	3.10
KKFD-C1	2.80	3.36	0.03	0.42	65.86	3.07
KKFD-A2	56.33	66.64	0.60	9.33	61.42	3.29
KKFD-B2	60.68	71.68	0.64	11.31	65.58	3.13
KKFD-B3	43.96	50.49	0.45	28.93	63.48	3.25
KKFD-C3	48.35	56.34	0.50	24.78	64.71	3.30
KKFD-A4 (1)	26.62	32.40	0.30	5.97	64.21	2.92
KKFD-A4 (2)	33.61	40.27	0.37	7.15	66.23	3.12
KKFD-84	10.35	12.58	0.12	2.89	62.72	3.17
KKFD-C4	17.91	22.17	0.20	4.72	65.45	3.06
KKFD-D4 (1)	6.21	7.43	0.07	2.43	65.15	3.21
KKFD-D4 (2)	4.73	5.61	0.05	2.31	65.70	3.25
KKFD-A5 (1)	0.44	0.50	0.00	0.45	65.62	3.20
KKFD-A5 (2)	0.52	0.58	0.00	0.66	58.71	3.21
KKFD-B5	0.85	0.92	0.01	0.67	65.92	2.83
KKFD-B6	46.32	55.44	0.50	7.11	61.71	3.33
KKFD-C6	40.78	47.99	0.44	9.44	62.61	3.166
KKFD-D6	47.70	57.31	0.52	7.77	65.55	3.00
KKFD-B7 (1)	57.44	66.57	0.59	30.55	63.34	3.31
KKFD-B7 (2)	56.31	64.82	0.57	28.08	62.76	3.27
KKFD-D7	60.82	68.39	0.60	26.32	65.48	3.03
KKFD-A8 (1)	65.71	76.34	0.68	12.20	64.28	3.09
KKFD-A8 (2)	68.30	79.10	0.70	10.97	62.03	3.08
KKFD-C8	63.86	73.92	0.66	13.35	64.24	3.03
KKFD-A9 (1)	28.95	33.47	0.30	18.50	64.29	3.06
KKFD-A9 (2)	-	-	-	-	-	-
KKFD-D9	33.28	38.52	0.34	19.16	62.70	3.01
KKFD-A10 (1)	35.72	42.56	0.39	6.02	64.23	3.07
KKFD-A10 (2)	37.99	45.34	0.41	6.61	64.03	3.15
KKFD-C10	30.47	36.68	0.34	5.37	65.64	3.13
KKFD-D10	40.21	48.93	0.45	3.90	62.30	2.94
KKFD-A11 (1)	1.77	2.04	0.02	1.09	61.32	3.23
KKFD-B11	1.22	1.33	0.011	1.15	64.46	3.23
KKFD-A12	65.92	77.52	0.69	17.52	62.04	3.31
KKFD-B12	64.90	76.86	0.68	15.24	65.58	2.87
KKFD-A13 (1)	67.17	76.98	0.67	31.31	66.16	3.19
KKFD-A13 (2)	-	-	-	-	-	-
KKFD-B13	67.76	78.08	0.68	33.97	64.31	2.98
KKFD-A14 (1)	48.57	57.39	0.52	12.08	65.99	3.13
KKFD-A14 (2)	48.37	57.97	0.52	11.14	65.64	3.12
KKFD-B14	39.56	46.59	0.42	6.67	66.10	2.95
KKFD-C14	34.81	42.52	0.39	5.56	65.30	3.06
KKFD-A15	0.66	0.78	0.01	0.50	64.26	3.29
KKFD-B15	1.06	1.27	0.01	0.54	64.63	2.88
KKFD-A16	18.87	23.64	0.22	2.81	60.64	3.22
KKFD-B16	23.08	27.62	0.26	4.05	61.01	3.03

Table C.3(c_1): Yield and concentrate ash data used in modified Kleinkopje factorial design analysis

experimental	yield				concentrate ash			
conditions	A	B	C	D	A	B	C	D
1		1.18	2.79			8.06	7.43	
2	56.33	60.68			9.84	10.42		
3		43.96	48.35			11.86	10.93	
4	30.29	10.35	17.91	5.46	8.15	7.72	8.46	9.14
5	0.48	0.85			15.57	16.98		
6		46.32	40.78	47.70		8.97	9.14	8.80
7		56.88		60.82		11.53		11.91
8	66.98		63.86		11.07		10.74	
9	28.08			33.28	11.49			11.23
10	36.87		30.47	40.21	8.44		8.14	8.43
11	1.77	1.22			10.18	16.28		
12	65.92	64.89			11.28	11.10		
13	67.01	67.76			13.11	12.89		
14	48.47	39.56	34.81		9.89	10.37	8.02	
15	0.66	1.06			10.83	9.95		
16	18.87	23.08			7.01	7.26		

Table C.3(c_2): Recovery and water recovery data used in modified Kleinkopje factorial design analysis

experimental	clean coal recovery				water recovery			
conditions	A	B	C	D	A	B	C	D
1		1.43	3.36			0.57	0.42	
2	66.64	71.68			9.33	11.31		
3		50.49	56.34			28.93	24.78	
4	36.55	12.58	22.17	6.5	6.56	2.89	4.72	2.37
5	0.54	0.92			0.55	0.67		
6		55.44	47.99	57.31		7.11	9.44	7.77
7		65.7		68.39		29.32		26.32
8	77.72		73.92		11.60		13.35	
9	32.53			38.52	17.51			19.16
10	43.97		36.68	48.93	6.32		5.37	3.90
11	2.04	1.33			1.09	1.15		
12	77.52	76.86			17.52	15.24		
13	76.85	78.08			30.38	33.97		
14	57.68	46.59	42.52		11.61	6.67	5.56	
15	0.78	1.27			0.50	0.54		
16	23.56	27.62			2.81	4.05		

Table C.3(d): Modified Kleinkopje factorial design error analysis

experimental conditions	yield (%)		concentrate ash (%)		clean coal recovery (%)		water recovery (%)	
	s^2	av	s^2	av	s^2	av	s^2	av
1	1.30	1.99	0.20	7.75	1.86	2.40	0.01	0.50
2	9.46	58.51	0.17	10.13	12.70	69.16	1.96	10.32
3	9.64	46.16	0.43	11.40	17.11	53.42	8.61	26.86
4	350.87	16.00	1.07	8.37	514.71	19.45	10.89	4.14
5	0.07	0.67	0.99	16.28	0.07	0.73	0.01	0.61
6	26.83	44.93	0.06	8.97	48.62	53.58	2.88	8.11
7	7.76	58.85	0.07	11.72	3.62	67.05	4.50	27.82
8	4.87	65.42	0.05	10.91	7.22	75.82	1.53	12.48
9	13.52	30.68	0.03	11.36	17.94	35.53	1.36	18.34
10	49.00	35.85	0.06	8.34	75.94	43.19	2.97	5.20
11	0.15	1.50	18.61	13.23	0.25	1.69	0.00	1.12
12	0.53	65.41	0.02	11.19	0.22	77.19	2.60	16.38
13	0.28	67.39	0.02	13.00	0.76	77.47	6.44	32.18
14	96.18	40.95	3.08	9.43	123.13	48.93	20.75	7.95
15	0.08	0.86	0.39	10.39	0.12	1.03	0.00	0.52
16	8.86	20.98	0.03	7.14	8.24	25.59	0.77	3.43
total	579.39		25.29		832.50		65.29	
dof		21		21		21		21
MSe		27.59		1.20		39.64		3.11
se		5.25		1.10		6.30		1.76

Table C.3(e_1): Contrasts for modified Kleinkopje factorial design main effects

	yield contrast		concentrate ash contrast		clean coal recovery contrast		water recovery contrast	
parameter	lk	MSlk	lk	MSlk	lk	MSlk	lk	MSlk
Ao/Au	166.47	216.49	-0.55	0.00	189.49	280.51	93.96	68.97
Lc/dc	-163.87	209.79	-5.12	0.20	-187.18	273.73	-41.54	13.48
Ainlet	14.45	1.63	3.13	0.08	15.22	1.81	-1.55	0.02
UF	229.66	412.08	0.22	0.00	265.74	551.71	110.92	96.12
Air	-99.87	77.93	5.72	0.25	-115.97	105.07	-28.49	6.34
Lvf/dc	61.16	29.22	12.57	1.23	71.39	39.82	10.96	0.94

Table C.3(e_2): Contrasts for modified Kleinkopje factorial design interaction terms

	yield contrast		concentrate ash contrast		clean coal recovery contrast		water recovery contrast	
parameter	lk	MSlk	lk	MSlk	lk	MSlk	lk	MSlk
AB+CE+DF	-43.96	15.10	-6.07	0.29	-48.17	18.13	-10.25	0.82
AC+BE	-19.08	2.84	2.38	0.04	-23.87	4.45	0.15	0.00
AD+BF	-139.96	153.04	20.65	3.33	-173.63	235.52	39.94	12.46
AE+BC	-36.79	10.57	-11.24	0.99	-41.92	13.73	-8.44	0.56
AF+BD	-50.93	20.27	-9.24	0.67	-58.32	26.57	-18.39	2.64
CD+EF	5.79	0.26	0.91	0.01	9.76	0.74	-9.55	0.71
CF+DE	-9.86	0.76	-14.13	1.56	-12.69	1.26	-18.74	2.74
ACD+BDE+BCF+AEF	-28.92	6.53	-1.44	0.02	-30.99	7.50	-5.71	0.26
ACF+BEF+BCD+ADE	50.48	19.91	14.40	1.62	57.34	25.69	4.17	0.14

Table C.3(f_1): F-Ratios for modified Kleinkopje factorial design main effects

parameter	yield F-ratio	concentrate ash F-ratio	clean coal recovery F-ratio	water recovery F-ratio
Ao/Au	7.85	0.00	7.08	22.18
Lc/dc	7.60	0.17	6.90	4.34
Ainlet	0.06	0.06	0.05	0.01
UF	14.94	0.00	13.92	30.92
Air	2.82	0.21	2.65	2.04
Lvf/dc	1.06	1.02	1.00	0.30

Table C.3(f_2): F-Ratios for modified Kleinkopje factorial design interaction terms

parameter	yield F-ratio	concentrate ash F-ratio	clean coal recovery F-ratio	water recovery F-ratio
AB+CE+DF	0.55	0.24	0.46	0.26
AC+BE	0.10	0.04	0.11	0.00
AD+BF	5.55	2.77	5.94	4.01
AE+BC	0.38	0.82	0.35	0.18
AF+BD	0.73	0.55	0.67	0.85
CD+EF	0.01	0.01	0.02	0.23
CF+DE	0.03	1.30	0.03	0.88
ACD+BDE+BCF+AEF	0.24	0.01	0.19	0.08
ACF+BEF+BCD+ADE	0.72	1.34	0.65	0.04

C.2 Kleinkopje Pulp Density / Air Rate Investigation

C.2.1 Pulp density/air rate investigation results

A total of 12 pulp density/air rate investigation runs, at 4 pulp densities and 3 air rates were carried out. The experimental results are listed in **Table C.4(a)** and the calculated values indicating the performance of the ASH are listed in **Table C.4(b)**.

The calculated values listed in Tables C.4(a) and C.4(b) were obtained in the same way as those for Tables B.4.x_k(a) and B.4.x_k(b), respectively (see Appendix B). The calculations used are detailed in Section B.4 of Appendix B.

Table C.4(a): Results obtained during the pulp density/air rate investigation

	sampling time (s)		wet sample mass (kg)		dry sample mass (g)		ash content (%)		
sample	of	uf	of	uf	of	uf	of	uf	feed
KKPD-1a	10	10	3.85	7.01	564.06	407.77	13.01	39.23	24.01
KKPD-1b	10	10	2.78	7.29	617.06	309.21	12.48	46.05	23.69
KKPD-1c	10	10	2.03	8.86	544.84	441.91	11.33	37.54	23.07
KKPD-2a	10	10	3.49	7.62	341.96	230.46	13.09	40.52	24.13
KKPD-2b	10	10	3.26	8.19	375.66	209.76	12.59	45.69	24.45
KKPD-2c	10	10	1.99	8.87	322.36	262.46	11.45	38.50	23.59
KKPD-3a	10	10	3.14	6.96	209.06	120.66	13.19	42.41	23.88
KKPD-3b	10	10	3.22	8.05	221.56	122.66	12.65	43.64	23.69
KKPD-3c	10	10	1.99	8.66	193.76	150.26	11.53	36.79	22.56
KKPD-4a	10	10	3.52	7.17	103.56	67.16	12.97	38.63	23.06
KKPD-4b	10	10	2.94	7.82	105.86	64.46	12.39	39.36	22.60
KKPD-4c	10	10	2.17	8.97	98.86	78.86	11.39	36.30	22.44

Table C.4(b): Calculated results obtained during the pulp density/air rate investigation

sample	coal yield (%)	coal recovery (%)	sep. coef.	water recovery (%)	slurry rate (l/min)	pulp density (%)
KKPD-1a	58.04	66.44	0.58	33.21	62.92	9.27
KKPD-1b	66.62	76.40	0.67	23.69	58.35	9.53
KKPD-1c	55.22	63.64	0.56	14.99	63.09	9.38
KKPD-2a	59.74	68.44	0.59	29.89	65.39	5.25
KKPD-2b	64.17	74.24	0.65	26.53	67.34	5.22
KKPD-2c	55.12	63.88	0.57	16.26	63.87	5.49
KKPD-3a	63.41	72.31	0.63	29.98	59.85	3.31
KKPD-3b	64.37	73.68	0.64	27.46	66.83	3.09
KKPD-3c	56.32	64.35	0.57	17.46	63.15	3.27
KKPD-4a	60.66	68.62	0.60	32.44	63.75	1.61
KKPD-4b	62.15	70.35	0.62	26.74	64.18	1.59
KKPD-4c	55.63	63.55	0.56	18.91	66.43	1.61

C.2.2 Repeat and duplicate run error analysis

The error analysis carried out below makes use of the duplicate and repeat runs carried out during the factorial design investigation (Section C.1 above). This was done to determine the error between duplicates and repeats, i.e. the errors involved when the ASH was not dissembled and then reassembled. This was the case when the pulp density/air rate investigation was carried out.

The experimental results of these runs are listed in **Table C.5(a)** below. The calculated values indicating the performance of the ASH are listed in **Table C.5(b)**. The data used in the statistical analysis of the errors between duplicate and repeat runs is given in **Tables C.5(c_1)** and **(c_2)**. The average response (yield, concentrate ash content, coal recovery and water recovery) values and their respective variances are listed in **Table C.5(d)**.

The values listed in Tables C.5(a) and C.5(b) were obtained from Tables 4(a) and (b), respectively. The values listed in Tables C.4(c_1) and (c_2) and Table C.5(d) were calculated in the same way as those for Tables C.x_k(c_1) and (c_2) and C.x_k(d), above, respectively.

Table C.5(a): Results of factorial design repeat and duplicate runs used in the pulp density/air rate investigation error analysis

	sampling time (s)		wet sample mass (kg)		dry sample mass (g)		ash content (%)		
sample	of	uf	of	uf	of	uf	of	uf	feed
KKFD-B1 (1)	20	10	0.13	11.07	7.54	337.31	8.07	24.92	24.73
KKFD-B1 (2)	20	10	0.13	10.80	8.34	329.17	8.05	24.08	23.88
KKFD-A3 (2)	10	10	1.69	9.10	135.36	206.48	10.08	31.56	23.05
KKFD-A3 (3)	10	10	1.45	9.39	133.69	201.73	9.78	32.08	23.19
KKFD-A4 (1)	10	10	0.71	10.11	83.14	229.16	8.06	30.39	24.45
KKFD-A4 (2)	10	10	0.89	10.28	115.82	228.79	8.24	31.09	23.41
KKFD-D4 (1)	20	10	0.56	10.71	43.21	326.43	8.67	24.65	23.66
KKFD-D4 (2)	20	10	0.53	10.82	33.68	339.16	9.61	24.45	23.75
KKFD-A7 (1)	10	10	2.45	7.93	159.34	179.58	10.63	35.39	23.75
KKFD-A7 (2)	10	10	2.88	7.75	175.57	170.26	11.28	39.26	25.06
KKFD-B7 (1)	10	10	3.36	7.33	200.94	148.91	11.68	40.16	23.80
KKFD-B7 (2)	10	10	3.07	7.52	192.45	149.30	11.38	37.99	23.01
KKFD-C7 (1)	10	10	2.09	8.88	200.12	133.50	10.73	45.54	24.66
KKFD-C7 (2)	10	10	2.20	8.75	203.55	126.83	10.90	45.46	24.17
KKFD-A8 (1)	10	10	1.50	9.34	217.59	113.56	10.98	47.14	23.38
KKFD-A8 (2)	10	10	1.33	9.13	217.81	101.10	11.16	49.42	23.29
KKFD-A10 (1)	10	10	0.75	10.08	117.37	211.18	8.36	31.25	23.07
KKFD-A10 (2)	10	10	0.82	9.98	127.89	208.75	8.51	32.44	23.35
KKFD-A14 (1)	10	10	1.47	9.66	167.36	177.24	9.94	36.85	23.78
KKFD-A14 (2)	10	10	1.36	9.71	164.87	175.97	9.83	38.75	24.76

Table C.5(b): Calculated results obtained during the pulp density/air rate investigation

sample	coal yield (%)	coal recovery (%)	sep. coef.	water recovery (%)	slurry rate (l/min)	pulp density (%)
KKFD-B1 (1)	1.11	1.35	0.01	0.57	66.03	3.10
KKFD-B1 (2)	1.25	1.51	0.01	0.58	64.43	3.10
KKFD-A3 (2)	39.60	46.27	0.42	14.88	63.96	3.21
KKFD-A3 (3)	39.86	46.82	0.42	12.53	64.27	3.13
KKFD-A4 (1)	26.62	32.40	0.30	5.97	64.21	2.92
KKFD-A4 (2)	33.61	40.27	0.37	7.15	66.23	3.12
KKFD-D4 (1)	6.21	7.43	0.07	2.43	65.15	3.21
KKFD-D4 (2)	4.73	5.61	0.05	2.31	65.70	3.25
KKFD-A7 (1)	47.01	55.10	0.49	22.81	61.51	3.31
KKFD-A7 (2)	50.77	60.10	0.53	26.30	62.99	3.29
KKFD-B7 (1)	57.44	66.57	0.59	30.55	63.34	3.31
KKFD-B7 (2)	56.31	64.82	0.57	28.08	62.76	3.27
KKFD-C7 (1)	59.98	71.07	0.63	17.77	65.06	3.08
KKFD-C7 (2)	61.61	72.39	0.64	18.80	64.95	3.05
KKFD-A8 (1)	65.71	76.34	0.68	12.20	64.28	3.09
KKFD-A8 (2)	68.30	79.10	0.70	10.97	62.03	3.08
KKFD-A10 (1)	35.72	42.56	0.39	6.02	64.23	3.07
KKFD-A10 (2)	37.99	45.34	0.41	6.61	64.03	3.15
KKFD-A14 (1)	48.57	57.39	0.52	12.08	65.99	3.13
KKFD-A14 (2)	48.37	57.97	0.52	11.14	65.64	3.12

Table C.5(c_1): Yield and concentrate ash data used in pulp density/air rate investigation error analysis

run	yield			concentrate ash		
number	1	2	3	1	2	3
B1	1.11	1.25		8.07	8.05	
A3		39.60	39.86		10.08	9.78
A4	26.62	33.61		8.06	8.24	
D4	6.21	4.73		8.67	9.61	
A7	47.01	50.77		10.63	11.28	
B7	57.44	56.31		11.68	11.38	
C7	59.98	61.61		10.73	10.90	
A8	65.71	68.30		10.98	11.16	
A10	35.72	37.99		8.36	8.51	
A14	48.57	48.37		9.94	9.83	

Table C.5(c_2): Recovery and water recovery data used in pulp density/air rate investigation error analysis

run	clean coal recovery			water recovery		
number	1	2	3	1	2	3
B1	1.35	1.51		0.57	0.58	
A3		46.27	46.82		14.88	12.53
A4	32.40	40.27		5.97	7.15	
D4	7.43	5.61		2.43	2.31	
A7	55.10	60.10		22.81	26.30	
B7	66.57	64.82		30.55	28.08	
C7	71.07	72.39		17.77	18.80	
A8	76.34	79.10		12.20	10.97	
A10	42.56	45.34		6.02	6.61	
A14	57.39	57.97		12.08	11.14	

Table C.5(d): Pulp density/air rate investigation error analysis

run number	yield (%)		concentrate ash (%)		clean coal recovery (%)		water recovery (%)	
	s^2	av	s^2	av	s^2	av	s^2	av
B1	0.01	1.18	0.00	8.06	0.01	1.43	0.00	0.50
A3	0.03	39.73	0.05	9.93	0.15	46.55	2.76	13.71
A4	24.43	30.12	0.02	8.15	30.97	36.34	0.70	6.56
D4	1.10	5.47	0.44	9.14	1.66	6.52	0.01	2.37
A7	7.07	48.89	0.21	10.96	12.50	57.60	6.09	24.56
B7	0.64	56.88	0.04	11.53	1.53	65.70	3.05	29.32
C7	1.33	60.80	0.01	10.82	0.87	71.73	0.53	18.29
A8	3.35	67.01	0.02	11.07	3.81	77.72	0.76	11.59
A10	2.58	36.86	0.01	8.44	3.86	43.95	0.17	6.32
A14	0.02	48.47	0.01	9.89	0.17	57.68	0.44	11.61
total	40.56		1.00		122.75		14.52	
dof		10		10		10		10
MSe		4.06		0.10		12.28		1.45
se		2.01		0.32		3.50		1.21

C.3 Kleinkopje Collector Dosage Investigation

A total of seven runs were carried out during the collector dosage investigation, at collector dosages ranging from 1.0 to 35.0 kg/ton. In addition size analyses were carried out on the flotation concentrate and tails samples from selected runs (KKCD1, KKCD4 and KKCD6).

The results of the collector dosage experiments carried out are listed in **Table C.6(a)**. The calculated values indicating the performance of the ASH are listed in **Table C.6(b)**. The results of size analyses carried out on particular runs, and the calculated reconstituted feed and concentrate yield in each size fraction are listed in **Tables C.7(a), (b)** and **(c)**.

The values listed in Tables C.6(a) and (b) were obtained in the same way as those for Tables B.4.x_k(a) and (b), respectively (see Appendix B). The calculations used are detailed in Section B.4 of Appendix B.

The values listed in each Tables C.7(a), (b) and (c) were obtained in the same way as those for Tables B.2.x_k(b) and B.4.3(d) and (f) (see Appendix B). The calculations used are detailed in Sections B.2 and B.4 of Appendix B.

Table C.6(a): Results obtained during the collector dosage investigation

	sampling time (s)		wet sample mass (kg)		dry sample mass (g)		ash content (%)		
sample	of	uf	of	uf	of	uf	of	uf	feed
KKCD1	10	10	2.99	7.66	51.65	290.43	18.07	26.70	25.40
KKCD2	10	10	3.10	7.61	94.78	250.20	14.01	28.69	24.66
KKCD3	10	10	3.24	7.42	131.69	209.88	13.21	31.92	24.71
KKCD4	10	10	3.41	7.07	174.35	149.83	12.81	39.44	25.12
KKCD5	10	10	3.44	7.09	195.00	123.07	12.95	43.33	24.70
KKCD6	10	10	3.71	7.02	224.84	94.58	12.92	50.44	24.03
KKCD7	10	10	3.81	7.09	243.55	85.64	12.81	54.44	23.64

Table C.6(b): Calculated results obtained during the collector dosage investigation

sample	coal yield (%)	coal recovery (%)	sep. coef.	water recovery (%)	slurry rate (l/min)	pulp density (%)
KCD1	15.10	16.58	0.14	28.51	63.12	3.25
KCD2	27.47	31.36	0.27	28.99	63.47	3.26
KCD3	38.55	44.44	0.39	30.12	63.18	3.24
KCD4	53.78	62.62	0.55	31.86	62.14	3.13
KCD5	61.31	70.88	0.62	31.78	62.45	3.06
KCD6	70.39	80.68	0.70	33.48	63.65	3.01
KCD7	73.98	84.48	0.74	33.74	64.65	3.06

Table C.7(a): Size analyses of run KKCD1 concentrate and tails samples and the concentrate yield in each size fraction

	concentrate		tails		feed	concentrate
size fraction (micron)	mass (g)	% in size fraction	mass (g)	% in size fraction	% in size fraction	(yield) (%)
+425	0.02	0.04	1.75	3.50	2.98	0.21
-425+212	0.41	0.87	6.06	12.12	10.42	1.25
-212+150	0.36	0.76	4.60	9.20	7.93	1.45
-150+106	0.69	1.46	4.69	9.38	8.19	2.69
-106+ 75	1.02	2.15	5.82	11.64	10.21	3.19
- 75+ 45	1.82	3.84	1.45	2.90	3.04	19.07
- 45	43.04	90.88	25.62	51.25	57.23	23.98
overall	47.36	100.00	49.99	100.00	100.00	15.10

Table C.7(b): Size analyses of run KKCD4 concentrate and tails samples and the concentrate yield in each size fraction

	concentrate		tails		feed	concentrate
size fraction (micron)	mass (g)	% in size fraction	mass (g)	% in size fraction	% in size fraction	(yield) (%)
+425	0.04	0.09	2.45	5.09	2.40	2.03
-425+212	0.25	0.57	10.02	20.81	9.92	3.07
-212+150	1.12	2.54	4.51	9.37	5.69	23.98
-150+106	2.57	5.83	7.03	14.60	9.88	31.71
-106+ 75	4.19	9.50	5.68	11.80	10.56	48.37
- 75+ 45	5.88	13.33	2.00	4.15	9.09	78.88
- 45	30.06	68.15	16.46	34.18	52.45	69.88
overall	44.11	100.00	48.15	100.00	100.00	53.78

Table C.7(c): Size analyses of run KKCD6 concentrate and tails samples and the concentrate yield in each size fraction

	concentrate		tails		feed	concentrate
size fraction (micron)	mass (g)	% in size fraction	mass (g)	% in size fraction	% in size fraction	(yield) (%)
+425	0.02	0.04	2.76	6.37	1.92	1.63
-425+212	1.21	2.69	9.71	22.42	8.53	22.17
-212+150	2.60	5.77	5.15	11.89	7.59	53.58
-150+106	3.77	8.37	3.52	8.13	8.30	71.00
-106+ 75	5.02	11.15	2.66	6.14	9.67	81.19
- 75+ 45	3.83	8.51	2.10	4.85	7.42	80.66
- 45	28.58	63.47	17.41	40.20	56.58	78.96
overall	45.03	100.00	43.31	100.00	100.00	70.39

C.4 Analysis of Particle Size Effects

In addition to the size analysis work carried out in Chapter Four, and in the collector dosage investigation, particle size analyses were carried out on flotation concentrates and tails samples from selected runs from both the factorial design (runs KKFD-A8(2), KKFD-B16 and KKFD-D6) investigation. The material remaining in each of the different size fractions was then subjected to float-and-sink analysis. The same was done with concentrate and tailings samples from KKB3 (batch flotation-Chapter Five) and KKCD1, KKCD4 and KKCD6 (collector dosage investigation-Chapter Six).

In the float-and-sink analyses carried out, the SG of the heavy liquid was chosen so as to detect the "misplaced" material in both the concentrate and tailings fractions of each of the runs investigated.

The results of the float-and-sink analyses are listed in **Tables C.8(a)** to **(g)** below. The size analyses of the concentrate, tails and reconstituted feed (calculated), and the concentrate yield in each of the size fractions are listed in **Tables B.2.3(b)** and **(c)** in Section B.2.3 of Appendix 3 (KKB3), **Tables C.7(a)**, **(b)** and **(c)** in Section C.3 above (KKCD1, KKCD4 and KKCD6) and **Tables 9(a)**, **(b)** and **(c)** below (KKFD-A8(2), KKFD-B16 and KKFD-D6).
In Tables 8(a) to (g) a "-" indicates that there was insufficient material in the size fraction to carry out float-and-sink or ash analyses. Where insufficient material was present in a particular size fraction the material was added to the material in the next largest size fraction. The values in the various columns of Tables C.8(a) to (g) signify the following.

i) The **sample mass** is the mass of concentrate, in column 2, or tails, in column 6, remaining in each of the size fractions (i) after sieving. Fractional shovelling (as described in Appendix A) was used to produce concentrate and tails samples small enough for size analysis.

ii) The **% floats** is the amount (percent) of concentrate, in column 3, or tails, in column 7, which floats at the RD used.

iii) The **% ash floats** is the ash content of the material in the concentrate, in column 4, or tails, in column 8, which reported to the "floats" at the RD used.

iv) The **% ash sinks** is the ash content of the material in the concentrate, in column 4, or tails, in column 8, which reported to the "sinks" at the RD used.

The values listed in each Tables C.9(a), (b) and (c) were obtained in the same way as those for Tables B.2.x_k(b) and B.4.3(d) and (f) (see Appendix B). The calculations used are detailed in Sections B.2 and B.4 of Appendix B.

Table C.8(a): Size and float-and-sink analyses of run KKCD1 concentrate and tails samples

	concentrate (SG=1.35)				tails (SG=1.30)			
size fraction (micron)	sample mass (g)	% floats	% ash floats	% ash sinks	sample mass (g)	% floats	% ash floats	% ash sinks
+425	0.02	-	-	-	1.75	5.74	-	43.47
-425+212	0.41	-	-	-	6.06	5.49	-	39.27
-212+150	0.36	-	-	-	4.60	7.25	-	28.64
-150+106	0.69	-	-	-	4.69	6.71	-	21.63
-106+ 75	1.02	29.90	-	17.83	5.82	6.22	-	19.69
- 75+ 45	1.82	26.10	-	15.83	1.45	6.44	-	18.55
- 45	43.04	11.30	2.92	19.8	25.62	1.88	-	25.87

Table C.8(b): Size and float-and-sink analyses of run KKCD4 concentrate and tails samples

	concentrate (SG=1.50)				tails (SG=1.45)			
size fraction (micron)	sample mass (g)	% floats	% ash floats	% ash sinks	sample mass (g)	% floats	% ash floats	% ash sinks
+425	0.04	-	-	-	2.45	33.01	4.9	53.20
-425+212	0.25	-	-	-	10.02	33.16	5.38	-
-212+150	1.12	-	-	-	4.51	36.34	5.52	42.62
-150+106	2.57	88.74	4.41	20.5	7.03	34.27	5.93	41.64
-106+ 75	4.19	79.09	5.94	21.26	5.68	27.24	5.75	41.89
- 75+ 45	5.88	73.80	5.99	25.94	2.00	18.70	-	56.01
- 45	30.06	73.18	6.01	39.64	16.46	15.06	5.78	56.11

Table C.8(c): Size and float-and-sink analyses of run KKCD6 concentrate and tails samples

	concentrate (SG=1.60)				tails (SG=1.55)			
size fraction (micron)	sample mass (g)	% floats	% ash floats	% ash sinks	sample mass (g)	% floats	% ash floats	% ash sinks
+425	0.02	-	-	-	2.76	51.23	7.43	57.76
-425+212	1.21	99.04	7.43	57.76	9.71	39.52	9.44	56.71
-212+150	2.60	97.72	10.10	55.20	5.15	32.52	10.10	56.04
-150+106	3.77	95.02	10.10	56.87	3.52	24.94	10.00	63.69
-106+ 75	5.02	91.55	10.00	65.64	2.66	18.90	-	67.58
- 75+ 45	3.83	87.24	-	71.06	2.10	14.19	-	71.06
- 45	28.58	86.38	19.71	64.31	17.41	24.20	19.71	64.31

Table C.8(d): Size and float-and-sink analyses of run KKFD-8(2) concentrate and tails samples

	concentrate (SG=1.60)				tails (SG=1.55)			
size fraction (micron)	sample mass (g)	% floats	% ash floats	% ash sinks	sample mass (g)	% floats	% ash floats	% ash sinks
+425	0.03	-	-	-	4.04	54.76	7.65	55.42
-425+212	2.23	97.81	6.36	-	7.49	36.06	10.01	55.47
-212+150	3.23	94.57	7.04	-	3.85	28.11	10.27	60.31
-150+106	4.25	91.74	7.52	-	2.82	28.55	10.17	63.12
-106+ 75	9.32	89.68	7.98	-	2.41	24.54	10.20	65.13
- 75+ 45	1.97	87.41	6.65	-	0.66	-	-	-
- 45	27.88	86.00	7.65	44.11	23.79	31.61	12.63	66.26

Table C.8(e): Size and float-and-sink analyses of run KKFD-B16 concentrate and tails samples

	concentrate (SG=1.45)				tails (SG=1.40)			
size fraction (micron)	sample mass (g)	% floats	% ash floats	% ash sinks	sample mass (g)	% floats	% ash floats	% ash sinks
+425	-	-	-	-	1.25	34.17	3.90	38.61
-425+212	-	-	-	-	4.96	33.02	3.80	36.02
-212+150	0.23	-	-	-	3.97	35.57	3.83	31.51
-150+106	1.58	89.08	3.59	-	4.04	30.30	3.78	28.15
-106+ 75	2.79	80.40	4.03	15.82	1.19	31.86	3.84	25.39
- 75+ 45	8.40	72.77	4.16	17.32	5.74	23.90	3.98	27.92
- 45	34.52	74.08	3.95	20.16	21.24	15.84	4.63	36.05

Table C.8(f): Size and float-and-sink analyses of run KKFD-D6 concentrate and tails samples

	concentrate (SG=1.50)				tails (SG=1.45)			
size fraction (micron)	sample mass (g)	% floats	% ash floats	% ash sinks	sample mass (g)	% floats	% ash floats	% ash sinks
+425	-	-	-	-	2.24	37.51	5.39	45.73
-425+212	0.28	-	-	-	7.68	36.20	5.29	43.20
-212+150	1.33	96.64	3.93	-	5.20	33.00	5.71	41.78
-150+106	2.87	89.81	4.95	-	4.22	28.53	6.07	42.39
-106+ 75	4.17	83.53	5.45	21.47	2.97	23.93	5.63	40.99
- 75+ 45	4.96	79.11	5.98	24.71	2.93	19.70	5.58	49.13
- 45	23.56	80.84	5.00	29.15	17.75	19.45	7.49	50.24

Table C.8(g): Size and float-and-sink analyses of run KKB3 concentrate and tails samples

	concentrate (SG=1.60)				tails (SG=1.55)			
size fraction (micron)	sample mass (g)	% floats	% ash floats	% ash sinks	sample mass (g)	% floats	% ash floats	% ash sinks
+425	0.14	-	-	-	2.11	-	-	-
-425+212	3.44	-	-	-	4.59	36.50	10.21	69.84
-212+150	3.37	83.03	7.68	-	3.30	42.62	9.24	67.10
-150+106	3.46	84.50	7.11	34.64	3.33	50.59	9.25	66.44
-106+ 75	4.32	84.56	7.36	-	3.91	56.41	9.47	64.53
- 75+ 45	4.23	82.66	7.02	-	2.70	48.76	9.41	66.47
- 45	24.05	86.26	6.72	40.94	19.87	28.22	11.74	72.85

Table C.9(a): Size analyses of run KKFD-A8(2) concentrate and tails samples and the concentrate yield in each size fraction

	concentrate		tails		feed	concentrate
size fraction (micron)	mass (g)	% in size fraction	mass (g)	% in size fraction	% in size fraction	(yield) (%)
+425	0.03	0.06	4.04	8.97	2.88	1.45
-425+212	2.23	4.56	7.49	16.62	8.38	37.14
-212+150	3.23	6.60	3.85	8.54	7.22	62.48
-150+106	4.25	8.69	2.82	6.26	7.92	74.95
-106+ 75	9.32	19.06	2.41	5.35	14.71	88.47
- 75+ 45	1.97	4.03	0.66	1.46	3.22	85.56
- 45	27.88	57.00	23.79	52.80	55.67	69.93
overall	48.91	100.00	45.06	100.00	100.00	68.30

Table C.9(b): Size analyses of run KKFD-B16 concentrate and tails samples and the concentrate yield in each size fraction

	concentrate		tails		feed	concentrate
size fraction (micron)	mass (g)	% in size fraction	mass (g)	% in size fraction	% in size fraction	(yield) (%)
+425	-	0.00	1.25	2.95	2.27	0.00
-425+212	-	0.00	4.96	11.70	9.00	0.00
-212+150	0.23	0.48	3.97	9.37	7.32	1.53
-150+106	1.58	3.32	4.04	9.53	8.10	9.48
-106+ 75	2.79	5.87	1.19	2.81	3.51	38.56
- 75+ 45	8.40	17.68	5.74	13.54	14.50	28.15
- 45	34.52	72.64	21.24	50.11	55.31	30.31
overall	47.52	100.00	42.39	100.00	100.00	23.08

Table C.9(c): Size analyses of run KKFD-D6 concentrate and tails samples and the concentrate yield in each size fraction

	concentrate		tails		feed	concentrate
size fraction (micron)	mass (g)	% in size fraction	mass (g)	% in size fraction	% in size fraction	(yield) (%)
+425	-	0.00	2.24	5.21	2.73	0.00
-425+212	0.28	0.75	7.68	17.86	9.70	3.70
-212+150	1.33	3.58	5.20	12.10	8.03	21.25
-150+106	2.87	7.72	4.22	9.82	8.82	41.77
-106+ 75	4.17	11.22	2.97	6.91	8.96	59.69
- 75+ 45	4.96	13.34	2.93	6.82	9.93	64.10
- 45	23.56	63.38	17.75	41.29	51.83	58.34
overall	37.17	100.00	42.99	100.00	100.00	47.70